

A multilevel study of platelet activation at biomaterial surface:  
from evaluating to controlling hemocompatibility

Zur Erlangung des akademischen Grades eines  
DOKTORS DER NATURWISSENSCHAFTEN  
(Dr. rer. nat.)

der KIT-Fakultät für Chemie und Biowissenschaften  
des Karlsruher Instituts für Technologie (KIT)

genehmigte

DISSERTATION

von

M. Sc. Alessia Donati

aus

Taranto, Italien

KIT-Dekan: Prof. Dr. Willem Klopper

Referent: Prof. Dr. Martin Bastmeyer

Korreferent: Prof. Dr. Ute Schepers

Tag der mündlichen Prüfung: 16.12.2016

# Eidesstattliche Erklärung

Hiermit erkläre ich,

1. dass es sich bei der eingereichten Dissertation zu dem Thema „A multilevel study of platelet activation at biomaterial surface: from evaluating to controlling hemocompatibility“ um meine eigenständig erbrachte Leistung handelt.
2. nur die angegebenen Quellen und Hilfsmittel benutzt und mich keiner unzulässigen Hilfe Dritter bedient zu haben. Insbesondere habe ich wörtlich oder sinngemäß aus anderen Werken übernommene Inhalte als solche kenntlich gemacht.
3. dass ich die Regeln zur Sicherung guter wissenschaftlicher Praxis im Karlsruher Institut für Technologie (KIT) in der gültigen Fassung beachtet habe.
4. dass die elektronische Version der Arbeit mit der schriftlichen übereinstimmt.
5. dass die Abgabe und Archivierung der Primärdaten gemäß Abs. A (6) der Regeln zur Sicherung guter wissenschaftlicher Praxis des KIT beim Institut gesichert ist.
6. diese Arbeit oder Teile davon bislang nicht an einer Hochschule des In- oder Auslands als Bestandteil einer Prüfungs- oder Qualifikationsleistung vorgelegt zu haben.

Die Richtigkeit der vorstehenden Erklärungen bestätige ich.

Die Bedeutung der eidesstattlichen Versicherung und die strafrechtlichen Folgen einer unrichtigen oder unvollständigen eidesstattlichen Versicherung sind mir bekannt.

Ich versichere an Eides statt, dass ich nach bestem Wissen die reine Wahrheit erkläre und nichts verschwiegen habe.

Karlsruhe, den 02.11.2016

Alessia Donati

# Acknowledgements

For this work of Thesis, I would like to thank:

Prof. Dr. Martin Bastmeyer for having accepted to be my *Doktorvater*.

Dr. Ilya Reviakine, for his continuous supervision during my Ph.D study. He encouraged my research and allowed me to grow as a research scientist. His guidance was essential for me at all the time of research and writing of this thesis.

Prof. Dr. Matthias Franzreb and Prof. Dr. Ute Schepers, for being part of my Thesis Advisory Committee and for their valuable support.

Dr. Cornelia Lee-Thedieck for giving me access to her laboratory and use her equipment.

Prof. Dr. Aldo Jesorka who provided me the opportunity to join his group at Chalmers University (Gothenburg, Sweden), where I worked with the multifunctional pipette.

Prof. Dr.-Ing. Friedrich Jung, Dr. Steffen Braune for giving me the possibility to work at Helmholtz-Zentrum Geesthacht, where I performed the experiments with the shear channels.

Prof. Dr. Hans Peter Wendel, Dr. Stefanie Krajewski, Dr. med Andreas Straub and Dr. Thiago Folgosa Granja at the University Hospital of Tübingen for the collaboration on the shear channel project.

Prof. Grunze for the collaborations on the shear channel and the microfluidic projects, and to Dr. Kwan Cho who worked with me on the microfluidic project.

Dr. Alexander Welle who realized the surface coatings, and to Dr. Alexei Nefedov who performed the X-ray photoelectron spectroscopy analysis for this study.

Alexander Kueller (Celanova Biosciences) for providing the CoCr sputtering target used in the coating of the shear channels and Bertram Kuntz (KIT Technik-Haus—TEC) for fabricating the shear channels and the steel sputtering target for their coating.

George Albert (IFG, KIT) and Michael Horisberger (Paul Scherer Institute—PSI, CH) for the shear channel coating.

Dr. Volker List, M.D. and Ms. Ingrid Schaefer from the KIT Medical Service, and Ms. Sabina Santa and Ms. Eva Flenner (Sahlgrenska Univeritetssjukhuset, Klinisk kemi, Goteborg,

Sweden) for organizing blood donations, and Dr. Angela Weiss, who helped to obtain the Ethical approval.

BiF (Biointerfaces International Graduated School) and KHYS (Karlsruhe House of Young Scientists) for the funding and the travel scholarship to Chalmers University, respectively.

A special thank to:

My mom, my dad and my sister, for their support and love

My friends: Paola, Cristina, Alice, Rita, Ilaria, Gabriella, Yelitza and Kurt for being always next to me, for their constant help and support.

Christian and Natalie, because you let me feel at home, always.

# Abstract

Cardiovascular disorders (CVDs) are the major cause of death world-wide. Their management relies on artificial materials in implants and external devices such as stents and cardiopulmonary bypass equipment. All currently used artificial materials cause thrombotic and inflammatory complications and require anticoagulant and antiplatelet therapies that are costly and dangerous for the patient. So far, research into blood-material interactions failed to find materials free from these complications, an adequate *in vitro* test for evaluating material hemocompatibility, or appreciate the complexity of the blood-biomaterial interactions. I address these problems by designing two *in vitro* hemocompatibility tests. One is a whole-blood quasi-static test where thrombotic and inflammatory responses to three clinically used biomaterials (Ti, CoCr, steel) are evaluated using a multi-parametric assay assessing thrombin generation, platelet and leukocyte activation and aggregation, and complement activation. The second one is a small volume, rapid, microfluidic assay where platelet-surface interactions in platelet-rich plasma are evaluated by measuring platelet detachment from and activation at biomaterial surfaces. Because of the novelty of this test system, model surfaces were used: TiO<sub>2</sub>, glass, hydrophobically modified glass, and glass coated with a polymer, poly[bis(trifluoroethoxy)phosphazene] (PTFEP), that has recently attracted attention as stent coating. The key feature of my approach in both cases was to identify blood activation parameters sensitive to differences between materials, such as platelet consumption (decrease in the platelet count due to contact with the material) and the activation of platelet-leukocyte aggregates in the whole-blood test and platelet spreading and platelet-surface adhesion strength in the microfluidic test. Analysis of correlations between parameters showed that different surfaces acted as platelet agonists of different strength and highlighted platelet-mediated interactions between the inflammatory and thrombotic reactions. Titanium emerged as a superior material in the whole-blood test.

The future of artificial material integration is in their ability to activate native wound healing pathways. Normally platelets initiate them by secreting growth factors and cytokines. By selectively activating platelets at biomaterial surfaces, it should be possible to induce a healthy wound healing response. Unfortunately, not enough is known about the underlying mechanisms, but there is evidence of differently activated platelet subpopulations causing

different reactions. As a first step towards understanding and controlling platelet secretion reactions, I developed, for the first time, a single-platelet microfluidic assay for studying platelet secretion reactions that could access platelets in different subpopulations.

## Zusammenfassung

Herz-Kreislauf-Erkrankungen sind die Haupttodesursache weltweit. Ihre Behandlung stützt sich aktuell auf synthetische Materialien, die in Implantaten, Stents sowie externen Geräten wie z.B. Herz-Lungen-Maschinen zum Einsatz kommen. Alle derzeit eingesetzten synthetischen Materialien verursachen Komplikationen wie Thrombosen und Entzündungen und benötigen die Blutgerinnung sowie die Thrombozytenfunktion hemmende Therapien, welche für die Patienten kostenintensiv und gefährlich sind. Bislang waren die Versuche im Bereich Blut-Biomaterial-Interaktion, Materialien frei solcher Komplikationen oder einen geeigneten in vitro Test für Hämokompatibilität zu finden, sowie das komplexe Zusammenspiel von Blut und Biomaterial näher zu verstehen, nur wenig erfolgreich. Ziel dieser Arbeit war es, diese Problematik aufzugreifen und zwei in vitro Hämokompatibilitätstest zu entwickeln. Der erste ist ein quasistatischer Vollbluttest, bei welchem die thrombotischen und entzündlichen Reaktionen auf drei klinisch genutzten Biomaterialien (Ti, CoCr, Stahl) unter Verwendung von multiparametrischen Tests unter Beurteilung der Bildung von Thrombin, der Aktivierung und Aggregation von Thrombozyten und Leukozyten sowie der Komplementaktivierung untersucht werden.

Der zweite ist ein auf geringen Probenvolumen basierender, schneller mikrofluidischer Test, welcher Interaktionen zwischen Thrombozyten und den Oberflächen in einem thrombozytenreichen Blutplasma aufgrund der Ablösung der Thrombozyten von den Biomaterialoberflächen sowie der Thrombozytenaktivierung an selbigen Oberflächen beurteilt. Da es sich bei diesen Verfahren um neue Testsysteme handelt, kamen folgende Modelloberflächen zur Verwendung: TiO<sub>2</sub>, Glas, hydrophob-modifiziertes Glas und Glas beschichtet mit dem Polymer Poly(Bis(Trifluoroethoxy)Phosphazen), welches kürzlich als Stentbeschichtung in den Fokus der Aufmerksamkeit rückte. Das wesentliche Merkmal meines Ansatzes in beiden Fällen war das Ermitteln bezüglich Materialunterschiede sensitiver Blutaktivierungsparametern, wie dem Thrombozytenverbrauch (Abnahme der

Thrombozytenanzahl bei Kontakt mit dem Material) und der Aktivierung von Thrombozyten-Leukozyten-Aggregationen im Vollbluttest, sowie der Thrombozytenverteilung und der Oberflächenhaftung der Thrombozyten im mikrofluidischen Test. Die Analyse der Zusammenhänge ergab, dass die unterschiedlichen Oberflächen in unterschiedlicher Stärke als Thrombozytenagonisten agieren, und hob die Thrombozyten-vermittelten Wechselwirkungen zwischen entzündlichen und thrombotischen Reaktionen hervor. Titan ging aus den Vollbluttests als herausragendes Material hervor.

Die Integration der synthetischen Materialien wird in der Zukunft von ihrer Fähigkeit abhängen, die natürlichen Wundheilungsprozesse zu initiieren. Üblicherweise aktivieren Thrombozyten diese durch Absonderung von Wachstumsfaktoren oder Zytokinen. Durch das selektive Aktivieren von Thrombozyten an Biomaterialoberflächen sollte es möglich werden, den Wundheilungsprozess einzuleiten. Leider sind die zugrunde liegenden Mechanismen nur unzureichend bekannt, jedoch gibt es den Nachweis für unterschiedlich aktivierte Thrombozyten-Untergruppen, welche unterschiedliche Reaktionen verursachen. Als ersten Schritt zum Verständnis und zur Kontrolle der Sekretionsreaktionen von Thrombozyten habe ich - zum ersten Mal - einen Einzelthrombozyten Mikrofluidik-Test, welcher Thrombozyten in unterschiedlichen Untergruppen erfassen kann, entworfen.

# List of Publications

Alessia Donati, Swati Gupta, Ilya Reviakine. Subpopulations in Purified Platelets Adhering On Glass. *Biointerphases* **11**, 029811 (2016)

Eva Uhl, Alessia Donati, Ilya Reviakine. Platelet immobilization on supported phospholipid bilayers for single platelet studies. *Langmuir* **32**(33), 8516–8524 (2016)

Swati Gupta, Alessia Donati, Ilya Reviakine. Differences in intracellular calcium dynamics cause differences in  $\alpha$ -granule secretion and phosphatidylserine expression in platelets adhering on glass and TiO<sub>2</sub>. *Biointerphases* **11**, 029807 (2016)

# Abbreviations

A5	Annexin A5
ACD	Acid Citrate Dextrose
ACT	Anticoagulant Therapy
APT	Antiplatelet Therapy
APTES	(3-Aminopropyl)trimethoxysilane
AT	Anti-Thrombin (coagulation inhibitor)
BMS	Bare Metal Stent
CABG	Coronary Artery Bypass Grafting
CAD	Coronary Artery Disease
CaloP	Calcium Ionophore A23187
COX	Cyclooxygenase
CPB	Cardiopulmonary Bypass
CTGF	Connective Tissue Growth Factor
CVDs	Cardiovascular Disorders
DAG	1,2-Diacyl-Glycerol
DAPT	Dual Antiplatelet Therapy
DES	Drug Eluting Stent
Det50	Shear Stress at which 50% of the platelet detach from the surface
DTS	Dense Tubular System
ECMO	Extracorporeal Membrane Oxygenator
ECs	Endothelial Cells
EGF	Epidermal Growth Factor
FGF	Fibroblast Growth Factor
FSC	Forward Scattered Light
G-CSF	Granulocyte-Colony Stimulating Factor
GM-CSF	Macrophage-Colony Stimulating Factor
GP	Glycoprotein
GPCRs	G-protein Coupled Receptors
HCV	Hydrodynamically Confined Volume

HEMA	Hydroxyethyl methacrylate
HGF	Hepatocyte Growth Factor
HMWK	High Molecular Weight Kininogen
IGF	Insulin-like Growth Factor
IL	Interleukin
IP <sub>3</sub>	Inositol-1,4,5-Triphosphate
IP <sub>3</sub> R	Inositol-1,4,5-Triphosphate Receptor
LPS	Lyppolysaccharides
LVAD	Left Ventricular Assist Devise
MAC	Membrane Attack Complex
MACE	Major Adverse Cardiac Events
MBL	Mannose-binding Lectin
MFI	Median Fluorescence Intensity
MMP	Matrix Metalloproteinase
MON	Monocyte
NEU	Neutrophil
NO	Nitric Oxide
OCS	Open Canalicular System
OTS	Octadecyltrichlorosilane
PAF	Platelet Activating Factor
PAR	Protease Activated Receptor
PC	Phosphorylcholine
PCI	Percutaneous Coronary Intervention
PDGF	Platelet Derived Growth Factor
PDMS	Polydimethoxysiloxane
PEG	Polyethylene Glycol
PF4	Platelet Factor 4
PfP	Platelet poor Plasma
PGI <sub>2</sub>	Prostaglandin I <sub>2</sub>
PIP <sub>2</sub>	Phosphatidylinositol 4,5-bisphosphate
PLC	Phospholipase C
PLT	Platelet

PMA	Phorbol 12-myristoyl Acetate
PMN	Polymorphonuclear (leukocyte)
PrP	Platelet rich Plasma
PS	Phosphatidylserine
PSGL-1	P-selectin Glycoprotein Ligand-1
PTFE	Polytetrafluoroethylene
PTFEP	Poly[bis(trifluoroethoxy)phosphazene]
PVC	Polyvinyl Chloride
RBC	Red Blood Cell
SDF1 $\alpha$	Stromal Derived Growth Factor 1 $\alpha$
SDS	Sodium Dodecyl Sulfate
SOCE	Store-Operated Calcium Entry
SSC	Side Scattered Light
ST	Stent Thrombosis
STIM1	Stromal Interaction Molecule 1
TAT	Thrombin-anti-Thrombin complex
TF	Tissue Factor
TFPI	Tissue Factor Pathway Inhibitor
TIMPs	Tissue Inhibitor of metalloproteinases
TNF- $\alpha$	Tumor Necrosis Factor
t-PA	Tissue Plasminogen Activator
TRAP6	Thrombin Receptor Activating Peptide (SFLLRN)
TSP-1	Thrombospondin
TXA2	Thromboxane A2
UNT	Untreated
VAD	Ventricular Assist Devise
VEGF	Vascular Endothelial Growth Factor
vWF	von Willebrand Factor
WBC	White Blood Cell
XPS	X-ray Photoelectron Spectroscopy
$\beta$ -TG	$\beta$ -Thromboglobulin

# Content

<b>1. Introduction</b> .....	1
1.1 Cardiovascular disorders: a global problem .....	1
1.2 CVD management strategies .....	2
1.3 Use of Artificial Devices for CVD management .....	2
1.4 Adverse reactions to the materials: activation of the body's defenses systems .....	6
1.5 Hemostasis .....	7
1.5.1 Vascular spasm .....	7
1.5.2 Platelets .....	8
1.5.3 Coagulation .....	12
1.6 Inflammation .....	14
1.6.1 Complement .....	14
1.6.2 Leukocytes .....	15
1.7 Hemostasis and Inflammation: one system for wound healing and material-induced thrombosis .....	16
1.8 Pharmacological management of the adverse effects caused by the artificial devices	17
1.9 Mechanisms of blood activation at the biomaterial surface: the role of adsorbed proteins .....	18
1.10 Failed Attempts to Find Hemocompatible Materials .....	20
1.11 Evaluating hemocompatibility: thrombotic and embolic events .....	22
1.12 The future of implant integration: directing platelet responses towards wound healing	25
1.13 Objectives of the work .....	29
<b>2. Materials and Methods</b> .....	30
2.1 Cell Labeling Reagents .....	30
2.2 Other Chemicals .....	30
2.3 Equipment .....	30
2.4 Incubation Setup .....	31
2.5 Buffers .....	31
2.6 Blood Collection .....	32
2.7 Methods for material hemocompatibility testing .....	33

2.7.1	Shear Channels .....	33
2.7.2	Surface coating and surface characterization .....	34
2.7.3	Shear Channel cleaning .....	35
2.7.4	Shear Channel experiments .....	35
2.7.5	Blood Cell Count .....	35
2.7.6	Six color Flow cytometric Assay .....	36
2.7.7	Flow cytometry data analysis .....	37
2.7.8	ELISA sample preparation and measurements .....	37
2.7.9	Statistical analysis .....	38
2.8	Methods for platelet detachment studies .....	38
2.8.1	Platelet Rich Plasma (PrP) Preparation .....	38
2.8.2	Blood Cell Count .....	39
2.8.3	Analysis for Platelet Activation in PrP by Flow Cytometry .....	39
2.8.4	Substrate preparation and characterization .....	40
2.8.5	Shear forces apparatus for analyzing platelet detachment .....	41
2.8.6	Detachment studies in the shear forces apparatus .....	42
2.8.7	Detachment studies under static condition .....	43
2.8.8	Detachment studies: data analysis and statistics .....	44
2.9	Methods for studying platelets at single platelet level.....	44
2.9.1	Platelet isolation and purification.....	44
2.9.2	Platelet characterization by flow cytometry .....	45
2.9.3	Substrate preparation and characterization .....	46
2.9.4	Preparation of surface adhering platelets .....	46
2.9.5	Open volume microfluidic pipette .....	46
2.9.6	Open volume microfluidic pipette experiments and relevant controls .....	47
2.9.7	Data analysis.....	48
<b>3.</b>	<b>Material Hemocompatibility Testing: Quantifying Blood Responses.....</b>	<b>50</b>
3.1	Summary .....	50
3.2	Shear Channel system .....	52
3.3	Surface characterization of the coated shear channels.....	54
3.4	Whole blood cell count analysis.....	56
3.5	Quantitative evaluation of the coagulation cascade activation .....	61
3.6	Quantitative evaluation of the material-induced platelet activation and inflammatory responses.....	63

3.7	Quantitative evaluation of the solution and surface-phase events with the six-color flow cytometric assay and ELISA .....	68
3.8	Morphological effects of ageing of the shear channel coatings .....	79
3.9	Summary of the statistically significant material-induced changes in the blood activation according to the assay parameters measured in the study .....	81
3.10	Discussion .....	82
3.10.1	Differences between materials and the evaluation of the most sensitive assay parameters .....	83
3.10.2	Blood-material interaction mechanisms .....	87
3.10.3	Limitation of the study .....	92
3.10.4	Experimental model .....	93
3.11	Conclusion .....	95
<b>4.</b>	<b>Testing: a simple in vitro test for distinguishing between materials.....</b>	<b>96</b>
4.1	Summary .....	96
4.2	Surfaces .....	98
4.3	Platelet characterization by flow cytometry .....	99
4.4	Dynamically initiated platelet detachment.....	100
4.5	Platelet detachment in the static system .....	103
4.6	Platelet activation: area and CD62P expression .....	104
4.6.1	Platelet spreading.....	104
4.6.2	Platelet CD62P expression under dynamic and static conditions.....	106
4.7	Summary of the statistically significant material-induced changes in platelet detachment and activation according to the assay parameters measured in the study .....	109
4.8	Discussion .....	110
4.8.1	Material screening: sensitivity of various parameters to the differences between materials.....	111
4.8.2	What do the detachment measurements reveal about platelet-biomaterial interactions?.....	113
4.8.3	What does the microfluidic assay reveal about hemocompatibility of the tested materials? .....	116
4.8.4	Limitation of the study .....	118
4.8.5	Conclusion and outlook .....	118
<b>5.</b>	<b>A Method for Studying Platelet Activation at the Single Platelet Level ...</b>	<b>119</b>
5.1	Summary .....	119

5.2	The multifunctional pipette .....	120
5.3	Assay design .....	122
5.4	Platelet isolation, purification and analysis .....	123
5.5	Triggering $\alpha$ -granule secretion in individual platelets .....	124
5.6	Triggering PS expression in individual platelets.....	127
5.7	Quantitative analysis of the multifunctional pipette performance.....	128
5.8	Discussion.....	132
5.8.1	Multifunctional pipette for single platelet assay .....	132
5.8.2	Expression of CD62P and PS .....	133
5.9	Conclusion and Outlook .....	134
<b>6.</b>	<b>Discussion .....</b>	<b>135</b>
<b>7.</b>	<b>Conclusions.....</b>	<b>137</b>
	<b>Appendix .....</b>	<b>138</b>
	<b>References .....</b>	<b>140</b>

# List of Figures

Figure 1-1. Artificial Devices.....	3
Figure 1-2. Overview of blood-material interactions showing the components of the hemostatic and inflammatory systems relevant to thrombotic complications .....	7
Figure 1-3. Platelet Structure .....	8
Figure 1-4. Platelet activation. ....	11
Figure 1-5. Blood Coagulation Cascade.....	13
Figure 1-6. Complement Cascade .....	15
Figure 1-7. Approaches to developing hemocompatible materials.....	20
Figure 1-8. Thrombotic and embolic responses to the materials.....	22
Figure 1-9. In vivo hemocompatibility tests.....	23
Figure 1-10. Directing platelet activation towards the wound healing. ....	26
Figure 2-1. Shear channels schematic.....	34
Figure 2-2. Fluid cell design.....	41
Figure 2-3. Shear Force Apparatus.....	42
Figure 3-1. Testing strategy.....	51
Figure 3-2. Chandler Loop and Shear Channel design. ....	53
Figure 3-3. Platelet activation: CD62P expression in baseline blood and upon contact with PVC tube .....	53
Figure 3-4. Surface Characterization of the coated shear channels by XPS: Survey Spectra. .	54
Figure 3-5: Expanded view of the Ti2p region of the XPS spectrum of the Ti coating. ....	55
Figure 3-6: Detailed spectra of the Cr 2p and Co2p regions of the CoCr alloy coating. ....	55
Figure 3-7: Detailed spectrum of the Cr2p and Fe2p regions of the steel coating.....	56
Figure 3-8. Whole blood cell count analysis. RBC: red blood cells.....	57,58
Figure 3-9: Fractional decrease in PLT counts for the three materials used in this study.....	59
Figure 3-10. Thrombin generation evaluated by measuring thrombin-anti-thrombin III (TAT) complex in the blood.....	61
Figure 3-11. Flow cytometry analysis of whole blood: Scatter plots. ....	64
Figure 3-12. Strategy to identify and evaluate the activation of platelets and leukocytes in the platelet population and platelet aggregates with different types of leukocytes. ....	65
Figure 3-13. Titration assays .....	66
Figure 3-14. Scatter Plots depicting platelet population and platelet-leukocyte aggregates before and after the blood interaction with different materials.....	67
Figure 3-15. Quantification of platelet activation and aggregation with leukocytes. ....	70
Figure 3-16. Platelet aggregation with monocytes and neutrophils. ....	72
Figure 3-17. The activation state of platelets and monocytes in the platelet-monocyte aggregates. ....	74

Figure 3-18. The activation state of platelets and neutrophils in the platelet-neutrophil aggregates. ....	77
Figure 3-19. Complement activation: levels of sC5b-9. ....	78
Figure 3-20. State of the coatings .....	80
Figure 3-21. Thrombin generation versus platelet activation and inflammatory responses ..	88
Figure 3-22. Correlation between different ways to evaluate platelet activation .....	89
Figure 3-23. PMN-elastase release versus platelet activation .....	90
Figure 3-24. sC5b-9 generation versus platelet activation and PMN-elastase release. ....	91
Figure 4-1. Experimental strategy. ....	98
Figure 4-2. Platelet characterization by flow cytometry.....	99
Figure 4-3. Dynamic platelet detachment experiments. ....	101
Figure 4-4. Static platelet detachment experiments. ....	104
Figure 4-5. Analysis of platelet activation: platelet spreading.....	105
Figure 4-6. Platelet Activation: CD62P expression .....	107
Figure 4-7. Correlations between detachment and activation parameters .....	114
Figure A-1. XPS analysis of TiO <sub>2</sub> glass surfaces.....	139
Figure A-2. XPS analysis of PTFEP coating on glass .....	139

# List of Tables

Table 1-1. Major classes of Platelet $\alpha$ -granule content and their function .....	27
Table 2-1. Incubation setup types used in the thesis.....	31
Table 2-2. Buffers used in this study and the chapters in which they were used. ....	32
Table 2-3. Anticoagulant of choice.....	33
Table 2-4. Blood cell count in whole blood, Platelet free Plasma (PfP) and Diluted Platelet rich Plasma (PrP). ....	39
Table 2-5. Blood cell count in whole blood and in purified platelet suspension.....	45
Table 3-1. Experiments and measured parameters.....	52
Table 3-2. Raw blood cell count data.....	60
Table 3-3. Panel of the six antibodies used in the flow cytometry assay and the volumes used in the assay.....	66
Table 3-4. Material-induced blood activation.....	81
Table 4-1. Significant differences between materials in terms of the fraction of remaining platelets.....	102
Table 4-2. Significant differences between materials in det50. ....	103
Table 4-3. Significant differences between materials in platelet spreading .....	106
Table 4-4. Significant differences between materials in CD62P expression.....	108
Table 4-5. Summary of the significant differences between materials in the measured parameters.....	109

# 1. Introduction

## 1.1 Cardiovascular disorders: a global problem

Cardiovascular disorders (CVDs) are diseases of the heart and blood vessels. Coronary Artery Disease (CAD), heart attacks, stroke, arrhythmias, heart failure, congenital and acquired heart valve abnormalities, are prominent examples.<sup>1</sup> CVDs represent a global concern, poised to become more severe with the increase of the lifespan and acquisition of lifestyle-related risk factors (smoking, alcohol consumption, obesity, diabetes). CVDs are the major contributors to mortality world-wide, causing the death of around 18 million people every year. CAD alone is responsible for 8 million of these deaths, strokes account for 5.5 million of deaths annually.<sup>2</sup> The primary cause of CAD, heart attacks, and strokes, is atherosclerosis.

Atherosclerosis is the formation of a plaque in the artery wall that narrows the artery and limits the blood flow. The plaque formation results from a progressive accumulation of lipid and cholesterol, inflammatory cells, and fibrous elements--such as smooth muscle cells and extracellular matrix-- in the wall of the artery.<sup>3</sup> In an advanced state, the plaque can calcify and become increasingly big and complex. Non-occlusive obstructions of the artery--due to the growth of the atherosclerotic plaque--clinically manifest as ischemic events and disabling chest pain.<sup>4,5</sup> Acute occlusion of the artery occurs when a thrombus or blood clot forms at the atherosclerotic plaque. Usually, thrombus forms when the atherosclerotic plaque ruptures or erodes, due to the activation and aggregation of platelets and the initiation of the coagulation cascade.<sup>6</sup> Clinical manifestations of acute occlusions of the artery are heart attacks and strokes.

Other pathological conditions such as hypertension greatly contribute to the epidemiology and mortality of atherosclerotic-related diseases. It is estimated that close to 9 million deaths world-wide are related to hypertensive complications.<sup>7</sup> Another example is atrial fibrillation. It affects 33.5 million of individuals and greatly contributes to the occurrence of thrombotic events and heart failure.<sup>8</sup>

Congenital or acquired abnormalities of the structure and function of the heart also contribute to the high mortality of CVDs. To give some examples, heart failure--defined as the impaired heart's pumping ability--affects more than 23 million of people world-wide and causes nearly

300,000 deaths annually.<sup>9,10</sup> Equally, structural heart diseases such as dysfunctional heart valves cause nearly 40,000 deaths every year.<sup>11</sup>

## 1.2 CVD management strategies

There is no cure for CVDs, but there are preventative approaches and/or strategies to manage their progress that save patients' lives and restore their quality of life. Preventative approaches focus on the lifestyle improvements (healthy diet, physical activity, quitting of smoking and alcohol consumption). Their application is rewarded with the reduction of CVD mortality. For examples, Finland achieved 80% reduction in CAD mortality during the period 1992-1972; Ireland of 50% during the period 1985-2000.<sup>12</sup> Despite these successes in some countries, in others the reduction is not so impressive and CVD prevention is still a faraway goal on the global scale.<sup>13</sup>

On the other hand, preventative approaches alone are not sufficient for the patients who are already at high risk or those with existing, developed CVDs. They require effective treatment measures to thrombotic complications of CVDs such as heart attacks and strokes. Examples of preventative therapies include those aimed at normalizing blood pressure, statins to lower cholesterol levels, and preventative antiplatelet therapies (aspirin) to reduce thrombosis risk. Thrombolytic agents are applied in the event of an acute thrombotic occlusion.<sup>14</sup> Surgical interventions (angioplasty, stenting, cardiovascular bypass grafting, etc.) are used in severe cases. Patients with implants have to be treated pharmaceutically with anticoagulant and/or antiplatelet drugs.

## 1.3 Use of Artificial Devices for CVD management

Surgical interventions rely on the use of artificial devices that substitute, or augment the function of the damaged vessel or heart. They represent a key strategy in the management of CVDs. Examples of such devices are stents, vascular grafts, mechanical heart valves, ventricular assist devices (VADs) and extracorporeal oxygenator systems (Figure 1-1 A-D).

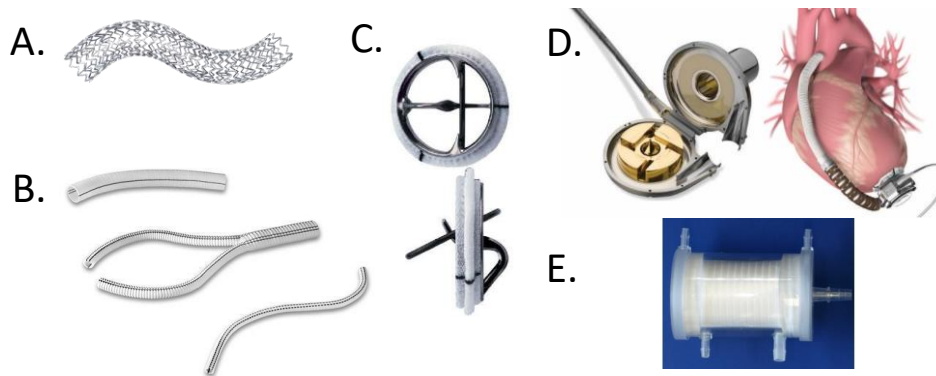


Figure 1-1. Artificial Devices. A. Coronary stent, B. Vascular bypass graft, C. Mechanical heart valves, D. Ventricular Assist Device (VAD), E. Membrane oxygenator used for extracorporeal membrane oxygenation systems.

The use of these devices saves millions of lives. Furthermore, the progress in their design allowed complex and challenging surgical procedures to become routine, although limitations remain.<sup>15</sup>

Key among these limitations are the adverse thrombotic and inflammatory reactions to the artificial materials used in the devices.

The introduction of coronary stents has revolutionized percutaneous coronary intervention (PCI, or angioplasty) for the management of CADs. Close to half a million of cardiac stents are implanted in the US annually, three quarters of million in Europe, and around 100,000 in the UK for the treatments of CAD.<sup>16-18</sup> Initially PCI was performed without stenting by balloon angioplasty (the first PCI was performed by Gruntzig in 1977).<sup>19</sup> The technique consisted in inserting a balloon catheter in the narrowed artery and inflating it at the atherosclerotic site, in order to compress the plaque against the artery's wall.<sup>19</sup> However, the outcomes were compromised by the acute collapse of the arterial wall (minute-hours after the angioplasty) and longer-term post-angioplasty restenosis (re-narrowing) of the arteries due to vascular remodeling and neo-intima proliferation.<sup>20</sup> The balloon angioplasty also suffered from thrombotic complications due to the tearing of the vessel.<sup>21</sup>

Bare metal stents (BMS) were developed to prevent the collapse of the vessel by scaffolding the balloon-dilated artery.<sup>22</sup> However, they resulted in high incidence of in-stent thrombosis (ST) and consequent embolic events. The breakthrough in the use of the stents was the introduction of dual antiplatelet therapy (DAPT, aspirin/ticlopidine, later replaced by aspirin/clopidogrel), which significantly reduced the occurrence of CAD treatment.<sup>23</sup>

While the thrombosis problem was addressed by DAPT, BMS suffer from significant rate of medium- and long-term in stent restenosis due to neo-intima proliferation.<sup>24</sup> To address this problem, drug eluting stents (DES) were developed. DES have polymer-coated metal framework eluting anti-proliferative and anti-inflammatory drugs (Sirolimus, Everolimus, Paclitaxel). With respect to reducing restenosis, DES were successful, but the first generation DES stents turned out suffer from late stent thrombosis (1 – 5 years after the intervention).<sup>25</sup> The long-term performance of BMS and first generation DES turned out to be similar in terms of the rate of adverse cardiac events such as heart attacks and strokes.<sup>26</sup> As the reasons behind late stent thrombosis became better understood, second-generation DES stents are now being introduced in the clinic, with better outcomes. Nevertheless, compared to the BMS, much longer duration of DAPT regiment (1-3 months for BMS, 6-12 months for DES) is recommended by the European guidelines.<sup>27,28</sup>

Alternative method to PCI with stents for the treatment of CAD, is the more invasive coronary artery bypass grafting (CABS). This is an open heart surgery to redirect the blood flow by sewing the vascular graft to the target vessel.<sup>29</sup> According to the current guidelines, CABS is the treatment of choice for patients with severe CAD.<sup>30,31</sup> The implantation of artificial vascular graft is, analogous to coronary stents, associated with thrombotic complications that are treated with DAPT. Artificial vascular grafts also suffer from restenosis due to intimal hyperplasia.<sup>15</sup>

A common and important problem of coronary stents and vascular grafts is their inability to promote the growth of a continuous endothelium over the surface of the implant. This limits the integration of the stents or graft and impairs the physiological wound healing.<sup>25</sup> Another example of the impact artificial devices have on the modern health-care is the implantation of artificial heart valves: world-wide approximately 280,000 artificial heart valves are implanted per year.<sup>32</sup> The introduction of valve replacement surgery in the early 1960s has dramatically improved the outcome of patients with congenital or acquired heart valve diseases.<sup>33</sup> During the evolution of the artificial heart valves, several models were designed and optimized with respect to their geometry, materials and hemodynamics properties. The most recent advances are represented by aortic valves design for minimally invasive, trans-catheter replacement.<sup>34</sup> Heart valve prosthetics are not free from drawbacks either. Patients with mechanical heart valve are at risks of thromboembolic complications, systemic embolization (usually cerebral), valve obstruction and/or regurgitation due to the thrombosis.

The problem is more severe than in the case of the stents, and patients with mechanical heart valves require life-long anti-coagulation and antiplatelet therapy.<sup>32</sup>

Yet another example is the implantation of left ventricular assist devices (LVADs) in patients with end-stage heart failure. It has increased considerably (from 246 patients in 2007 to circa 2,500 patients in 2014),<sup>35</sup> as LVAD design was recently improved. The change from the pulsatile to continuous flow greatly contributed to decrease the mortality rates.<sup>36</sup> VADs suffer from the same thrombotic and embolic complications as other devices, requiring life-long anti-coagulant and antiplatelet therapy regimens. Despite these regimens, the rates of thromboembolic complications in VAD patients remain significant (9% patients after 1 year).<sup>37,38</sup>

Finally, the use of external devices such as cardiopulmonary bypass (CPB) and external extracorporeal membrane oxygenators (ECMO) is a key element in modern surgical and intensive care procedures. These devices take over the heart and/or lung functions maintaining blood oxygenation.<sup>39</sup> Since their first introduction in 1953, their development went through several changes, particularly concerning the oxygenator design.<sup>39,40</sup> The gas exchange in the blood was initially achieved by direct contact bubble oxygenator, successively replaced by membrane oxygenator, and finally by the current used hollow fiber oxygenator that greatly increase the gas exchange in the blood passing through the device (Figure 1-1 D).<sup>41</sup> The performance of the external devices is also limited by thromboembolic complications and consequent strokes. Therefore, they require anti-coagulant therapies (heparin). Furthermore, they also cause the so-called systemic inflammatory responses that are not alleviated by the use of anti-coagulants.<sup>41-43</sup>

In summary, blood-contacting artificial devices save millions of patients affected by CVDs. However, it should be clear from the preceding discussion that their performance is limited by thromboembolic complications. All of the materials used in the construction of the artificial devices--metals and their oxides, polymers, pyrolytic and diamond-like carbon--are not hemocompatible.<sup>44</sup>

Hemocompatibility is defined as the ability of a material to be used in contact with blood without causing harm. Instead, all of these materials activate body's defense systems: coagulation, complement, and cellular inflammation pathways. Consequently, thrombotic and embolic complications of these reactions lead to major adverse cardiac events (MACE) such as heart attacks and strokes.<sup>45</sup> These complications are managed pharmaceutically with

anticoagulant and antiplatelet therapies. While this approach is successful at saving lives and improving the quality of life of millions of patients, it is fraught with complications. MACE rates are still significant in patients on the ACT/APT therapies and so is the risk of bleeding. Careful monitoring of patients with chronic application of ACT/APT therapies is also required to manage the bleeding risk, incurring considerable costs for the healthcare systems. With the ageing of the world-wide population, these costs will continue to rise. Much effort is therefore devoted to finding a material that avoids thrombotic and inflammatory complications—a so-called hemocompatible material—but none has been found till now. Further information on this subject can be found in a recent review from our group.<sup>46</sup>

I now discuss in detail what is known about adverse thrombotic and inflammatory reactions of blood to artificial materials.

#### 1.4 Adverse reactions to the materials: activation of the body's defenses systems

Contact of blood with artificial materials causes the activation of the body's defenses systems: hemostasis and inflammation. Hemostasis is a physiological process that is activated in response to the injury to stop the bleeding. Platelets are the key component of hemostasis, as they catalyze the formation of thrombin by the cascade of the plasmatic coagulation factors.<sup>47</sup>

Inflammation is a protective response of the body to infection and injuries. Its purpose is to localize and eliminate the injurious agent and to remove damaged tissue components, paving the way to the regenerative stages of the wound-healing cascade. It can be viewed as a combination of cellular reactions involving the activation of various leukocytes, and acellular reactions of the complement cascade.<sup>48,49</sup> Platelets are the first cellular structures to arrive at the injury site, and they prime and orchestrate the subsequent inflammatory and wound healing reactions. The connection between hemostatic and inflammatory responses is schematically depicted in Figure 1-2.

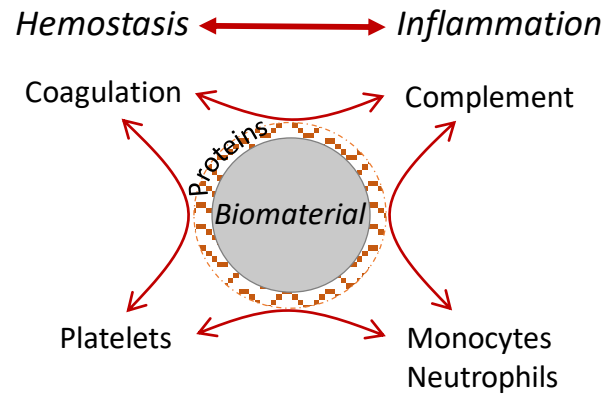


Figure 1-2. Overview of blood-material interactions showing the components of the hemostatic and inflammatory systems relevant to thrombotic complications. Adapted from Gorbet et al.<sup>45</sup>

Hemostatic and inflammatory systems are highly interconnected both in physiological and pathological conditions. However, under physiological condition the activation and the interplay of these systems lead to the wound healing, while in the pathological condition of blood-material contact lead to thrombotic complications.<sup>45</sup>

I now describe in detail the components of the hemostatic and inflammatory reactions.

## 1.5 Hemostasis

Hemostasis is a defense mechanism to stop the bleeding after the injury of the vessel wall. It consists of three major phases: 1) vascular spasm or vasoconstriction; 2) platelet activation and aggregation resulting in the formation of a platelet plug and amplification of the coagulation (primary hemostasis); 3) blood coagulation with the formation of the fibrin clot that seals the wound and stops the bleeding (secondary hemostasis).<sup>50</sup> Fibrin clot also serves as the natural tissue-regeneration scaffold for the subsequent wound healing reactions.

### 1.5.1 Vascular spasm

The vascular spasm, occurring immediately after the injury, is the reduction of the vessel lumen to limit the blood loss. It is produced by a contraction of the vessel wall and the smooth muscle cells as an immediate reflex to the injury.<sup>51</sup> Serotonin and thromboxane-A<sub>2</sub> (TXA<sub>2</sub>), released by the platelets activated at the injury site, contributes to this reaction.<sup>52</sup>

## 1.5.2 Platelets

Platelets are small anuclear cell fragments circulating in the blood. They originate from megakaryocytes in the bone marrow.<sup>53</sup> Platelets circulate at a concentration ranging from 150 to  $400 \times 10^6$  platelets/ml with a life span of 7-10 days.<sup>50</sup> They are the main players in the hemostatic process.

### 1.5.2.1 Platelet Structure

Platelets are the smallest elements circulating in the blood, averaging only 2 to 5  $\mu\text{m}$  in diameter. They have a discoid shape in their resting state. At high magnification in the low-voltage high-resolution scanning electron microscope the plasma membrane has a rugose appearance, resembling the surface of the brain (Figure 1-3 A). The tiny folds of the so-called open canalicular system (OCS) provide additional membrane surface needed when platelets spread and expand upon activation (Figure 1-3B).<sup>54</sup> Platelet membrane supports numerous receptors that respond to a very diverse variety of stimuli regulating the activation process.<sup>55</sup>

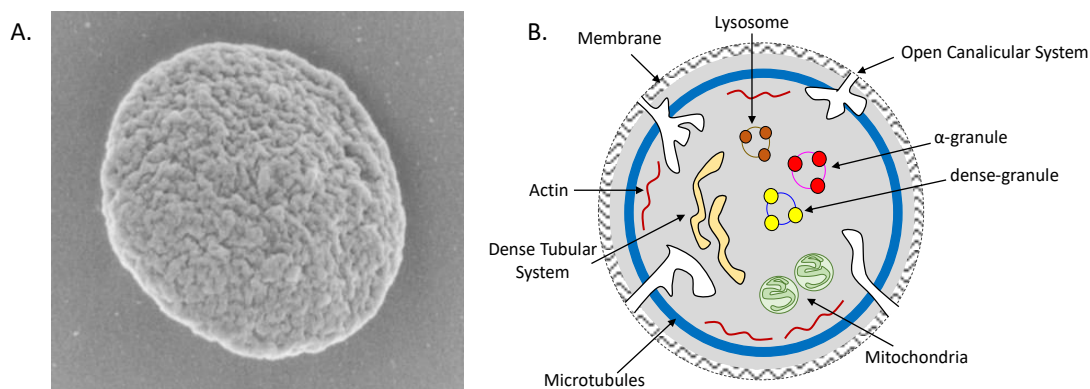


Figure 1-3. Platelet Structure. A. Discoid platelet photographed in low-voltage high-resolution scanning electron microscope. The platelet membrane resembles the surface of the brain. B. Figure summarizing the ultrastructure of a discoid platelet.

Microtubules and actin, underlying the membrane, support membrane rearrangement during activation.<sup>56</sup>

Platelet cytoplasm contains three major types of intracellular granules:  $\alpha$ -granules, dense-granules, and lysosomes.  $\alpha$ -granules are the most numerous platelet granules, ranging from 40 to 80 granules per platelet. They contain up to 300 different active biomolecules with different functions (for example pro-and anti-inflammatory molecules, pro-and anti-

angiogenic molecules, cytokines, growth factors). Dense-granules are less abundant than  $\alpha$ -granules.<sup>56,57</sup> They contain ions and small molecules such as ADP, calcium, and serotonin. Lysosomes (no more than three per platelet) contain degrading enzymes such as glycohydrolases.<sup>58</sup> Platelet activation triggers the release of the granule content and the expression of the granule-specific glycoproteins on the platelet surface. One of the most important glycoproteins is CD62P (P-selectin), a commonly used marker of platelet activation that mediates platelet-leukocyte and platelet-endothelium interactions.<sup>59,60</sup>

Other elements embedded in the cytoplasm include mitochondria and the dense tubular system DTS (Figure 1-3 B). DTS originates from the rough endoplasmic reticulum in the parent megakaryocyte. It functions as one of the major calcium storage pool, and participates in platelet activation by releasing calcium in a signal-dependent manner.<sup>56,61</sup>

### 1.5.2.2 Platelet in Hemostasis

Platelets play a key role in hemostasis. They circulate in a resting state in close proximity to the vessel wall.<sup>62</sup> The healthy endothelium provides a natural barrier to their activation by releasing inhibitor mediators such as nitric oxide (NO) and prostaglandin I<sub>2</sub> (PGI<sub>2</sub>).<sup>63</sup> Following vascular injury they quickly adhere, activate, and aggregate forming the platelet plug. Most importantly, activated platelets catalyze thrombin formation at their surface.<sup>64</sup>

#### *Platelet adhesion*

Vascular injury cause the disruption of the vascular wall, with the consequent exposure of the sub-endothelial matrix proteins—such as collagen, fibronectin and laminin—to the circulating blood components.<sup>63</sup>

Plasmatic von Willebrand factor (vWF), normally circulating in an inactive globular conformation, binds to the exposed collagen, changes conformation, and becomes competent to bind the platelet receptor glycoprotein (GP) Ib-IX-V. This binding initiates platelet tethering to the site of vascular injury.<sup>65</sup> Following the tethering, platelets adhere stably to the vWF and collagen via GPIV and GPIa/IIa binding.<sup>66</sup>

## *Platelet activation*

Platelet activation is initiated by their adhesion to the sub-endothelial proteins, as well as by soluble agonists. The most potent agonist is thrombin; other important agonists include ADP and TXA<sub>2</sub>, secreted or produced by the activated platelets themselves. Stimulation of the platelet signaling pathways by the interaction of agonists with platelet receptors leads to morphological and biochemical changes—such as spreading, exposure of phosphatidylserine (PS), activation of the integrin GPIIb/IIIa, production of TXA<sub>2</sub> and exocytosis of  $\alpha$ - and dense-granules.<sup>67</sup> These are schematically shown in Figure 1-4. Exposed PS serves as the assembly site for the plasmatic coagulation cascade proteins, leading to thrombin generation at the platelet surface. Activated integrin GPIIb/IIIa binds fibrinogen and/or plasmatic fibrin, cross-linking the platelets during the platelet plug formation.<sup>66,68</sup> TXA<sub>2</sub> and ADP (the latter comes from the dense granules), together with thrombin, activate more platelets through the autocatalytic feedback loops, amplifying hemostatic responses.<sup>69</sup> Thrombin activates protease activated receptor 1 and 4 (PAR1 and PAR4) on the platelet membrane by proteolytic cleavage of the N-terminal domain. The N-terminal peptide that is released in turn binds PAR1 and PAR4 initiating multiple signaling cascade via G-proteins.<sup>70</sup> ADP, released from dense-granules, binds its receptor P2Y<sub>1</sub> and P2Y<sub>12</sub> inducing further platelet activation and secretion events.<sup>71</sup> TXA<sub>2</sub> is produced by Cyclooxygenase (COX) mediated conversion of arachidonic acid (stored as phospholipid in the plasma membrane). TXA<sub>2</sub> binds to its receptors TP- $\alpha$  and TP- $\beta$  on platelet membrane, amplifying the activation process and GPIIb/IIIa inside-out signaling, which in turn recruits more platelets for the aggregation.<sup>72</sup> These autocatalytic feedback loops serve as the targets for antiplatelet therapy drugs. Thus, the most common antiplatelet agent, aspirin, inhibits the biosynthesis of TXA<sub>2</sub> by the platelets. In particular, aspirin inhibits the enzyme responsible for the conversion of Arachidonic acid in TXA<sub>2</sub>.<sup>73</sup> Another effective oral antiplatelet agent for long-term use, clopidogrel, blocks the action of ADP on the P2Y<sub>12</sub> receptor. Another type of antiplatelet agent is abciximab, a monoclonal antibody. Abciximab inhibits platelet aggregation through blockage of GPIIb/IIIa.<sup>74</sup> It is used intravenously or intra-arterially during cardiac interventions, but is too potent for long term use.<sup>71</sup> The combination of aspirin and clopidogrel forms the most effective antiplatelet regimen to date, DAPT used to manage patients with stents and other implants as described above in section 1.8.<sup>75</sup>

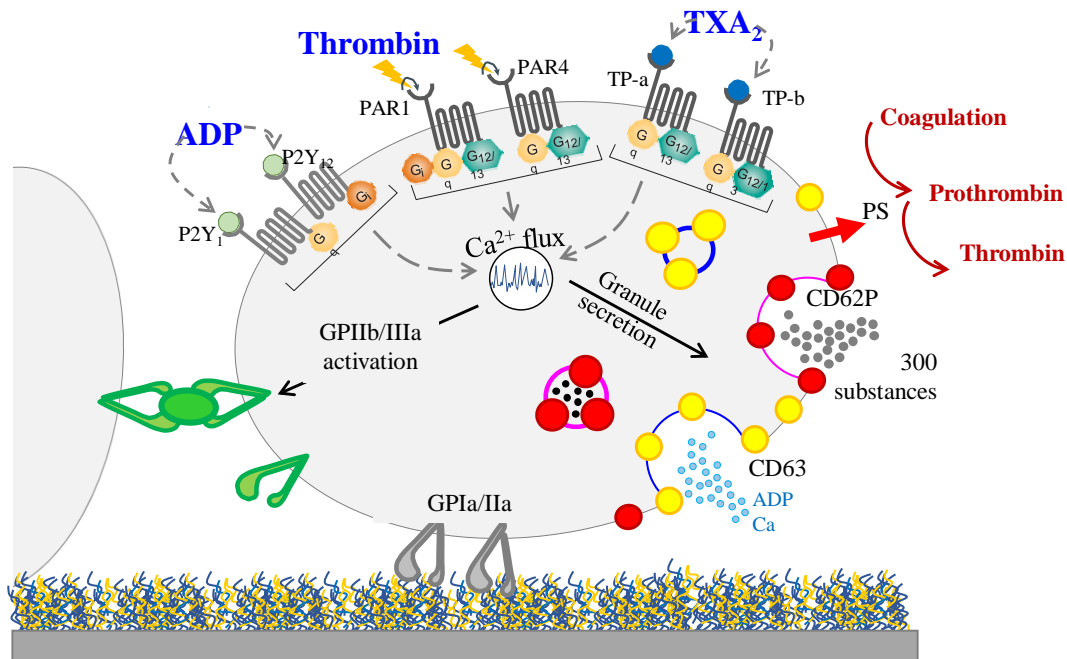


Figure 1-4. Platelet activation. Schematic representation of the major events characterizing platelet activation. Common platelet agonists (soluble: ADP, thrombin, TXA<sub>2</sub>; extracellular matrix proteins: collagen and collagen-bound von Willebrand factor) are indicated in blue. Soluble agonists bind to the G-protein receptors (black) that activate various platelet responses through the associated signaling pathways involving intracellular calcium rise. Matrix proteins bind to the integrin-type receptors (gray, GPIa/IIa; green, GPIIb/IIIa). Responses include PS expression, granule secretion, GPIIb/IIIa activation, and thromboxane synthesis. Note that ADP and TXA<sub>2</sub> are both released during activation and serve as platelet agonists, forming autocatalytic feedback loops amplifying platelet activation. PS catalyzes thrombin formation. The signaling through GPIIb/IIIa is bi-directional: it can be activated by soluble agonists (inside-out), making it competent to bind fibrinogen and cross-linking the platelets, as well as by binding to the fibrin or von Willbrand factor in the clot or injury site (outside-in), activating other platelet responses.

All these events are associated with an increase in the concentration of cytosolic calcium ( $[Ca^{2+}]_i$ ) triggered by the agonist-receptor interaction. The source of  $Ca^{2+}$  in platelet activation is both intracellular (DTS described above) and extracellular.<sup>76</sup> Intracellular  $Ca^{2+}$  release from the DTS involves the activation of phospholipase C (PLC), which hydrolyzes phosphatidylinositol 4,5-bisphosphate ( $PIP_2$ ) to inositol-1,4,5-trisphosphate ( $IP_3$ ) and 1,2-diacyl-glycerol (DAG).  $IP_3$  in turns triggers  $Ca^{2+}$  release by interacting with its receptors ( $IP_3R$ ) on the DTS, which themselves are  $Ca^{2+}$  permeable ion channels. The drop in the DTS  $Ca^{2+}$  is sensed by the stromal interaction molecule (STIM1) which triggers the extracellular  $Ca^{2+}$  influx into the cytoplasm through the channel Orai1. This mechanism is called SOCE (store-operated calcium entry) and it is reviewed by Varga-Szabo et al.<sup>77</sup>

The content of platelet granules deserves further comment. Dense granules contain small molecules—such as serotonin, ADP, ATP,  $Ca^{2+}$ .  $\alpha$ -granules contain proteins, growth factors,

cytokines, coagulation cascade proteins, etc. Altogether, some 300 molecules have been identified in the  $\alpha$ -granules. They include hemostatic factors (fibrinogen, Factor V, vWF, GPIIb/IIIa), growth factors (Stromal Derived Growth Factor 1 $\alpha$  /SDF1 $\alpha$ , Platelet-Derived Growth Factor/PDGF), proteases (Matrix Metalloproteinase 9/MMP9, Matrix Metalloproteinase 2/MMP2), pro-angiogenic factors (angiogenin, Vascular Endothelial Growth Factor/VEGF), anti-angiogenic factors (Platelet Factor-4/PF4, angiostatin), pro-inflammatory factors (e.g. P-selectin, RANTES, Interleukin 8/IL-8 and Interleukin 2/IL-2), and anti-inflammatory factors (e.g. IL4, Hepatocyte Growth Factor/HGF, Tumor Necrosis Factor- $\alpha$ /TNF- $\alpha$ ). These molecules control and regulate the wound microenvironment following the injury.<sup>78-80</sup> Many of them have contradictory functions, for example pro-and anti- angiogenic factors such as VEGF and angiostatin, pro- and anti- inflammatory factors such as interleukins and HGF.

### *Platelet aggregation*

Activated platelets form stable aggregates through the binding of the integrin GPIIb/IIIa to fibrinogen, fibrin and vWF. It is notable that following the engagement of ligands, GPIIb/IIIa can deliver outside-in signals, which further enhance platelet activation, cytoskeleton rearrangement, and granule secretion. These signal events facilitate the formation of the platelet plug.<sup>72,81</sup>

### *1.5.3 Coagulation*

The formation of the clot that stops the bleeding—coagulation—involves a series of enzymatic reactions in which a zymogen (inactive enzyme) present in the blood plasma becomes activated through cleavage and catalyzes the activation of the following component of the cascade.<sup>82</sup> Figure 1-5 schematically depicts the coagulation cascade. Coagulation is initiated by the damage to the vascular bed with the exposure of Tissue Factor (TF) on the damaged cells. TF binds FVII, which activates to VIIa to form extrinsic tenase, TF/FVIIa. The latter converts FX in to FXa, a key reaction needed to form the prothrombinase complex for catalyzing thrombin formation from prothrombin. Tenase complex consists of FXa and FVa, and is formed on the PS exposed at the activated platelet surface. Vitamin K and calcium serve as co-factors. TF also activates platelets.

Once formed, thrombin amplifies, propagates and sustains the coagulant response by further activating factors V, VIII, and XI. The FVIIIa that is formed assembles into the intrinsic tenase complex together with FIXa on the platelet surface. Thrombin also cleaves fibrinogen and FXIII to form the insoluble cross-linked fibrin clot.

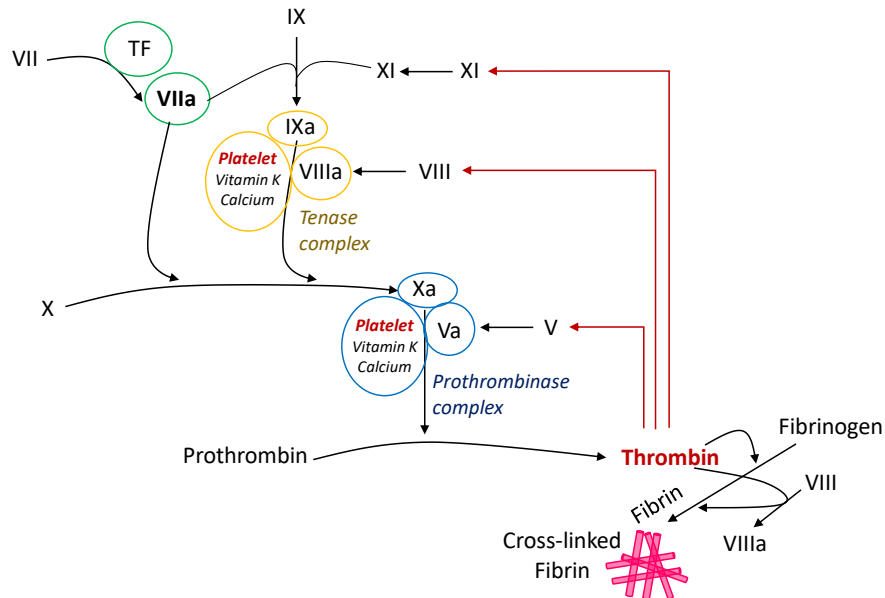


Figure 1-5. Blood Coagulation Cascade

Other initiation reactions, possibly relevant to some biomaterials, include prekallikrein, high molecular weight kininogen/HMWK, and FXII of the contact activation pathway are not shown in Figure 1-5. *In vivo* they are not involved in the initiation of coagulation, because patients with deficiency in these proteins do not have bleeding disorders.<sup>56</sup> Their physiological role is not known.<sup>45</sup>

Activated platelets are directly involved in the coagulation cascade in several ways. Firstly, the enzymatic reactions leading to the formation of thrombin are catalyzed by PS exposed on the surface of the activated platelets. Secondly, activated platelets release from their intracellular granules blood coagulation factors V, factor XI, fibrinogen and factor XIII (that combine with the pool of plasmatic coagulation proteins). If platelets are deficient in these factors, patients suffer bleeding disorders.<sup>83</sup> Third, activated platelets release TXA<sub>2</sub>, which is a vasoconstrictor.<sup>52</sup> They also release the trace amounts of thrombin needed for the initial activation of FVII on the TF-FVII complex.

The process of coagulation is controlled and restricted to the site of vascular injury by natural anticoagulants. These inhibitors of coagulation are: anti-thrombin (AT), the protein C and protein S, and the TF pathway inhibitor system (TFPI). Dissolution of blood clots (fibrinolysis) is regulated by the plasminogen–plasmin system. This system, activated by tissue plasminogen activator (t-PA), breaks down fibrin and controls fibrin polymerization.<sup>84</sup>

## 1.6 Inflammation

Inflammatory response entails the activation of cellular (leukocytes) and acellular (complement) components. It defends the organism against damage from external factors, both biological (pathogens) and non-biological. Under normal physiological conditions, inflammation leads to wound healing and regeneration of functional tissue. Acute inflammation occurs over the period of a few weeks, but under pathological conditions it can turn chronic and persist indefinitely.

### *1.6.1 Complement*

The complement system is a sequential cascade of more than twenty plasmatic proteins. Similar to the coagulation cascade, each factor catalyzes the activation of the subsequent factor. These steps culminate in the assembly of a membrane attack complex (MAC). Its function is to destroy the invading pathogen by lysis. Soluble components released as a part of the complement cascade reactions activate platelets and leukocytes, participating in the overall inflammatory cascade.<sup>49</sup> (Figure 1-6).

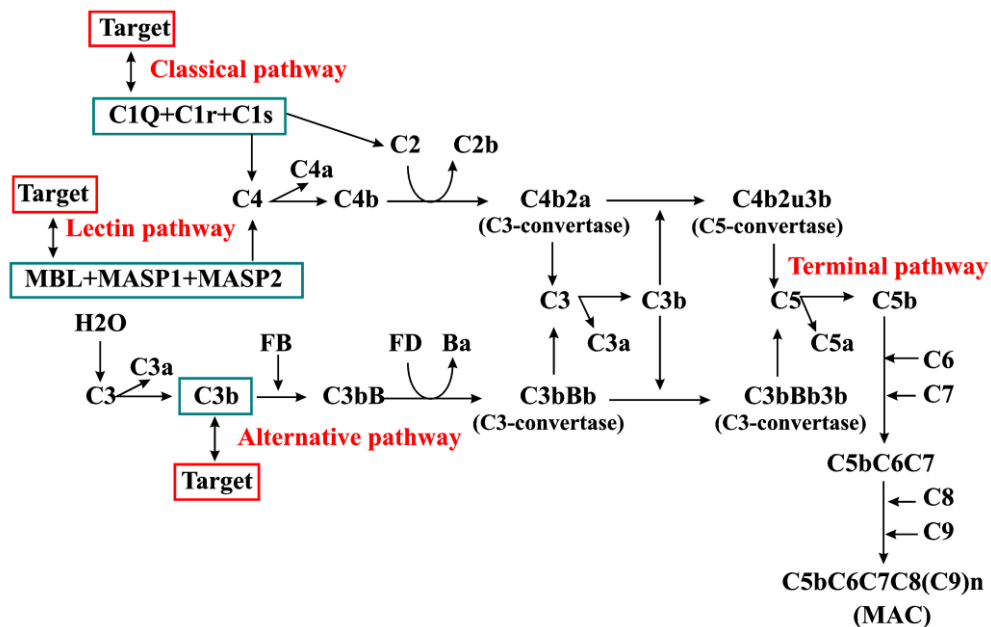


Figure 1-6. Complement Cascade.

Activation of complement occurs through the classical, lectin, or alternative pathways. The classical and lectin pathways are homologous, differing only in the initiation. The classical pathway is initiated by antigen-antibody complex, while the lectin pathway by mannose-binding lectin (MBL) binding to carbohydrates on microorganisms. The alternative pathway is initiated by any foreign elements—such as fungal, bacteria, lipopolysaccharides (LPSs) or biomaterials surfaces<sup>45</sup>. The three pathways merge at the formation of C5 convertase that catalyzes the assembly of the MAC.

In the absence of lipid membranes susceptible to the attack, MAC is inactivated by the S-protein (vitronectin) to form the soluble sC5b-9 complex.<sup>85</sup> This occurs when complement is activated by biomaterials, and sC5b-9 levels are used to measure complement activation.<sup>45</sup>

### 1.6.2 Leukocytes

Circulating leukocytes comprise neutrophils, monocytes, lymphocytes, basophils and eosinophils. Neutrophils and monocytes are the major players in the initiation and maintenance of the inflammation. Neutrophils circulate at a concentration of  $3-5 \times 10^6$  cells/ml, while monocytes at a concentration of  $0.2-1 \times 10^6$  cells/ml<sup>45</sup>. Under conditions of inflammation they activate, adhere to the endothelial cells (ECs) of the vasculature and migrate to the injured site. At the injury site, monocytes undergo to maturation and differentiate in macrophages. The activation of neutrophils and monocytes entails several

responses: synthesis and expression of TF, increased capacity to adhere to endothelium and other surfaces thanks to the upregulation of CD11b and the shedding of L-selectin.<sup>86</sup> Neutrophil activation results in the release of inflammatory mediators from the intracellular granules (gelatinase, specific and azurophil granules). Important inflammatory mediators are elastase, cathepsin G and lactoferrin, as well cytokines such as IL -1, -6, -8, TNF- $\alpha$ , Granulocyte colony-stimulating factor (G-CSF) and Granulocyte macrophage colony-stimulating factor (GM-CSF). Neutrophils also produce and release arachidonic acid metabolites, such as leukotriene B4 and platelet activating factor (PAF). The released inflammatory mediators are chemoattractant for leukocytes, promote adherence to ECs, and further activate platelets or leukocytes.<sup>87,88</sup>

Neutrophils and monocytes can also release oxidants, such as O<sub>2</sub><sup>-</sup> and H<sub>2</sub>O<sub>2</sub>. This products damaged tissue and activate cells,<sup>89</sup> but they are also powerful enough to erode most biomaterials.

## 1.7 Hemostasis and Inflammation: one system for wound healing and material-induced thrombosis

Hemostasis and inflammation are highly interrelated process that considerably affect each other.

The cross-talk between hemostasis and inflammation occurs at level of all components of the two systems: platelets, plasmatic coagulation, leukocytes, and complement.

Platelets occupy a central role in the relationship between hemostasis and inflammation. Upon activation, platelets release from the intracellular granules cytokines, growth factors and numerous pro-inflammatory mediators.<sup>80</sup> In addition, platelets recruit monocytes and neutrophils to the site of the injury by forming platelet-leukocyte aggregates. The aggregate formation is mediated by P-selectin on the activated platelets and its counter-receptor on leukocytes (P-selectin Glycoprotein Ligand-1, PSGL-1).<sup>90</sup> Also, cellular interaction via P-selectin markedly enhances the production of pro-inflammatory cytokines and chemokines in neutrophils and monocytes, increases the expression of adhesion molecules (CD11b) and TF on both leukocytes and ECs.<sup>91</sup>

In turn, platelet activation is enhanced by the complement factors. Incorporation of the terminal complement C5b-9 complex into the cell membrane activates platelets and results in

the exposure of PS, thereby enhancing the pro-coagulant activity of platelets, and granule secretion from the cytoplasm of platelets.<sup>92</sup> Binding of C1q to its receptor on the surface of platelets induces the expression of P-selectin.<sup>93</sup> The complement factors (C3a, C4a and C5b) also induce the activation of leukocytes and augment the expression of TF, which is the key initiator of the coagulation cascade (Figure 1-5). On the other hand, thrombin produced in the coagulation cascade induces leukocyte activation through the PAR-receptors expressed on the leukocyte surface.<sup>94</sup> The thrombin-mediated activation of leukocytes leads to increased production of inflammatory mediators and increased leukocytes adhesion and chemotaxis. Thrombin is also involved in the activation of C3, C5 and C6 in the complement cascade.<sup>45</sup> Finally, the clot scaffolding made of fibrin recruits activated platelets through GPIIb/IIIa binding, as well as leukocytes through interaction with the active form of the integrin CD11b. Leukocyte binding to fibrin leads to production of chemokines and cytokines and degranulation.<sup>95</sup>

The bidirectional relationship of hemostasis and inflammation is also apparent in the anti-coagulant pathways. All the three major natural anticoagulants (AT, TFPI, Protein C/S) also possess anti-inflammatory properties.<sup>96</sup>

In summary, coagulation, platelets, leukocytes and complement act in concert creating a hemostatic-inflammatory cycle, in which the activated processes promotes the others in a positive feed-back loop (Figure 1-2). Under physiological conditions the close relationship between hemostasis and inflammation leads to the wound healing. In pathological conditions this relationship greatly contributes to the etiology or progression of the disease. This is what happens when blood contacts the artificial device: coagulation, platelets, leukocytes and complement activate and closely interact leading to thrombotic and inflammatory complications.

## **1.8 Pharmacological management of the adverse effects caused by the artificial devices**

Clinicians have learned to manage the complications associated with the artificial devices pharmacologically through APT, ACT, or combination of the two. The breakthrough in the management of artificial devices was the combination of different antiplatelet agents (DAPT).<sup>23,71,97</sup> DAPT considerably reduced the thromboembolic complications associated with

stent implantation, underscoring the importance of platelets in adverse reactions to biomaterials.

DAPT relies on the combination of aspirin and clopidogrel. These two antiplatelet agents have the greatest clinical successes in reducing thromboembolic complications.<sup>23,98</sup> This success could be attributed to the ability of both aspirin and clopidogrel in modulating the amplification of platelet activation. Aspirin, by preventing the generation of TXA<sub>2</sub>, and clopidogrel, by inhibiting the ADP binding to its receptor P2Y<sub>1</sub>, eliminates important feedback loops for the amplification of the activation.<sup>71</sup>

In addition to APT, ACT are used for the prevention of thrombotic complications in a variety of interventions. Heparin and warfarin are the most common anticoagulants. Heparin exerts its action by binding and activating anti-thrombin III, which in turn inactivates thrombin, FXa and FIXa. Intravenous heparin-based ACT is used to prevent thromboembolic complications during CPB and ECMO.<sup>39,99,100</sup> Warfarin is a vitamin K antagonist, important cofactor for the activation of many coagulation factors (prothrombin, FVII, IX, X). Differently from heparin, it is administered orally and it is used for long-term anticoagulation treatments, e.g. after mechanical heart valve replacement or VADs implantation, alone or in combination with APT.<sup>36,101,102</sup>

However, the use of APT and ACT is not free of drawbacks. They are associated with increased risks of hemorrhagic complications. Heparin further causes thrombocytopenia.<sup>71,103</sup>

Balancing between thrombosis and hemorrhagic risks requires complex decisions in terms of drug combinations, dosage and duration, and as well constant monitoring.

## 1.9 Mechanisms of blood activation at the biomaterial surface: the role of adsorbed proteins

In this section, we discuss what is known about the mechanisms, by which biomaterials activate body's defense systems that have been described in the previous sections.

The first event occurring at the blood-material interface is the adsorption of plasma proteins. The adsorption phenomena are thought to be key to the development of the subsequent cellular reactions.<sup>104</sup>

The composition and the conformation of the adsorbed protein layer are considered particularly important in influencing these reactions. For example, the adsorption of

fibrinogen, vWF, vitronectin, coagulation proteins such as FXII and HMWK is favorable in inducing platelet adhesion.<sup>105</sup>

In particular, it has been known for a long time that the amount of fibrinogen was always associated to the platelet adhesion response.<sup>106</sup> However, the group of Latour demonstrated that the conformational changes occurring at the surface are more important mediators of platelet adhesion. The adsorption-induced conformational changes of fibrinogen led to the exposure of platelet binding motif, otherwise hidden in the native state of the circulating protein.<sup>107</sup> This notion, of surface-induced conformational changes, was actually inspired by vWF that undergoes such a conformational change upon adsorption to collagen, to biomaterial surfaces, and in turbulent flow.<sup>108</sup>

Interestingly, a similar unfolding mechanism leading to platelet activation was recently found in albumin,<sup>109</sup> even though this protein is usually considered passivating and unable to induce platelet adhesion due to the lack of binding motif in its sequence.<sup>110</sup>

Albumin is the main protein constituent of plasma (40 mg/ml). These conformational changes were found to be surface-specific (e.g., dependent on the chemical nature of the surfaces studied), and they occurred in a time-dependent manner.

However, despite several studies only partial data on adsorbed protein profiles on different surfaces have been obtained.<sup>110</sup> It is important to remember that blood contains several hundred of different proteins and that the adsorption phenomena are complex and time-dependent. The phenomenon known as Vroman effect describes how the layer composition evolves with time, such that the highest mobility proteins are adsorbed earlier (seconds) and are displaced later (minutes) by proteins with higher surface affinity. The classic Vroman effect example is the initial adsorption of albumin and fibrinogen, subsequently replaced by the coagulation protein HMWK or FXII.<sup>111,112</sup>

Finally, the dynamics of protein adsorption is also related to the physicochemical properties of the surface.<sup>113</sup> For example, there are differences between hydrophobic and hydrophilic surfaces. Fibrinogen retention is greater on hydrophobic surfaces than on the hydrophilic ones. Some materials sequester complement factor C3b and may cause less activation of the plasmatic coagulation by the complement system.<sup>114</sup> Dynamic Vroman effects are seen mainly for hydrophilic surfaces on which the proteins are less tightly bound than on hydrophobic ones.<sup>110</sup>

In other words, the composition of the adsorbed protein layer, as well as the conformation of the proteins in that layer, are important in the interaction between surfaces of artificial implants and platelets. Both evolve with time and depend on the surface chemistry of the material. However, despite many years of research, the detailed mechanisms of pro-coagulatory and pro-inflammatory events upon blood contact with artificial surfaces are only poorly understood. If on one hand the basic mechanisms of those interaction have to be investigated, on the other hand a systematic evaluation and comparison between biomaterials still makes sense, in order to predict the performance *in vivo*.

## 1.10 Failed Attempts to Find Hemocompatible Materials

We saw above that adverse reactions to biomaterials begin with the absorption of proteins to the biomaterial surface. Therefore, the main approach of the past 70 years of research to developing hemocompatible materials was to reduce protein adsorption and cell adhesion; in other words, it was to make the materials “inert”. In many hemocompatibility tests, resistance to protein adsorption and platelet adhesion was used as a marker in lieu of hemocompatibility.<sup>110,115</sup>

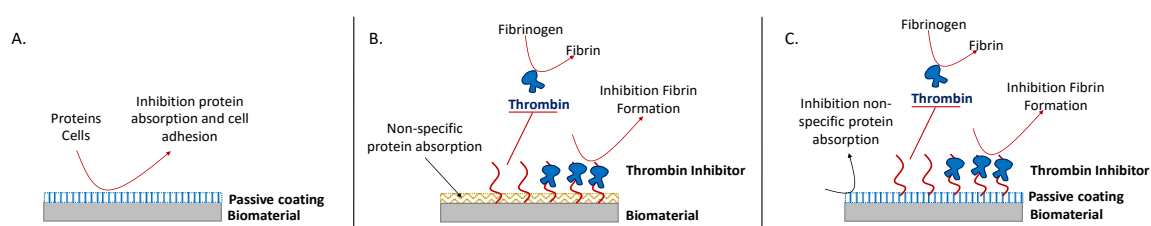


Figure 1-7. Approaches to developing hemocompatible materials. A. Passivating coatings. B. Immobilization of bioactive molecules for the inhibition of thrombin. C. Bifunctional surface: the passivating coating reduces the non-specific protein absorption; the immobilized bioactive molecule promotes specific reactions with thrombin modulating coagulation.

This strategy typically entailed the modification of the material surface with passivating coatings -such as Polyethylene Glycol (PEG) or phosphorylcholine (PC) coatings- in order to weaken and ideally eliminate the interaction of proteins and cells with the surface (Figure 1-7 A). It is now clear, that this approach failed rather spectacularly.

While both PEG and PC exhibit significant reduction in protein adsorption and platelet adhesion *in vitro*,<sup>116-121</sup> this had not translated into *in vivo* success.<sup>122,123</sup> For example, PC polymer-coated stents had no advantages over uncoated stents in porcine or rabbit

angioplasty models.<sup>124</sup> Although they showed reduced protein absorption and platelets adhesion, they had no significant effect in reducing coagulation activation. Indeed, studies showed that coagulation still took place on these so-called “inert” surfaces.<sup>125</sup> The only instance of a passivating coating used in an implant to date is in the Endeavor stent from Medtronic, where PC coating is used together with drug-elution. This stent has been introduced recently and clinical outcomes are not clear.<sup>126</sup> All other coatings used in the clinic to date are of the “active” type, such as heparin modified materials for the CPB, ECMO, and dialysis circuits (Figure 1-7 B).<sup>127</sup> But even these, active-type coatings, did not find application in implant surface modification: when heparin coated implantable artificial devices—such as coronary stents and vascular graft—underwent to clinical trials, they did not show any significant improvement in the long-term thrombosis compared to the uncoated stents.<sup>128 129</sup> Stents and other implants are constructed of materials that are certainly far from “inert” (metals, carbons, other polymers). One can speculate that bioactive coatings are not suitable for long-time blood-material contact, because the enzymatic degradation that occurs over time causes the loss of activity of the coating.

Once again, existing active coatings (heparin-coated CPB, ECMO, and dialysis devices) still rely on soluble heparin injections and other anticoagulants to function. Heparin coating improves the situation, but does not solve the problem.

Modern extensions of the active coating approach focus on bifunctional surface modified with PEG—for protein resistance—and direct thrombin inhibitor (hirudin) – for the specific protein binding (Figure 1-7 C).<sup>130</sup> These are sought for applications in CPB, hemodialysis, ECMO, catheters, and other external medical devices.

The biomaterials currently used in clinical practice include metals and metallic alloys (Titanium, Nitinol, surgical grade-steel, cobalt chromium alloys), polymers (Dacron, Teflon, Polyurethane, Polyethylene, Polytetrafluoroethylene—PTFE), and carbon modifications (diamond-like and pyrolytic).<sup>131,132</sup> All of them, without exception, activate adverse thrombotic and inflammatory responses when they come into contact with the blood. These lead to thrombotic and inflammatory complications that need to be managed with anticoagulant and antiplatelet treatment. Inertness does not equal hemocompatibility, and tests that evaluate protein adsorption or platelet adhesion are poor predictors of hemocompatibility. The question becomes, what has to be tested to evaluate material hemocompatibility, and how can the situation be improved.

## 1.11 Evaluating hemocompatibility: thrombotic and embolic events

The best information we have about the behavior of various materials in blood comes from animal tests. It was shown early on (1970s) by Kusserow and later by Ratner that platelets may not adhere to the material surface, but may become activated by the surface and aggregate in solution, causing emboli that travel downstream from the device and occlude vessels in the lung, heart, brain or kidney.<sup>133,134</sup> Thus, a direct parallel between platelet adhesion and the material hemocompatibility is erroneous. Instead, there is the need to evaluate not only the events occurring at the surface but also the ones occurring in solution, referred to by the thrombotic and embolic potential of the surface, respectively. Indeed, as early as 1972 Kusserow wrote: “*The need for careful evaluation of a given prosthetic device or surface for its embolic propensity is apparent*” (Figure 1-8).

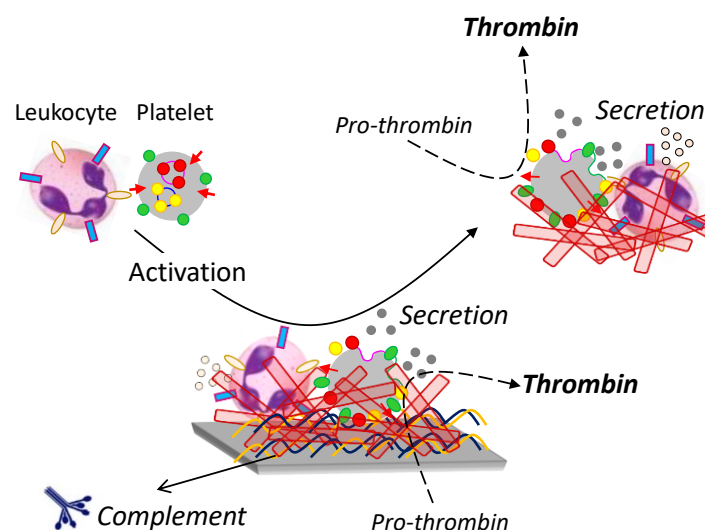


Figure 1-8. Thrombotic and embolic responses to the materials. The nomenclature refers to the early work of Kusserow.<sup>134</sup> Since in this thesis we are concerned not only with thrombotic adverse reactions, but also inflammatory, we refer to these as surface-phase and solution phase thrombotic and inflammatory responses. It is to be understood that “thrombotic” in this case includes thrombotic (surface-phase) and embolic (solution-phase) reactions.

Kusserow studied the thromboembolic properties of ring implants, composed of several materials, placed in the renal artery of dogs (Figure 1-9 A). As well, other investigators tested the thrombotic and embolic events following materials implantation in the vena cava, using canine models, or in baboons having arteriovenous (A-V) shunts (Figure 1-9 B and C).<sup>135,136</sup>

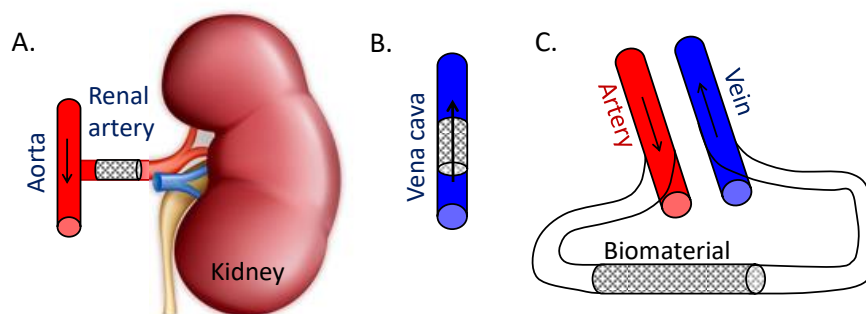


Figure 1-9. In vivo hemocompatibility tests. A. Renal embolus test: the stent made of the material of interest is implanted in the renal artery of the dog, B. Vena cava test: the stent implanted in the superior and/or inferior vena cava of the animal. C. Arteriovenous shunt: the shunt is insert between an artery and a vein of the experiment animal, the test materials is interposed between the inlet and the outlet of the shunt.<sup>134,137,138</sup>

These studies invariably revealed that materials could have thrombotic potential, embolic potential, or both, and that all materials activated hemostasis to some extent. They also revealed that platelet depletion from the fluid phase was the best parameter to assess both the thrombotic and embolic propensities of the implanted materials that could be correlated with *in vitro* results in some cases.<sup>131</sup> However, animal experiments have always been a complicated topic, especially in the case of primates and canines. Economic and ethical issues ultimately led to a reduction of animal experiments or their complete prohibition.<sup>139,140</sup> Translation of the animal test results to the humans is also a complex problem that will not be considered here: blood from different species behaves differently, for example the adhesiveness of dog- and human platelets differs by orders of magnitude; pig and human platelets differ in functional responses, while murine and human platelets express different receptor repertoires.<sup>44,141,142</sup> Finally, there is the lack of a reliable correlation between *in vitro* and in animal studies. All of this drives the need to design reliable *in vitro* tests.

It turns out that despite the past 70 years of hemocompatibility research, there is actually no standard *in vitro* test for evaluating hemocompatibility, and no universal agreement for the parameters that need to be measured to evaluate hemocompatibility. Some standards are being worked out (ISO 10993-Part 4), but this is very much a work in progress.<sup>143</sup> However, some lessons have been learned. Based on the animal experiments, we can surmise that a reliable *in vitro* test has to meet these requirements:

- Thrombin levels should be measured, because thrombotic complications of biomaterials are most severe;

- Platelet counts should be measured, because it is the one parameter that has exhibited some correlation between *in vitro* and *in vivo* results;
- Any other parameter that is measured (e.g., platelet activation, cellular or acellular inflammatory responses) cannot be restricted to surface- or solution-phase reactions. Measurements should either reflect both, or separately measure the two, for the reasons discussed above;
- Of these, platelet activation is particularly important because of their unique position in the hemostatic, inflammatory, and regenerative responses (section 1.7 above).

The next point concerns the measurement conditions under which all these parameters need to be measured so that the results of these measurements are useful. There is a general consensus that the testing should be performed under flow, if nothing else than avoid cell sedimentation.<sup>46,144</sup> The geometry should be circular for mimicking *in vivo* flow conditions and, more likely, for reflecting physiological distribution of cells in the flowing blood with platelets pushed to the periphery. Several models for *in vitro* circulation have been employed. Examples are the Chandler loop system and the rolled-pump closed loop. However, each of them have their drawbacks and complications, and arguments about their physiological relevance continue.<sup>145,146</sup> Perhaps the future is with micro-fluidic systems, which required small blood volumes, are easy to control and to standardize.<sup>46,147,148</sup> The drawback of the micro-fluidic systems is an increased surface area-to-volume ratio. Microfluidic technologies have been widely used to study platelet functions, activation and thrombus formation under flow and at protein-coated surfaces (for simulating the vascular injury).<sup>147,149,150</sup> To my knowledge, microfluidic technologies have been rarely applied to the biomaterial testing.

So-called quasi-static measurement protocols also exist. They are based on systems for blood incubation under static conditions, in which the sedimentation of the blood cells is prevented by agitation. The quasi-static measurements show similar sensitivity in distinguishing between materials of the *in vitro* circulation models.<sup>151</sup>

In general, the idea that only measurements that mimic “physiological conditions” are useful is somewhat dogmatic. It cannot be considered proven, because so far, correlations between *in vitro* measurements and *in vivo* performance have not really been established. Indeed, there are several arguments against the blind “mimicking” approach. Firstly, blood, taken out of the body, will coagulate if left on its own; therefore, none of the *in vitro* situations are physiological.<sup>152</sup> Secondly, all of the currently used *in vitro* tests hemocompatibility tests

struggle with predicting long-term (3 – 5 years) effects from short-term (15 – 90 minute) measurements. This timescale gap actually points to the need for a test that strives away from physiological conditions to be predictive, because a predictive test run under “physiological” conditions would have to run for 3 – 5 years! (The timescale problem is illuminated in the work of Latour et al. already mentioned above, who showed that surface-adsorbed proteins may take months to change conformation<sup>153</sup>). This topic is also discussed in Reviakine et al.<sup>152</sup> Therefore, in my view, the search for adequate in vitro hemocompatibility test has to focus not on attempts to mimic physiological conditions, but on clinical correlations, independently of how they are obtained. In this spirit, Chapters 3 is concerned with the development of a quasi-static whole blood hemocompatibility assay that is based on the principles outlined above, while Chapter 4 is concerned with the development of a platelet-rich-plasma (PrP) based hemocompatibility assay that searches for a parameter displaying maximum sensitivity to the differences between material properties.

## 1.12 The future of implant integration: directing platelet responses towards wound healing

The more fundamental question than how to test material hemocompatibility is related to the desired outcome of the blood-biomaterial interaction. What are the properties of the vascular implant that are needed for it to be hemocompatible? For a long time, it was considered that minimizing thrombotic and inflammatory responses was the goal of material science and modification approaches to synthesizing materials for vascular implants. This is still the prevailing point of view today, despite 70 years of consistent failure. Testing strategies were developed and used accordingly.

The view taken in my group, as well as shaped by my own work presented in Chapters 3 and 4, is that minimizing the initial adverse reactions to biomaterial is not the relevant goal of, or an approach to, the material hemocompatibility. The ultimate goal should be to “hide” the biomaterial from the bloodstream altogether. No other material is more hemocompatible than vascular endothelium, and therefore, after a short healing period, any vascular implant should be covered with it. This idea is very old, but my work represents a radical departure from how it has been approached until now.

Until now, the two strategies to implant endothelialization entailed either “seeding” ECs on the surface of an implant or tissue engineering scaffold ex vivo, or catalyzing the formation of

the endothelium formation *in vivo*.<sup>154,155</sup> The second strategy, entails modification of the implant or scaffold surface with antibodies or peptides able to capture the endothelial progenitor cells (EPCs) from the blood, or with growth factors that stimulate endothelialization.<sup>155,156</sup>

Up to now, neither strategy has been successful. First clinical trials of the EPC capture stents have not shown improvement compared to the drug-eluting stents.<sup>157,158</sup> Their failure of the endothelialization approaches, in my view, is related to the fact that platelets have been missing from the picture.

*In vivo*, platelets are the first cellular elements that interact with the implant. Under physiological conditions platelets orchestrate wound healing reactions, but at the implant surface they cause thrombosis and inflammation. Therefore, I believe that controlling platelet activation is the key to promote the wound healing at the site of the implant (Figure 1-10).

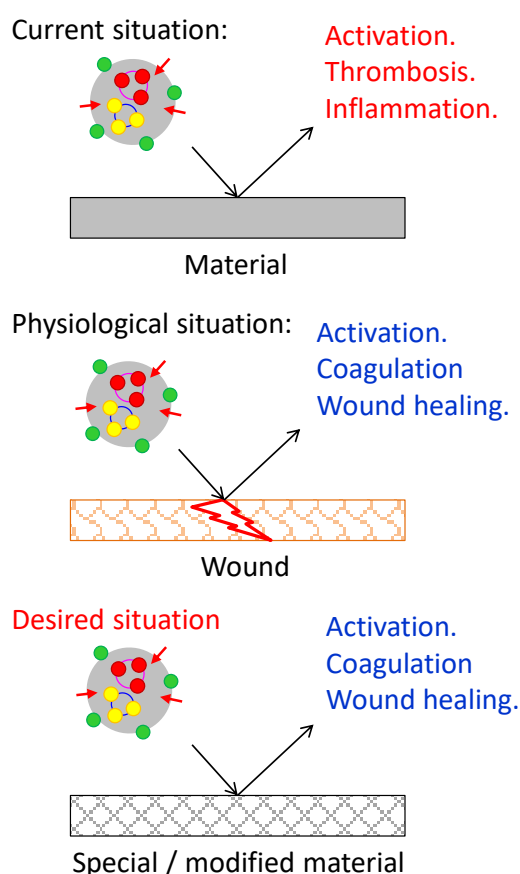


Figure 1-10. Directing platelet activation towards the wound healing.

The question then becomes, how do we control platelet activation to achieve the desired wound healing response? The answer is thought to be related to controlling platelet secretion

responses. Upon activation, platelets release a plethora of molecules to finely orchestrate wound healing. These molecules are stored in the  $\alpha$ -granules of the resting platelets, but are released upon activation. A lot of these factors have contradictory properties and how their release is controlled is not understood. Some of those factors are listed in Table 1-1.

**Pro-angiogenic, vascular remodeling, recruitment, growth and proliferation of ECs and fibroblast**<sup>159 160</sup>

<i>Growth Factors</i>	VEGF, PDGF, fibroblast growth factor (FGF), epidermal growth factor (EGF), HGF, insulin-like growth factor (IGF), connective tissue growth factor (CTGF)
<i>Chemokines, cytokines and others</i>	RANTES, IL-8, angiopoietin, SDF-1, and $\beta$ -thromboglobulin ( $\beta$ -TG), MMP-1, -2, and -9

**Anti-angiogenesis, inhibition of endothelial cell proliferation, interference with pro-angiogenic factors**<sup>78,161</sup>

<i>Glycoprotein, cytokines and others</i>	Thrombospondin-1 (TSP-1), PF4, angiostatin, endostatin, tissue inhibitors of metalloproteinases (TIMPs-1 and -4)
---	--

Table 1-1. Major classes of Platelet  $\alpha$ -granule content and their function. More than 300 factors have been identified by proteomics analysis so far.<sup>162</sup>

It is notable that platelets accumulate at the site of injury very rapidly, much more so than the other circulating blood cells, making platelets the most important source of the wound-healing mediators.<sup>80</sup> For example, VEGF concentrations are elevated 3-fold during the first minutes after plug formation following forearm incision.<sup>163</sup> Therefore, the future of hemocompatibility is not behind minimizing the activation of the defense systems, but in inducing specific activation, in directing platelet responses to the wound healing and implant integration reactions. To achieve this, the triggers controlling their secretion reactions need to be understood and harnessed in the biomaterials. There is evidence in the literature that this approach is viable. Firstly, platelet secretion may be agonist-specific. For example, ADP is a more potent mediator of VEGF and CTGF release from platelet than endostatin.<sup>164-166</sup>

Secondly, PrP is used in a number of therapeutic applications in dental, orthopedic, and plastic surgery where rapid wound healing is required.<sup>160,167</sup> PrP is also used for promoting the proliferation of mesenchymal stem cells (MSCs).<sup>168</sup>

Third, it has been shown by us and others that platelets activate in biomaterial surfaces in different ways: differential expression of GPIIb/IIIa was also reported in response to the interaction with different materials;<sup>131</sup> differential  $\alpha$ -granule secretion in platelets adhering to different surfaces or surfaces modified with different plasma proteins has been reported by several authors under different conditions.<sup>169-172</sup>

Furthermore, several studies of platelet activation in solution report that different stimuli induce platelet subpopulations in term of the expression of PS and GPIIb/IIIa,<sup>173-175</sup> while we reported that such phenomena are observed in surface-adhering platelets.<sup>176</sup>

Altogether, these observations point to the fact that platelet activation and secretion patterns at biomaterial surfaces can in principle be controlled, and that control could lead to beneficial, wound-healing reactions. For this reason, in Chapter 5 I develop and validate an assay for evaluating platelet secretion. Because of the discovery of platelet subpopulations with different activation profiles, the assay is focused on individual platelets approached with a microfluidic technique.

### 1.13 Objectives of the work

It is widely recognized that there is an urgent need for improving the performance of the artificial devices used to treat CVDs. All the artificial materials currently in use induce thrombotic and inflammatory complications that lead to heart attacks and strokes. Platelets play a central role in these complications. Clinicians manage the thrombotic complication therapeutically through anticoagulant and antiplatelet agents. However, their clinical use is accompanied by significant risk of bleeding. Until now, research into blood-material interaction failed in finding a material free from these complications, or devising an *in vitro* test for characterizing material hemocompatibility that could reasonably and rapidly guide the search for such a material. Therefore, **the first objective of this work was** to identify sensitive and robust blood activation parameters for *in vitro* material testing. Two *in vitro* test systems are used for this purpose. First is a whole-blood quasi-static test system, where I evaluate the effectiveness of various *in vitro* measures of blood activation in distinguishing between similar clinically used biomaterials (Ti, CoCr, steel) and examine the underlying activation mechanisms. Blood activation is evaluated using a multiparametric assay I develop that measures solution- and surface-phase reactions contributing to the thrombotic and inflammatory responses. These include thrombin production, platelet consumption and activation, and leukocyte and complement activation. This aspect is described in Chapter 3. Second is a simple biophysical system based on measuring platelet-surface interactions in platelet-rich plasma with the goal of identifying a platelet activation parameter that is most sensitive to differences between materials. This aspect of the work is described in Chapter 4. **The second objective of this work** was to pave the way for the developing future biomaterial integration strategies based on platelet regenerative functions. Based on the notion that platelet secretion is the key to the regenerative functions of the platelets, I develop and validate a single platelet assay for studying platelet secretion. This aspect is described in Chapter 5. Chapter 6 provides the overall conclusions.

## 2. Materials and Methods

### 2.1 Cell Labeling Reagents

PerCPCy5.5-conjugated anti-CD41a, PE-conjugated anti-CD62P, BV450-conjugated anti-CD63, FITC-conjugated anti-CD45, V450-conjugated anti-CD66b, BV605-conjugated anti-CD14, APC-conjugated anti-CD14, BV510-conjugated anti-CD11b, as well as BV605- and Cy5-conjugated phosphatidylserine binding protein Annexin A5, were purchased from BD Biosciences (Heidelberg, Germany).

### 2.2 Other Chemicals

Vacutainers for blood collection containing 0.105 M Sodium Citrate, 170 I.U. Sodium Heparin, or 109 M CTAD (Buffered Sodium Citrate, Theophylline, Adenosine, Dipyridamole) were purchased from BD Biosciences (Heidelberg, Germany). BD Cell Fix and 10X concentrated BD Lysis solution were from BD Biosciences (Heidelberg, Germany). Acid citrate dextrose (ACD), sodium dodecyl sulfate (SDS), calcium chloride hexahydrate  $\geq 99.0\%$ ,  $\alpha$ -D-glucose anhydrous 96%, magnesium chloride anhydrous  $\geq 98.0\%$ , potassium nitrate  $\geq 99\%$ , sodium chloride  $\geq 99.5\%$ , TRAP6 (thrombin receptor activating peptide 6), PMA (phorbol 12-myristoyl acetate) and Calcium Ionophore A23187 (CaloP) were obtained from Sigma-Aldrich (Steinheim, Germany). HEPES (4-(2-hydroxyethyl) piperazin-1-ylethanesulfonic acid), OTS Octadecyltrichlorosilane and APTES: (3-Aminopropyl)trimethoxysilan were purchased from VWR International GmbH (Bruchsal, Germany). PMN-elastase ELISA assay was purchased from Demeditec Diagnostics GmbH (Kiel, Germany), MicroVue complement sC5b-9 Plus ELISA assay from Quidel (San Diego, USA), TAT ELISA assay from BioCat GmbH (Heidelberg, Germany) and  $\beta$ -TG ELISA assay from Diagnostica Stago (Asnieres, France).

### 2.3 Equipment

All of the experiments were performed in a sterile, dust-free environment provided by the sterile laminar flow cabinet (Biomedis<sup>®</sup>, laborservice GmbH & Co.KG, Gießen, Germany). Centrifugations were performed with temperature-controlled Sigma 3-30KHS centrifuge (Sigma Laborzentrifugen GmbH, Osterode am Harz, Germany), blood cell count with ABX

Pentra 60+ (Horiba Medical, Kyoto, Japan). The flow cytometric analysis were performed using anAttune® Acoustic Focusing Cytometer (AB applied biosystems, Foster City, CA, USA) or a Guava® easyCyte™ 8HT flow cytometer (Millipore, Darmstadt, Germany) or a MACSQuant® Analyzer 10 flow cytometer (Miltenyi Biotec, Bergisch Gladbach, Germany). Fluorescence pictures were acquired using an Axio Observer.Z1 inverted fluorescence microscope (Carl Zeiss AG, Oberkochen, Germany), a Leica DM-IRB optical inverted microscope (Leica Microsystem, Stockholm, Sweden) and a home-made scanning laser confocal ThorLabs confocal scanner (ThorLabs, Mölndal, Sweden). Surfaces used in the experiments were cleaned with an UV-Ozone cleaner (Jelight Company Inc., Irvine, CA, USA) and sonication steps were done in an Ultrasonic Cleaning Unit (Elma, Singen, Germany). Samples were incubated at 37°C in an incubating mini shaker (VWR, Darmstadt, Germany).

## 2.4 Incubation Setup

In the thesis different types of cells were used for incubating the blood samples. The type of incubation setup are indicated in Table 2-1.

Incubation setup	Chapter
Shear Channels	3
Teflon cells	4
Metallic screw cells with Teflon insert	4, 5

Table 2-1. Incubation setup types used in the thesis

The shear channels are made of aluminum and coated with the material of interest. They will be described in section 2.7.1. The Teflon cells are circular home-made hollow cells with dimension of 1 cm high and 25 mm wide. The test surface (25 mm glass slide) is mounted in the center of the cell using dental glue. The screw cells consist of titanium rings used to keep a 25 mm test surface and a Teflon insert, separated by a Viton O-ring, sealed securely together.

## 2.5 Buffers

The buffers used throughout the thesis are listed in Table 2-2 together with the chapter in which they were used.

Buffer	Composition	pH	Purpose	Chapter
CITRATE Buffer	100 mM NaCl, 5 mM KCl, 1 mM MgCl <sub>2</sub> , 15 mM citrate, 5 mM Glucose	6.5	Platelet purification	5
Calcium-free HEPES Buffer	145 mM NaCl, 5 mM KCl, 1 mM MgCl <sub>2</sub> , 10 mM HEPES, 5 mM Glucose	7.4	Platelet re-suspension	3,4,5
Calcium-containing HEPES Buffer	145 mM NaCl, 5 mM KCl, 1 mM MgCl <sub>2</sub> , 10 mM HEPES, 2 mM CaCl <sub>2</sub> , 5 mM Glucose	7.4	Platelet re-suspension	5

Table 2-2. Buffers used in this study and the chapters in which they were used.

All buffers were freshly prepared in nano-pure water and autoclaved 24 hrs prior to the experiments. Glucose was added after autoclaving, immediately before use. After the addition of glucose, buffers were filtered through 200 nm sterile syringe filters (Whatman GE Healthcare Life Sciences, Freiburg, Germany).

## 2.6 Blood Collection

Blood collection was organized at Karlsruhe Institute of Technology (KIT), Chalmers University (Sweden) and at Helmholtz Zentrum Geesthacht (HZG, Teltow, Berlin).

At KIT, the blood collection was organized by the KIT medical service. Study protocols were approved by the Ethics commission of Baden-Württemberg (approval #F-2014-077). Informed consent was obtained from all the donors by the KIT medical staff.

At the HGZ was organized according to the review board of the Charité - Universitätsmedizin Berlin (Application number: EA2/018/16).

At Chalmers, the blood collection was organized by the Sahlgrenska Univeritetssjukhuset (Klinisk kemi, Goteborg, Sweden) and was also performed with informed consent according to the appropriate legal and ethical guidelines (approval ID #s15010). In all cases, the donors were healthy volunteers without history of exposure to antiplatelet medication (such as aspirin) or exposure to alcohol in the two weeks prior to collection. Phlebotomy was performed by a trained nurse.

For every experiment, blood was collected by venipuncture with a 21-gauge needle into BD Vacutainer® tubes containing the anticoagulant of choice (Table 2-3).

Anticoagulant	Chapter
170 I.U. Sodium Heparin	3, 4
0.105 M Sodium Citrate	5

Table 2-3. Anticoagulant of choice.

First 2 ml of blood was discarded during the collection to avoid platelet activation by residual thrombin and/or tissue factor. Tubes were pre-warmed to 37 °C prior to collection and stored without agitation at 37 °C until used (< 30 minutes).

## 2.7 Methods for material hemocompatibility testing

Blood-material interactions were evaluated in order to assess the effects of different clinically used materials on blood response. To this purpose a home-made system called shear channels was used to expose the blood to the materials of interest.

### 2.7.1 Shear Channels

The experiments were performed using the shear channels system. The system was developed at KIT, in collaboration with Prof. Grunze. The system consists of two aluminum valves containing a channel (Figure 2-1). The two halves are closed together in a sandwich-structure, embedding the channel. Two ports for filling the channels with blood and withdrawing it are present on one aluminum halves. The ports are tightly closed with the lids equipped with O-rings to prevent evaporation (box on the right in Figure 2-1). The maximal channel volume is 20 ml.



### 2.7.3 Shear Channel cleaning

The cleaning protocol of the coated shear channels involved several sonication steps, using a water-bath Ultrasonic cleaning unit (Elma, Singen, Germany). The assembled systems were sonicated for 10 minutes filled with 2% SDS solution (1X), nano-pure water (2X), ethanol (3X) and again nano-pure water (3X). Between each sonication step the systems were washed under a constant flow of nano-pure water. Excess water was then removed with a stream of filtered nitrogen gas. The channels were disassembled in a sterile laminar flow cabinet and further cleaned for 15 min in a UV-Ozone cleaner (Jelight Company Inc., Irvine, CA, USA) that was pre-heated 30 min prior the use. The UV-Ozone cleaning is effective in removing organic contaminants from the surfaces.<sup>179</sup>

The cleaning protocol was executed the day before each experiment and immediately after each experiment. Cleaned channels were stored under sterile conditions overnight.

### 2.7.4 Shear Channel experiments

Within 15 minutes after blood collection, each of the three shear channels (Ti, CoCr, steel) was filled with 6 ml of blood using a pipette through the filling ports. This was done slowly and in the most gentle way possible as to not activate the blood during the filling stage. In each experiment, only blood from one donor was used.

The shear channels were placed in a shaker horizontally and shaken at 200 rpm at 37°C for 30 min. Blood samples were taken prior (baseline) and after the incubation in the shear channels for flow cytometry, cell count, and ELISA analysis as described below. Blood from the shear channels was withdrawn through the filling ports with a pipette, again, this was done gently to avoid activation.

### 2.7.5 Blood Cell Count

The counts of red blood cell, leukocytes and platelets were measured in an ABX Pentra 60+ cell counter. Blood cell counts were performed immediately—after collection, or after the relevant experimental steps. The blood cell count is presented in Chapter 3.

### 2.7.6 Six color Flow cytometric Assay

Baseline blood and blood-contacting material were sampled for flow cytometric analysis. Sample volume was 50  $\mu$ l. Samples were incubated for 30 min at 37°C with a mix of six antibodies: 2.5  $\mu$ l of PerCPCy5.5-conjugated anti-CD41a was used to identify platelets and 1.25  $\mu$ l of PE-conjugated anti-CD62P to evaluate their activation state; 2.5  $\mu$ l of FITC-conjugated anti-CD45 was used for identification of leukocytes, 2.5  $\mu$ l of V450-conjugated anti-CD66b for identification of neutrophils and 2.5  $\mu$ l of BV605-conjugated (or APC-conjugated) anti-CD14 for identification of monocytes; 2.5  $\mu$ l of BV510-conjugated anti-CD11b was used to evaluate the activation of neutrophils and monocytes. The antibody volumes were chosen after performing titration experiments for each employed antibody. After staining, positive controls were prepared by activating blood with the agonists TRAP6, at a final concentration of 70  $\mu$ M, and PMA at a final concentration of 10  $\mu$ M, for 30 min at 37°C.

Isotype matched-controls were run in parallel to all monoclonal antibodies. Subsequently to agonist stimulation and staining, the blood samples were fixed with BD Cell Fix solution 1X for 45 min, at room temperature in the dark. Afterwards, erythrocytes were lysed using BD FACS lysis solution 1X.

Flow cytometry was performed within 4 hours of the sample preparation. At KIT we used an Attune® Acoustic Focusing Cytometer equipped with a blue laser (488 nm, 20 mW) and a violet laser (405 nm, 50 mW) calibrated before each experiments with the Attune® Performance Tracking Beads. At HZG the measurements were performed on a MACSQuant® Analyzer 10 flow cytometer equipped with a blue laser (488 nm, 30 mW diode pumped solid state), a violet laser (405 nm, 40 mW diode) and a red laser (638 nm, 20 mW diode) routinely calibrated with MACSQuant Calibration Beads. In the assay, an electronic threshold was applied in the forward scattered light (FSC) and in the side scattered light (SSC) channels in order to eliminate very small events such as debris and to display a correct blood picture. FSC is proportional to the cell surface area or size, while SSC is proportional to cell granularity and internal complexity. Correlated measurements of FSC and SSC allowed the differentiation of platelets and different types of leukocytes. For the fluorescence signals, a proper compensation matrix was design on both the Attune and MACSQuant flow cytometers, in order to correct the overlap of one fluorophore's emission into another fluorophore's emission. The compensation matrix was defined using single stained controls for all the antibodies used in the assay.

The samples were acquired at a low flow rate. The acquisition was stopped when 10,000 events positive for the platelet identification marker CD41a were reached. Forward scatter, side scatter, and fluorescence data were collected using all detectors in logarithmic scale.

### 2.7.7 Flow cytometry data analysis

The data were analyzed using the Flowjo software. The strategy of the analysis aimed to evaluate platelet activation and interaction with leukocytes, and differentiate the composition of platelet/leukocyte aggregates.

The antibody binding is presented as frequency of positive events for the antibody staining over the recorded 10,000 events CD41a+. Positive events were defined by drawing an exclusion gate based on the fluorescence histograms of the isotypes. Activated platelets are identified by the expression of the activation marker CD62P on their surface (CD41a+/CD62P+ events). Platelet/leukocyte aggregates are considered as the events positive for both CD41a and CD45 markers (CD41a+/CD45+). Within the platelet/leukocyte aggregates, leukocytes are differentiated in neutrophils expressing CD66b+ (CD41a+/CD45+/CD66b+), and monocytes expressing CD14 (CD41a+/CD45+/CD14b+). The activation of the platelet/leukocyte aggregates was evaluated analyzing the expression of the activation marker CD11b on neutrophils (CD66b+/CD11b+) and monocytes (CD14+/CD11b+), and of CD62P on platelets in the aggregates. Via back-gating the fluorescence signals, the different populations identified in the strategy analysis are depicted in the FSC/SSC plot (scatter plot).

### 2.7.8 ELISA sample preparation and measurements

ELISA samples were prepared from baseline blood and blood-contacting materials for the measurements of the activation of platelets ( $\beta$ -TG secretion); coagulation (thrombin-anti-thrombin complex, TAT), leukocytes (PMN-elastase release), and complement (sC5b-9).

For  $\beta$ -TG evaluation, blood was sampled in tubes containing 109 M CTAD (Buffered Sodium Citrate, Theophylline, Adenosine, Dipyridamole, BD Biosciences, Heidelberg, Germany) and kept in ice 15-60 min. The samples were centrifuged twice for 20 min at 2500xg at 4°C, aliquoted in 100  $\mu$ l samples, shock-frozen in liquid nitrogen and stored at -20°C for further ELISA analysis.

For TAT, PMN-elastase and sC5b-9, the blood was sampled in 0.105 M sodium-citrate tubes and immediately centrifuged for 20 min at 2000xg at room temperature. Plasma from blood

samples was aliquoted in 250  $\mu$ l samples, shock-frozen in liquid nitrogen. Samples for TAT and PMN-elastase were stored at -20°C for further ELISA analysis. Samples for sC5b-9 were stored at -80°C for further ELISA analysis.

ELISA measurements were performed using  $\beta$ -TG ELISA kit (Stago, Germany), Thrombin-Antithrombin Complexes ELISA Kit (AssayMax, Germany), PMN elastase ELISA Kit (Demeditec Diagnostics, Germany) and SC5b-9 Plus ELISA Kit (Quidel, USA) according to manufacturer's specifications.

### 2.7.9 Statistical analysis

The fluorescence data from the flow cytometry are presented as frequency of the CD41a+ events.

The data are presented as arithmetic mean  $\pm$  standard deviation. At KIT 4 different experiments from 1 donor were performed. In HZG, 5 experiments with the blood from 5 donors were run.

Activation and aggregate levels are presented as normalized data by the positive control (blood treated with TRAP6 or PMA) data normalized by the baseline. For the ELISA measurements, the data are presented as raw data and data normalized by the baseline. All the data were then analyzed using paired t-test or unpaired two-sample equal variance t-test to reveal difference between the groups. Statistical significance was defined as  $p < 0.05$ .

## 2.8 Methods for platelet detachment studies

### 2.8.1 Platelet Rich Plasma (PrP) Preparation

PrP was prepared from freshly withdrawn heparin anticoagulated whole blood. PrP was obtained by centrifuging whole blood at 40xg, for 20 min at 37°C. Platelet concentration in PrP was adjusted to a final concentration of  $5 \times 10^4/\mu$ l using Platelet Free Plasma (PfP). PfP was prepared from PrP through a two-step centrifugation. First, a certain volume of PrP was centrifuged for 20 min at 700 xg at 22°C. The supernatant was collected and centrifuged a second time for 15 min at 5000 xg at 22°C. The entire procedure was performed under sterile conditions to avoid contamination. Immediately after preparation, platelet activation in PrP was analyzed by flow cytometry. PrP was then used in the following experiments in the Shear Force Apparatus or in static condition.

## 2.8.2 Blood Cell Count

Blood cells were counted using an ABX Pentro 60+ cell counter. Red Blood Cell, Leukocyte and Platelet count was measured in whole blood prior the PrP preparation. Platelet number was measured in undiluted PrP, in PpP to ascertain the absence of platelets, and finally in the diluted PrP (Table 2-4).

Donors	Whole Blood			PpP			Diluted PrP		
	RBC ( $10^{12}/l$ )	WBC ( $10^9/l$ )	PLT ( $10^9/l$ )	RBC ( $10^{12}/l$ )	WBC ( $10^9/l$ )	PLT ( $10^9/l$ )	RBC ( $10^{12}/l$ )	WBC ( $10^9/l$ )	PLT ( $10^9/l$ )
01	4.51	6.5	254	0	0	0	0	0.3	62
	4.45	8.0	238	0	0	0	0	0.2	66
	4.99	6.0	435	0	0	0	0	0.2	69
02	4.59	7.8	276	0	0	0	0	0.1	55
	5.38	5.2	108	0	0	0	0	0	42
	4.30	7.6	291	0	0	0	0	0.2	45
	4.26	6.7	452	0	0	0	0	0.2	62
03	4.61	8.8	545	0	0	0	0	0	59
04	4.99	9.6	552	0	0	0	0	0.2	77
	4.87	8.9	547	0	0	0	0	0.1	65

Table 2-4. Blood cell count in whole blood, Platelet free Plasma (PpP) and Diluted Platelet rich Plasma (PrP).

## 2.8.3 Analysis for Platelet Activation in PrP by Flow Cytometry

Prior to each experiment, flow cytometry was performed to ensure that platelets in the PrP were minimally activated and properly responded to the agonists. PrP volume used for flow cytometry sample was 25  $\mu$ l. 1.5  $\mu$ l of PerCPCy5.5-conjugated anti-CD41a antibody was used for platelet identification. 1.5  $\mu$ l of PE-conjugated anti-CD62P, 1  $\mu$ l of BV450-conjugated anti-CD63, 1  $\mu$ l of BV605-conjugated phospholipid binding protein Annexin A5 were used to evaluate platelet activation. TRAP6 at the final concentration of 70  $\mu$ M and PMA at the final concentration of 10  $\mu$ M were added to the samples for 30 min at 37°C in order to activate the platelets. After agonist stimulation and staining, PrP was diluted to 2 ml in HEPES Buffer. Isotype-matched controls were run in parallel to all monoclonal antibodies. Forward scatter,

side scatter, and fluorescence data from 10,000 events were collected with all the detectors in the logarithmic mode. Data analysis was performed using Flow Jo software (Tree Star Inc, USA).

#### 2.8.4 Substrate preparation and characterization

For the substrates preparation, 25 #1 mm glass slides (VWR, Darmstadt, Germany) were coated with titanium dioxide ( $\text{TiO}_2$ ), modified with Octadecyltrichlorosilane (OTS), coated with poly[bis(trifluoroethoxy)phosphazene] (PTFEP), or left unmodified.

*TiO<sub>2</sub> Substrate.* 20 nm  $\text{TiO}_2$  coating was deposited by magnetron reactive sputtering as previously described<sup>178</sup> in a Leybold dc-magnetron Z600 sputtering unit at the Paul Scherrer Institute (PSI, Villigen, Switzerland). The coatings were characterized by XPS (X-ray photoelectron spectroscopy) to ascertain their quality and purity. The results are presented in the Appendix.

Prior to each detachment experiment, the unmodified glass and  $\text{TiO}_2$  coated glass surfaces were cleaned for 30 min in the 2% SDS solution that was filtered through 0.2  $\mu\text{m}$  pore diameter syringe filters, washed under a stream of Nano-pure water, and cleaned for 30 min in a UV-Ozone cleaner (pre-heated for 40 min immediately prior).

*OTS Substrate.* Unmodified glass slides were cleaned using Piranha cleaning. Freshly cleaned, dried slides were incubated in solution of 0.1% OTS in Toluene overnight. The substrates were then rinsed with chloroform and dried under a stream of filtered nitrogen gas. The OTS coated surfaces emerged dry from Toluene and were hydrophobic as judged by the water rolling on the slide.

*PTFEP Substrate.* Cleaned glass slides in Piranha solution were pre-treated with APTES. To this end, the glass slides were immersed for 30 min in a solution of 94 ml methanol, 5 ml nano-pure water, 5  $\mu\text{l}$  Acetic Acid concentrate containing 1 ml of APTES. The pre-treated slides were then removed from the solution while rinsing with nano-pure water and dried under a stream of nitrogen. Subsequently, they were heated at 105°C for 1 hour and then cooled to room temperature. They were then immersed in a freshly prepared solution of PTFEP in ethyl acetate (450 mg/10 ml) and incubated overnight. PTFEP coated slides were then rinsed with ethyl acetate and dry under a stream of filtered nitrogen gas. PTFEP coatings were characterized by XPS. OTS and PTFEP coating was performed by Dr. Kwan Cho and Dr. Alexander Welle (IFG, KIT).

### 2.8.5 Shear forces apparatus for analyzing platelet detachment

The shear force apparatus used in these experiments was based on a microfluidic channel assembly previously described in ref. 180. The original system consisted of a polydimethylsiloxane (PDMS) channel sealed by an upper glass slide and the sample substrate on the bottom. For the purposes of this experiment, the fluid cell geometry was inverted so that it could be placed on the stage of an inverted fluorescence microscope (Axio Observer.Z1 equipped with a 37 °C incubator) and observed with a 63x oil-immersion high-numerical aperture objective. To do so, we used our home-made incubation set-up consisting of a screw-together metal housing that pressed a Teflon insert and a substrate glass coverslip together. Sealing was achieved by viton O-rings placed between the glass and the Teflon. A PDMS spacer with a thickness of 200  $\mu\text{m}$  was placed on top of the substrate. The PDMS spacer contained a channel formed by impressing it with a polished micro-machined brass mold to form the channel with dimensions 150  $\mu\text{m}$  high, 1500  $\mu\text{m}$  wide, and 2500  $\mu\text{m}$  long. According to the calculations in ref. 181, the flow regime for the entire experiment can be considered laminar. The spacer was finally sealed with a PDMS top cover containing inlet and outlet fluid flow holes cut in the PDMS cover. This structure is shown in Figure 2-2.

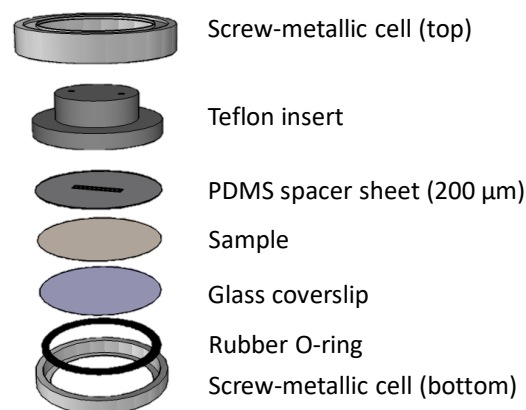


Figure 2-2. Fluid cell design. The PDMS channel is embedded by a PDMS top cover and the substrate (sample). They are kept together in a chamber consisting of two aluminum rings (bottom and top), a rubber O-ring and a blank glass cover slip on which the channels system is placed.

Through a six-way valve the tubing allow the connection of two fluidic cells to a pressurized liquid reservoir filled with HEPES buffer (pH 7.4) on the inlet and a syringe pump (PI, Physics Instruments GmbH & Co. Karlsruhe, Germany) on the outlet. The six-way valve also allows the

injection of the sample in the system and a channel switch enables to control the flow direction. Figure 2-3 describes the shear force apparatus.

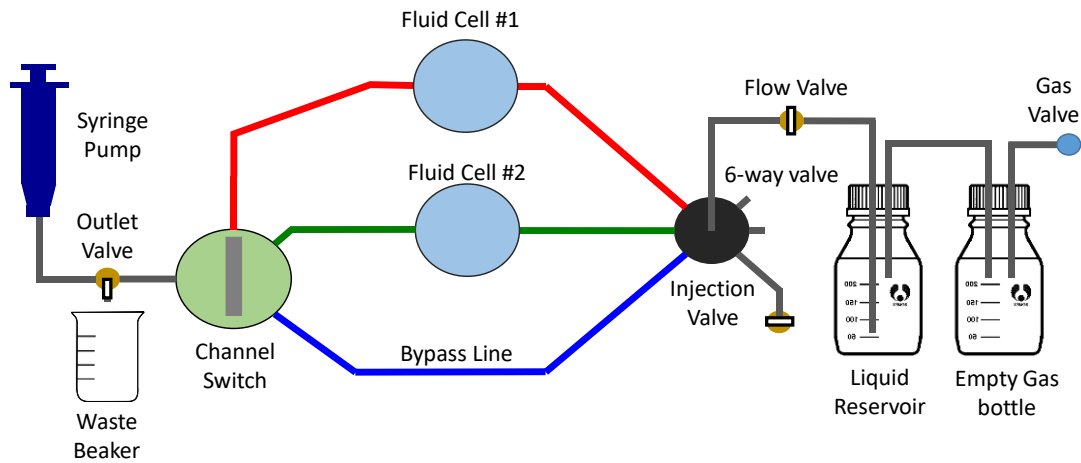


Figure 2-3. Shear Force Apparatus.

Fluid flow is supplied by the liquid reservoir, and the flow rate is regulated by the syringe pump in incremental steps determined by computer software (Mikromove).

Before sample injection the channel was flushed with HEPES buffer (pH 7.4).

### 2.8.6 Detachment studies in the shear forces apparatus

The shear force apparatus was mounted on the stage of the inverted fluorescence microscope. 300  $\mu$ l of PrP were gently injected into the apparatus using a syringe. Unstimulated and agonist-stimulated PrP samples were prepared for the detachment experiments. In the experiments with stimulated PrP, TRAP6 at the final concentration of 70  $\mu$ M was added to PrP for 30 min at 37°C prior the injection.

Stimulated or unstimulated PrP was incubated with the substrates in the shear force apparatus undisturbed for time periods of 10 minutes or 1 hour to allow platelets to adhere. Following the incubation, adhering platelets were immuno-stained with 5  $\mu$ l PerCpCy5.5-conjugated anti-CD41a for platelet identification, and 5  $\mu$ l PE-conjugated anti-CD62P for the evaluation of platelet activation state. The staining was performed by injecting 300  $\mu$ l of antibodies solution in HEPES buffer into the apparatus and incubating for 20 min at 37°C in the dark. Particular care was taken during the injection of the antibody solution to avoid moving or detachment of the platelets from the surface. After the staining, images were

acquired using simultaneously the fluorescence channels for PerCpCy5.5-conjugated anti-CD41a and for PE-conjugated anti-CD62P. Following the acquisition of images, the syringe pump was activated to induce detachment. The pump speed was increased every 5 seconds at predetermined exponential rates ( $\alpha$ ) to generate shear stresses from 0 to  $\sim 5000$  dyn/cm<sup>2</sup> so that the shear stress as function of time ( $\tau(t)$ ) was given by:

$$\tau(t) = \tau_0 e^{\alpha t}$$

Platelet detachment was recorded in a time series format acquired with an interval of 1850 milliseconds, for a total duration of 4 minutes. The interval time was calculated based in the exponential increase of the shear stress, so that a different value of the shear stress corresponds to every image. For platelet detachment, only the fluorescence channels for PerCpCy5.5-conjugated anti-CD41a was used to improve time resolution. Finally after detachment, a fluorescence image was acquired using both the fluorescence channels for the CD41a and CD62P. These experiments are referred to as dynamic experiments.

### 2.8.7 Detachment studies under static condition

Experiments in static condition were performed mounting the test surfaces in the teflon cells. Immediately after the glue has set, the surfaces were washed with HEPES Buffer to reduce the chances of contamination. The volume of PrP was 500  $\mu$ l, incubation periods were of 10 minutes and 1 hour, and TRAP6 (70  $\mu$ M final concentration) and PMA (10  $\mu$ M final concentration) were used to stimulate platelets for 30 min at 37°C prior the incubation.

After incubation, PrP was immunostained using 1  $\mu$ l of PerCpCy5.5-conjugated anti-CD41a and 1  $\mu$ l of PE-conjugated anti-CD62P for 20 min at 37°C in the dark.

To induce the detachment, the samples were washed by adding and withdrawing 250  $\mu$ l of the HEPES Buffer for 10 times. Particular care was taken not to touch the surface with the pipette tip, not to introduce bubbles, and not to dry the sample out.

Considering a volumetric flow rate of 250  $\mu$ l/sec, the shear stress acting on the bottom surface of the center of the well (the point of lowest shear stress) could be approximate to:

$$\tau = 0.526 \text{ dyn/cm}^2$$

Fluorescence images using the fluorescence channels for CD41a and CD62P were acquired prior and after the detachment induced by the washing. The experiments were performed at 37°C in an Axio Observer.Z1 inverted fluorescence microscope.

## 2.8.8 Detachment studies: data analysis and statistics

*Platelet count, area and activation.* Fluorescence images from static and dynamic experiments were analyzed using the Fiji Software. First, the multi-channel images were split into separate channels: one corresponds to the PerCpCy5.5-conjugated anti-CD41a fluorescence and one corresponds to PE-conjugated anti-CD62P.

Platelet were counted manually to separate individual platelets and platelet aggregates. For counting the platelets, the fluorescence channel for PerCpCy5.5-conjugated anti-CD41a was used. Regions of interest (ROIs) around the platelets were drawn using the free hand selection tool. The ROIs were as well used for area calculation. For the evaluation of the activation, the fluorescence intensities of individual platelets in the channel for the PE-conjugated anti-CD62P were calculated. The ROI data in the channels for PerCpCy5.5-conjugated anti-CD41a were used as mask and applied to the CD62P channel. Mean intensity levels of the platelets were extracted from these ROIs to fluorescence intensity per platelets. Background fluorescence was calculated manually drawing ROIs outside of the platelets in the same images. The intensity for each platelet in a given image was then background-subtracted,  $I = I(\text{platelet}) - I(\text{background})$ , and this value was taken to indicate activation level.

*Platelet detachment.* For studying the detachment, platelet were counted in each fluorescence image of the time series as described above. This resulted in the detachment curves in which the fraction of platelets still adhering on the surface was plotted versus the applied shear stress ( $\text{dyn}/\text{cm}^2$ ). The critical shear stress at which 50% of the platelets are detached from the surface is referred in the text as Detachment50 (Det50). Det50 was calculated from the detachment curves for each material.

The statistical significance of the data was then evaluated using paired t-test. Statistical significance was defined as  $p < 0.05$ .

## 2.9 Methods for studying platelets at single platelet level

### 2.9.1 Platelet isolation and purification

Platelets were isolated from sodium-citrate anticoagulated whole blood by a three-step centrifugation. Identical protocols were used at Chalmers University and at KIT. This protocol has been previously used by us in other studies.<sup>171,172,176</sup> The first step involved centrifugation at 40  $\times g$ , for 25 min at 37°C to separate platelet-rich plasma (PRP) from the cells. PRP layer

was collected into a 15 ml falcon tube and incubated with acid-citrate-dextrose (ACD, Sigma, Germany) in a ratio 1 : 6 by volume for 10 min at 37°C. To separate the platelets from the plasma, the samples were then centrifuged the second time for 20 min at 700 ×g at 22°C. Platelets were gently re-suspended in the citrate buffer and centrifuged for 10 min at 700g 22°C to remove the residual proteins. Finally, the pellet of platelets was re-suspended in the HEPES isolation buffer at a platelet concentration of ~ 1 x 10<sup>8</sup> cells per ml.

Blood cell count was performed in whole blood and in the purified platelet suspension (Table 2-5).

Donors	Whole Blood			Adjusted Platelet suspension		
	RBC (10 <sup>12</sup> /l)	WBC (10 <sup>9</sup> /l)	PLT (10 <sup>9</sup> /l)	RBC (10 <sup>12</sup> /l)	WBC (10 <sup>9</sup> /l)	PLT (10 <sup>9</sup> /l)
<b>01</b>	4.20	6.3	315	0	0	122
<b>02</b>	4.01	5.9	359	0	0	105
<b>03</b>	4.43	4.8	202	0	0	145

Table 2-5. Blood cell count in whole blood and in purified platelet suspension.

### 2.9.2 Platelet characterization by flow cytometry

Flow cytometry was performed to analyze the purity, basal activity, and response to agonists, of the purified platelets. At Chalmers, a Guava® easyCyte™ 8HT flow cytometer (Millipore, Darmstadt, Germany) was used. At KIT, the Attune® Acoustic Focusing Cytometer (Life Technologies, Darmstadt, Germany) was used. Sample volume was 25 µl. Platelets were identified by staining samples with PerCPy5.5-conjugated anti-CD41a antibody. TRAP6 at a final concentration of 70 µM and CaloP at a final concentration of 5 µM were used to stimulate the platelets for 30 minutes at 37°C. Activation was evaluated staining with the PE-conjugated anti-CD62P (P-selectin), PECy7-conjugated anti-CD63 antibodies and FITC – annexin A5. For the staining, samples were incubated for 30 min at 37°C in the dark. 1.5 µl of the relevant antibody solution was used. After incubation with the agonist and staining, samples were diluted to 600 µl in the HEPES Ca-containing buffer for the experiments performed at Chalmers, and to 2 ml for the experiments performed at KIT. Isotype-matched controls were run in parallel to all monoclonal antibodies. Forward scatter, side scatter, and fluorescence

data from 10,000 events were collected with all the detectors in the logarithmic mode. Data analysis was performed using Flow Jo software (Tree Star Inc, USA).

### 2.9.3 Substrate preparation and characterization

Surfaces used were 47 mm and 25 mm #1 glass slides (from Willco Wells, Amsterdam, the Netherlands and VWR, Darmstadt, Germany, respectively). 20 nm TiO<sub>2</sub> coating was deposited by magnetron reactive sputtering as previously described<sup>178</sup> either in a FHR MS 150 sputter instrument at the process lab MC2 at Chalmers University, or a Leybold dc-magnetron Z600 sputtering unit at the Paul Scherrer Institute (PSI, Villigen, Switzerland). Prior to each experiment, surfaces were cleaned for 30 min in the 2% SDS solution, filtered through 0.2 μm pore diameter syringe filters. Following, surfaces were washed under a stream of Nano-pure water, and cleaned for 30 min in a UV-Ozone cleaner (pre-heated for 30 min immediately prior). The coatings were characterized by XPS to ascertain their quality and purity.

### 2.9.4 Preparation of surface adhering platelets

Freshly purified platelets were incubated with the freshly cleaned TiO<sub>2</sub> or glass surfaces at a platelet concentration of 10<sup>5</sup> – 10<sup>7</sup> ml<sup>-1</sup> for 10 minutes in a calcium-free HEPES buffer at 37°C. The surface-adherent platelets were gently washed with the same buffer. Care was taken not to touch the surface with the pipette tip, not to introduce bubbles and not to dry the sample out. Subsequently, these samples were either installed in the scanning laser confocal microscope at Chalmers or in an inverted fluorescence microscope at KIT for the microfluidic pipette studies, or used in the analysis of platelet activation directly by adding the relevant antibodies and CaloP to the buffer above the platelets. These latter experiments are referred to as “bulk experiments”.

### 2.9.5 Open volume microfluidic pipette

The open volume microfluidic pipette was a gift from Prof. Aldo Jesorka, Chalmers University (Gothenburg, Sweden). The pipette is an open-volume microfluidic device that operates by generating a hydrodynamically confined, localized perfusion zone at its tip (HCV). It consists of a pen-shaped silicon polymer (poly(dimethyl siloxane), PDMS) body, housing eight integrated wells for injection and collection of solution to and from the adhering cells. Detailed

descriptions of the multifunctional pipette geometry and functionality are in Chapter 5 in section 5.2.

### 2.9.6 Open volume microfluidic pipette experiments and relevant controls

Pipette wells were loaded with 30  $\mu\text{l}$  of Ca-containing HEPES buffer containing the PE-conjugated anti-CD62P antibody, Cy5-conjugated phospholipid binding protein Annexin A5, CaloP solutions. Pressure balance was optimized to achieve an HCV of  $\sim 100 \mu\text{m}$  in diameter. The pipette was mounted on an XYZ manipulator an MH-3 micromanipulator (Narishige, Japan) that was attached to the microscope frame and can be operated independently of the microscope stage, on which the sample is mounted. Prior to each pipette experiment, the adhering platelets were stained with the PerCPCy5.5-conjugated anti-CD41a antibody (5  $\mu\text{l}$ , 30 min, in the dark, at 37°C). The pipette was then approached to the surface. An experimental cycle consisted of exposing the adhering platelets to the staining solution, to the calcium containing buffer alone, then to CaloP, and then again to the staining solution. Images were recorded during the delivery of the staining as well as after. Staining solutions contained 5  $\mu\text{l}$  of anti-CD62P antibody, 5  $\mu\text{l}$  of annexin A5, or both, in a calcium-containing buffer. In a set of experiments, the adhering platelets inside the HCV were exposed to solutions containing increasing concentration of CaloP. 0  $\mu\text{M}$ , 5  $\mu\text{M}$ , 10  $\mu\text{M}$  and 20  $\mu\text{M}$  CaloP and 5  $\mu\text{M}$  of annexin A5 were delivered to the platelets for the evaluation of the effects of CaloP concentration on PS exposure. Different individual platelets or groups of platelets, depending on the number of platelets on the surface, were accessed by translating the microscope sample stage underneath the pipette.

For the pipette and the bulk experiments, two microscopes were used. At Chalmers, a confocal microscope consisting of a Leica DM-IRB optical inverted microscope and a ThorLabs confocal scanner equipped with a 63x oil immersion objective with a NA of 1.25 and filter sets appropriate for the dye wavelength selected. At KIT, we used the Zeiss Observer Z1 inverted fluorescence microscope located in the laboratory of Dr. Cornelia Lee-Thedieck, equipped with the COLIBRY illumination system, a high-pressure Xenon lamp, an appropriate set of filter cubes, an AxioCam camera, and a Pecon environmental chamber with temperature control. All experiments were performed at 37°C.

### 2.9.7 Data analysis

Image analysis. Fluorescence images were analyzed using the Fiji software. First, the multi – channel images were split into separate channels: one corresponding to the aCD41a fluorescence and one corresponding to aCD62P or PS fluorescence. Fluorescence intensities of individual platelets in each channel were calculated as follows.

The channel for CD41a fluorescence was thresholded in order to obtain a binary image. The command “Analysis Particles” was then used to define regions of interest (ROIs) around the platelets. The ROI data from the binary image were used as a mask, applied to the CD62P and PS channels. Mean intensity levels of the platelets were extracted from these ROIs to fluorescence intensity per platelets. Background fluorescence was calculated manually using ROIs outside of the platelets in the same images, while background deriving from the surface itself was calculated in the channel for CD62P or PS in absence of anti-CD62P antibody or A5. The intensity for each platelet in a given image was then background-subtracted,  $I = I(\text{platelet}) - I(\text{background})$ , and this value was indicative of the level of CD62P or PS expression.

The effect of CaloP on the level of marker expression was determined by subtracting fluorescence intensities before and after the addition of CaloP:  $\Delta I = [I(\text{after CaloP}) - I(\text{before CaloP})]$ . The resulting fluorescence intensity differences were finally plotted as histograms displaying the frequencies of cells with given intensities on linear and logarithmic scales.

*Dose – response curves.* The dose – response curves show the effects of CaloP concentration on PS expression. The frequency of PS expressing platelets for each CaloP concentration was calculated for the adhering platelets (single platelets and bulk experiments) and for the platelets in solution.

Adhering platelets: fluorescence intensities of adhering platelets at each CaloP concentration were calculated as described in the section “image analysis” above. The frequency of PS+ platelets was obtained by dividing the number of platelets with  $\Delta(I_a - I_b) > 0$  by the total number of observed platelets.

Platelets in solution: the fluorescence intensities were analyzed by flow cytometry. The frequency of PS expressing platelets was determined using the FlowJo software.

The estimation of the EC50 was done on the sigmoid fitted dose – response curve according the following equation:

$$(A) \quad Y = \frac{\exp(\text{slope} * (X - IP))}{1 + \exp(\text{slope} * (X - IP))} * SP$$

Where IP is the inflection point and SP the saturation point.

## 3. Material Hemocompatibility Testing: Quantifying Blood Responses

### 3.1 Summary

Blood-material interactions limit the performance of the biomedical devices. In the Introduction, I made a case for the need to develop *in vitro* testing strategies for biomaterials and to quantify the blood responses to the materials used in clinical practice. This part of the work addresses this need.

The starting point for our investigation are the observations of Kusserow,<sup>134</sup> who showed that both the reactions that occur at the material surface and in the solution phase have to be tested for to build an accurate, clinically relevant, picture of the blood-biomaterial interactions. He calls these “thrombotic” and “embolic” reactions. Transcending his focus on hemostasis and thrombosis caused by biomaterials, my aim is to develop a multi-parametric *in vitro* test to simultaneously quantify the propensity of materials to activate coagulatory and the inflammatory defense mechanisms. Therefore, I will refer to the two types of reactions as solution-phase and surface-phase instead of embolic and thrombotic, respectively.

In the assay described in this chapter, whole human blood was used. It was exposed to the materials of interest using a custom-made system that we call “shear channels”. The system and its validation are presented in section 3.2. The inner surface of the shear channels was coated with the materials of interests. The surface chemical composition was characterized by XPS and results are presented in section 3.3.

To test the solution- and surface- phase reactions of blood to biomaterials, I used a six-color flow cytometric and ELISA assays, augmented by cell count measurements before and after exposure of blood to the materials of interest. The flowchart in Figure 3-1 illustrates the steps in the test strategy.

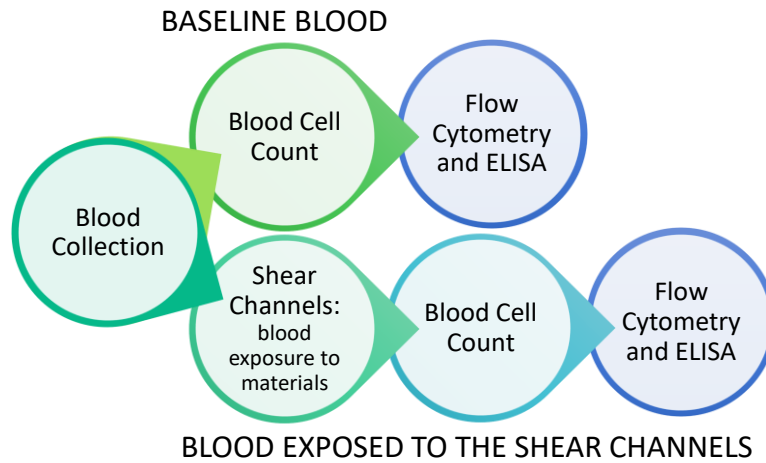


Figure 3-1. Testing strategy. After blood collection, blood prior (baseline) and after the exposure to the shear channels was used for the cell count and the preparation of the flow cytometric and ELISA samples.

The six-color flow cytometric assay was used to quantify platelet activation using CD62P as activation marker (expressed upon  $\alpha$ -granule secretion), platelet-leukocyte interactions using the platelet-specific marker CD41a and the leukocyte-specific marker CD45, and leukocyte activation in the platelet-leukocyte aggregates using the activation marker CD11b before and after exposure of blood to the biomaterials. These events characterize solution-phase reactions of blood to biomaterials. Assay design and results are presented in section 3.6 and 3.7. To characterize both the solution and surface-phase reactions of blood to biomaterials, I used a set of well-established ELISA assays for quantifying thrombin production, platelet activation using  $\beta$ -TG secretion as a marker, neutrophil activation using of PMN-elastase secretion as a marker, and complement activation using the formation of the soluble complement factor sC5b-9 as a marker<sup>147</sup>. The results are presented in section 3.7.

In a first phase, the experiments were conducted at University Hospital of Tubingen (Universitätsklinik Tuebingen), in collaboration with Dr. med. Andreas Straub. These measurements failed. In a second phase, I designed a new flow cytometric assay at KIT and the experiments were performed using this assay with the blood from one donor. Experiments with multiple (five) donors were then conducted at Helmholtz Zentrum Geesthacht (HZG) in Teltow, in collaboration with Prof. Friedrich Jung and Dr. Steffen Braune, because the donor pool at KIT was limited. Throughout the Chapter, I present the results of individual experiments both to show the donor-to-donor variation and to illustrate the effect of ageing of the surface coatings that we encountered during the experiments. The results of each

experiment are presented in the order they were performed so that the effect of ageing of the channel coatings could be examined. Table 3-1 lists the experiments and the relative measured parameters.

<i>Date</i>	27Jan	03Feb	01Apr	06 Apr	14 Jun	21 Jun	23 Jun	28 Jun	29 Jun	02 Aug
	<b>1</b>	<b>2</b>	<b>3</b>	<b>4</b>	<b>5</b>	<b>6</b>	<b>7</b>	<b>8</b>	<b>9</b>	<b>10</b>
<b>TAT</b>	n.m.	n.m.	•	•	•	•	•	•	•	•
<b>b-TG</b>	•	•	•	•	•	•	•	•	•	•
<b>PMN-elastase</b>	n.m.	n.m.	•	•	•	•	•	•	•	•
<b>sC5b9</b>	n.m.	n.m.	•	•	•	•	•	•	•	•
<b>Platelet (CD62P)</b>	•	•	•	•	•	•	•	•	•	•
<b>PLT-LEU</b>	•	•	•	•	•	•	•	•	•	•
<b>PLT-MON</b>	•	•	•	•	n.m.	n.m.	n.m.	•	•	•
<b>PLT-MON (CD11b)</b>	•	•	•	•	n.m.	n.m.	n.m.	•	•	•
<b>PLT-MON (CD62P)</b>	•	•	•	•	n.m.	n.m.	n.m.	•	•	•
<b>PLT-NEU</b>	•	•	•	•	•	•	•	•	•	•
<b>PLT-NEU (CD11b)</b>	•	•	•	•	•	•	•	•	•	•
<b>PLT-NEU (CD62P)</b>	•	•	•	•	•	•	•	•	•	•

Table 3-1. Experiments and measured parameters. “n.m.” stands for “not measured”. PLT: Platelets. MON: monocytes. NEU: neutrophils.

### 3.2 Shear Channel system

To expose blood to the materials of interest, I used the so-called shear channels. This is a system introduced by prof. Grunze, consisting of closed-loop metallic analogues of the Chandler loop system. Figure 3-2 shows the Chandler loop (A) and the shear channel (B) setup. Further details of the shear channel setup can be found in Chapter 2 (Materials and Methods), on page 33.

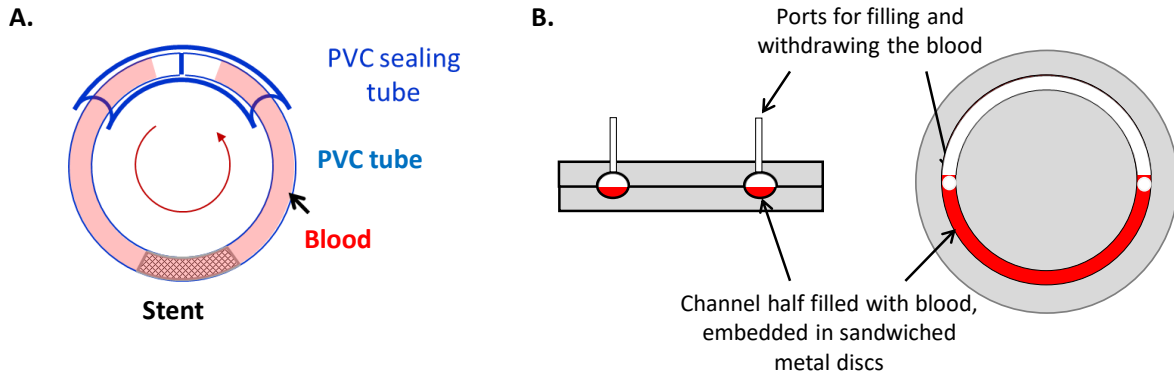


Figure 3-2. Chandler Loop (left) and Shear Channel (right) design. In both cases, experiments are performed at 37 °C.

Briefly, the Chandler Loop system consists of a polyvinyl chloride (PVC) tube in which is inserted the stent material to be tested (Figure 3-2 A). It is partially filled with blood and rotated in a water-bath to mimic physiological or pathological shear stresses. The experiments are performed at 37°C. The Chandler loop system presents several disadvantages, well known in literature.<sup>145</sup> On rotation, the stents in the loop repetitively come into contact with the air/blood interface. This induces artefacts due to the activation of platelets and leukocytes on the protein denatured due to the contact with the air. Also, the blood contact with two materials (PVC and the material of interest) causes artefacts: PVC significantly activates platelets, as shown in Figure 3-3. Here, we measured platelet activation caused by the PVC tube using the expression of the platelet activation marker CD62P by flow cytometry. This result is consistent with the literature.<sup>145</sup>

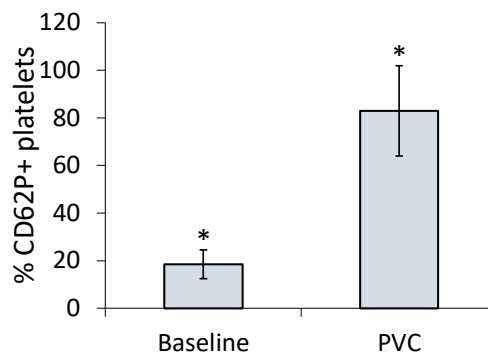


Figure 3-3. Platelet activation: CD62P expression in baseline blood and upon contact with PVC tube. I acquired these data at the laboratory of Prof. H. P. Wendel at the University Hospital Tubingen together with Dr. S. Krajewski and Dr. med. A. Straub.

The shear channel system overcomes these disadvantages. Firstly, here blood contacts only one material. This is possible because the entire inside of the channel is coated with the material of interest. Secondly, I chose not to rotate the shear channels but partially fill them with blood and shake the channels horizontally in a shaker/incubator at 37°C for 30 min. This avoids repeated passage of the air/water interface over the proteins adsorbed at the biomaterial surface. As we show below, this procedure enabled us to distinguish between different clinically used materials, and is therefore validated *post hoc*. Finally, the area of the blood-material contact is higher in the shear channels than in the Chandler loop system.

### 3.3 Surface characterization of the coated shear channels

The shear channels, identically polished, were coated with metallic titanium, cobalt-chromium (CoCr) alloy and stainless steel. The coating of each channel was characterized by XPS. Figure 3-4 shows the composition of the coatings.

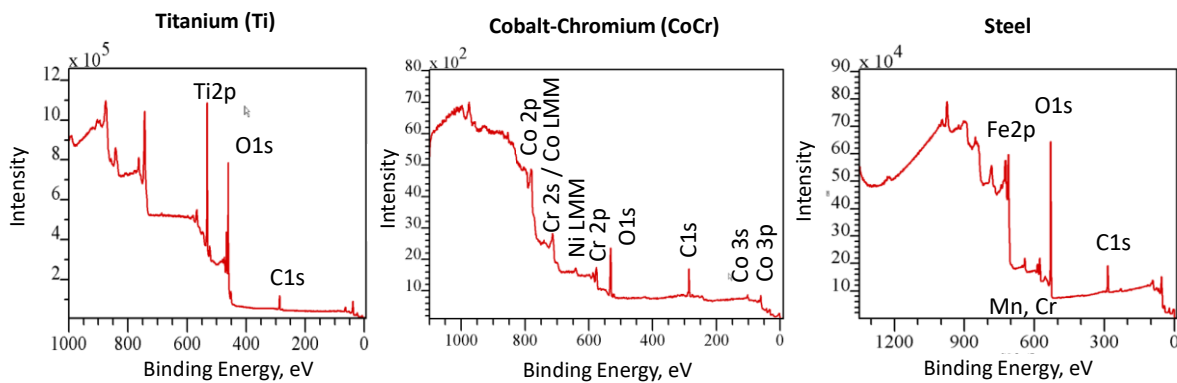


Figure 3-4. Surface Characterization of the coated shear channels by XPS: Survey Spectra.

Targets used in the sputtering process were metallic Ti, L605 CoCr alloy, and 316 Ti stainless steel, respectively, for the three materials. Accordingly, in the case of Ti coating, Ti and oxygen are expected to be present in the Ti coating, because Ti rapidly oxidizes in air and its surfaces will be covered by a native oxide layer (see below). These are the elements found by XPS on the Ti coating, together with the adventitious carbon contamination (Figure 3-4).

The L605 CoCr alloy consists predominantly (~ 50%) of Co, with Cr (~ 20%), W (~ 15%), and Ni (~ 10%) as the most significant additives. The elements found in the CoCr coating (Co, Cr, Ni, C; Figure 3-4) reflect this composition with the notable absence of W and the presence of the adventitious carbon.

316 Ti stainless steel target consists of Fe (62%), Cr (18%), Ni (14%), Mn (2%) and Mo (3%), with trace amounts of Ti, P, S, Si, and C. Of these, Fe, Cr, and traces of Mn are found in the coating, together with the carbon contamination (Figure 3-4).

Detailed examination of the XPS spectra for the 2p regions of Ti, Co, Cr, and Fe, in these materials indicates, not surprisingly, that the surfaces are dominated by the oxides. In particular in the case of Ti (Figure 3-5), three peaks of the Ti2p 3/2 – Ti2p 1/2 doublet are visible:

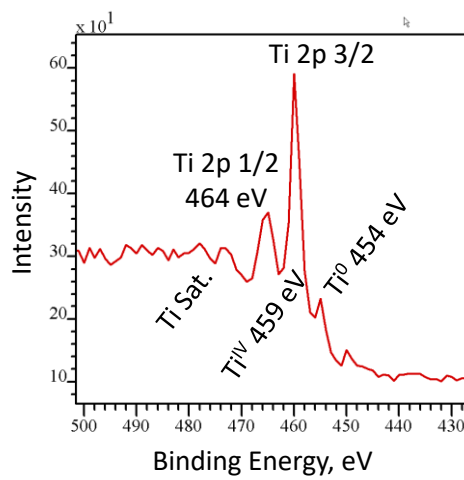


Figure 3-5: Expanded view of the Ti2p region of the XPS spectrum of the Ti coating with the assignment of the three peaks indicated above the spectrum.

The Ti2p 1/2 of the oxide at  $\sim 464$  eV, Ti2p 3/2 of the oxide mixed with Ti2p1/2 of the metal at  $\sim 459$  eV, and Ti2p 3/2 of the metal at 454 eV.<sup>182 183 184,185</sup> The visibility of the metallic titanium indicates that the oxide thickness is  $< 10$  nm.

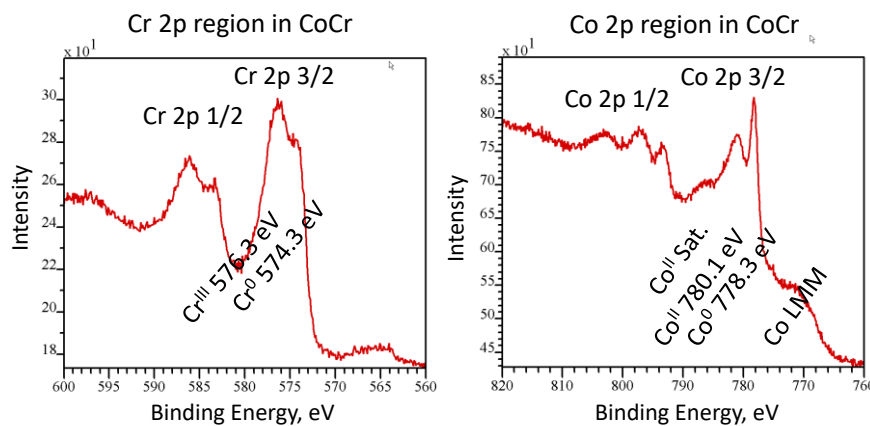


Figure 3-6: Detailed spectra of the Cr 2p (left) and Co2p (right) regions of the CoCr alloy coating.

The characteristic multiplet splitting of the Co and Cr 2p peaks indicates that in the CoCr alloy coating, these elements are also present in the form of the oxides, and that in both cases, the contributions of the metallic states are visible (Figure 3-6). The presence of Cr<sup>III</sup> and Co<sup>II</sup> oxidation states, in addition to the metal, is inferred from the peak binding energies and, in the case of Co, characteristic satellite pattern (Co<sup>II</sup> sat. marked in Figure 3-6).

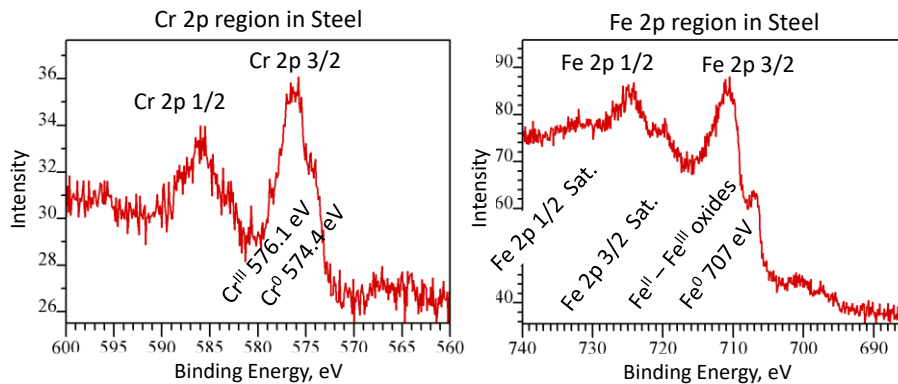


Figure 3-7: Detailed spectrum of the Cr2p (left) and Fe2p (right) regions of the steel coating.

Similarly, in the case of steel (Figure 3-7), Cr and Fe are present in the form of the Co<sup>III</sup> oxide and, most likely, mixture of Fe<sup>II</sup> and Fe<sup>III</sup> oxides. The contribution of the metallic species to the spectrum of Cr on steel is smaller than on CoCr, as the metal peak appears as a shoulder only (c.f. the left panels in Figure 3-6 and Figure 3-7). Metallic iron is visible in the spectrum of the Fe2p region (Figure 3-7, right panel), as expected. No Cl was detected on the steel coating by XPS (Figure 3-4), ruling out the contribution of the chlorinated iron species to the Fe2p region (they would appear at the same binding energies).

### 3.4 Whole blood cell count analysis

Before and after the incubation in the shear channels, whole cell counts in whole blood were characterized. Red blood cell, platelet, and white blood cell (total, monocyte, and neutrophil) counts are shown in Figure 3-8. Both the raw data and the data normalized to the baseline counts are shown. It is easier to detect trends in the normalized data.

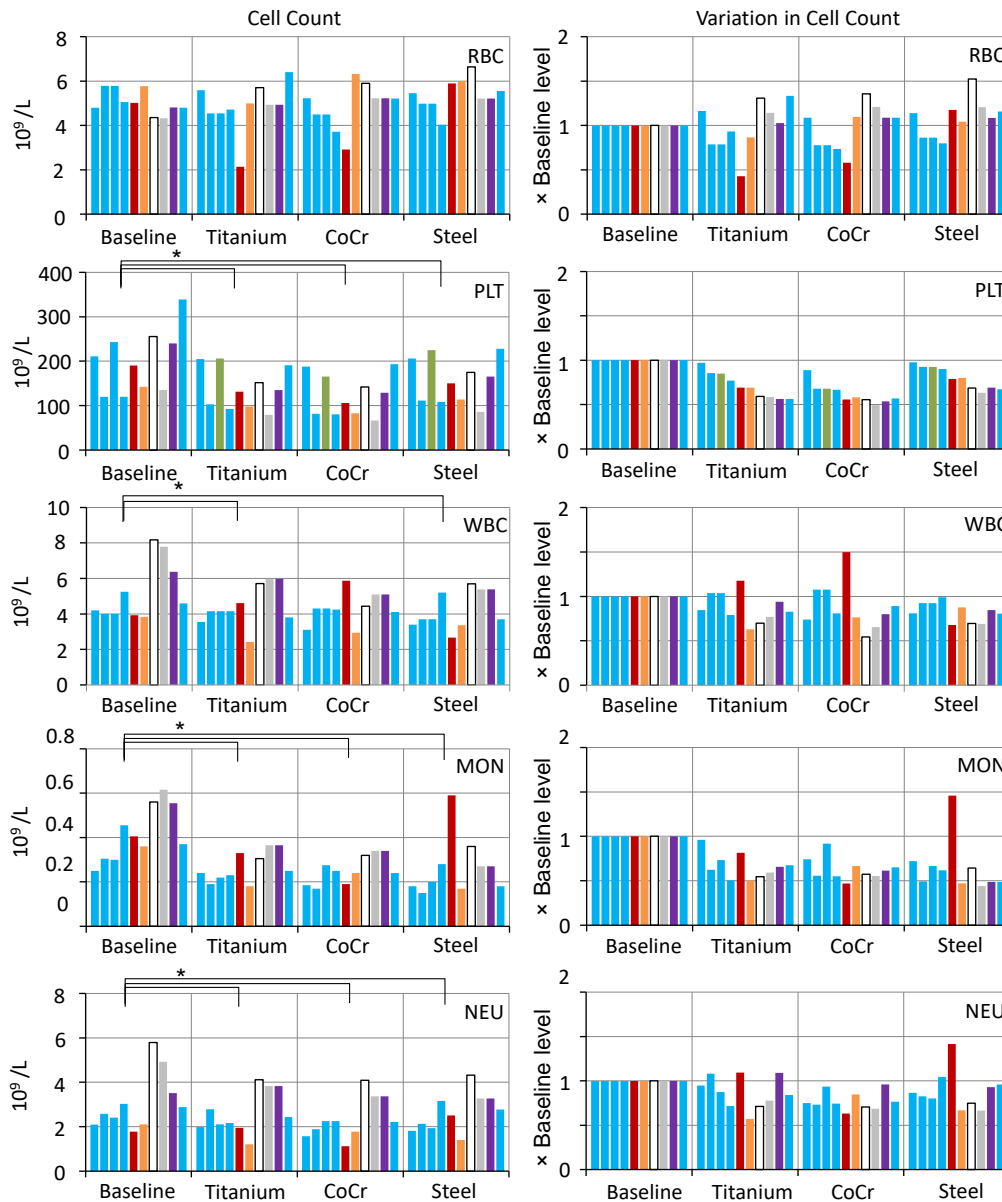


Figure 3-8. Whole blood cell count analysis. RBC: red blood cells. PLT: Platelets. WBC: White blood cells. MON: monocytes. NEU: neutrophils. Left column: raw data. Right column: data, normalized to the count before exposure to the material (baseline). Bar colors represent donors. Light blue bars (experiments 1 – 4 and 10, Table 3-1) were performed at KIT with the blood from one donor. The 10<sup>th</sup> experiment is referred to as the “stability” experiment in the text. Other colors refer to the experiments performed in Teltow (experiments 5 – 9, Table 3-1). Results are shown in chronological order so that the effect of ageing of the channel coatings could be examined. The color coding of the donors and the abbreviations are used throughout the chapter. Statistical significance of the differences in the cell counts between baseline and materials were evaluated with a paired two-sample t-test. Statistically significant differences ( $p < 0.05$ ) are indicated with the black asterisks and the corresponding brackets. Raw blood cell count data for all of the experiments is presented in Table 3-2.

Examining Figure 3-8, one observes material-induced variations in the counts for all of the cells. For the most part, cell counts decrease, as would be expected for cell adsorption,

aggregation, and damage. Some instances of material-induced increase in cell counts are also observed with RBCs and WBCs, but not with the platelets. The effects of the materials on RBC counts were not statistically significant ( $p > 0.05$  evaluated by the paired two-sample t-test), while the effects of the materials on the PLT, MON, and NEU counts were ( $p = 0.01, 7.4E-5, 0.002$  for the changes in the platelet counts;  $p = 0.0001, 6.3E-6, 0.004$  for the changes in the monocyte counts;  $p = 0.02, 0.001, 0.04$  for the changes in the neutrophil counts; in all cases, values for the baseline-Ti, baseline-CoCr, and baseline-steel comparison are listed in that order). In the case of the WBC counts, the changes induced by Ti and steel were significant ( $p = 0.02$  and  $0.002$ , respectively), but the changes induced by CoCr were not ( $p = 0.06$ ).

The most striking effect of materials is on the platelet counts. Platelet counts are seen to decrease systematically from the baseline level in each successive experiment for each of the materials. This effect is more significant than the variation between the donors, because it is visible for all the donors. We interpret this as evidence of the ageing (corrosion) of the shear channel coatings upon successive exposure to blood and washing procedures between the experiments that were performed over a period of 8 month. A total of 10 experiments were performed, first four and the last one with the blood from the same donor (light blue bars in Figure 3-8). In each of the successive figure in this Chapter, we present the results in chronological order to highlight the effect of ageing, as we do in Figure 3-8.

In Figure 3-9, the decrease in platelet count relative to the baseline values is shown for the three materials. Over time, all three materials lead to the same level of PLT reduction ( $\sim \times 0.6$ ), but for CoCr, this happens faster than for steel or for Ti. Also, in the case of CoCr, PLT reduction occurs already in the first experiment.

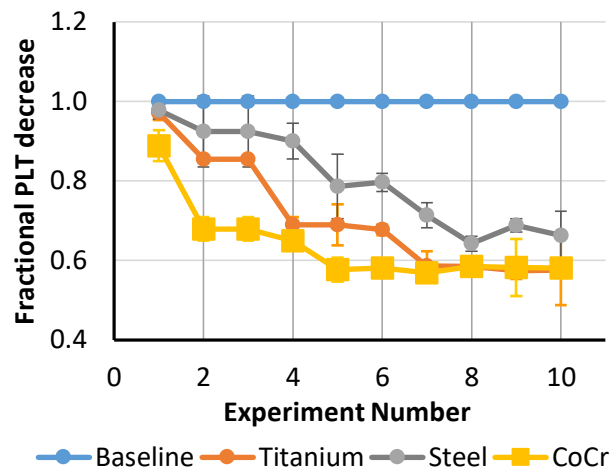


Figure 3-9: Fractional decrease in PLT counts (relative to the baseline level) for the three materials used in this study. The number of the experiment, in chronological order, is plotted on the x-axis. The corresponding data are shown in Table 3-2. Error bars are standard deviations.

In summary, blood contact with biomaterials resulted in significant reduction in the platelet, monocyte, and neutrophil counts. Significant ageing effects were observed, with platelet reduction getting progressively worse with every experiment. This effect was worse for CoCr than for other materials.

#	Cells	Baseline	Ti	CoCr	Steel
1	RBC × 10 <sup>9</sup> /L	4.80	5.59	5.22	5.46
	PLT × 10 <sup>9</sup> /L	211	205	187.5	206
	WBC × 10 <sup>9</sup> /L	4.2	3.6	3.1	3.4
	MON × 10 <sup>9</sup> /L	0.25	0.24	0.19	0.18
	NEU × 10 <sup>9</sup> /L	2.09	1.98	1.57	1.81
2	RBC × 10 <sup>9</sup> /L	5.78	4.55	4.50	4.98
	PLT × 10 <sup>9</sup> /L	120	102.5	81.5	111
	WBC × 10 <sup>9</sup> /L	4.0	4.2	4.3	3.7
	MON × 10 <sup>9</sup> /L	0.31	0.19	0.17	0.15
	NEU × 10 <sup>9</sup> /L	2.58	2.79	1.89	2.13
3	RBC × 10 <sup>9</sup> /L	5.78	4.55	4.50	4.98
	PLT × 10 <sup>9</sup> /L	243	206	165	225
	WBC × 10 <sup>9</sup> /L	4.0	4.2	4.3	3.7
	MON × 10 <sup>9</sup> /L	0.30	0.22	0.28	0.20
	NEU × 10 <sup>9</sup> /L	2.41	2.11	2.26	1.93
4	RBC × 10 <sup>9</sup> /L	5.06	4.71	3.72	4.03
	PLT × 10 <sup>9</sup> /L	120	92.5	80	108
	WBC × 10 <sup>9</sup> /L	5.3	4.2	4.3	5.2
	MON × 10 <sup>9</sup> /L	0.46	0.23	0.25	0.28
	NEU × 10 <sup>9</sup> /L	3.03	2.17	2.26	3.16
5	RBC × 10 <sup>9</sup> /L	5.02	2.14	2.91	5.89
	PLT × 10 <sup>9</sup> /L	190	131	106	150
	WBC × 10 <sup>9</sup> /L	3.9	4.6	5.9	2.7
	MON × 10 <sup>9</sup> /L	0.41	0.33	0.19	0.59
	NEU × 10 <sup>9</sup> /L	1.78	1.94	1.12	2.51
6	RBC × 10 <sup>9</sup> /L	5.77	5.00	6.32	6.01
	PLT × 10 <sup>9</sup> /L	142	98	82.5	113.5
	WBC × 10 <sup>9</sup> /L	3.8	2.4	2.9	3.4
	MON × 10 <sup>9</sup> /L	0.36	0.18	0.24	0.17
	NEU × 10 <sup>9</sup> /L	2.10	1.20	1.78	1.41
7	RBC × 10 <sup>9</sup> /L	4.36	5.70	5.90	6.64
	PLT × 10 <sup>9</sup> /L	256	152	142	175
	WBC × 10 <sup>9</sup> /L	8.2	5.7	4.4	5.7
	MON × 10 <sup>9</sup> /L	0.56	0.31	0.32	0.36
	NEU × 10 <sup>9</sup> /L	5.79	4.12	4.09	4.33
8	RBC × 10 <sup>9</sup> /L	4.33	4.94	5.23	5.21
	PLT × 10 <sup>9</sup> /L	135	79	67	86
	WBC × 10 <sup>9</sup> /L	7.8	6.0	5.1	5.4
	MON × 10 <sup>9</sup> /L	0.62	0.37	0.34	0.27
	NEU × 10 <sup>9</sup> /L	4.92	3.83	3.37	3.27
9	RBC × 10 <sup>9</sup> /L	4.81	4.94	5.23	5.21
	PLT × 10 <sup>9</sup> /L	240	135	129	166
	WBC × 10 <sup>9</sup> /L	6.4	6.0	5.1	5.4
	MON × 10 <sup>9</sup> /L	0.56	0.37	0.34	0.27
	NEU × 10 <sup>9</sup> /L	3.52	3.83	3.37	3.27
10	RBC × 10 <sup>9</sup> /L	4.80	6.40	5.22	5.55
	PLT × 10 <sup>9</sup> /L	339	191	194	228
	WBC × 10 <sup>9</sup> /L	4.6	3.8	4.1	3.7
	MON × 10 <sup>9</sup> /L	0.37	0.25	0.24	0.18
	NEU × 10 <sup>9</sup> /L	2.89	2.43	2.21	2.77

Table 3-2. Raw blood cell count data. The experiment number corresponds to the experiment date shown in Table 3-1.

### 3.5 Quantitative evaluation of the coagulation cascade activation

The most severe adverse reaction to foreign materials placed in the vascular system is thrombosis. Therefore, the most direct way to evaluate the effect of the material is to measure the levels of thrombin in whole blood in contact with the material. Here, thrombin levels were evaluated by quantifying the levels of thrombin-antithrombin complex (TAT) in the blood before (baseline) and after contact with the surfaces of different materials. The results are shown in Figure 3-10.

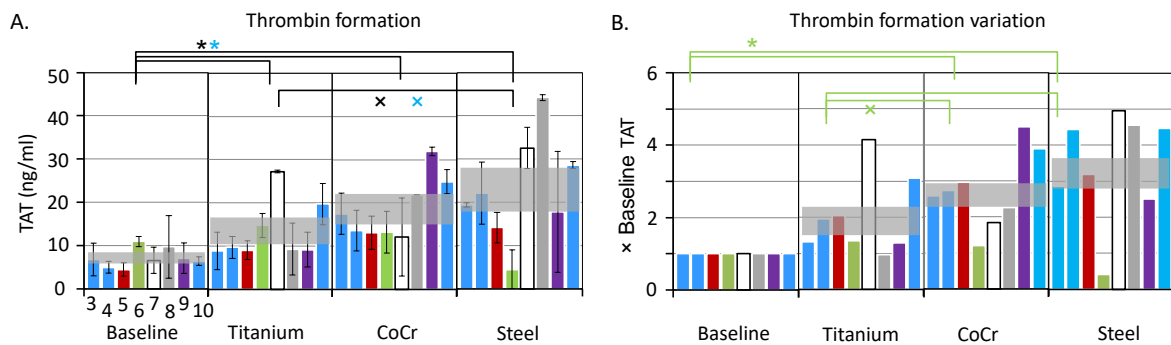


Figure 3-10. Thrombin generation evaluated by measuring thrombin-anti-thrombin III (TAT) complex in the blood. (A). TAT levels in ng/ml. (B). Time-fold variation of the TAT levels calculated by normalizing the data measured after contact with the shear channels to the baseline values. Error bars in (A) are standard deviations.

Color coding of the donors is the same as in Figure 3-8: each color refers to a unique donor; light blue bars (experiments 3, 4 and 10, Table 3-1) reflect experiments performed at KIT with the blood from one donor; other colors refer to the experiments performed in Teltow (experiments 5 - 9, Table 3-1). Results are shown in the order in which the experiments were performed so that the effect of ageing of the channel coatings could be examined.

Gray horizontal regions are means calculated over all of the donors for each condition (baseline, Ti, CoCr, steel). The widths of these regions correspond to the standard errors of the mean.

Brackets and symbols above the plots refer to the evaluation of the statistical significance: black – calculated for all of the donors; blue – calculated only for the KIT donor (light-blue bars); green – same as light blue, but without the last (10<sup>th</sup>) experiment to evaluate the effect of ageing. Asterisks refer to the statistical significance of the difference between baseline and the materials ( $p \leq 0.05$  by paired t-test), while crosses refer to the statistical significance of the difference between the materials ( $p \leq 0.05$  by the unpaired two-sample equal variance t-test). Further details are in the main text of the chapter. The color code for the donors and statistical significance evaluation remains the same throughout this chapter.

It is evident from the results presented in Figure 3-10 that all three materials—titanium, CoCr, and steel—induce thrombin generation in whole blood after incubation. Compared with the TAT level of  $7.1 \pm 0.8$  ng/ml in the blood before exposure to the materials (baseline), each of them led to a significant increase in the TAT concentration to  $14 \pm 2$  ng/ml for Ti,  $19 \pm 3$  ng/ml

for CoCr, and  $23 \pm 4$  ng/ml for steel. These values are obtained by averaging the data over 8 experiments (experiments 3 – 10, Table 3-1) with five donors. Each of these increases was statistically significant when compared to the baseline level (black asterisks in Figure 3-10; p-values of 0.02, 0.001, and 0.04 for the differences between baseline and Ti, baseline and CoCr, and baseline and steel, respectively).

When comparing thrombin generation between the three materials, only the difference between titanium and steel was statistically significant (black cross in Figure 3-10,  $p = 0.044$ ). TAT level induced by the contact with CoCr was between those induced by Ti and steel, but the differences between Ti and CoCr and CoCr and steel were not statistically significant. We attribute this to the effects of the donor-to-donor variation and coating ageing.

To evaluate the effect of the ageing of the coatings on the observations, the statistical significance of the measured differences in the TAT levels was evaluated considering only the experiments with the blood from one donor done at KIT (light-blue asterisk and cross in Figure 3-10 A); in this case, they are the same as for all the donors (black asterisks and cross in Figure 3-10A). However, when the results of the last (10<sup>th</sup>) experiment were excluded from the evaluation of the experiments done at KIT (green asterisk and crosses in Figure 3-10 B), the following differences emerged: on the one hand, the difference between the baseline and Ti was no longer statistically significant ( $p=0.1$ ). This is most likely due to the insufficient number of measurements. On the other hand, the difference between Ti and CoCr was statistically significant ( $p=0.04$ ). This reflects the effect of ageing on the CoCr coating.

(Note that results of 10 experiments are shown in Figure 3-8, but of 8 in Figure 3-10. This is because TAT levels could not be measured in the first two experiments done at KIT; other parameters had been measured, as described below and in Table 3-1).

## 3.6 Quantitative evaluation of the material-induced platelet activation and inflammatory responses

Thrombin production is an integral response to the biomaterial that draws on several mechanisms, of which platelet activation is arguably the most important. Inflammatory responses also contribute to the generation of thrombin, and are important in their own right. To evaluate these individual contributions in the solution phase, we developed a six-color flow cytometry assay that measures CD62P expression on the platelets, platelet-leukocyte aggregation, and activation of monocytes and neutrophils in the aggregates with the platelets. The contribution of the surface-phase reactions was evaluated using ELISA assays for platelet activation ( $\beta$ -TG secretion), neutrophil activation (PMN elastase) and complement activation (sC5b-9). Flow cytometry assay design is described first, and then its results are presented together with the ELISA results.

### 3.6.1 The design of the six color flow cytometric assay for measuring platelet activation, platelet-leukocyte interactions, and activation of leukocytes in platelet-leukocyte aggregates in solution

Flow cytometric assay for characterizing the solution-phase responses of platelets and leukocytes to the materials was developed and implemented at KIT. As a starting point, we used the six color assay established at University Hospital Tubingen.<sup>186</sup>

In the six color flow cytometric assay the evaluation of platelet and leukocyte populations was based on their phenotypical characteristics revealed by immunostaining with a panel of six antibodies. This assay focused on the platelets. Therefore, only CD41a<sup>+</sup> events were recorded (PLTs and PLT-LEU aggregates). The forward light scatter (FSC) and the side light scatter (SSC) were set to capture the platelets and the platelet-leukocyte aggregates in the appropriate detector range, as shown Figure 3-11. Figure 3-11A depicts platelet and platelet-leukocyte populations in an unstimulated sample. Here, platelets appear at the bottom of the scatter plot, while platelet-leukocyte aggregates appear above and to the right, indicating larger size and greater complexity. Identification is confirmed with the antibody staining. Antibodies against CD41a for platelets, CD45 for leukocytes, CD66b for neutrophils and CD14 for monocytes were used (the complete panel of antibodies is presented in Table 3-3). Figure 3-

11 B and C show platelet and leukocyte populations in samples stimulated with the agonists TRAP6 and PMA, respectively.

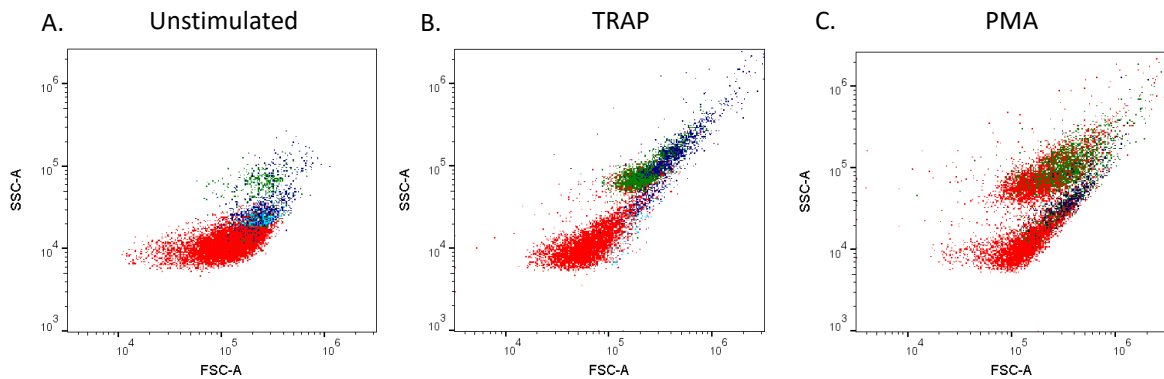


Figure 3-11. Flow cytometry analysis of whole blood: Scatter plots. Colors represent populations of different cells identified through with antibodies against CD62P for the platelets, CD66b for the neutrophils, CD14 for the monocytes. A. unstimulated whole blood. B. TRAP6 stimulated whole blood. C. PMA stimulated whole blood.

The agonists, TRAP6 and PMA, activate platelets (TRAP6, PMA) and leukocytes (PMA), causing changes to the scatter plots. In particular, in stimulated samples, platelet and platelet-leukocyte populations assume a more elongated shape (Figure 3-11 B and C). Furthermore, in the TRAP6-stimulated samples (Figure 3-11 B) platelet-neutrophil (green) and platelet-monocyte (blue) aggregates appear overlaid. On the contrary, in the PMA stimulated sample (Figure 3-11 C) the two types of aggregates are well separated in distinct populations. The difference between TRAP6- and PMA-stimulated samples is related to the different effects that these agonists have on platelets and leukocytes: TRAP6 is platelet-specific, while PMA is an agonist for leukocytes as well as platelets.<sup>56</sup>

The changes in the scatter plots illustrate qualitative changes in the platelet and leukocyte populations caused by activation. In order to quantify these changes, I evaluated expression levels of the activation markers CD62P and CD11b on the platelets and different types of platelet-leukocyte aggregates according to the strategy shown in Figure 3-12. The different types of PLT-LEU aggregates were distinguished by the expression of the monocyte- and neutrophil- specific markers CD14 and CD66.

**CD41a+ events ( Platelets; 10000 recorded)**

- CD45+ ..... *Platelet/Leukocyte aggregates*
- CD14+ ..... *Platelet/Monocyte aggregates*
- CD11b+ ..... *Platelet/ Active Monocyte aggregates*
- CD62P+ ..... *Active Platelet/ Active Monocyte aggregates*
- CD66b+ ..... *Platelet/Neutrophil aggregates*
- CD11b+ ..... *Platelet/Active Neutrophil aggregates*
- CD62P+ ..... *Active Platelet/Active Neutrophil aggregates*
- CD62P+ ..... *Active Platelet*

Figure 3-12. Strategy to identify and evaluate the activation of platelets and leukocytes in the platelet population and platelet aggregates with different types of leukocytes (monocytes, CD14+; and neutrophils, CD66+).

This strategy allowed me to quantitatively evaluate the effect of biomaterials.

The first step towards implementing the strategy shown in Figure 3-12 was to define the volume of each antibody that was needed to reliably identify the relevant populations without saturating the photomultipliers of the flow cytometers or causing cell aggregation due to excessive amount of antibodies used.<sup>187</sup> Thus, minimal antibody volumes needed to detect stained cells were determined by titrations, the results of which are shown in Figure 3-13. Here, the median fluorescence intensities (MFI) are plotted as a function of the antibody volume used. MFIs reflect the level of staining.

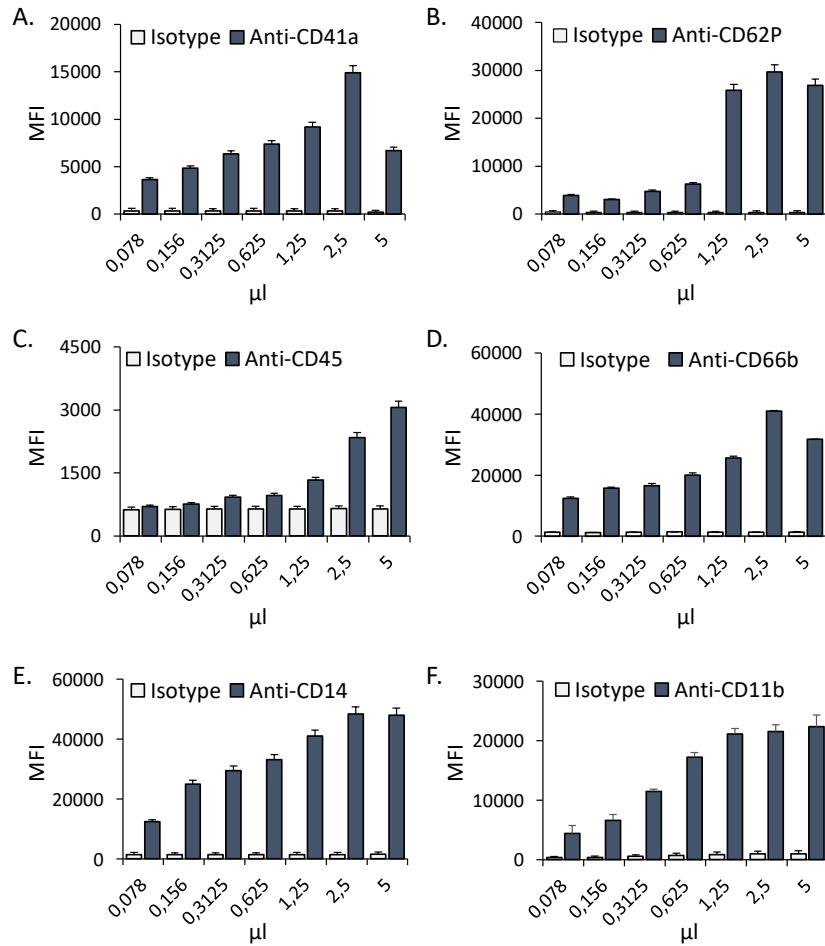


Figure 3-13. Titration assays. Whole blood samples were stained with increasing concentrations of anti-CD41a (A), anti-CD62P (B), anti-CD45 (C), anti-CD66b (D), anti-CD14 (E), anti-CD11b (F).

The necessity to choose appropriate volumes of the antibodies has been extensively discussed in the flow cytometry literature. The Table 3-3 shows the panel of the six antibodies and the respective volumes used.

Antibody against	Volumes	Target
CD41a	2.5 μl	Platelets
CD62P	1.25 μl	Activated platelets
CD45	2.5 μl	Leukocytes
CD66b	2.5 μl	Neutrophils
CD14	2.5 μl	Monocytes
CD11b	2.5 μl	Activated neutrophils, activated monocytes

Table 3-3. Panel of the six antibodies used in the flow cytometry assay and the volumes used in the assay.

### 3.6.2 Platelet and leukocyte interaction and activation at the material surface

Once the appropriate antibody volumes were chosen, the flow cytometric assay was used to evaluate and quantify platelet activation, platelet-leukocyte aggregation, and the activation of neutrophils and monocytes in the PLT-LEU aggregates in the blood samples collected before (baseline) and after the blood contact with the shear channels. TRAP6- and PMA-stimulated samples were used as positive controls for the evaluation of the activation state of platelets and leukocytes. Figure 3-14 A shows platelet and leukocyte populations in the baseline blood and Figure 3-14 B-D show these populations upon contact with the shear channels. The fluorescence signals were overlaid on the scatter plots in order to highlight different populations such as single platelets (red), and platelet-leukocyte aggregates (turquoise). Within the population of the aggregates, platelet-monocyte aggregates (blue) and platelet-neutrophils aggregates (green) are distinguished.

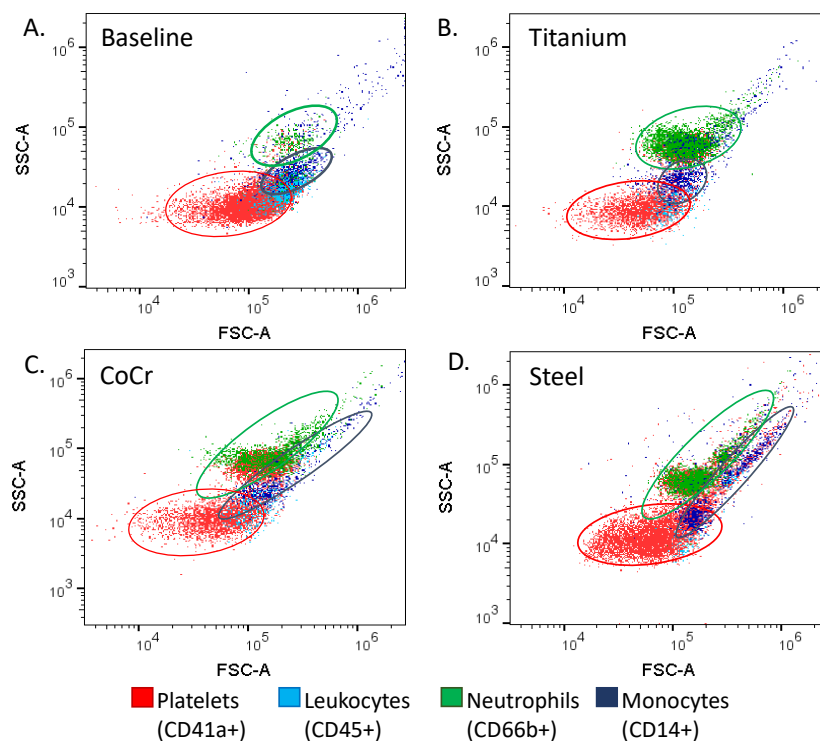


Figure 3-14. Scatter Plots depicting platelet population (red) and platelet-leukocyte aggregates (green) before (A) and after the blood interaction with different materials: titanium (B), CoCr (C) and steel (D).

The overlaid fluorescence signals are commonly referred to as “back-gating”. The back-gating allows highlighting of the differences in the scatter plots between the baseline samples and

blood samples exposed to the shear channels coated with different materials. It can be seen in Figure 3-14 B that the contact with the titanium-coated shear channels does not induce a drastic change in the appearance of the scatter plot. This signifies that platelet and leukocyte populations are not significantly affected by this material. On the contrary, CoCr and Steel cause clearly evident changes in the morphology of the scatter plots (Figure 3-14 C, D). It is noteworthy that these changes are comparable with those caused by PMA (Figure 3-11 C). They therefore indicate activation. It is important to note that we observe *qualitative* differences between materials already at the stage of examining the scatter plots. Different materials cause different reactions in the blood.

### 3.7 Quantitative evaluation of the solution and surface-phase events with the six-color flow cytometric assay and ELISA

Having designed and validated the six-color flow cytometry assay, I had at my disposal the tools I needed to characterize the effect of the materials on platelets and leukocytes in the platelet-leukocyte aggregates.

#### 3.7.1 Quantitative evaluation of platelet activation and aggregation with leukocytes

Platelet activation was quantified by measuring the expression of the platelet activation marker CD62P (also called P-selectin) and platelet-leukocyte aggregation by flow cytometry and the secretion of  $\beta$ -TG by ELISA. The results are presented in Figure 3-15.

Concerning platelet activation measured by evaluating CD62P expression (Figure 3-15 A, B), CoCr and steel induce a statistically significant increase in the level of expression of this marker as compared to the baseline level, while titanium does not (black asterisk and brackets in Figure 3-15 A;  $p = 0.021, 0.044, 0.39$  for baseline-CoCr, baseline-steel, and baseline-Ti; here, results from all the donors are considered). This difference between the effect of Ti and of the other two materials is striking. It is more significant than the donor-to-donor variation.

When the results of the experiments performed at KIT with the blood from one donor (light blue bars in Figure 3-15 A, B) are considered, an additional, statistically significant difference in the level of CD62P expression between Ti and CoCr and Ti and steel is revealed (blue cross, and the corresponding brackets, in Figure 3-15 A;  $p = 0.014$  and  $0.02$  for baseline-CoCr and

baseline-steel, but 0.42 for baseline-Ti;  $p = 0.015$  for Ti-CoCr and Ti-steel, but 0.4 for CoCr-steel).

When the results of the experiments performed at KIT with the blood from one donor are considered without the last “stability” experiment, the effects are the same (green asterisk, cross, and the corresponding brackets in Figure 3-15 B;  $p = 0.018$  and  $0.027$  for the baseline-CoCr and baseline-steel, respectively;  $0.015$  and  $0.016$  for the Ti-CoCr and Ti-steel, respectively, but  $0.47$  and  $0.35$  for baseline-Ti and CoCr-steel, respectively). Therefore, the effect of ageing on the activation of platelets as measured by CD62P expression levels is not apparent. On the other hand, the low CD62P expression observed in the three experiments conducted in Teltow (white, gray, and purple bars) is surprising.

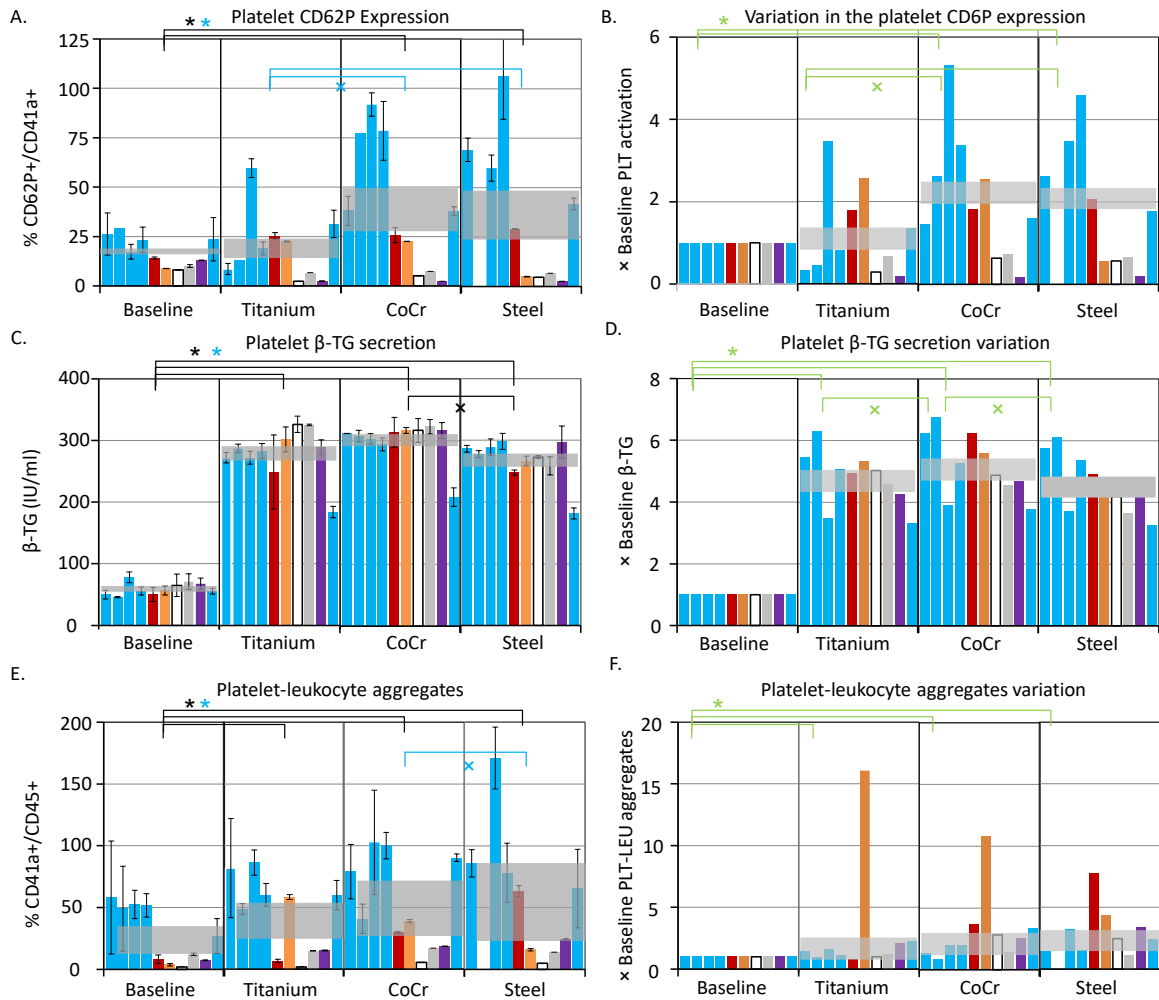


Figure 3-15. Quantification of platelet activation and aggregation with leukocytes. A, C, E: raw data; B, D, F: data normalized by the baseline levels.

(A), (B): Evaluation of platelet activation by measuring CD62P expression on platelets by flow cytometry. Activation level is calculated as the fraction of CD62P+ events out of the total CD41a+ events, normalized by the same fraction in the positive control (TRAP6-stimulated platelets).

(C), (D): Evaluation of platelet activation by quantification of  $\beta$ -TG secretion by ELISA.

(E), (F) Evaluation of platelet activation by measuring platelet-leukocyte aggregation by flow cytometry. In (E), the data are presented as frequency of CD45+ events out of the total CD41a+ events, normalized by the same frequency in the positive control (PMA-stimulated samples).

Error bars are standard deviations. Gray horizontal bars are means calculated over all of the donors. Their widths correspond to the standard error of the mean in each case. The color of each bar represents a unique donor. E.g., light blue bars stem from experiments performed with the blood from one donor at KIT (experiments 1 – 4 and 10, Table 3-1), while bars of other colors stem from the experiments performed with the blood of different donors at Teltow (experiments 5 - 9, Table 3-1). Experiments are presented in the order they were performed so that the effect of ageing of the channel coatings could be examined.

Statistical significance of the differences between baseline and materials (asterisks) was evaluated with a paired two-sample t-test. Statistical significance of the difference between materials (crosses) was evaluated using an unpaired two-sample t-test assuming equal variance. The colors of the symbols, and the corresponding brackets (black, blue, green) refer to the evaluation of statistical significance for all of the donors (black), KIT donor only (blue), and KIT donor only without the last “stability” experiment.

When the activation of platelets is measured in terms of the  $\beta$ -TG secretion (Figure 3-15 C, D), the results are strikingly different. All three materials induce  $\beta$ -TG secretion. Statistically significant changes in the  $\beta$ -TG levels between baseline and Ti, CoCr, and steel are observed (black asterisks and the corresponding brackets in Figure 3-15 C;  $p = 1.2E-9$ ,  $1.4E-9$ ,  $5.0E-9$ , respectively, considering results for all the donors). Moreover, statistically significant difference in the  $\beta$ -TG levels was observed between CoCr and steel (black cross and the corresponding bracket in Figure 3-15 C;  $p = 0.02$ ;  $p = 0.1$ ,  $0.26$  for the differences between Ti-CoCr and Ti-steel, respectively).

Ageing of the coatings had a significant effect in the case of CoCr, and possibly, Ti. Indeed, when considering the results obtained using blood from one donor in the experiments performed at KIT (light blue bars in Figure 3-15C), one finds no statistically significant difference between the materials. On the contrary, when the last “stability” experiment is excluded from this analysis, statistically significant differences between Ti and CoCr and CoCr and steel emerge (green crosses and the corresponding bars in Figure 3-15D;  $p = 0.002$  and  $0.015$ , respectively).

The differences between baseline  $\beta$ -TG levels and the levels induced by the materials are statistically significant independently of how they are evaluated: for all the donors (black asterisk), KIT donor (blue asterisk), or KIT donor without the “stability” experiment (green asterisk and the corresponding brackets in Figure 3-15 D).

Exposure of whole blood to all three materials also induced statistically significant levels of PLT-LEU aggregates, as indicated in Figure 3-15 E and F. This conclusion is valid when the statistical significance is valued for all the donors (black asterisk and the corresponding brackets in Figure 3-15 E;  $p = 0.012$ ,  $0.004$ ,  $0.012$  for baseline-Ti, baseline-CoCr, and baseline-steel, respectively), KIT donor (blue asterisk,  $p = 0.022$ ,  $0.026$ ,  $0.048$ ), or KIT donor without the last “stability” experiment ( $p = 0.06$ ,  $0.068$ ,  $0.026$ ). Indeed, no effect of material aging was observed, but a statistically significant difference in the level of PLT-LEU aggregates between blood exposed to CoCr and steel emerged when evaluating experiments performed with the blood from one donor at KIT (blue cross and asterisk in Figure 3-15 E,  $p = 0.25$ ).

### 3.7.2 Quantitative evaluation of platelet-monocyte and platelet-neutrophil aggregates.

Within the platelet-leukocyte aggregates, the platelet interactions with monocytes and neutrophils were quantified separately. The results are shown in Figure 3-16.

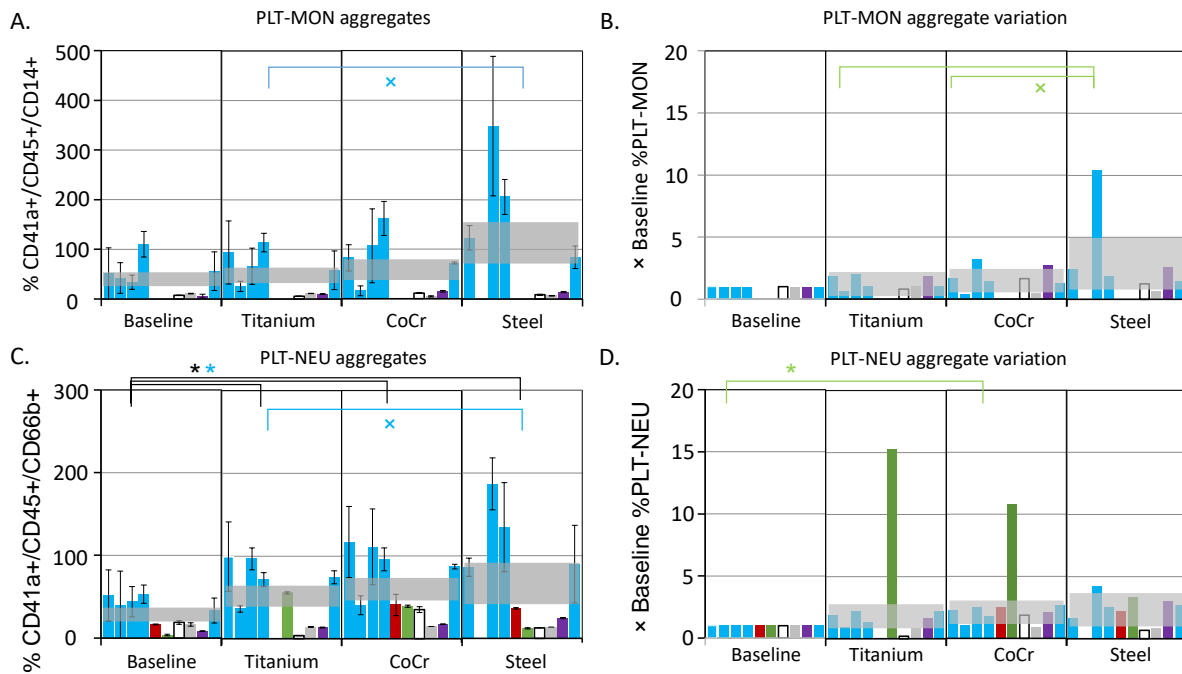


Figure 3-16. Platelet aggregation with monocytes and neutrophils. (A), (B). Quantification of platelet-monocyte aggregates. (C), (D). Quantification of platelet-neutrophil aggregates.

PLT-MON aggregates were identified as events positive for CD41a, CD45, and CD14; PLT-NEU aggregates were identified as events positive for CD41a, CD45, and CD66b. In (A) and (C), their levels are presented, normalized to the levels of these events in PMA-stimulated samples. In (B) and (D), the levels of the aggregates are further normalized by the baseline levels to indicate fold-changes. Error bars in (A) and (C) are standard deviations. Gray horizontal regions are means calculated over all of the donors; their widths correspond to the standard error of the mean in each condition. Different donors are indicated by the differently colored bars. The color code is the same as in the other figures of this chapter. The corresponding experiments appear in Table 3-1. Experiments are presented in the order they were performed so that the effect of ageing of the channel coatings could be examined.

Statistical significance of the differences between the baseline and the materials was evaluated with the paired two-sample t-test (asterisks). That for the difference between the different materials—with the unpaired two-sample equal-variance t-test (crosses). This was done for all of the donors (black symbols and the corresponding brackets), the KIT donor (light blue symbols/brackets) and the KIT donor without the last “stability” experiment (green symbols and brackets).

None of the materials induced statistically significant change in the PLT-MON aggregates levels as compared to the baseline (Figure 3-16 A, B), but a statistically significant difference

between Ti and steel was observed when the results from the KIT donor were considered (blue cross and bracket in Figure 3-16 A). Ageing had a discernable effect on the CoCr coating, as evaluated from the PLT-MON aggregation. This was evident from the statistically significant difference in the PLT-MON levels between CoCr and steel that emerged when this difference was evaluated for the experiments performed with the blood from the KIT donor without considering the last “stability” experiment (green cross and brackets in Figure 3-16 B;  $p = 0.048$ ), but not when it was evaluated for the experiments performed with the blood from the KIT donor including the last “stability” experiment ( $p = 0.06$ ). The difference between titanium and steel was statistically significant in both of these cases.

The case of the PLT-NEU aggregates is quite different (Figure 3-16 C, D). Here, all of the materials induced statistically significant changes in the aggregate levels when the results of all the donors were evaluated (black asterisk and the corresponding brackets in Figure 3-16 C,  $p = 0.02, 0.002, 0.02$  for the baseline-Ti, baseline-CoCr, and baseline-steel, respectively), or when the results for the experiments performed with the KIT donor were evaluated (blue asterisk in Figure 3-16 C,  $p = 0.018, 0.009, 0.02$ , respectively). In this case, the difference in the PLT-NEU aggregate levels between Ti and steel was also statistically significant ( $p = 0.04$ ).

Ageing had no significant effect on the PLT-NEU aggregation levels, since only loss of statistical significance was observed when the last “stability” experiment was excluded from the analysis (c.f. green and blue symbols in Figure 3-16 D).

Surprisingly, much lower aggregate levels were detected in the experiments performed in Teltow than at KIT.

Next, the activation states of the platelets and leukocytes in the PLT-MON and PLT-NEU aggregates were evaluated. The results are presented in Figure 3-17 and Figure 3-18 for the PLT-MON and PLT-NEU aggregates, respectively.

CoCr and steel caused statistically significant increase in the CD62P expression level on the PLT-MON aggregates (Figure 3-17 A, B). This was observed independently of whether the statistical significance was evaluated for all the donors (black asterisk and brackets in Figure 3-17 A;  $p = 0.006, 0.028$ , respectively), KIT donor (blue asterisk in Figure 3-17 A;  $p = 0.041, 0.047$ , respectively), or for the KIT donor without the last “stability” experiment (green asterisk and brackets in Figure 3-17 B;  $p = 0.041, 0.047$ , respectively), indicating that ageing did not have a significant effect. On the contrary, Ti did not cause a statistically significant increase in

the CD62P expression on PLT-MON aggregates compared to the baseline levels ( $p = 0.058, 0.1, 0.1$  for all the donors, KIT donor, KIT donor without the last “stability” experiment).

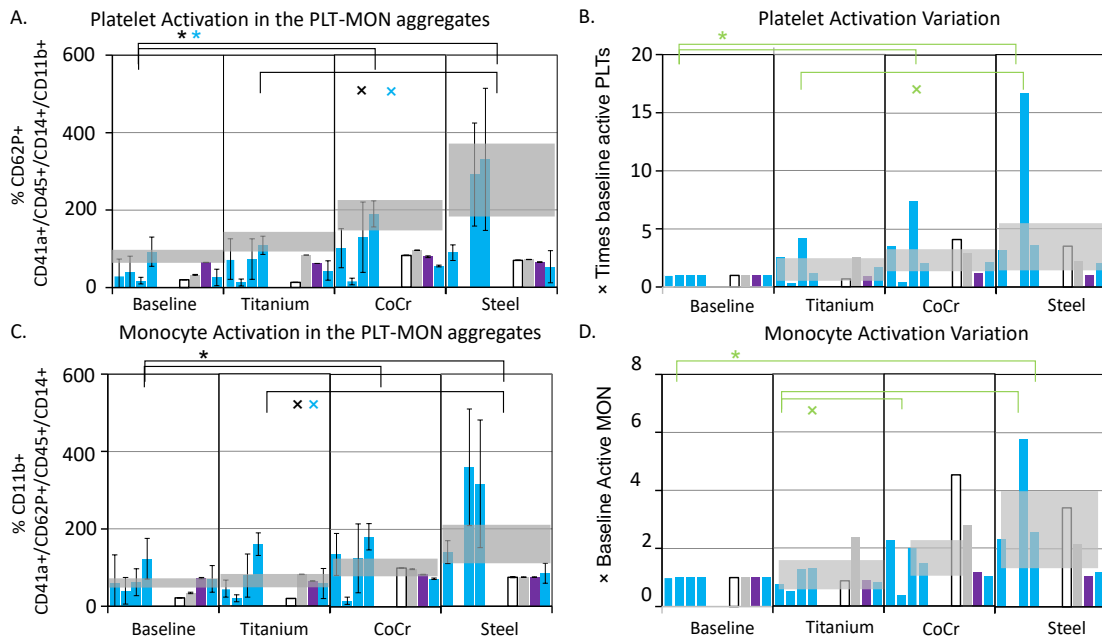


Figure 3-17. The activation state of platelets and monocytes in the platelet-monocyte aggregates. (A), (B). Platelet activation in platelet-monocyte aggregates evaluated by quantifying the level of CD62P expression. (C), (D) Monocyte activation in platelet-monocyte aggregates evaluated by quantifying CD11b expression. In (A), the fraction of CD62P events in the CD41a+/CD45+/CD14+/CD11b+ population was normalized by that fraction in agonist-treated samples. In (C), the same was done for the fraction of the CD11b+ events in the CD41a+/CD45+/CD14+/CD62P+ population. In (B) and (D), the data were further normalized to the baseline levels in order to obtain fold changes relative to the baseline levels.

Error bars in (A) and (C) are standard deviations. Gray horizontal regions are means calculated over all of the donors; their widths correspond to the standard error of the mean in each condition.

Different donors are indicated by the differently colored bars. The color code is the same as in the other figures of this chapter. The corresponding experiments appear in Table 3-1. Experiments are presented in the order they were performed so that the effect of ageing of the channel coatings could be examined.

Statistical significance of the differences between the baseline and the materials was evaluated with the paired two-sample t-test (asterisks). That for the difference between the different materials—with the unpaired two-sample equal-variance t-test (crosses). This was done for all of the donors (black symbols and the corresponding brackets), the KIT donor (light blue symbols/brackets) and the KIT donor without the last “stability” experiment (green symbols and brackets).

Statistically significant difference in the CD62P expression level was also observed between titanium and steel ( $p = 0.0045, 0.043, 0.043$ , when evaluated for all the donors (black cross and the corresponding bracket in Figure 3-17 A), KIT donor (blue cross in Figure 3-17 A) or KIT donor without the stability experiment (green cross and bracket in Figure 3-17 B)). This, once again, indicates that ageing did not have a significant effect.

Considering monocyte activation in the PLT-MON aggregates, CoCr and steel, but not Ti, induced statistically significant changes in the CD11b expression as compared to the baseline levels (black asterisk and brackets in Figure 3-17 C;  $p = 0.011$  and  $0.027$  for baseline/CoCr and baseline/steel vs.  $0.29$  for baseline/Ti when results from all the donors were evaluated); a statistically significant difference between titanium and steel was also observed (black cross and bracket in Figure 3-17 C,  $p = 0.031$ ). In this case, ageing did have a significant effect: the differences between baseline and steel and CoCr and steel were statistically significant when evaluated for the results obtained with the KIT donor without the stability experiment ( $p = 0.047$  and  $0.037$ , respectively; green asterisk and cross, and the corresponding brackets in Figure 3-17 D) but not significant when evaluated for the results obtained with the KIT donor including the stability experiment. In this case, it is the ageing of steel that appears to be relevant.

The activation of platelets and neutrophils in PLT-NEU aggregates is presented in Figure 3-18. All three materials induce statistically significant CD62P and CD11b expression levels on PLT-NEU aggregates (Figure 3-18 A - D), as well as PMN elastase release (Figure 3-18 E), as compared to the levels in the baseline samples, when these parameters are evaluated for all of the donors (black asterisks and brackets in Figure 3-18A, C, E;  $p = 0.029$ ,  $0.003$ ,  $0.011$  for the differences in the CD62P expression levels between baseline and Ti, baseline and CoCr, and baseline and steel samples, respectively;  $p = 0.019$ ,  $0.004$ , and  $0.016$  for the differences in the CD11b expression levels; and  $p = 6.96E-9$ ,  $8.51E-4$ ,  $0.001$  for the differences in the PMN elastase levels).

When evaluated for all the donors, differences in the CD62P or CD11b expression levels on the different materials were not statistically significant. On the other hand, the differences in the PMN elastase levels induced by Ti and CoCr were statistically significant (black cross and bracket in Figure 3-18 E,  $p = 7E-4$ ).

Ageing did not have an effect on the CD62P or CD11b expression levels on the PLT-NEU aggregates, but it did have a significant effect on the PMN elastase levels: when the results for the KIT donor were evaluated with and without the stability experiment (blue vs. green asterisks, crosses, and the corresponding brackets in Figure 3-18 E), the difference in PMN elastase between baseline and steel was significant in the latter case but not the former case, and so was the difference in the PMN elastase level between titanium and steel ( $p = 0.001$  and  $0.042$ , respectively). This indicates that the ageing effect was relevant for steel.

Interestingly, PMN elastase levels were lower for CoCr than for Ti; this difference was statistically significant (black crosses and brackets in Figure 3-18 E;  $p = 7E-4$ ). The level for steel was also lower than for Ti, but this difference was not statistically significant when evaluated for all of the donors ( $p = 0.134$ )—only when it was evaluated for KIT donor, with or without the stability experiment (blue and green symbols and brackets in Figure 3-18 E;  $p = 0.014$  and  $0.001$ , respectively). These observations were not affected by the ageing of the coatings (c.f. blue and green symbols and brackets in Figure 3-18 E).

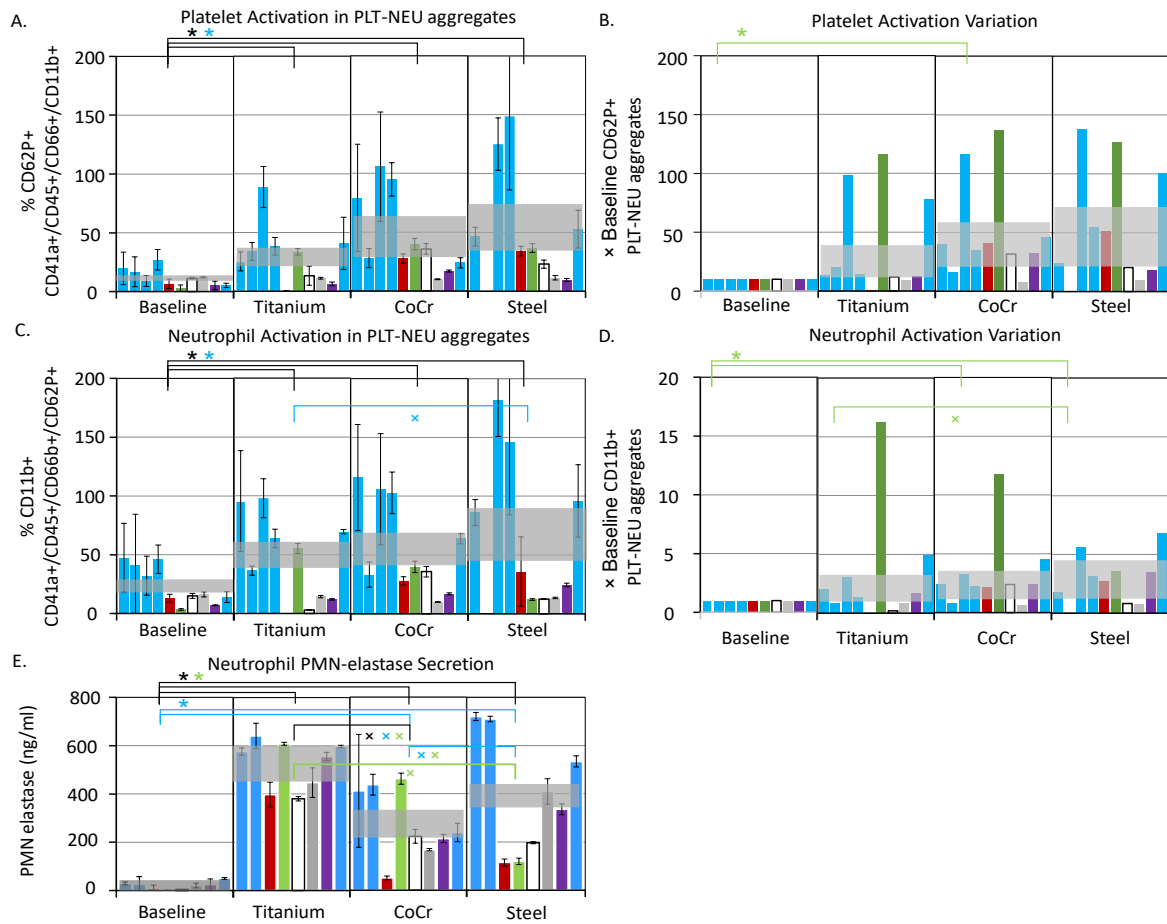


Figure 3-18. The activation state of platelets and neutrophils in the platelet-neutrophil aggregates. (A), (B). Flow cytometric evaluation of platelet activation in the PLT-NEU aggregates by quantifying CD62P expression. (C), (D). Flow cytometric evaluation of neutrophil activation in the PLT-NEU aggregates by quantifying CD11b expression. (E) Neutrophil activation evaluated by quantifying PMN elastase levels.

In (A) and (C), the data are presented in terms of the fraction of CD62P+ or CD11b+ positive events on the CD41a/CD45+/CD66b+/CD11b+ or CD41a/CD45+/CD66b+/CD62P+ populations, normalized by the same fraction in PMA-treated samples (positive controls). In (B) and (D), the same data are further normalized by the baseline levels to obtain fold-changes over the baseline.

Error bars in (A), (C) and (D) are standard deviations. Gray horizontal regions are means calculated over all of the donors; their widths correspond to the standard error of the mean in each condition. Different donors are indicated by the differently colored bars. The color code is the same as in the other figures of this Chapter. The corresponding experiments appear in Table 3-1. Experiments are presented in the order they were performed so that the effect of ageing of the channel coatings could be examined. Statistical significance of the differences between the baseline and the materials was evaluated with the paired two-sample t-test (asterisks). That for the difference between the different materials—with the unpaired two-sample equal-variance t-test (crosses). This was done for all of the donors (black symbols and the corresponding brackets), the KIT donor (light blue symbols/brackets) and the KIT donor without the last “stability” experiment (green symbols and brackets).

### 3.7.3 Quantitative evaluation of complement activation

Finally, the effects of the three materials on complement activation were evaluated. This was done by quantifying the formation of sC5b-9, the final complex of the complement cascade.

Figure 3-19 shows the results of the quantification.

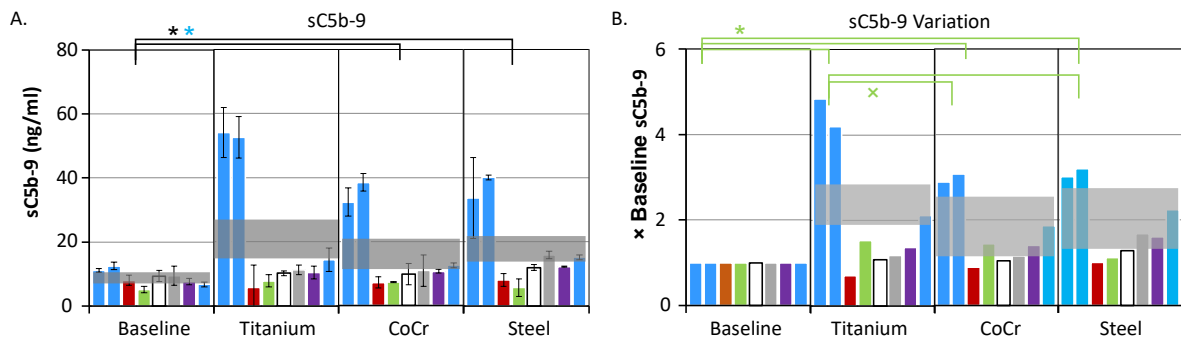


Figure 3-19. Complement activation: levels of sC5b-9. (A). Plasmatic sC5b-9 levels in ng/ml. Error bars are standard deviations. (B). sC5b-9 levels normalized to the baseline values. The color code is the same as in Figure 3-9 on page 59: the color of each bar represents a unique donor and experiments are presented in the order they were performed. The corresponding experiments appear in Table 3-1. Gray horizontal bars are means calculated over all of the donors; their widths correspond to the standard error of the mean in each case. Asterisks indicate statistically significant ( $p \leq 0.05$ ) baseline-material differences evaluated with the paired two-sample t-test; crosses—statistically significant ( $p \leq 0.05$ ) differences between materials evaluated with the unpaired two-sample equal variance t-test. Their colors, and those of the corresponding brackets, refer to the donors over which the statistical significance was evaluated: black, all donors; blue, KIT donor (light blue bars); green, KIT donor (light blue bars) without the last experiment to evaluate the effect of ageing.

It is evident from the results shown in Figure 3-19 that contact with the three materials induces complement activation. The effect is statistically significant in the case of CoCr and steel (black asterisks in Figure 3-19A;  $p = 0.04$  and  $0.021$ , respectively) despite rather drastic variation between the donors, but the donor-to-donor variation obscures the differences between materials ( $p = 0.3, 0.4, 0.4$  for the differences between Ti and CoCr, Ti and steel, CoCr and steel, respectively, evaluated for all the donors).

Material ageing also has a significant effect on complement activation. This can be inferred from the analysis of the results of the experiments conducted with one donor (light blue bars in Figure 3-19). Here, only the baseline/CoCr and baseline/steel differences were found to be statistically significant (light blue asterisk in Figure 3-19 A,  $p = 0.038$  and  $p = 0.050$ , respectively), but not baseline/Ti ( $p = 0.058$ ) or differences between materials ( $p = 0.23, 0.26$ ,

0.46 for the differences between Ti/CoCr, Ti/steel and CoCr/steel, respectively). On the other hand, when the results of experiments conducted with the blood from this donor are evaluated without the last (stability) experiment (green asterisk, cross, and the corresponding brackets in Figure 3-19 B), the changes between the baseline and all of the three materials become statistically significant ( $p = 0.011$ ,  $0.033$ ,  $0.032$  for the difference between baseline and Ti, baseline and CoCr, and baseline and steel, respectively), and so do the differences between Ti and CoCr and Ti and steel ( $p = 0.015$  and  $0.019$ , respectively; for CoCr-steel,  $p = 0.038$ ), despite a smaller number of experiments. This indicates that material ageing effects on complement activation are significant for Ti and CoCr. Interestingly, ageing decreases the level of complement activation as measured with the sC5b-9 levels. Indeed, the levels of this molecule become very low in the experiments performed in Teltow and the last KIT stability experiment.

### 3.8 Morphological effects of ageing of the shear channel coatings

During the experiments with the shear channels, we noticed deterioration of the inner channel surfaces with each subsequent experiment. It was particularly noticeable with steel. We therefore acquired microscopy images of the coated channels. Figure 3-20 shows the state of the titanium, CoCr and steel coatings when the shear channels were freshly coated (Figure 3-20 top) and after repetitive use of the shear channels in six experiments during approximately 8 months (Figure 3-20 bottom).

The surfaces of the freshly coated shear channels show small defects, particularly visible on steel (Figure 3-20 E). After repetitive use, the surfaces exhibit white structures as well as pits channel surfaces. They are small but numerous for titanium and CoCr coatings (visible as white spots in Figure 3-20 B and D). On steel coating, the damage to the surface is far more significant. Larger scratches and pits are visible, and they exhibit an orange color, possibly reflecting the remaining blood (Figure 3-20 F).

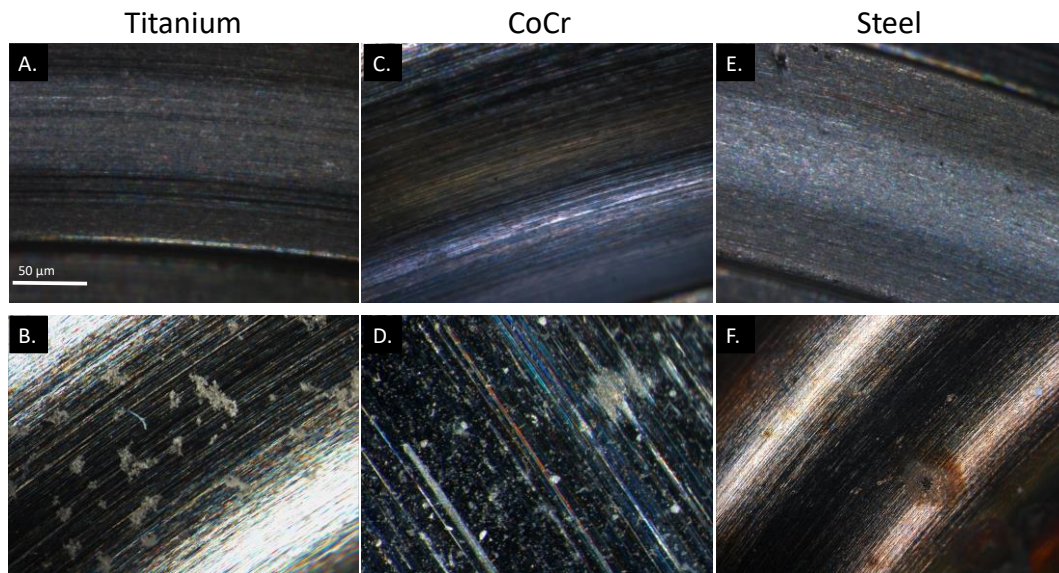


Figure 3-20. State of the coatings. Top: freshly coated shear channels. Bottom: aged shear channels. Images of the titanium (A and B), CoCr (C and D) and steel (E and F) coated channels.

### 3.9 Summary of the statistically significant material-induced changes in the blood activation according to the assay parameters measured in the study

Table 3-4 summarizes the significant differences in the measured parameters with respect to the baseline, between materials, and induced by the ageing of the coatings.

PARAMETER/ MATERIAL	BASELINE			MATERIAL DIFFERENCES			AGEING		
	Ti	CoCr	Steel	Ti/Cr	Ti/steel	CoCr/steel	Ti	CoCr	Steel
<b>PLT COUNTS</b>	–	–	–	<i>Not tested</i>	<i>Not Tested</i>	<i>Not Tested</i>	Yes	Yes	Yes
<b>TAT</b>	*	*	*	ns	*	ns	No	Yes	No
<b>PLT ACTIVATION</b>									
<b>CD62P</b>	ns	*	*	ns	ns	ns	No	No	No
<b>BTG SECRETION</b>	*	*	*	ns	ns	*	?	Yes	No
<b>PLT-LEU</b>	*	*	*	ns	ns	ns	No	No	No
<b>PLT-MON</b>	ns	ns	ns	ns	ns	ns	No	Yes	?
<b>PLT-NEU</b>	*	*	*	ns	ns	ns	No	No	No
<b>PLT ACTIVATION IN PLT-LEU AGGREGATES</b>									
<b>PLT-MON</b>	ns	*	*	ns	*	ns	No	No	No
<b>PLT-NEU</b>	*	*	*	ns	ns	ns	No	No	No
<b>INFLAMMATION</b>									
<b>MON ACTIVATION</b>	ns	*	*	ns	*	ns	No	Yes	No
<b>NEU ACTIVATION</b>	*	*	*	ns	ns	ns	No	No	No
<b>PMN ELASTASE RELEASE</b>	*	*	*	*	*	ns	No	No	Yes
<b>COMPLEMENT</b>	ns	*	*	ns	ns	ns	Yes	No	Yes

Table 3-4. Material-induced blood activation: summary of the effects observed in this study. “\*” stands for significant increase; “–” stands for significant decrease. “Yes” and “no” refer to the effects of the aging.

### 3.10 Discussion

The work reported in this chapter pursued several goals. The first goal was to examine differences in the way different metallic materials activated the hemostatic and inflammatory defense systems when brought into contact with whole human blood *ex vivo*. To do this, I evaluated the activation of the coagulation, platelets, inflammation and complement. The second goal was to evaluate different parameters that were measured with respect to their sensitivity, both to the experimental variables such as material chemistry, and to the noise factors such as the variation in the results between experiments performed with the blood obtained from different donors.

The third goal was to shed light on the mechanism by which materials activate these systems. Here, we note that we used a number of different assays to measure various activation responses; for example, platelet activation was evaluated by measuring  $\beta$ -TG release, CD62P expression, and platelet-leukocyte aggregation; inflammatory responses were measured by evaluating monocyte and neutrophil activation in PLT-LEU aggregates as well as by evaluating PMN-elastase release and complement activation; while all of these parameters reflect platelet activation or inflammatory responses, there are mechanistic differences between them. We consider these differences in terms of the mechanism of blood-biomaterial interactions.

When evaluating the experimental data that were finally obtained against these goals, we encountered a complication: we found a time-dependent process, referred as to “ageing”, that manifested itself as a change in the measured parameters from one experiment to the next, and a decrease in sensitivity of the experiments to the differences between the materials. This, and other limitations of the assay, will also be addressed in this section.

Finally, the *in vitro* hemocompatibility testing system we used—the shear channels that were shaken to prevent red blood cell sedimentation rather than rotated to induce shear—differs from the conventional approach of mimicking the physiological situation adopted by most authors, and I therefore comment on the general validity of our conclusions with respect to other studies and the physiological situation. I refer to our system as “quasi-static”, because shaking prevented RBC sedimentation, but did not induce shear typical of the dynamic systems (e.g, Chandler loop).

### 3.10.1 Differences between materials and the evaluation of the most sensitive assay parameters

The first inescapable conclusion is that all materials activate all defense systems: titanium, CoCr, and steel all lead to thrombin generation, platelet activation, and inflammatory responses above the baseline levels. This conclusion is consistent across multiple donors and is independent of the way in which various activation parameters were evaluated. As such, it correlates with the clinical situation and validates our approach to measuring blood-biomaterial interactions in the quasi-static shear channel system. This point is discussed in more detail further below.

The second, and the most important, conclusion of this work is that there are differences in the way the three different materials—Ti, CoCr, steel—activate blood. These differences are manifested in several respects. Statistically significant differences in the level of thrombin production between titanium and steel were observed across multiple donors (Figure 3-10 and Table 3-4). Perhaps the most striking example of the difference between materials is visible in the flow cytometry scatter plots shown in Figure 3-14: blood contact with titanium vs. that with steel or CoCr induces different patterns of platelet activation and aggregation. Unfortunately, this effect was only manifested in the experiments performed at KIT with the blood from one donor. On the other hand, when I quantitatively evaluated platelet activation by measuring CD62P expression, I found that titanium did not induce a significant increase in the CD62P expression, but CoCr and steel did. This difference between Ti and CoCr or steel was observed when the measurements performed with all of the donors were taken into account and is therefore robust (Figure 3-15 A and B).

When evaluating the levels of CD62P expression induced by the three materials, no statistically significant differences were observed. At the first glance, this leads to a paradox: when evaluating baseline-material differences, Ti behaves differently from the two other materials, but when evaluating material-material differences, this conclusion is not confirmed. This situation arises from the fact that baseline-material differences are correlated (their statistical significance is evaluated with a paired t-test corresponding to the levels measured “before” and “after” the exposure of the material to blood), but material-material differences are independent, and are therefore more susceptible to the noise arising from donor-to-donor variation and other sources. Sources of the noise in my assay are discussed in section 3.10.3 “Limitations of the study”. In what follows, I discuss both the significance of the baseline-

material differences and material-material differences; the most robust assay parameters are the ones that are sensitive to both, but the baseline-material differences are assigned a greater significance due to the above argument (they are less susceptible to the noise).

In my assay, platelet activation was evaluated in several different ways, and it is interesting to consider differences between them. In particular, platelet consumption is a parameter that has been considered useful for over 70 years of evaluating materials both *in vivo* and *in vitro*. Arguably, it is the only parameter that was shown to correlate between *in vitro* and *in vivo* experiments, reflecting both the degree of platelet adhesion to the materials and platelet aggregation in solution (thrombotic and embolic potentials of the material in the language of Kusserow,<sup>134</sup>).<sup>131,135</sup> My observations confirm that this parameter is indeed sensitive: there is a consistent drop in the platelet counts upon exposure of blood to the materials for all experiments, all materials, and all donors; subtle differences between materials are also evident: CoCr appears worse (greater decrease) than titanium or steel for all experiments, while titanium is worse compared steel (Figure 3-9). Platelet consumption is sensitive to the ageing of the coatings, because it becomes worse with every subsequent experiment, revealing changing in the material composition.

Platelet activation as measured by  $\beta$ -TG release turned out to be entirely insensitive to the difference between materials but somewhat sensitive to the effect of ageing (Figure 3-15 C, D and Table 3-4).  $\beta$ -TG level was high for all materials and all donors, and decreased with the ageing of the coatings. At least in some of the studies reported in the literature the release of  $\beta$ -TG was always high on all materials without marked differences between them.<sup>131</sup> Significant differences in the release of  $\beta$ -TG were found in some cases, e.g., between materials with very high and very low thrombogenic propensities, such as Cu-coated and Parlyne C-coated stents (but these materials are not used in clinical practice).<sup>188,189</sup> Furthermore, *in vivo* results show that high levels of  $\beta$ -TG are observed in trauma patients, PCI and in perioperative myocardial infarction following CABG, and aspirin administration fails to lower  $\beta$ -TG levels.<sup>190-192</sup> In one of these studies, it was noted that  $\beta$ -TG levels in trauma patients were invariably high even though the levels of other platelet activation markers, such as PF4, varied.<sup>191</sup> The same study noted a correlation between  $\beta$ -TG level and inflammation. All together, these observations raise questions concerning the sensitivity of  $\beta$ -TG measurements to subtle differences between materials.

Platelet aggregation with leukocytes, monocytes and neutrophils is another interesting parameter to measure platelet activation. There has been some discussions in the literature that PLT-MON aggregates are more sensitive to PLT activation than parameters such as CD62P expression.<sup>193 194</sup> However, not all authors agree. I would like to first note that in the baseline samples, the PLT-MON, and more generally, PLT-LEU aggregate levels, are much higher, than CD62P levels (Figure 3-15 and Figure 3-16). This is particularly evident in the case of the KIT donor, where the baseline activation is relatively high, on the order of 20 – 25% (light blue bars in Figure 3-15 E). In that regard, aggregate formation does appear to be more sensitive to platelet activation than CD62P expression level.

Secondly, neither platelet-leukocyte nor platelet-monocyte aggregates reveal differences between materials (Figure 3-16 A, B and Table 3-4). The parameter that was sensitive to the differences between the materials is the activation of platelets in the aggregates with monocytes, both when baseline-material difference and material-material differences are considered (Figure 3-17 A and Table 3-4). Titanium is the only material not causing a significant increase in the level of PLT activation in the PLT-MON aggregates relative to the baseline level. A significant difference between Ti and CoCr was also noted. These conclusions are confirmed for all the donors.

Platelet-neutrophil aggregate levels increase on all materials but do not reveal any differences between them (Figure 3-16 C and D). The same trend is observed for platelet activation in the aggregates with neutrophils (Figure 3-18 A). These conclusions are also confirmed across all of the donors.

Further differences between materials were observed when evaluating inflammatory responses. These were evaluated in terms of PMN elastase release, complement activation, and the activation of monocytes and neutrophils in PLT-LEU aggregates. PMN-elastase release was higher on titanium than on CoCr or steel (Figure 3-18 E); this effect was consistent across multiple donors and independent from the ageing. However, the aging effects is visible on steel, on which the levels of PMN-elastase decrease over time. The evaluation of complement activation reveals that titanium does not induce a significant increase compared to the baseline, but CoCr and steel do. However, there are no differences between materials, partially due to donor-to-donor variation and partially due to aging effects that manifest themselves as a reduction in the measured levels of sC5b-9 for all materials. In the literature, an increase in PMN-elastase and complement is reported on different materials, polymeric

and metallic, without any marked differences.<sup>188,189</sup> The same effects as for the complement are visible for monocyte activation in the aggregates with platelets: while titanium does not cause an increase, CoCr and steel do. Further, monocyte activation reveals significant differences between titanium and CoCr across the multiple donors. The effects of aging can also be observed on CoCr. On the contrary, the activation of neutrophils in the aggregates was significantly increased on all materials, but reveals no difference between materials. Notably, the activation levels of neutrophils in platelet-neutrophil aggregates were lower than of monocytes in the platelet-monocyte aggregates. Also, the effects of aging are not visible for neutrophil activation. The activation of monocytes in PLT-MON aggregates appears to be the most sensitive parameter in revealing differences between materials. This conclusion is supported by similar findings, when material hemocompatibility is tested under shear.<sup>195</sup> This supports the idea put forth in the literature that PLT-MON aggregates represent an important factor reflecting hemostatic-inflammatory axis connection in vivo.<sup>193</sup>

In summary, my results highlight the different propensities of metallic materials in inducing hemostatic and inflammatory blood responses. Particularly, titanium appears to be the best material in respect to the activation of the coagulation and platelets as measured by CD62P expression and aggregation with leukocytes. However, it induces a high secretion of  $\beta$ -TG from platelets just like the other two materials, and high pro-inflammatory responses (as measured as PMN-elastase and sC5b-9 generation), higher than the other two materials. CoCr and steel appear to be similarly highly thrombogenic (more so, than the Ti) and pro-inflammatory (less so than the Ti).

In the context of identifying the most sensitive parameter for revealing differences between materials, the activation of platelet-monocyte aggregates as measured by CD62P and CD11b expression appears to be the most sensitive parameters for the evaluation of material performance. Contrary to the other parameters measured, the activation of platelet-monocyte aggregates was the only one able to reveal differences between materials, independently of the donor-to-donor variation and aging of the coating. Supporting this conclusion, an increase in the level of the circulating platelet-leukocyte aggregates has been observed in different cardiovascular diseases, such as stable and unstable angina, myocardial infarction, and in patients undergoing percutaneous coronary interventions and heart valve

replacement; in addition, platelet-leukocyte aggregate level is a predictive index of acute re-occlusion following coronary angioplasty.<sup>193,196,197</sup>

I expect that the assay parameters, such as PLT-MON aggregation and activation, reveal differences between material surface chemistry. Indeed, XPS analysis of the coatings (Figure 3-4, Figure 3-5, Figure 3-6 and Figure 3-7) reveals that the materials are chemically different. The three coatings I used were prepared by sputtering on the identically polished Al channels. Therefore, the differences in roughness are expected to be minimal. Supporting this interpretation are several observations. Firstly, CoCr and steel coatings behaved similar in several tests but different from Ti. Indeed, steel and CoCr coatings are more similar to each other, both having the chromium oxide species on their surface, than to Ti, which only has TiO<sub>2</sub> (c.f. Figure 3-5 with Figure 3-6 and Figure 3-7). Secondly, ageing in most cases led to the loss of the ability to distinguish between materials. This would be expected as effects of roughness and perhaps the appearance of the underlying Al of the channel base reduced the differences due to material chemistry.

### 3.10.2 Blood-material interaction mechanisms

I now turn to the discussion of the activation mechanisms on the different materials. To this end, I introduce the correlation plots, where the relationships between the different parameters are examined. For example, it is known that most of the thrombin that is produced during coagulation is produced at the platelet membranes. Therefore, it is interesting to examine the relationship between thrombin production and platelet activation. In Figure 3-21, I plot the thrombin generation as a function of the various platelet activation and inflammatory response markers. Surprisingly, it turns out that thrombin generation is not correlated with platelet activation measured in terms of  $\alpha$ -granules secretion (CD62P expression or  $\beta$ -TG release). What it does correlate with is platelet-leukocyte ( $R^2=0.8$ ), PLT-MON ( $R^2=0.8$ ) and PLT-NEU aggregates levels ( $R^2=0.9$ ) (Figure 3-21 B-D). Thrombin production was also found to correlate with the activation of platelets and monocytes in PLT-MON aggregates ( $R^2=0.9$  and  $0.8$ ), and platelets and neutrophils in PLT-NEU aggregates ( $R^2=0.9$  and  $0.9$ ) (Figure 3-21 E-H). We can conclude that thrombin production correlates not with the PLT activation alone (at least when it is measured by focusing on  $\alpha$ -granule secretion), but with reactions that involve both platelet activation and cellular inflammatory responses. On the other hand, thrombin production did not show a clear correlation with PMN-elastase release

from granulocytes (but it is interesting that titanium stands apart from the trend that is apparent when the baseline, CoCr and steel data are considered, see Figure 3-21 J), while complement activation and thrombin production were anti-correlated (Figure 3-21 K), pointing to the complexity in the interplay between the different pathways and their measurement parameters.

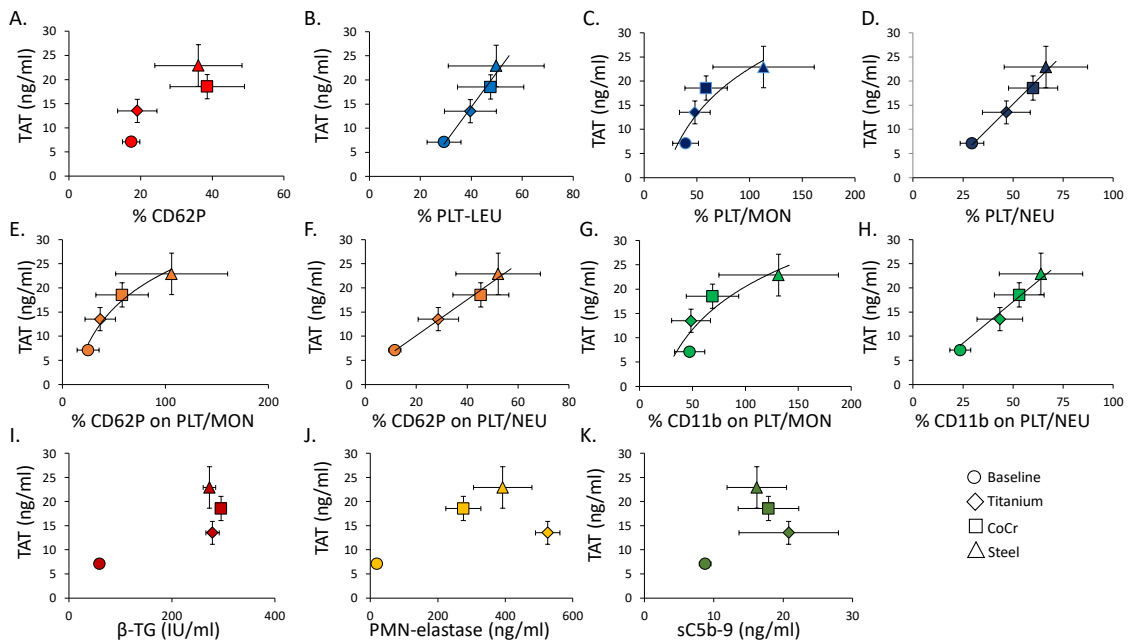


Figure 3-21. Thrombin generation versus platelet activation and inflammatory responses. The generation of thrombin is plotted versus A. CD62P expression, B. platelet-leukocyte aggregates, C. platelet-monocyte aggregates, D. platelet-neutrophil aggregates, E. CD62P expression on platelets in the aggregates with monocytes, F. and in the aggregates with neutrophils, G. CD11b expression on monocytes and H. on neutrophils in the aggregates with platelets, I. secretion of  $\beta$ -TG, J. release of PMN-elastase and K. generation of sC5b-9.

Similar correlations can be examined for the various ways of evaluating PLT activation (Figure 3-22). The secretion of  $\beta$ -TG is not correlated with the expression of CD62P or the aggregation with leukocytes (Figure 3-22 A-H), because its release is always high.

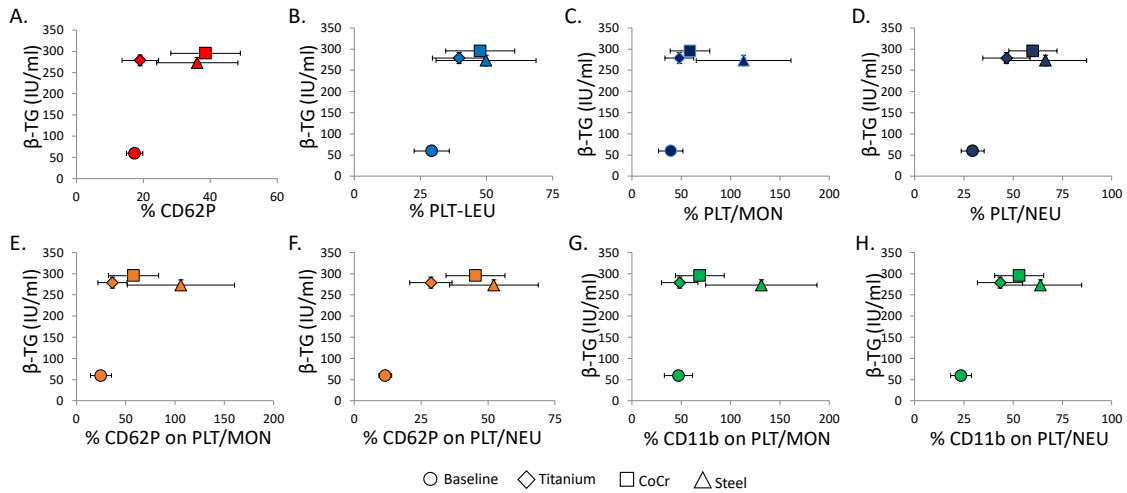


Figure 3-22. Correlation between different ways to evaluate platelet activation. The secretion of  $\beta$ -TG from activated platelets is plotted versus A. CD62P expression, B. platelet-leukocyte aggregates, C. platelet-monocyte aggregates, D. platelet-neutrophil aggregates, E. CD62P expression on platelets in the aggregates with monocytes, F. and in the aggregates with neutrophils, G. CD11b expression on monocytes and H. on neutrophils in the aggregates with platelets.

The link between inflammation and platelet activation can be examined by evaluating the correlations between inflammatory factors—such as PMN elastase release or sC5b-9 generation—and platelet activation factors (Figure 3-23 and Figure 3-24). For PMN-elastase release and complement activation, there is no correlation with the CD62P expression, platelet aggregation with monocyte and neutrophils, activation of the aggregates, or  $\beta$ -TG release (Figure 3-23 A-I, and Figure 3-24 A-I). Similarly to thrombin/PMN-elastase correlation, titanium stands apart from the trend visible for baseline, CoCr and steel in Figure 3-21 J. My measurements therefore do not reveal a correlation between inflammatory pathway activation and platelet activation as measured by the  $\alpha$ -granule release.

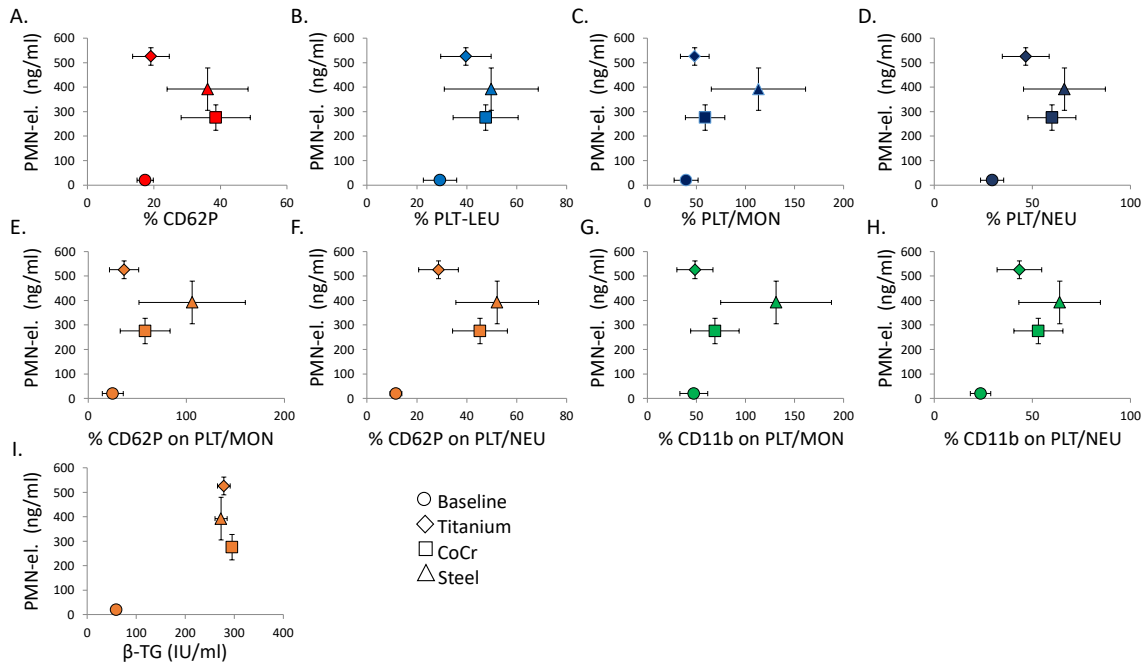


Figure 3-23. PMN-elastase release versus platelet activation. The release of PMN-elastase from granulocytes is plotted versus A. CD62P expression, B. platelet-leukocyte aggregates, C. platelet-monocyte aggregates, D. platelet-neutrophil aggregates, E. CD62P expression on platelets in the aggregates with monocytes, F. and in the aggregates with neutrophils, G. CD11b expression on monocytes and H. on neutrophils in the aggregates with platelets and I. secretion of  $\beta$ -TG.

Finally, the two ways of evaluating the inflammation—PMN-elastase release and sC5b-9- do correlate with each other ( $R^2=0.9$ ) (Figure 3-24 J), as expected.

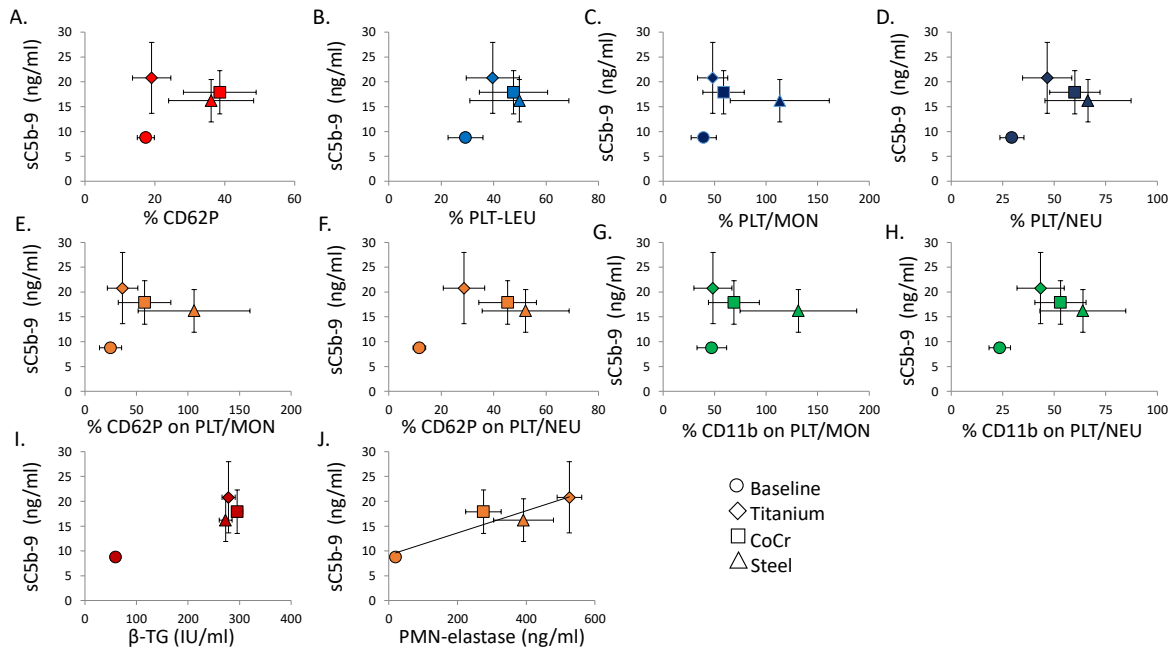


Figure 3-24. sC5b-9 generation versus platelet activation and PMN-elastase release. The generation of sC5b-9 is plotted versus A. CD62P expression, B. platelet-leukocyte aggregates, C. platelet-monocyte aggregates, D. platelet-neutrophil aggregates, E. CD62P expression on platelets in the aggregates with monocytes, F. and in the aggregates with neutrophils, G. CD11b expression on monocytes and H. on neutrophils in the aggregates with platelets, I. secretion of  $\beta$ -TG and PMN-elastase release. A-H were measured by flow cytometry. I-J were measured by ELISA assay. The full colored makers indicate the results with the freshly coated shear channels, while the open markers the results with the aged shear channels with the blood from one donor. The patterned markers indicate the results from multiple donor.

The above correlation analysis can be looked at from two perspectives. On one hand, it emerges that  $\alpha$ -granule secretion markers such as CD62P or  $\beta$ -TG are not the right ones to evaluate platelet activation in the context of biomaterial reactions, because they are not correlated to thrombin production or inflammation. Indeed, others have also remarked on the lack of correlation between CD62P expression,  $\beta$ -TG secretion, and coagulation.<sup>198</sup> From this perspective, the most robust parameters characterizing blood activation by the materials are, once again, PLT-LEU aggregates, particularly PLT-MON aggregates and their activation as measured by the expression of CD62P and CD11b (Figure 3-21 C-H), because they correlate with the thrombin levels.

On the other hand, the connection between coagulation, platelet activation, and inflammation evident at the level of platelet aggregation with leukocytes (monocytes and neutrophils) and in the degree of their activation points to a biological mechanism. Indeed, in the literature, this connection is explained by the fact that the aggregation of platelets with monocytes and neutrophils through CD62P induces TF expression on the leukocytes. The

aggregates expressing TF are therefore directly related to thrombin generation, since TF is an initiator of the coagulation cascade (Figure 1-5 on page 13 in the Introduction).<sup>197,199</sup> Furthermore, platelet-monocyte and platelet-neutrophil aggregates, but not neutrophils or monocytes alone, bind FXa and fibrinogen. The binding is dependent on the adhesion of platelets to these cells.<sup>200</sup>

The anti-correlation between the thrombin generation and complement activation was surprising. This observation is against what is currently known about the interplay between the two systems: for example thrombin is known to cleave factor C3, C5 and C6 and so contributing to the amplification of the complement cascade.<sup>45</sup> Therefore, I cannot entirely explain the observed anti-correlation. Ageing of the coatings may have contributed to this observation, because it leads to the decrease in the levels of sC5b-9 measured in each subsequent experiment (Figure 3-19).

### 3.10.3 Limitation of the study

As any study, this one has several limitations. Firstly, I observed a consistent decrease in the parameters measured in Teltow (multiple donors) compared to those measures at KIT (one donor). In particular, the decrease is visible for CD62P expression (Figure 3-15 A), platelet aggregation with leukocytes (Figure 3-15 E), monocytes and neutrophils (Figure 3-16 A and C), activation of the platelet-leukocyte aggregates as measured by CD62P and CD11b expression (Figure 3-17 A, C for monocytes and Figure 3-18 A, C for neutrophils), and for the complement (Figure 3-19). The ageing process we describe in detail below is partially responsible for this. This is visible from Figure 3-15 A and B, which shows that CD62P expression levels decrease when blood from the same donor is allowed to contact aged vs. fresh shear channels. The decrease does not occur for the platelet-leukocyte aggregates (Figure 3-15 E and F). Therefore, ageing does not entirely explain the consisted decrease observed in the measured parameters. Another potential cause of this effect could be the differences in the starting activation levels (particularly evident for platelet-leukocyte aggregates-Figure 3-15 E and F). In the same vein, the differences in the starting activation levels do not appears for thrombin generation,  $\beta$ -TG secretion, PMN-elastase release and complement activation (Figure 3-15 C, Figure 3-18 E, and Figure 3-19) . The conclusions that are not affects by these problems are: thrombin generation,  $\beta$ -TG secretion, PMN-elastase release, CD62P and CD11b expression on platelet-monocyte aggregates.

The effect we call ageing represents another serious limitation of the study. Microscopy images of the channels show white structures and pits of different on Ti, CoCr and steel coatings (Figure 3-20 B, D and F). It appears that a combination of factors is responsible for this process. Firstly, the cleaning procedure (section 2.7.3 in the Materials and Methods) might not be sufficiently effective in removing traces of blood. The white structures might be traces of the clots consequent to blood exposure that are not removed by the washing (F. Jung, personal communication). More aggressive washing procedures were not possible to perform, as they tend to strip the sputtered coatings. The presence of pits is essentially an artifact of the procedure used to prepare the channels themselves, although it is noteworthy that the pits are more severe on the steel-coated shear channel (Figure 3-20 A, C and F). The pits may become damaged by the macrophages over time, explaining the visual deterioration we observed. Orange color also indicates that the washing procedure was not efficient. In retrospect, it would have been better to make the shear channels out of the different materials rather than coat the surfaces with the materials of interest, but the cost of such an approach was beyond the means of our laboratory. Another approach would be to re-polish and re-coat the channels before every experiment; this is also costly and prohibitively time consuming. This does, however, point to how careful one must be in designing hemocompatibility studies.

The shear channel approach is also limiting in the sense that their surfaces cannot be easily analyzed either by the biological or physical methods due to the sheer size and weight of the channels. Finally, the small number of different materials tested could also be considered a limitation.

#### 3.10.4 Experimental model

Finally, I comment on the validity of our conclusion using the “quasi-static” shear channel model with respect to other studies and physiological conditions.

The current dogma dominating the hemocompatibility field is that studies under flow are needed to evaluate blood-biomaterial interactions, because they mimic the physiological shear. The origin of the dogma is the regulation of platelet activation and adhesion under shear: different shear forces regulate the activation of vWF and of many platelet receptors (for example GPIb responds to high shear stress).<sup>201</sup> Also, under flow platelets are concentrated near the vessel wall.<sup>202</sup> Therefore, various in vitro circulation systems are widely

used in hemocompatibility studies. However, there are arguments against the dogma, as well. The question is not settled and below I discuss the different points of view.

Two types of *in vitro* circulation systems have been used extensively: the modified Chandler loop (Figure 3-2 on page 53 in the Results section) and the roller pump closed-loop system.

All of them include PVC tubing in which the material to be tested is inserted. The systems are rotated during the testing and the blood circulation through the tubing is implemented by air inside the system. The common drawbacks of these systems are: the blood contact with two materials and the presence of the air bubble. Both results in measurement artifacts. On rotation, the air bubble repetitively contacts the test material causing protein denaturation and damaged to the blood elements (platelet and leukocyte activation, detachment of the adhering blood cells). The rolled pump closed-loop system presents a further problem: the damaged of the blood elements caused by the pump.<sup>146</sup> For this reason, this system is suitable only for short-time testing, being not sensitive to reveal differences between materials. Evolution of these model systems is the hemobile: a simple mechanical device which generates a semicircular movement. Additionally, it does not contain air bubble. In this way is attempted to reduce the damaged and activation of the blood elements. In the system is applied a pulsatile flow in a frequency similar to the arterial circulation. The hemobile was compared with the Chandler loop and the roller pump, showing promising results.<sup>145</sup>

On the other hand, quasi static system models for testing material hemocompatibility are also used. The so called "screening chamber" represent an example. It consists of two stainless-steel cover plates that are screwed together to fix the test surface. A PTFE spacer forms a cavity in which the blood is exposed to the test materials. The system is shaken in an incubator to avoid red blood cell sedimentation.

Comparison of the quasi static with the *in vitro* circulation model did not show any significant advantages of the *in vitro* circulation model over the quasi-static one. The advantage of the more realistic application of flowing blood in the perfusion setup is in certain cases interfered with by the increased activation of the blood, which may reduce the sensitivity of the testing.

151

The shear channel I use in this study is a quasi-static model: it is not rotated but the sedimentation of the red blood cells is avoided by agitation. It has been developed to overcome the drawbacks of the Chandler loop system. In the shear channels the blood contacts only one material (because the entire inside of the channel is coated with the

material of interest). The system still contains the air/blood interface, but now the interface does not encounter the entire surface of the material but is restricted to its small fraction as the interface oscillates during the agitation. In the Chandler loop, the passage of the air/blood interface across all of the material would be expected to lead to the denaturation of the surface adsorbed proteins and in this way contribute to the noise in the hemocompatibility measurements. Some amount of air is nevertheless required to decouple the fluid (blood) from the surface. Ratner pointed out repeatedly that the ability to evaluate material hemocompatibility comes down to a signal-to-noise problem.<sup>131</sup> Approaches to minimize the noise are therefore important, and our system represents an example of a noise minimization strategy; perhaps this contributed to our ability to distinguish between materials.

In summary, there is universal agreement that red blood cell sedimentation has to be avoided, but beyond that, in my view, the jury is still out whether shear flow is actually needed for the testing. Indeed, my results with the quasi-static system show significant blood-biomaterial activation effects and the ability to distinguish between similar materials. Moreover, the results obtained are comparable with the *in vitro* and *in vivo* observations, among of them platelet count and the higher sensitivity of platelet-monocyte aggregates.<sup>131,193</sup>

### 3.11 Conclusion

In summary, taken together the results shows that this whole-blood quasi static test allows to distinguish between materials in inducing hemostatic and inflammatory responses. Titanium appears to be superior to CoCr and steel. I found that the most sensitive parameters in revealing such differences was the activation of platelet-leukocyte aggregates. Platelet consumption appeared to be sensitive to the material properties, as the most sensitive in revealing the effects of the ageing coatings. On the contrary, platelet activation markers such as CD62P expression and  $\beta$ -TG secretion are not the right ones to distinguish between materials. These conclusions are supported by the correlation plots. They also reveal interesting insights in the activation mechanisms on the materials. In particular, the interplay between the coagulatory and inflammatory responses clearly emerges from the correlation of platelet-leukocyte aggregates with thrombin generation. Finally, these results are comparable with other *in vitro* and *in vivo* observations.

## 4. Testing: a simple in vitro test for distinguishing between materials

### 4.1 Summary

In this Chapter, I present a simplified and rapid *in vitro* procedure for testing blood-biomaterial interactions. I use a microfluidic approach developed by Cho et al.<sup>181</sup> in which the detachment of platelets from the surface is initiated by applying tangential flow at controlled shear rates. In this way, the strength of the platelet-surface interactions is probed by measuring the shear rate at which 50% of the adhering platelets detached (Det50), and the fraction of adhering platelets that remained on the surface after detachment.

The assay is carried out in PrP. Four model surfaces are tested: glass, TiO<sub>2</sub>, glass functionalized with a hydrophobic Octadecyltrichlorosilane (OTS-glass), and glass functionalized with poly[bis(trifluoroethoxy)phosphazene] (PTFEP), a polymer that has recently generated some interest as a stent coating.<sup>203,204</sup> Microfluidic approaches have primarily been used for studying platelet biology and function in hemostasis, thrombosis and other coagulation pathologies.<sup>147</sup> These approaches have mainly been focused on the evaluation of platelet adhesion, aggregation, and thrombus formation under conditions mimicking the *in vivo* wall shear stress.<sup>147-149,205-207</sup> On the other hand, the application of microfluidic approaches in the context of blood-material interactions has been limited, as I already remarked in the Introduction.<sup>208,209</sup> The parameters typically evaluated in the blood-biomaterial interaction studies focusing on platelet adhesion and activation are platelet spreading and the expression of activation markers. This equally applies to microfluidic and regular studies. On the contrary, the stress needed to detach platelets from the surface has only been investigated in a few studies.<sup>210,211</sup> These studies showed that platelet detachment from the protein-coated surfaces was mainly dependent on the adsorbed protein composition and on the degree of platelet spreading.

As described extensively in the Introduction (section 1.9, page 18) the composition of the protein layer adsorbed at the biomaterial surface is related to the physicochemical properties of the material. Since the attachment strength depends on the adsorbed protein composition,

detachment parameters (Det50 and the remaining platelet fraction) may be suitable for distinguishing between materials with respect to their interactions with the platelets. Therefore the design of the assay presented in this Chapter is based on measuring Det50 and the remaining platelet fraction for platelets interacting with different materials under various conditions. The sensitivity of these parameters to differences between materials is examined, and correlated with the classical activation parameters such as platelet spreading and activation evaluated by measuring CD62P expression on the remaining platelets to establish biological context.

At the molecular level, platelet adhesion is mediated by the classical adhesion receptors expressed on the platelet surface (e.g., GPIIb/IIIa-integrin  $\alpha$ IIb/ $\beta$ 3 for the binding of fibrinogen and vWF, GPVI for the binding of collagen, or GPIb-IX-V for the binding of vWF).<sup>212,213</sup> This is true at the sites of the vascular injury as well as in the case of platelets interacting with the biomaterial surfaces, where the adsorbed protein layers mediate platelet-surface interactions.<sup>214,215</sup> The strength of these interactions depends on the degree and type of platelet activation. For example, platelets reversibly interact with the exposed vWF at the surface of activated ECs through GPIb-IX-V. This interaction activates the platelets, resulting in conformational changes of the platelet integrins, such as GPIIb/IIIa, that mediate irreversible adhesion of platelets at the injury site.<sup>56</sup> Similarly, at the biomaterial surface, platelets become activated and adhere via the irreversible interactions between the activated platelet surface receptors and the proteins adsorbed at the material surface.<sup>216</sup> This sets the biological context of the assay, through the dependence of the adhesion strength on the type and degree of platelet activation. In my assay, platelet activation either occurs spontaneously (by the biomaterial) or is artificially induced (by pre-incubating PrP with a platelet agonist TRAP6). The experimental strategy is described in Figure 4-1. Following the preparation of PrP from whole blood, PrP was characterized for the initial platelet activation and functionality by flow cytometry. PrP was incubated on the testing material surface (glass slides, coated or appropriately modified). Incubation times were either 10 min or 1 hr, and either untreated PrP, or PrP pre-activated with TRAP6, a platelet agonist, was used, in separate experiments. Following the incubation, antibodies against CD41a and CD62P were added to the incubation chambers to stain for platelet identification and activation, respectively. Fluorescence images were recorded to characterize the initial state of the surface. Then the detachment parameters were measured.

Detachment was initiated in two different ways. In one case, referred to as dynamic measurements, the detachment experiment was started by turning on the flow. Flow rate was increased exponentially every 5 seconds, and platelet detachment was recorded. The shear rates varied between 1 and 10 dyn/cm<sup>2</sup> (0.1 and 1 N/m<sup>2</sup>). In the other case, referred to as static measurements, the detachment was initiated with a hand-held pipette. The purpose of the static condition measurements was to further simplify the assay and avoid the use of bulky pumps and pressure chambers associated with the microfluidic experiments.

Finally, the fraction, the area, and the level of fluorescence intensity due to the binding of the anti-CD62P antibody on the remaining platelets were evaluated.

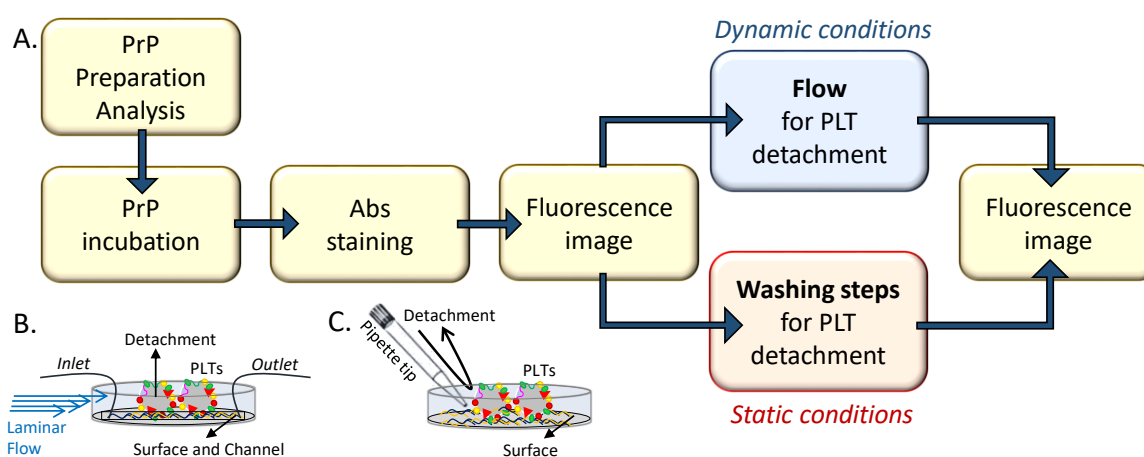


Figure 4-1. Experimental strategy. A. The overall experimental schematic. PrP was prepared from whole blood and the activation state of the platelets in PrP was analyzed by flow cytometry. It was incubated on the surfaces of interest. The incubation was followed by the antibody staining. Fluorescence images characterizing the state of the system were recorded, and then platelet detachment was initiated by turning on the flow under the dynamic conditions or rinsing under the static conditions. Under the dynamic conditions, fluorescence images were continuously recorded. Finally, the state after the detachment was recorded in both cases. B. and C. Schematic illustrations of the dynamic and static experiments, respectively. Platelets are shown as gray spheres.

## 4.2 Surfaces

The preparation and characterization of the surfaces used in this Chapter is described in detail in Chapter 2 (Materials and Methods) in section 2.8.4 at page 40. Briefly, unmodified glass, TiO<sub>2</sub>-coated glass, glass modified with OTS and glass coated with PTFEP were used. OTS-glass and PTFEP-coated glass are hydrophobic,<sup>203</sup> while freshly cleaned unmodified and TiO<sub>2</sub>-coated glass surfaces are hydrophilic; this was judged visually based on the water droplets rolling off

from the hydrophobic surfaces but spreading on the hydrophilic surfaces. The modification of glass with OTS and coating of glass with PTFEP were performed by Dr. Kwan Cho and Dr. Alex Welle according to the procedure published previously.<sup>203</sup>

TiO<sub>2</sub> and glass surfaces were freshly cleaned before each experiment. OTS-glass slides were prepared the night before. PTFEP-coated glass slides were prepared in batches, and stored for a period of less than one week in a desiccator.

XPS spectra illustrating the cleaning of the unmodified glass slides and TiO<sub>2</sub>-coated glass slides, as well as PTFEP coating, are shown in the Appendix. They confirm the surface cleanliness and composition.

### 4.3 Platelet characterization by flow cytometry

PrP was prepared from heparinized whole blood by centrifugation. Prior to each experiment, PrP was characterized by flow cytometry for ascertain initial platelet activation and functionality (Figure 4-2). The activation level and of untreated (UNT) PrP and PrP treated with TRAP6 and PMA was measured with respect to the expression of CD62P ( $\alpha$ -granule marker), CD63 (dense-granule marker) and PS.<sup>56,217</sup> Only the PrP with an activation level < 5% for CD62P and < 20% for both CD63 and PS was used for the experiments.

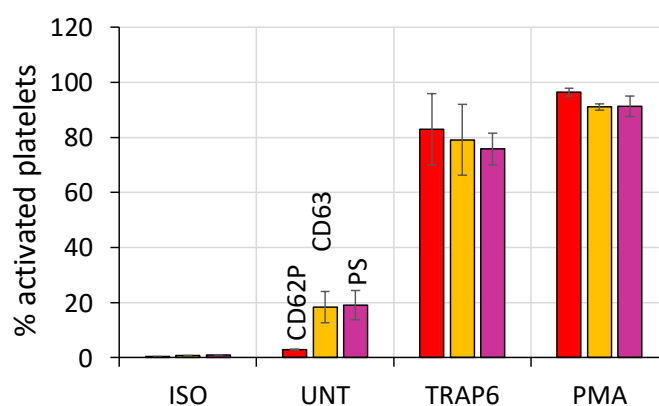


Figure 4-2. Platelet characterization by flow cytometry. The plot shows the initial activation levels and the response to the agonists of platelets in PrP. The results are present as averaged data of eight experiments performed with the blood from four different donors. Red bars: CD62P expression, yellow bars: CD63 expression, violet bars: PS exposure.

## 4.4 Dynamically initiated platelet detachment

After PrP incubation on the material surface, I measured the detachment of platelets by exposing them to the flowing buffer at different shear stresses in a custom-designed microfluidic cell, mounted in the fluorescence microscope (Figure 4-3 A, fluorescence images illustrating platelet detachment). It is evident from the images that the number of platelets adhering on the surface decreases with the increasing shear stress. The fraction of platelets remaining at the surface at each shear stress was calculated (Figure 4-3 B). From these detachment curves, it is evident that there are differences between conditions in terms of the final number of remaining platelets as well as in terms of the stress at which platelets detach (c.f. TRAP6-treated and untreated platelets, for example). Det50 and the remaining platelet fractions, measured from such curves, averaged over six experiments with blood from four different donors, are shown in Figure 4-3 C and Figure 4-3 D for the different materials and experimental conditions.

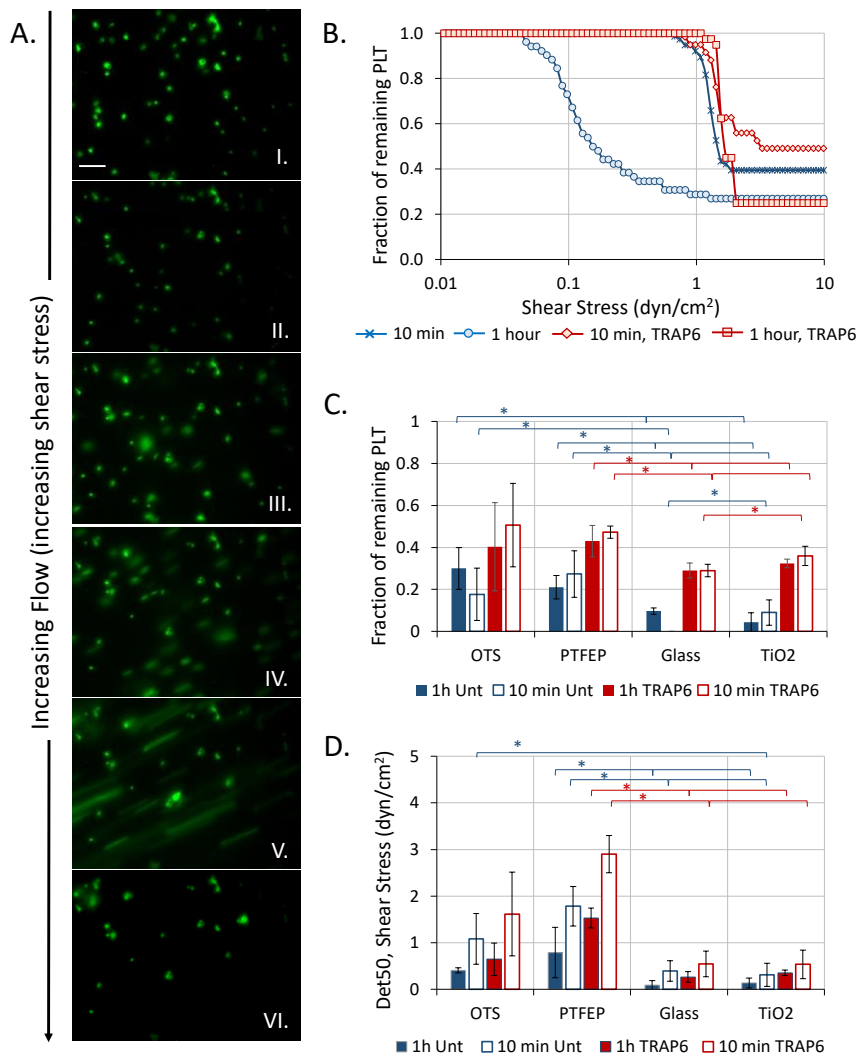


Figure 4-3. Dynamic platelet detachment experiments. A (I-VI). Sequence of representative images illustrating the detachment of adhering platelets under increasing flow. Platelets are stained for CD41a (green) for identification. B. Representative detachment curves of untreated (blue) and TRAP6-treated (red) platelets after 10 min and 1 hour incubation. The plot shows the fraction of platelets remaining on the surface at each shear stress level. In (A) and (B) the results of one experiment are shown from a total of six experiments. C. Average fraction of remaining platelets on the surface after detachment and D. Det50, obtained by measuring the shear stress at which 50% of the platelets detached from the surface. The plots in (C) and (D) were obtained by averaging the results from six independent experiments conducted with the blood from five different donors. Filled bars: 1 hr incubation, open bars: 10 min incubation. Blue: untreated PrP, red: TRAP6-treated PrP. Significant differences are calculated by unpaired two-sample equal-variance t-test and are indicated as “\*”. Blue colored “\*”: significant differences between materials for untreated PrP. Red colored “\*”: significant differences between materials for TRAP6-treated PrP.

From Figure 4-3 C it is evident that the fraction of remaining platelets depends on the material and the measurement conditions. More platelets remained attached to the hydrophobic surfaces (OTS-glass, PTFEP-glass) than to hydrophilic surfaces (glass, TiO<sub>2</sub>). This was true for both untreated PrP and TRAP6-treated PrP and for both incubation times. In the case of

untreated PrP incubated for 1 hr, the differences between hydrophobic and hydrophilic surfaces were statistically significant, while the differences within surface types (glass vs. TiO<sub>2</sub> or OTS-glass vs. PTFEP-glass) were not. In the case of TRAP6-treated PrP incubated for 1 hr, only the differences between PTFEP-glass and the hydrophilic surfaces (glass or TiO<sub>2</sub>) were statistically significant.

It is interesting to note that in the case of PrP incubated on the surfaces for 10 minutes, the fraction of the platelets remaining on the surface after detachment was also different between glass and TiO<sub>2</sub>. This was true for untreated or TRAP6-treated PrP. However, the difference between OTS-glass and TiO<sub>2</sub> was not significant in the case of PrP incubated on the surfaces for 10 minutes in untreated or TRAP6-treated PrP. The significant differences between materials are listed in Table 4-1.

	UNTREATED		TRAP6-TREATED	
	1 h	10 min	1h	10 min
<b>OTS/GLASS</b>	0.01	0.03	ns	Ns
<b>OTS/TIO<sub>2</sub></b>	0.007	ns	ns	Ns
<b>PTFEP/GLASS</b>	0.01	0.006	0.02	0.0008
<b>PTFEP/ TIO<sub>2</sub></b>	0.008	0.03	0.04	0.01
<b>GLASS/ TIO<sub>2</sub></b>	ns	0.03	ns	0.04

Table 4-1. Significant differences between materials in terms of the fraction of remaining platelets. The data presented in this table corresponds to Figure 4-3 C. Statistical significance was calculated by unpaired two-sample equal-variance t-test.

For all of the surfaces and incubation times, more platelets remained attached if they have been pre-activated with TRAP6, however, the difference with the non-activated PrP are not statistically significant for the hydrophobic surfaces (PTFEP- or OTS-modified glass).

Similarly, differences in the Det50 between materials and experimental conditions are visible in Figure 4-3 D. Det50 values were higher (stronger attachment of platelets) on the hydrophobic materials than on the hydrophilic materials under all of the measurement conditions. On the hydrophobic materials, in the case of PrP pre-treated with TRAP6, Det50 values were higher than in the case of untreated PrP, but due to variability, these differences were not statistically significant.

Differences between Det50 values on glass and TiO<sub>2</sub>, or PTFEP-glass and OTS-glass, were not statistically significant under any measurement conditions. Moreover, the differences in Det50 values between OTS-glass and untreated glass were not statistically significant for untreated PrP incubated for 10 minutes or TRAP6-treated PrP; differences between OTS-glass and TiO<sub>2</sub> were not significant for TRAP6-treated PrP.

The significant differences between materials in Det50 are listed in Table 4-2.

	UNTREATED		TRAP6-TREATED	
	1 h	10 min	1h	10 min
<b>OTS/GLASS</b>	0.004	ns	ns	ns
<b>OTS/ TiO<sub>2</sub></b>	0.009	0.04	ns	ns
<b>PTFEP/GLASS</b>	0.04	0.01	0.0004	0.002
<b>PTFEP/TiO<sub>2</sub></b>	0.04	0.003	0.0003	0.0006

Table 4-2. Significant differences between materials in det50. The data presented in this table corresponds to Figure 4-3 D. Statistical significance was calculated by unpaired two-sample equal-variance t-test.

Paradoxically, larger Det50 values were obtained in the case of PrP incubated for 10 min than for 1 hr for pre-treated as well as untreated platelets; remaining platelet fractions were also some times greater for the 10 min incubation.

## 4.5 Platelet detachment in the static system

To further simplify the measurement procedure, I measured the detachment of platelets by rinsing the surface with the buffer using a hand-held pipette rather than employing microfluidics cells with flow. Figure 4-4 A shows representative fluorescence images of the adhering platelets before and after the rinsing on OTS-modified glass, PTFEP-modified glass, unmodified glass, and TiO<sub>2</sub>. While differences between materials in terms of the fraction of platelets remaining on the surface can be observed in the fluorescence images, the results of the experiments varied too much for reliable conclusions to be drawn (Figure 4-4 B).

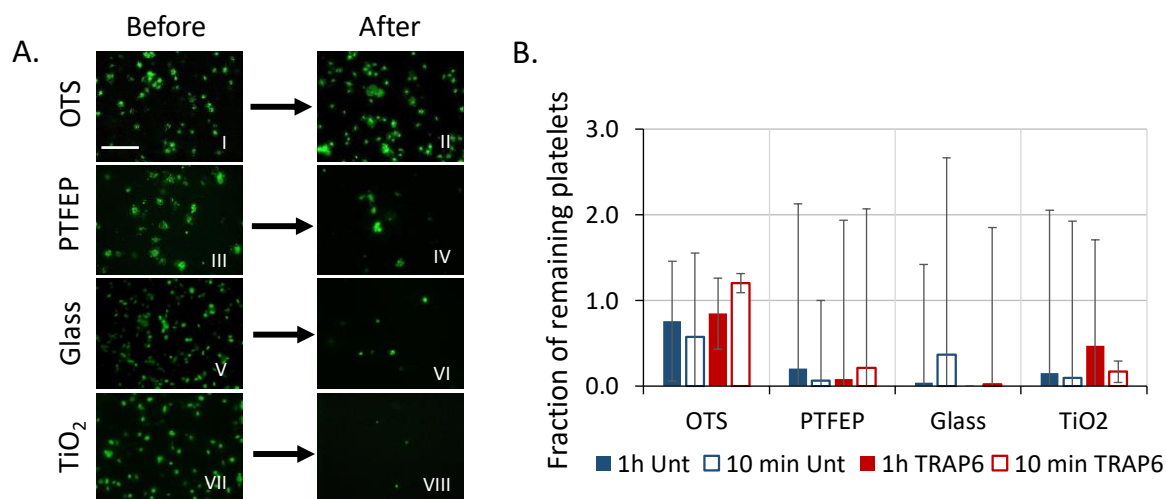


Figure 4-4. Static platelet detachment experiments. A. Images recorded before and after the platelet detachment induced by washing. The platelets are stained for CD41a for identification (green); staining was done after adhesion but before the washing. B. Fraction the platelets remaining on the surface after detachment. The plot shows results from 2 experiments, performed with blood from two different donors. Filled bars: 1h incubation, open bars: 10 min incubation. Blue: untreated PrP, red: TRAP6-treated PrP.

## 4.6 Platelet activation: area and CD62P expression

In this assay, I also examine the activation state of platelets adhering on the materials. Platelet activation was evaluated in terms of platelet spreading and expression of CD62P. The results of the static and dynamic experiments are presented together.

### 4.6.1 Platelet spreading

After platelet detachment, the spreading of the remaining platelets was evaluated. Figure 4-5 A and C show representative fluorescence images of adhering platelet after detachment for the dynamic and static measurements, respectively. The fluorescence images in Figure 4-5 A and C show the adhering platelet on OTS-glass, PTFEP-glass, unmodified glass and TiO<sub>2</sub> after detachment, in both dynamic and static conditions. In order to quantify the spreading, the area of the remaining platelets was measured. Averaged values of the area are presented in Figure 4-5 B and D for dynamic and static conditions, respectively. Six dynamic experiments were performed with the blood from four different donors; two static experiments were performed with the blood from two different donors. Note, that the number of platelets remaining on glass after detachment is very small. This is particularly true in the case of PrP incubated for the 10 minutes under dynamic condition, and for TRAP6-treated PrP incubated

for 10 min under the static condition. These results were therefore excluded from the statistical significance testing.

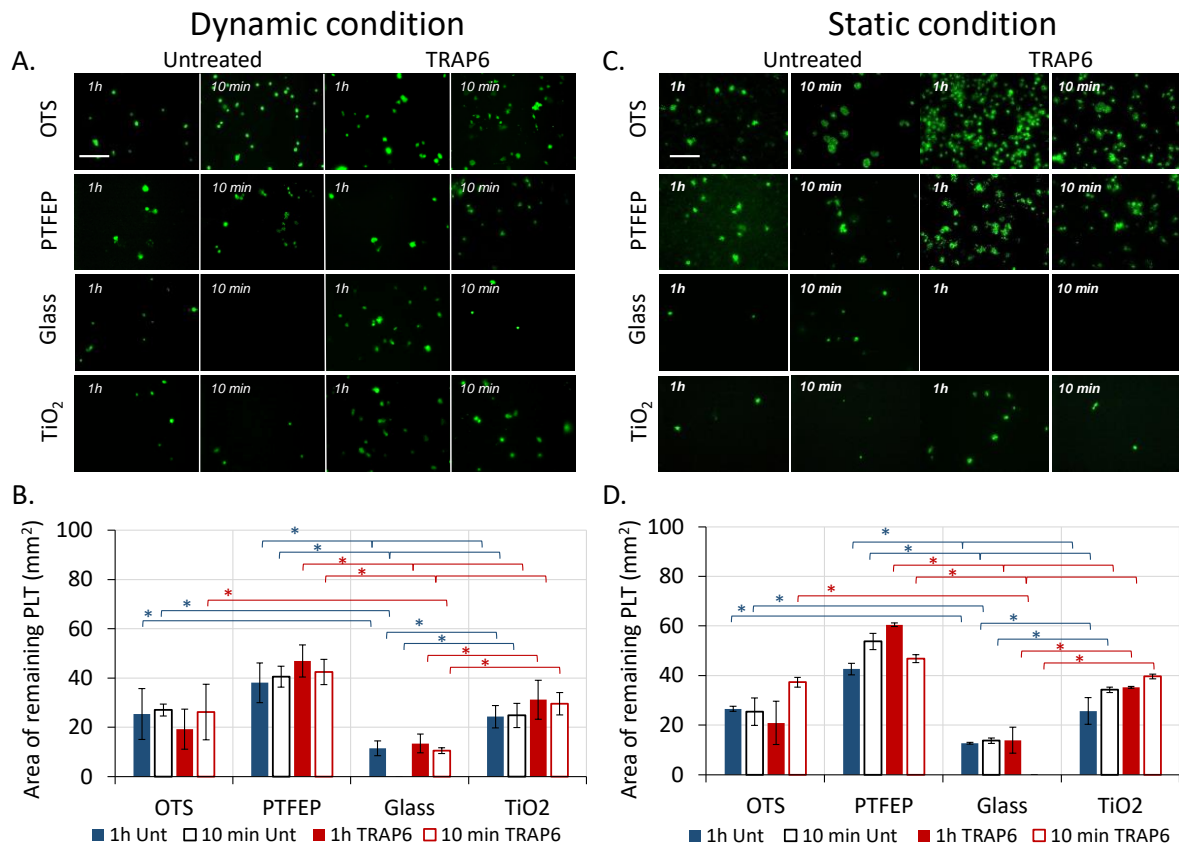


Figure 4-5. Analysis of platelet activation: platelet spreading. Images from experiments performed under dynamic and static conditions are shown (A, C). A and C. Pictures showing the remaining adhering platelets (green) after flow and after washing, respectively. The images are representative of one experiment. B and D Area of adhering platelets after flow and after washing, respectively. The plot in B show results from 6 experiments, the plot in D shows results from 2 experiments. Filled bars: 1h incubation, open bars: 10 min incubation. Blue: untreated PrP, red: TRAP6-treated PrP. Significant differences are calculated by unpaired two-sample equal-variance t-test and are indicated as “\*”. Blue colored “\*”: significant differences between materials for untreated PrP. Red colored “\*”: significant differences between materials for TRAP6-treated PrP.

As visible in Figure 4-5 B and C, both under the dynamic and the static conditions, the effects of materials on platelet spreading are the same. This is reassuring. In particular, the spreading of platelets adhering on the OTS-modified glass is greater than on unmodified glass when untreated PrP is incubated for 1h or 10 min, or when TRAP6-treated PrP is incubated for 10 min.

For all conditions (untreated- and TRAP6-treated PrP) and incubation times, the spreading of platelets adhering on PTFEP-modified glass is significantly greater than on unmodified glass or

TiO<sub>2</sub>, but no significant differences between PTFEP- and OTS-modified glass are observed. Differences are also visible in the spreading of platelets adhering on unmodified glass and TiO<sub>2</sub>, when PrP is incubated for 1hr or 10 min. Surprisingly, pre-activation with TRAP6 does not influence the degree of platelet spreading. Statistical significance values are listed in Table 4-3.

	DYNAMIC				STATIC			
	Untreated		TRAP6-treated		Untreated		TRAP6-treated	
	1 h	10 min	1 h	10 min	1h	10 min	1h	10 min
<b>OTS/GLASS</b>	0.04		ns	0.03	0.001	0.04	ns	
<b>PTFEP/GLASS</b>	0.002		0.0007	0.0002	0.001	0.001	0.003	
<b>PTFEP/TiO<sub>2</sub></b>	0.03	0.008	0.02	0.01	0.02	0.007	0.0002	0.01
<b>GLASS/TiO<sub>2</sub></b>	0.007		0.01	0.001	0.04	0.001	0.01	

Table 4-3. Significant differences between materials in platelet spreading. The data presented in this table corresponds to Figure 4-5 B and D. Statistical significance was calculated by unpaired two-sample equal-variance t-test.

#### 4.6.2 Platelet CD62P expression under dynamic and static conditions

After detachment, the activation state of platelets adhering on the materials was also evaluated in terms of CD62P expression. Figure 4-6 A and C show fluorescence images of the adhering platelets on the test materials. The adhering platelets are false-colored green, while the red color indicates CD62P expression. It can be observed in the fluorescence images that under static condition the CD62P fluorescence intensities are higher than in dynamic experiments. Particularly evident are the differences for OTS- or PTFEP-modified glass between static and dynamic experiments. Indeed, these differences are reflected in Figure 4-6 B and D (dynamic and static experiments, respectively), where the expression of CD62P is presented as geometric means of the fluorescence intensities. Averaged values of this parameter from six experiments for the dynamic conditions and two experiments for the static conditions are plotted. Geometric mean was chosen because of the log-normal distribution of the CD62P intensities (detailed explained in Chapter 5). Also in this case, the number of platelets remaining on glass after detachment is very small. This is true in the case of PrP incubated for the 10 minutes under dynamic condition, and for TRAP6-treated PrP incubated

for 10 min under the static condition. These results were therefore excluded from the statistical significance testing.

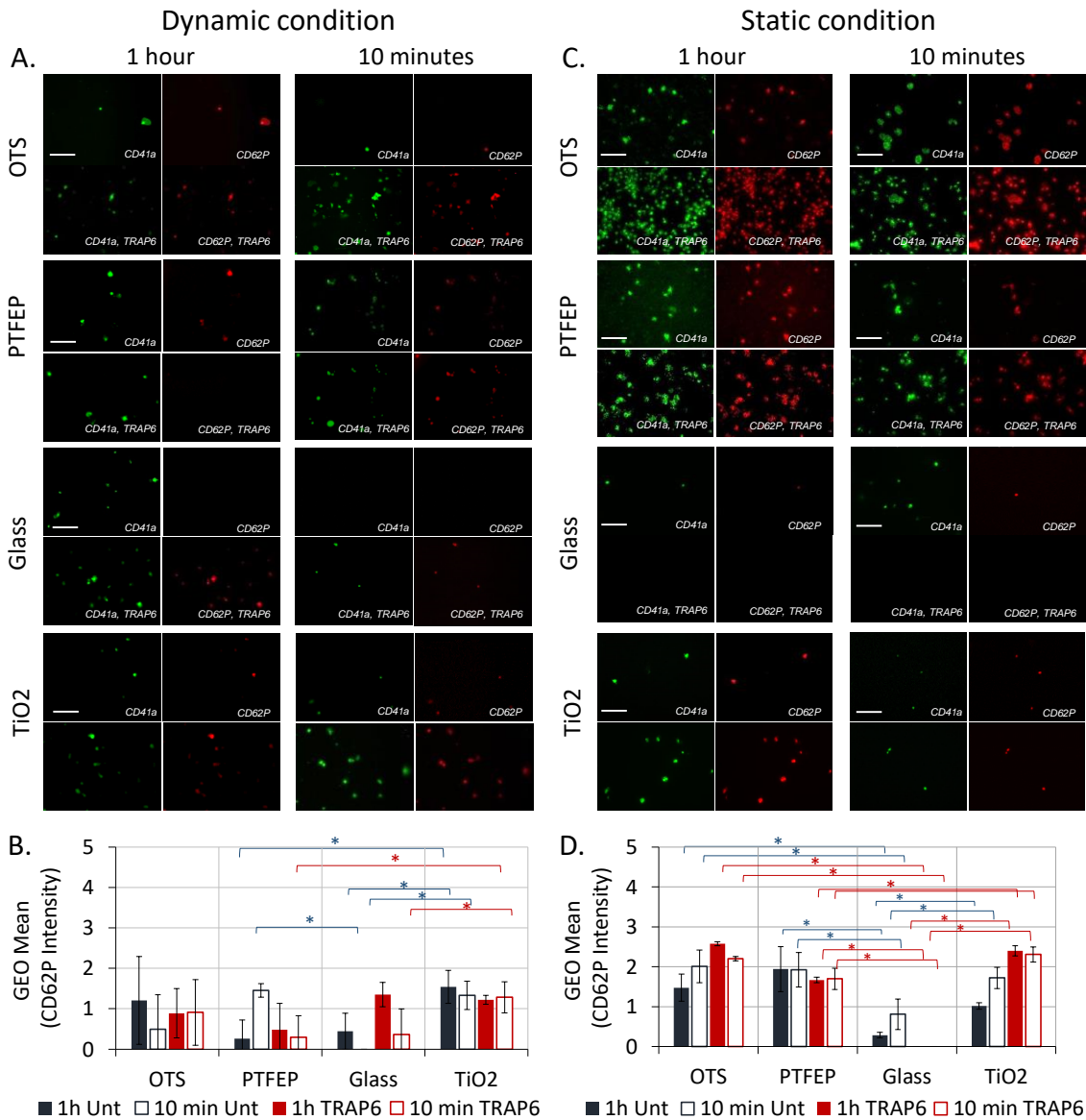


Figure 4-6. Platelet Activation: CD62P expression. Images from experiments performed under dynamic and static conditions are shown (A, C). A and C. Images showing the CD62P expression (red) on the remaining adhering platelets (green) after flow and after washing, respectively. The images are representative of one experiment. B and D Geometric mean of CD62P fluorescence intensities. The plot in B show results from 6 experiments, the plot in D shows results from 2 experiments. Filled bars: 1h incubation, open bars: 10 min incubation. Blue: untreated PrP, red: TRAP6-treated PrP. Significant differences are calculated by unpaired two-sample equal-variance t-test and are indicated as “\*”. Blue colored “\*”: significant differences between materials for untreated PrP. Red colored “\*”: significant differences between materials for TRAP6-treated PrP.

From Figure 4-6 B and D it is evident that dynamic and static experiments do not lead to the same results. I describe the results obtained in the dynamic experiments first (Figure 4-6 B).

Trends are difficult to discern. CD62P expression on remaining platelets on TiO<sub>2</sub> and OTS-modified glass was independent of the incubation time or platelet pre-activation with TRAP6. There were also no significant differences between these two surfaces. On the other hand, CD62P expression in platelets that remain adhering on PTFEP is significantly lower than on TiO<sub>2</sub>, except for the case of the TRAP6-treated PrP incubated on the surface for 10 minutes prior to the detachment, where it is the same on both surfaces. CD62P expression in platelets remaining on unmodified glass is lower than that in platelets remaining on PTFEP-modified glass in the case of TRAP6-treated PrP incubated for 1 hr, but similar in other cases (no platelets remained on glass in the case of TRAP6-treated PrP incubated for 10 minutes). Significantly less CD62P was expressed in platelets remaining on glass than on TiO<sub>2</sub> except in the case of TRAP6-activated PrP adhering for 1 hr.

Under static conditions (Figure 4-6 B), CD62P expression on platelets remaining on the OTS-modified glass, PTFEP-modified glass, and TiO<sub>2</sub> surfaces was similar to each other, but significantly different from glass. Table 4-4 lists the significant differences between materials in terms of CD62P expression.

	DYNAMIC				STATIC			
	Untreated		TRAP6-treated		Untreated		TRAP6-treated	
	1 h	10 min	1 h	10 min	1h	10 min	1h	10 min
<b>OTS/GLASS</b>	ns		ns	ns	0.02	0.04	0.0001	
<b>PTFEP/GLASS</b>	ns		ns	ns	0.02	0.05	0.0004	
<b>PTFEP/TIO<sub>2</sub></b>	0.01	ns	ns	0.04	ns	ns	0.009	0.001
<b>GLASS/TIO<sub>2</sub></b>	0.01		ns	0.04	0.005	0.05	0.0006	

Table 4-4. Significant differences between materials in CD62P expression. Significant differences between materials in det50. The data presented in this table corresponds to Figure 4-6 B and D. Statistical significance was calculated by unpaired two-sample equal-variance t-test.

No systematic effect of pre-activation with TRAP6 on the level of CD62P expression on platelets remaining on the different surfaces could be discerned under either static or dynamic conditions. In summary, the expression of CD62P distinguished TiO<sub>2</sub> from glass, but is not reliable for discerning OTS-modified glass from PTFEP-modified glass, or TiO<sub>2</sub>.

## 4.7 Summary of the statistically significant material-induced changes in platelet detachment and activation according to the assay parameters measured in the study

Table 4-5 summarizes the significant differences in the measured parameters between materials, with respect to dynamic and static experimental conditions.

	DYNAMIC				STATIC			
	Untreated		TRAP6-treated		Untreated		TRAP6-treated	
	1h	10min	1h	10min	1h	10min	1h	10min
FRACTION OF THE REMAINING PLATELETS								
OTS/PTFEP	ns	ns	ns	ns	ns	ns	ns	ns
OTS/GLASS	*	*	ns	ns	ns	ns	ns	ns
OTS/TiO <sub>2</sub>	*	ns	ns	ns	ns	ns	ns	ns
PTFEP/GLASS	*	*	*	*	ns	ns	ns	ns
PTFEP/ TiO <sub>2</sub>	*	*	*	*	ns	ns	ns	ns
GLASS/ TiO <sub>2</sub>	ns	*	ns	*	ns	ns	ns	ns
DET50								
OTS/PTFEP	ns	ns	ns	ns				
OTS/GLASS	*	ns	ns	ns				
OTS/ TiO <sub>2</sub>	*	*	ns	ns				
PTFEP/GLASS	*	*	*	*				
PTFEP/ TiO <sub>2</sub>	*	*	*	*				
GLASS/ TiO <sub>2</sub>	ns	ns	ns	ns				
SPREADING OF THE REMAINING PLATELETS								
OTS/PTFEP	ns	ns	ns	ns	ns	ns	ns	ns
OTS/GLASS	*	—	ns	*	*	*	ns	—
OTS/ TiO <sub>2</sub>	ns	*	*	*	*	*	*	*
PTFEP/GLASS	*	—	*	*	*	*	*	—
PTFEP/ TiO <sub>2</sub>	*	*	*	*	*	*	*	*
GLASS/ TiO <sub>2</sub>	*	—	*	*	*	*	*	—
CD62P EXPRESSION ON THE REMAINING PLATELETS								
OTS/PTFEP	ns	ns	ns	ns	ns	ns	ns	ns
OTS/GLASS	ns	—	ns	ns	*	*	*	—
OTS/ TiO <sub>2</sub>	ns	ns	ns	ns	ns	ns	ns	ns
PTFEP/GLASS	ns	—	ns	ns	*	*	*	—
PTFEP/ TiO <sub>2</sub>	*	ns	ns	*	ns	ns	*	*
GLASS/ TiO <sub>2</sub>	*	—	ns	*	*	*	*	—

Table 4-5. Summary of the significant differences between materials in the measured parameters. \* stand for “significantly different”. “—” refers to conditions where the number of the remaining platelets was too small for the significance of the results to be evaluated.

## 4.8 Discussion

The work presented in this Chapter represents another approach to the design of a simple and robust *in vitro* hemocompatibility test. All the current *in vitro* testing approaches are complex, time consuming, and require large amounts of blood (the test described in Chapter 3 is one case in point, the Chandler Loop test is another<sup>145</sup>). Therefore, I used a microfluidic approach reported by Cho et al.<sup>181</sup> which required 300  $\mu\text{l}$  of PrP per test (9 ml of whole blood for 8 experiments) instead of 6 ml of whole blood required for each shear channel test, so 18 ml of blood for one experiment, used in Chapter 3.

Unlike all of the other existing approaches to testing material hemocompatibility, this approach focuses on platelet detachment. Specifically, platelets adsorbed to the surfaces from PrP incubated under static conditions for 10 min or 1 hr were subjected to shear stress in the range of 0 – 10  $\text{dyn}/\text{cm}^2$ . For comparison, the highest physiological wall shear stress in arterial vasculature is  $\sim 10 \text{ dyn}/\text{cm}^2$ , while pathological shear stresses reach 80  $\text{dyn}/\text{cm}^2$ .<sup>218</sup> The fraction of platelets remaining at the surface at the end of an experimental run, and the shear stress at which 50% of platelets detached from the surface (Det50), were measured. These parameters have not been used to characterize material hemocompatibility previously, but they have been used to study phenomena such as bacteria-surface interactions in the biofilms and strength of attachment of diatoms to different surfaces.<sup>219,220</sup> Sensitivity to surface properties has been reported.<sup>219</sup>

I focused on evaluating the sensitivity of these parameters to the differences between different materials. Simultaneously I measured the extent of platelet spreading and activation (CD62P expression) in the remaining platelets to shed light on the biological context of the detachment parameters and biomaterial differences. To further simplify testing, the fraction of the platelets remaining on the surface and platelet activation parameters were evaluated in a “static” system where platelet detachment was initiated using a hand-held micropipette. This was also correlated with the activation parameters. It has to be noted that this assay was not designed to mimic physiological conditions. Platelet adhesion to implant surfaces or wound sites *in vivo* occurs under flow, while I incubate PrP with the surfaces under static conditions to give them time to interact and undergo activation. Such static incubation has been used by others to study platelet interactions with various surface-adsorbed proteins by

analyzing platelet detachment process and correlating it with the surface properties of the polymeric substrates, platelet spreading, and GPIIb-IIIa-vWF interaction.<sup>208-210</sup> However, caution must be exercised when interpreting the absolute values of the detachment stresses I report here, because they may not be physiologically relevant: Boudot et al showed that platelet adhesion under static and dynamic adhesion were different, and that different shear stresses influence the strength of platelet adhesion differently (for example GPIIb-IIIa promotes the adhesion at high shear stress, while at low shear stress the efficiency of GPIIb/IIIa is maximal).

106,221,222

In other words, my strategy for designing a hemocompatibility assay is, once again, not to mimic the physiological conditions—an approach that has not led to a successful hemocompatibility test strategy over the past 70 years—but to evaluate platelet activation and previously unexplored platelet-surface interaction parameters in a well-defined model system according to their ability to distinguish between materials. Other studies concerned themselves with the phenomenology of the platelet adhesion and detachment process to shed light on these important aspects of platelet physiology in hemostasis and thrombosis,<sup>147-149,205-207,209</sup> but this was not my goal at this point.

#### 4.8.1 Material screening: sensitivity of various parameters to the differences between materials

The first question I would like to address is, which of the parameters measured is better in distinguishing between the different surfaces and under which conditions. Det50 and the remaining platelet fraction were both able to distinguish between classes of surfaces (hydrophilic/hydrophobic) in dynamic experiments with untreated PrP incubated for 1 hr (Figure 4-3C and D, Table 4-5). Of the two, Det50 was more robust (greater differences and smaller variability), because the remaining platelet fraction involves taking a ratio between the remaining and the starting platelet numbers. Neither of the two parameters (Det50 or remaining platelet fraction) was good at telling apart the surfaces within the classes (glass from TiO<sub>2</sub> or PTFEP from OTS-glass), except in the case of PrP incubated for 10 minutes, treated or untreated with TRAP6, where the remaining platelet fraction was different for glass and TiO<sub>2</sub>.

On the other hand, when untreated PrP was incubated on the surfaces for 10 min, Det50 became less sensitive to the differences between the surfaces (e.g., not being able to

distinguish between OTS-glass and unmodified glass), while the remaining platelet fraction was insensitive to the difference between OTS-glass and TiO<sub>2</sub> (while being sensitive to the differences between glass and TiO<sub>2</sub>). Pre-treating PrP with TRAP6 in general diminished the sensitivity of these two parameters to the differences between materials in the dynamic experiments, with the exception of the TRAP6-treated PrP incubated on the surfaces for 10 min that could distinguish between glass and TiO<sub>2</sub>, as mentioned above. This is most clearly visible in Table 4-5.

The remaining platelet fraction measured in the static experiments was entirely insensitive to the differences between the surfaces. This is most likely because the application of the shear flow with a hand-held pipette failed to mimic the ramping conditions of the exponential increase in the shear rate used in the dynamic experiments, and too much variability in the remaining platelet fractions results. The detachment conditions were less controlled.

In the static experiments, the degree of spreading of the remaining platelets turned out to be the most sensitive parameter. Indeed, differences are observed not only between surfaces of different classes (hydrophobic/hydrophilic), but within the hydrophilic surfaces (TiO<sub>2</sub> vs. glass), both in the case of untreated and TRAP6-treated PrP. Again, pre-treatment with TRAP6 makes things somewhat worse (Table 4-5). Surprisingly, in the dynamics experiments, the interpretation of this parameter is more complex. Differences between glass and TiO<sub>2</sub> are still evident in the case of PrP incubated for 1 hr (treated or untreated), but in some cases no differences between OTS and TiO<sub>2</sub> or OTS and untreated glass are evident, which makes this parameter less reliable overall.

CD62P expression levels on the remaining platelets proved rather disappointing in regards to their sensitivity to the differences between the surfaces. Moreover, quite different results were obtained in the static and the dynamic experiments, pointing to the sensitivity of this parameter to the details of the flow conditions. Nevertheless, CD62P expression levels in platelets remaining on glass and TiO<sub>2</sub> were different, both in static and in the dynamic experiments, under several conditions (Table 4-5). Differences were evident between other surfaces under some conditions, but in no case between OTS and PTFEP or OTS and TiO<sub>2</sub>.

None of the measured parameters revealed differences between the two hydrophobic surfaces, OTS and PTFEP, while every other pair of surfaces could be distinguished at least in some of the tests, in every case, more than one test (see Table 4-5). For example, glass and TiO<sub>2</sub> could be distinguished from each other by measuring the area of the remaining platelets

in static or dynamic experiments by incubating untreated or pre-treated PrP for 1 hr; fraction of the remaining platelets in the dynamic experiments by incubating untreated or pre-treated PrP for 10 min; or CD62P expression levels in static or dynamic experiments by incubating untreated PrP for 1 hr.

I can therefore conclude that:

- Glass, TiO<sub>2</sub>, and the two hydrophobic surfaces (OTS- and PTFEP-coated glass) interact with PrP differently.
- A minimal combination of two parameters (Det50 and remaining platelet spreading), measured in the dynamic experiments with PrP incubated on the surfaces for 1 hr, is needed for maximal sensitivity that can be achieved with this assay (distinguishing between glass, TiO<sub>2</sub>, and the two hydrophobic materials).
- Spreading of the remaining platelets measured in static experiments with untreated PrP incubated at the surfaces for 1 hr could also be used as a parameter for distinguishing between materials, but there are some concerns about how controlled the static experiments are.
- To evaluate material hemocompatibility, a test based on these parameters should be designed and applied to a sufficiently large set of materials that have previously been examined in vivo (e.g., by Kusserow and Ratner<sup>134,135</sup>). It should be augmented by a thrombogenicity assay.
- Using TRAP6-pretreated PrP or evaluating the level of CD62P expression on the remaining platelets is not useful for distinguishing between materials.

#### 4.8.2 What do the detachment measurements reveal about platelet-biomaterial interactions?

My measurements offer insight into the platelet-surface interactions and platelet activation at biomaterial surfaces. Very little, is known about the details of how biomaterial surfaces activate platelets. There is strong evidence that different surfaces do so differently. For example, several authors report differential GPIIb/IIIa activation and  $\alpha$ -granule secretion in response to different surfaces and surfaces coated with different plasma proteins.<sup>131,169-172</sup>

The differences in the platelet reactions to different surfaces are thought to reflect the differences in the properties of the adsorbed protein films (composition and

conformation).<sup>223,224</sup> Consistent with these observations, I found differences between materials when probing the strength of platelet attachment to surfaces, the number, and the degree of spreading, of the platelets that remained attached to the surface after the detachment experiment. These can be better appreciated in the plots I introduce in Figure 4-7, where the correlations between various parameters are examined.

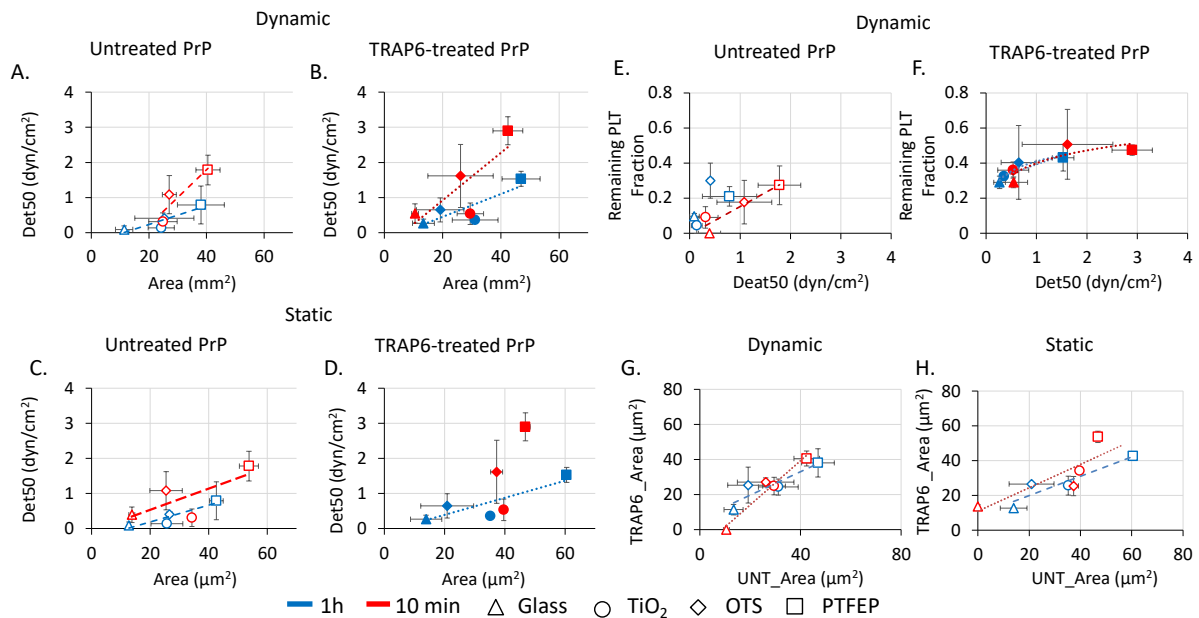


Figure 4-7. Correlations between detachment and activation parameters. A - D: Det50 vs. remaining platelet area for dynamic and static measurements performed with untreated and TRAP6-treated PrP, as indicated. E, F: dependence of the remaining platelet fraction on DET50 under dynamic conditions. G, H: Remaining platelet area for TRAP6-pretreated vs. untreated PrP in dynamic (G) and static (H) measurements.

In particular, Det50 correlates with the area of the remaining platelets (their degree of spreading) both in the dynamic and static experiments with untreated or TRAP6-pretreated PrP, except in the case of 10 min incubation of pretreated PrP under static conditions (Figure 4-7 A-D). The remaining platelet fraction correlates with Det50 for the dynamic experiments (Figure 4-7 E, F). Both of these are expected: in the first case, consider that the force that is needed to detach a platelet from a surface depends on the strength of the receptor-surface interactions and their number. To a first approximation, the number of the interactions is expected to scale with the area, assuming a uniform receptor distribution. A uniform distribution has indeed been observed for GPIIb/IIIa and GPIb-IX-V at the surfaces of activated platelets by electron microscopy.<sup>56</sup> Therefore, platelets that are spread to a greater degree

are expected to be attached to the surface stronger and require higher shear rates to detach. Indeed, others have shown that platelets that are spread to a greater degree detach at higher shear rates.<sup>210</sup>

The correlation between remaining platelet fraction and Det50 (Figure 4-7 E, F) is a manifestation of the fact that more platelets remain on the surface if they are attached stronger, given that the shear stress at the end of a detachment experiment is the same in all cases.

What is interesting is the effect of TRAP6 (Figure 4-7 G, H). Pre-treatment with TRAP6 does not affect the area of the remaining platelets, but it does affect Det50—the interaction strength. This effect is also visible in Figure 4-7 E and F. To understand this effect, I examine further the molecular details of the platelet-surface interaction.

The interactions between the platelets and biomaterial surfaces are thought to be mediated by the proteins adsorbed at the biomaterial surface.<sup>45</sup> At the molecular level, platelet surface adhesion receptors are responsible for the attachment of the platelets to the adsorbed proteins. Examples of these proteins include glycoproteins GPIIb/IIIa (integrin  $\alpha$ IIb/ $\beta$ 3) for binding fibrinogen and vWF, GPVI for the binding collagen, and the GPIb-IX-V complex that binds to vWF (see Figure 1-4 on page 11 in the Introduction).<sup>56,212,213</sup> These receptors bind to the specific sequences in the adsorbed proteins that become exposed when these proteins are adsorbed to biomaterial surfaces or at the sites of vascular injury. Initial interactions are reversible.<sup>225</sup> However, depending on the conformation of the adsorbed proteins, platelets may become activated, entailing conformational changes in the adhesion receptors to their active forms, platelet spreading, and granule secretion.<sup>216,225</sup> The active forms of the surface adhesion receptors promote stable (irreversible) adhesion (*in vivo*, such irreversibly adhering and aggregated platelets are removed only during the clot lysis stage of the wound healing process).<sup>50,216</sup> Subtle differences in the platelet responses to different proteins have been reported in the literature: for example collagen binding to GPIIb induce TXA<sub>2</sub> production and PS expression, while vWF binding to its receptor GPIb-IX-V leads to dense granule secretion (reviewed by Reviakine).<sup>69</sup>

The activation of the platelet surface adhesion receptors may also be triggered by soluble agonists, such as TRAP6 used in this study. TRAP6 is a PAR1 receptor agonist, a partial analogue of thrombin that strongly activates platelets promoting granule secretion, spreading, and the

activation of the GPIIb/IIIa integrin receptor complex that mediates adhesion and aggregation.<sup>226</sup> Soluble agonists activate platelets through G proteins coupled receptors (GPCRs) that in general involve different sets of pathways than integrin-mediated and other surface dependent activation pathways, and again, this may lead to different patterns or degrees of platelet activation.<sup>227</sup> The effects of the two sets of pathways are in some cases synergistic, in other cases permissive.

The fact that TRAP6 affects Det50 without affecting platelet area (Figure 4-7G, H) means that the assay is sensitive to the specific details of the platelet activation—whether it is triggered by the soluble or surface-adsorbed agonists. This is a specific effect, related to the different signaling pathways engaged by the soluble and surface-adsorbed agonists. The effect of soluble and surface agonists on the platelet adhesion strength appear to be synergistic (adhesion strength is higher in the case of TRAP6-preactivated platelets), while the spreading is controlled by the surface agonists only and is independent of the pre-treatment by TRAP6.

#### 4.8.3 What does the microfluidic assay reveal about hemocompatibility of the tested materials?

Attempting to draw conclusions about which material is more or less hemocompatible based on these results is dangerous. Many investigators fell into this trap in the past, by equating hemocompatibility with the number of adhering platelets or the degree of their spreading.<sup>46,135</sup> Drawing such conclusions should await the results of an extended test where the in vitro results are correlated with the vivo performance of different materials. However, some remarks can be made by comparing our results with the literature. For example, hydrophilic polymer surfaces (such as hydroxyethyl methacrylate—HEMA) have generally been shown to exhibit low platelet adhesion and easy detachment in the in vitro experiments. This is also our conclusion in the case of glass and TiO<sub>2</sub>, which are hydrophilic when freshly cleaned (Figure 4-3 B and C). However, the same hydrophilic polymer surfaces also showed high platelet consumption in the arterio-venous shunt experiments, and therefore poor hemocompatibility performance due to downstream emboli formation.<sup>228-230</sup>

On the other hand, hydrophobic materials have a long history of good in vitro and in vivo performance, from the initial experiments showing that Vaseline and paraffin coating of glass extended blood clotting time performed in the late 1880s/early 1900s/to the much more

recent observations have with PTFE (Teflon)-coated stents.<sup>231-233</sup> Similarly, the results obtained with the hydrophobic PTFEP in animal and human tests were also considered promising.<sup>234-237</sup> Our results show that platelets adhere stronger to the hydrophobic materials (higher Det50 values and larger remaining platelet fractions), and similar observations have been reported by others.<sup>209</sup> In particular in the case of PTFEP, Tur et al reported initial adhesion of platelets under flow that was not followed by detachment in an *in vivo* canine shunt systems (c.f. Figure 4A ref 238). Interesting is also not followed by growth of the thrombus.<sup>238</sup> It is possible, that increased platelet adhesion actually plays a protective role in some cases (the passivation discussed by several authors;<sup>131</sup>), but to prove that, an appropriate platelet activation parameter has to be evaluated concurrently. We attempted to do that by examining CD62P expression on the remaining platelets, but without success. It does not appear to be the relevant parameter.

It should also be noted that our results are in contradiction with those of Welle et al who showed that more platelets adhered on glass than on PTFEP under static conditions.<sup>203</sup> However, those authors used citrate-anticoagulated PrP diluted in PBS instead of undiluted, heparin-anticoagulated PrP used in my study, and the results are therefore difficult to compare.

Further concern is the ability of a short-time assay to predict long-term behavior of the materials. In particular, we observe a paradoxical result that the adhesion strength decreases with the PrP incubation time. Such observations also have been reported by others.<sup>209</sup> The most likely origin of this observation is the effect of platelet-released proteases on the underlying protein layer, but the conformational changes in the adsorbed proteins of the type reported by Latour et al are also possible.<sup>107,153</sup>

The approach to predicting clinical performance of materials I favor is through establishing the ranking of materials according to the parameters that are sensitive to material differences, and correlating this with their clinical performance. For example, I can rank materials according to the platelet adhesion strength, which decreases from hydrophobic to hydrophilic materials, and correlate that with the performance of the materials in animal and human tests. It appears to me that this approach would be superior to attempts of direct interpretation of physiological significance of the various parameters (e.g., equating lower

platelet adhesion to improved hemocompatibility), as the latter are often flawed due to significant differences in the timescales involved and the overall complexity of the process.

#### 4.8.4 Limitation of the study

This study has two main limitations: first, the number of the surfaces tested was limited to few model surfaces and, second, no other clinically relevant materials were tested. Furthermore, studies with platelet inhibitors, agonists other than TRAP6, and markers other than CD62P are needed to further understand activation mechanisms.

#### 4.8.5 Conclusion and outlook

In summary, this *in vitro* test is capable of distinguishing hydrophilic (glass and TiO<sub>2</sub>) from hydrophobic (OTS- and PTFEP-coated glass) surfaces and glass and TiO<sub>2</sub> from each other with respect to platelet adhesion strength (Det50) and the number of platelet remaining on the surfaces after the detachment runs. Pre-treatment of PrP with TRAP6 diminishes the sensitivity of the assay but reveals that it is sensitive to the particular details of platelet activation. This allows me to conclude that different surfaces act as agonists of different strength, activating platelets to a different degree, as revealed by the differences in the area of the remaining platelets. This difference was evident in experiments with the untreated as well as TRAP6 pre-treated PrP, consistent with the notion that soluble and surface agonists activate platelets via different pathways. Further comments on the mechanism of the platelet-surface interactions require detailed inhibitor studies. Evaluating platelet activation by measuring the level of CD62P expression on the remaining platelets was not useful for distinguishing between materials. This work paves the way for a comprehensive test of clinically relevant materials.

## 5. A Method for Studying Platelet Activation at the Single Platelet Level

### 5.1 Summary

In this Chapter, I present an assay for studying platelet activation at the single platelet level. It is by now well-established that all materials activate blood components, and previous Chapters revealed a certain selectivity in the way different materials do so that has also been noted by other authors.<sup>131,169,171,172,239,240</sup> This selectivity is particularly related to platelet activation at biomaterials. This idea is enunciated in a series of works from our group and articulated in a recent review.<sup>69</sup> Joining these ideas leads to the notion that platelet activation at biomaterial surfaces could be directed towards wound healing and implant integration, in the spirit of the approach proposed in ref. 46.

*In vivo*, platelets are the first cellular structures to interact with the implant. Their activation at the biomaterial surface leads to thrombus formation. This is quite different from what happens in the physiological, hemostatic conditions, where platelet activation leads to the formation of the clot and the consequent wound healing reactions. In order to direct platelet activation at the biomaterial surface towards the wound healing reactions, we need to understand how these reactions are triggered during the activation process of platelets. Secretion reactions are thought to play an important role in this process, because platelet granules contain cytokines, growth factors, and coagulation cascade mediators, with contradictory functions: pro- and anti-inflammatory, pro- and anti-angiogenic, etc.<sup>69,78,241-243</sup> These substances are secreted as a part of the activation process. Their secretion must be regulated, but until now, the regulation mechanisms have not been elucidated.<sup>161,244</sup>

Current understanding of platelet activation and its regulation, presented in the Introduction (section 1.5.2.2), is based on assays performed on the populations containing between tens of thousands and millions of platelets. It is an “average” view. It is becoming clear, however, that this “average” picture is incomplete. For example, it fails to explain the regulation of the granule secretion process described above. Another unexplained aspect is the observation, both *in vitro* and *in vivo*, of platelet subpopulations with different patterns of activation

marker expression; such platelet subpopulations have been observed in vivo and in vitro, including in my own work and the other works from our group.<sup>131,148,175,176,245</sup> These questions are a part of the broader challenge to understand how different, often redundant, platelet signalling pathways interact to elicit appropriate repertoire of responses under different physiological or pathological conditions.<sup>69</sup> Advances on these fronts that can take us past the “average” picture are expected to come from studies of single platelets.<sup>243</sup> These advance are expected to come, in part, from single platelet studies addressing the regulation of secretion. The objective of the work described in this Chapter was to design and validate such an assay. A method for studying single platelets should have the capability to analyse both the expression of the surface activation markers and the secretion of substances by the individual platelets. It should also have dynamic capabilities, enabling researchers to resolve the effects of combined (parallel) and sequential stimuli applied to the same platelet. To the best of our knowledge, such a method does not yet exist. Therefore, the method I developed is based on a multifunctional pipette mounted on the stage of a fluorescence microscope.<sup>246</sup>

## 5.2 The multifunctional pipette

The pipette is an open-volume microfluidic device that operates by generating a hydrodynamically confined, localized perfusion zone around the target cell. It consists of a pen-shaped silicon polymer (poly(dimethyl siloxane), PDMS) body, housing the four reagent wells, two collection wells, and two auxiliary wells for collecting the waste during switching operations (see below). The pipette is shown in Figure 5-1 A. The tip of the pipette contains the mixing unit connected to the aspiration channel, and peripherally to it, two injection channels. It is formed by a 10  $\mu\text{m}$  thin PDMS membrane (Figure 5-1 B). This defines the minimum distance between the aspiration channels and the surface.

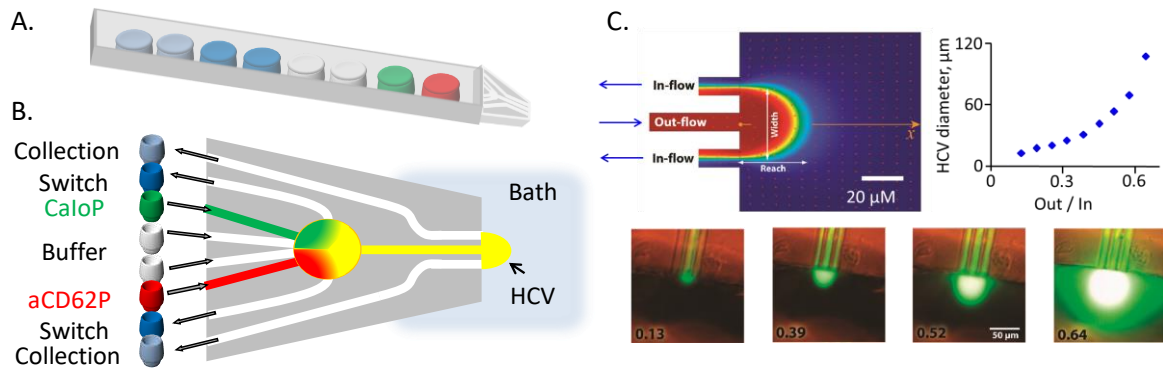


Figure 5-1. The view of the multifunctional pipette is shown in (A) and the schematic of its tip in (B). PDMS body is shown in gray; microfluidic channels are shown in white. The tip contains three channels, the central injection channel and two peripheral aspiration/collection channels. The injection channel is connected to the circular flow switching unit, which selects a single outflow solution from the four inflows. Wells are color-coded as shown in (B) on the right. The four wells in the front contain the solutions to be injected (in our case, the buffer, antibodies, and CaloP); followed by two switching wells connected to the flow selection unit by means of channels running at the bottom of the pipette body (not shown). The last two wells are connected directly to the aspiration /collection channels. The HCV is formed at the apex of the tip through the application of appropriately balanced positive and negative pressures to the injection, and aspirations channels as indicated by the arrows in (B). Details are provided in ref. 247. The concept of recirculation is shown in (C), which is taken from Ainla et al.<sup>247</sup> Simulation (top) and experimental (bottom) results are shown. The simulation results depict the view of the flow field from the top and the plot of the HCV diameter vs. the ratio of the outflow to the inflow. In the top view, the substrate concentration distribution is encoded with a color gradient (blue, 0% substrate; red, 100% substrate; the outflow/inflow ratio used in the simulation is 0.5). Orange arrow represents the distance from the channel outlet along the channel axis (x), and the white arrow depicts the diameter of the HCV. The size of the recirculation zone can be varied over 1 order of magnitude by adjusting the ratio between the pressures driving the flows, as shown in the series of experimental images below the simulation results.

Each of the reagent wells is connected through a dedicated to the mixing unit that leads to the injection channel (Figure 5-1 A). The collection wells are connected to the aspiration channels. The perfusion zone, referred to as the hydrodynamically confined volume (HCV), is generated by balancing the positive and negative flows through the central injection channel and peripheral aspiration channels located in the pipette tip (Figure 5-1 A). The flows are generated by applying positive pressures to the reagent wells and negative pressures to the collections wells. The pressures are balanced in such a way that the inflow rate is higher than the outflow rate, so that the fluid delivered through the injection channel is recirculated into the aspiration channels faster, than the solutes contained in it could diffuse outside of the HCV. This effectively isolates the HCV from the surrounding bath, as shown in Figure 5-1 C: there is a sharp fluorescence contrast between the HCV and the surrounding fluid. The size of the HCV is defined by the ration of the outflow to inflow rates (Figure 5-1 C), and optimal

ratios, the contrast can be maintained as long as there is fluid left in the wells (tens of minutes at a constant flow rate of 10 nl/sec). Figure 5-1 C shows both the results of a finite element method simulation and of actual experiments, both of which highlight the sharp definition of the HCV at appropriate flow rate ratios.

The pipette itself, and some of its biophysical, cell-, and tissue culture applications, have been described previously,<sup>246-248</sup> but this is the first quantitative evaluation of its performance. Others have used similar devices for applications such as whole cell lysis.<sup>249</sup>

### 5.3 Assay design

The multifunctional pipette works with surface-immobilized cells. Immobilizing platelets at surfaces is a problem, because they activate upon interaction with foreign materials.<sup>250,251</sup> To partially circumvent this problem and validate the functionality of the pipette in regards to studying individual platelets, we relied on the recent finding from my group that purified platelets adhering on TiO<sub>2</sub> in the absence of calcium do not spontaneously secrete  $\alpha$ -granules, as judged from the lack of CD62P expression and diminished  $\beta$ -TG secretion, or express PS (Figure 5-2).<sup>171,172</sup>

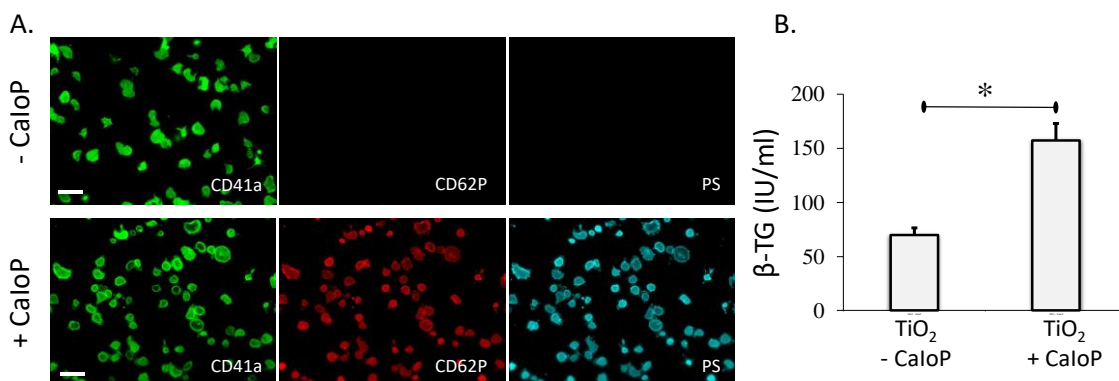


Figure 5-2. Purified platelets adhering on TiO<sub>2</sub>. A, top. Platelets (CD41a, green fluorescence) adhering on TiO<sub>2</sub> in absence of extracellular calcium do not express CD62P or PS. Bottom. Challenging them with CaloP leads to CD62P and PS expression. B.  $\beta$ -TG secretion: according to CD62P and PS expression, the treatment with CaloP increases the  $\beta$ -TG secretion. Statistical significance is calculated by paired t-test ( $p=0.001$ ). (My results shown in subfigure (B) appear in Gupta et al.,<sup>171</sup> while the results appearing in (A) are unpublished but reproduce those presented in Gupta et al.<sup>171</sup>).

Secretion and expression events in TiO<sub>2</sub>-adhering platelets could be triggered by treating them with calcium ionophore (CaloP).<sup>171</sup> This effect was shown to be surface-specific: identically prepared platelets adhering on glass under the same conditions did secrete  $\alpha$ -granules and

expressed PS spontaneously.<sup>171,172</sup> Hence, we approached individual platelets adhering on TiO<sub>2</sub> with the pipette that was used to deliver appropriate combinations of antibodies against platelet surface activation marker CD62P, annexin A5 (A5) to detect PS,<sup>252</sup> and CaloP to trigger activation. Platelet response was examined by fluorescence microscopy. The procedure is schematically shown in Figure 5-2 C – E.

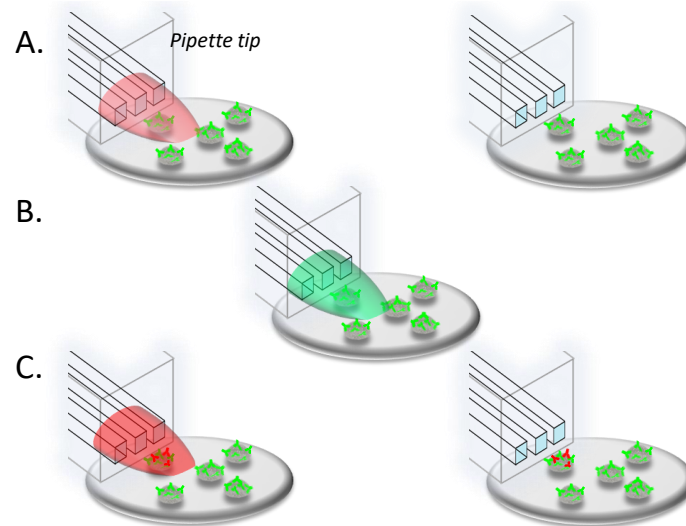


Figure 5-3. Experimental Strategy. Experimental strategy: Platelets (gray semi-spheres) adhering on TiO<sub>2</sub> (gray disk) in the absence of calcium are stained with a fluorescently labelled antibody against CD41a (aCD41a, green), a glycoprotein that is constitutively expressed on their surface, to aid identification. Individual platelets are approached with the pipette and exposed to a solution of fluorescently labelled anti-CD62P antibody in a calcium-containing buffer (A). Based on our previous results, no staining for CD62P is expected. The same platelet(s) are then exposed to the CaloP solution in a calcium-containing buffer injected through the pipette (B), and then again with the aCD62P solution, at which point CD62P expression is expected (C). To monitor PS expression, we used fluorescently labelled A5 in a calcium-containing buffer instead of, or together with, anti-CD62P.

## 5.4 Platelet isolation, purification and analysis

The platelets that we used were purified from citrate-anticoagulated whole human blood by centrifugation within 30 minutes after phlebotomy according to the protocol previously established in our group (see Materials and Methods for details).<sup>171,172,253,254</sup> Prior to each experiment, freshly purified platelets were characterized by flow cytometry to determine their activation levels and response to agonists (Figure 5-4). Platelets were used in further experiments only if their activation levels were below 7 % in terms of CD62P and PS expression.

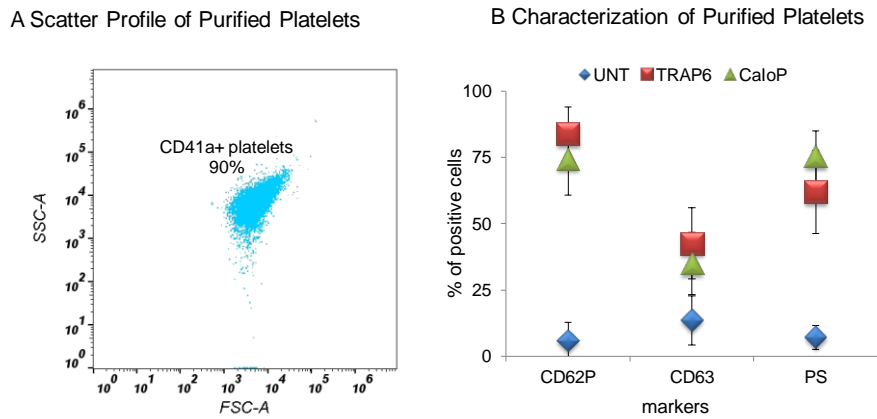


Figure 5-4. Platelet characterization by flow cytometry. A. Scatter plot showing the fraction of CD41a-positive events. 10,000 events were recorded. FSC and SSC refer to forward and side scatter, respectively. B. Activation level of untreated (UNT) platelets and platelets treated with TRAP6 or CaloP with respect to the expression of CD62P, CD63, and PS. The plot shows average results from thirteen experiments performed with blood from eight different donors.

## 5.5 Triggering $\alpha$ -granule secretion in individual platelets

Figure 5-5 shows the results of two representative experiments employing the multifunctional pipette. The HCV, false-colored red to represent the anti-CD62P antibody fluorescence, is seen surrounding one (Figure 5-5 A) or two (Figure 5-5 B) platelets (green, stained with anti-CD41a). CaloP treatment triggers CD62P expression in platelets confined to within the HCV (c.f. (Figure 5-5 II and IV)). Platelets adjacent to the HCV are not affected by the delivery of CaloP (Figure 5-5 III, IV). No aCD62P staining is observed without CaloP treatment (Figure 5-5 I, II). In total, nine such experiments with platelets purified from blood of three different donors were performed. Fluorescence intensity data was collected on 1141 individual platelets and analyzed; the results of the analysis are shown in Figure 5-5 C. It can be seen that outside the HCV (blue bars), the distribution of fluorescence intensity changes (after – before the CaloP treatment,  $\Delta(I_a - I_b)$ ) is approximately Gaussian, with a mean  $\pm$  std. dev. of  $5 \pm 35$ ; they are very similar to the background intensities (gray) and represent random noise. On the contrary, within the confines of the HCV (red bars), fluorescence intensity differences  $\Delta(I_a - I_b)$  are distributed log-normally (inset). Log-normal distributions commonly arise in biological systems due to coupling between random factors and existence of a lower boundary, such as the ligand and antibody concentrations and intensities that cannot be smaller than  $\sim$  zero.<sup>255,256</sup> These distributions appear “tailed” in linear coordinates but become symmetrical when transformed into logarithmic coordinates (c.f. main panels and insets in Figure 5-5 C and D). There are various ways of characterizing log-normal distributions. We follow Limpert et

al.<sup>255</sup> by presenting the geometric mean and multiplicative standard deviation,  $68 \times / 2$  in the case of  $\Delta(I_a - I_b)$  due to anti-CD62P binding to the platelets within the HCV.

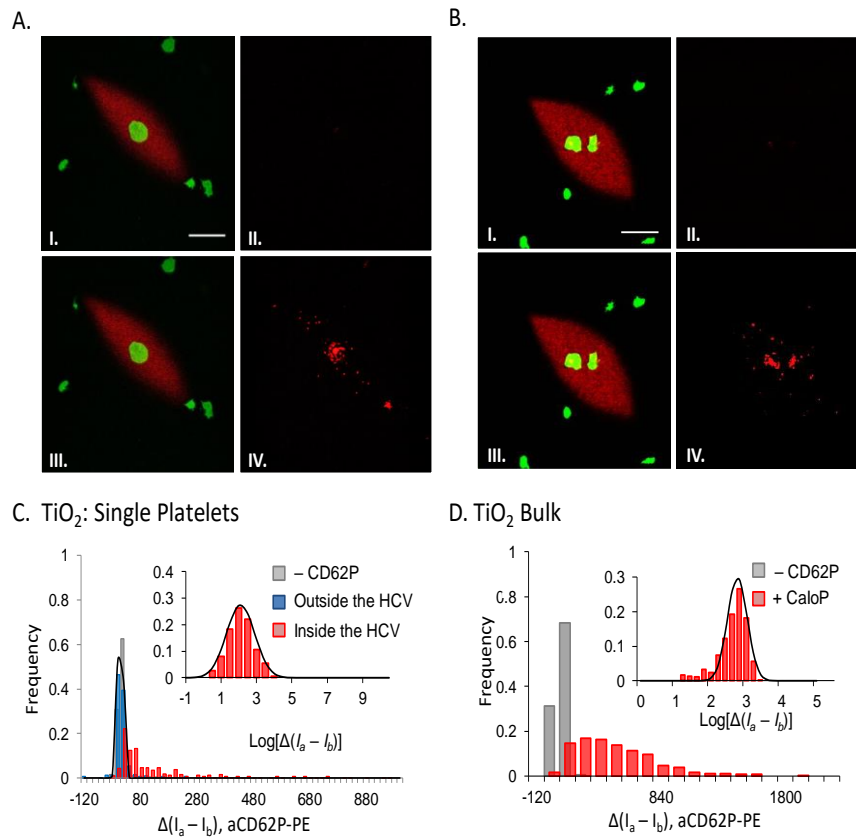


Figure 5-5. Sequences of fluorescence images illustrating the delivery of anti-CD62P and CaloP to single platelets. Left: merged images from the green (CD41a) and the red (CD62P) channels. Right: images from the red (CD62P) channel. (I) Platelets adhering on TiO<sub>2</sub> in the absence of extracellular calcium were stained for CD41a (green) and exposed to the HCV containing 2 mM Ca and anti-CD62P. No CD62P staining appears (II), ruling out platelet activation due to the flow from the pipette. They are then exposed to the HCV containing 5  $\mu$ M CaloP + 2 mM calcium (not shown) and subsequently to the anti-CD62P antibody (III). CD62P staining is now visible on the target platelets (IV), while platelets outside the HCV visible in (III), highlighted by the dashed circles, are not stained. Each set of four images (A and B) is taken from a single experiment with blood collected from one donor. The donors in the two experiments shown in (A) and (B) were different. Scale bar: 10  $\mu$ m. C and D. Distributions of fluorescence intensity differences,  $\Delta(I_a - I_b)$ , after and before CaloP treatment, for the platelets adhering on TiO<sub>2</sub> located outside (blue) and inside (red) of the HCV from the single platelet experiments (C) and from the bulk experiments (D). Background fluorescence intensities recorded before the addition of aCD62P are shown in gray. Insets show the same data plotted on the semi-log scale to highlight the log-normal distributions of the fluorescence intensities due to aCD62P binding. Black curves are Gaussian fits.

For comparison, we also show the effect of CaloP treatment of platelets adhering on TiO<sub>2</sub> (Figure 5-5 D) that was performed by adding the ionophore to the buffer above the adhering platelets; we refer to these as “bulk” experiments to distinguish them from the “single-

platelet" experiments discussed above. Here, fluorescence intensity differences,  $\Delta(I_a - I_b) \sim 308 \times / 4$ , are also distributed log-normally (inset).

## 5.6 Triggering PS expression in individual platelets

We then used the same approach to study PS expression on the TiO<sub>2</sub>-adhering platelets (Figure 5-6). These experiments followed the same protocol (Figure 5-4 C), but aCD62P was replaced with fluorescently labelled A5, and CaloP concentration was varied between 0 and 20 μM.

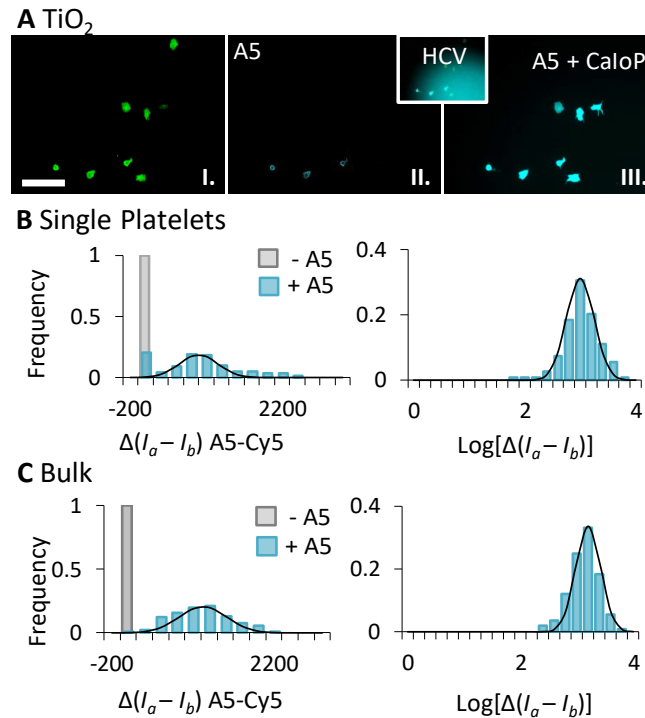


Figure 5-6. A. The sequence of fluorescence images illustrating PS expression in TiO<sub>2</sub>-adhering platelets before (II) and after (III) the delivery of 10 μM CaloP with the multifunctional pipette. Image I shows the CD41a expression (green), while the inset shows the HCV containing fluorescently labelled A5 (cyan) in a calcium-containing buffer. Calcium concentration was 2 mM. Some limited PS expression can be noted in II due to the residual activation of the purified platelets. Scale bar: 10 μm. B. Distribution of fluorescence intensity differences,  $\Delta(I_a - I_b)$ , after and before the delivery of 10 μM CaloP with the multifunctional pipette, for the platelets located within the boundaries of inside the HCV. Background fluorescence intensities recorded in the absence of A5 are shown in gray. Top: data plotted on the linear scale fit to a Gaussian distribution with a mean  $\pm$  std. dev. of  $890 \pm 548$ . Bottom: data plotted on the logarithmic scale fit to a log-normal distribution, with the mean  $\pm$  std. dev. of  $608 \times / 1$ . C. Same as (B), but for the “bulk” experiments. The data are plotted on the linear (left) and logarithmic (right) scale. Mean  $\pm$  std. dev:  $995 \pm 470$  ( $854 \times / 1$ ). The difference between  $\Delta(I_a - I_b)$  for the single platelet experiments shown in (B) and for the bulk experiments shown in (C) was statistically significant:  $t(89) = 1.7$ ,  $p = 0.03$ . In (B) and (C), the histograms contain data from 2 experiments performed with blood from 2 different donors.

The results from a representative experiment are shown in Figure 5-6 A. Analysis of the experiments performed with platelets from several donors (Figure 5-6 B) shows a reproducible increase of fluorescence intensity of individual platelets due to the binding of A5 as a result of

CaloP treatment, with  $\Delta(Ia - Ib) \sim 608 \times / 1$ . This situation mimics that found in the bulk experiments on  $TiO_2$  (Figure 5-6 C), where  $\Delta(Ia - Ib) \sim 854 \times / 1$  was observed.

## 5.7 Quantitative analysis of the multifunctional pipette performance

To further characterize the performance of the pipette, we compared the effect of the CaloP concentration on the expression of PS in the adhering platelets and in platelets in solution. The results of the experiments for the  $TiO_2$ -adhering platelets approached with the pipette are shown in Figure 5-7.

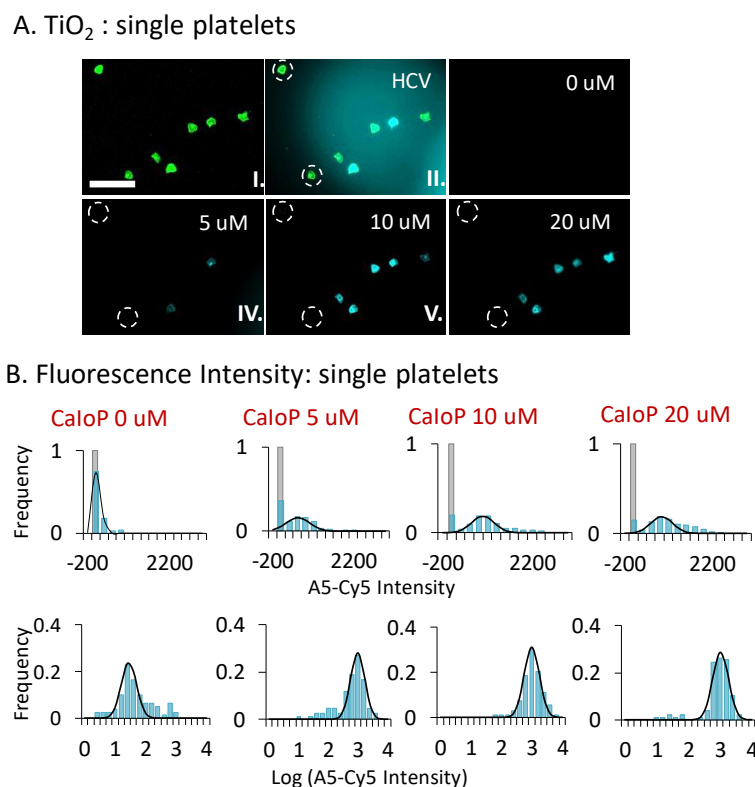


Figure 5-7. Effect of CaloP concentrations on PS exposure. A. Sequence of fluorescence images illustrating the effect of CaloP concentration on the PS expression in  $TiO_2$ -adhering platelets located within the confines of the HCV. I: image from the CD41a (green) channel. II: HCV containing A5 in a calcium-containing buffer. Ca concentration was 2 mM. III – IV: images from the PS (cyan) channel showing PS exposure after the delivery of CaloP with the multifunctional pipette. CaloP concentrations are indicated on the images. Note the two dashed circles highlighting platelets located outside the HCV that never express PS. Scale bar in I: 10  $\mu$ m. B. Histograms of fluorescence intensity for  $TiO_2$ -adhering platelets located inside the HCV exposed to increasing concentrations of CaloP. The fluorescence intensities represent the binding of A5 to the exposed PS on the adhering platelets. Gray: background fluorescence intensity. Top: data plotted on the linear scale. Bottom: data plotted on the logarithmic scale. Statistical significance of the changes in platelet fluorescence intensities as a function of CaloP concentrations was evaluated by a one-way ANOVA,  $F(3,472) = 2.62$ ,  $p = 4E-30$ .

In the images (Figure 5-7 A), it can be seen that as the concentration of CaloP delivered with the pipette increases, there is an increase in the number of PS+ platelets that bind A5. The increase is also visible in the average fluorescence intensity of these platelets (Figure 5-7 B). Untreated platelets (CaloP 0  $\mu$ M) present a minimal binding to A5, with a geometric mean  $\times$ /std. dev.  $\sim 35 \times / 2$ . The treatment with 5  $\mu$ M CaloP leads to a shift in the fluorescence intensity, with  $\Delta(I_a - I_b) \sim 350 \times / 2$ . A significant fraction of platelets still do not express PS. This is visible from the overlap with the background in the linear scale, and from the left tail in the logarithmic scale. Further increase in the fluorescence intensity occurs after treatment with 10  $\mu$ M CaloP, and 20  $\mu$ M CaloP,  $\Delta(I_a - I_b) \sim 608 \times / 1$  and  $685 \times / 1$ , respectively. Figure 5-8 shows the increase of fluorescence intensity on TiO<sub>2</sub>-adhering platelets treated with increasing CaloP concentrations by its addition to the subphase (bulk). The increase is evident from the sequence of images and from the shift in the fluorescence intensity, indicative of the A5 binding to the exposed PS (Figure 5-8 A and B). Untreated platelet (0  $\mu$ M CaloP) minimally bind A5, with fluorescence intensity ( $\Delta(I_a - I_b)$ )  $\sim 98 \times / 2$ . The treatment with increasing concentration of CaloP leads to a shift in the fluorescence intensity: 199  $\times / 2$  for 0.5  $\mu$ M CaloP; 375  $\times / 1$  for 1  $\mu$ M CaloP; 514  $\times / 1$  for 2.5  $\mu$ M CaloP; 522  $\times / 1$  for 5  $\mu$ M CaloP; 854  $\times / 1$  for 10  $\mu$ M CaloP. A decrease in fluorescence intensity is observed at 20  $\mu$ M CaloP: 504  $\times / 1$ . This can be ascribed to platelet damage caused by high CaloP concentrations.<sup>257</sup>

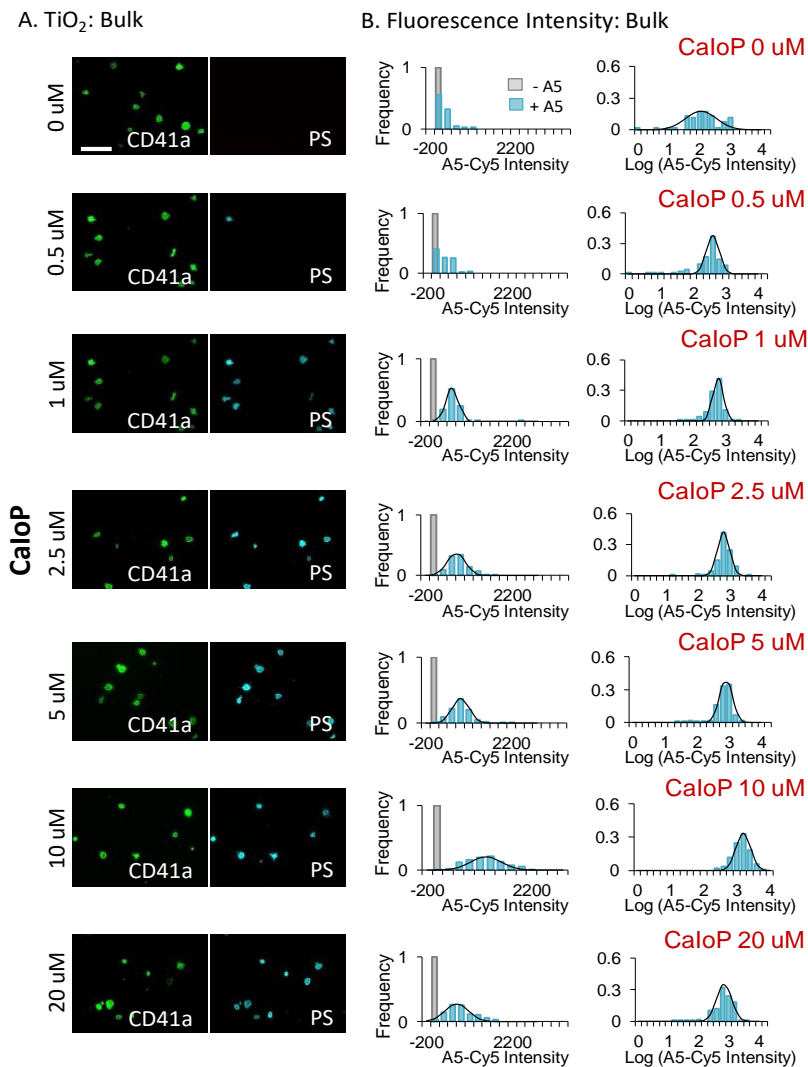


Figure 5-8. Bulk experiments: effect of CaloP concentrations on PS exposure on platelets in solution. A. Sequence of fluorescent images from the bulk experiments. Left column: individual images for CD41a staining. Right column: individual images for A5 staining (PS exposure). Each row corresponds to one CaloP concentration. The scale bar is 10  $\mu$ m. B. Histograms of fluorescence intensity for TiO<sub>2</sub> – adhering platelets treated with increasing CaloP concentrations by its addition to the subphase. The histograms originate from two separate experiments with blood obtained from two different donors. Left column: data plotted in the linear scale. Right column: data plotted in the logarithmic scale. Gray: background fluorescence intensity. Statistical significance of the changes in platelet fluorescence intensities as a function of CaloP concentrations was evaluated by a one-way ANOVA,  $F(6,623) = 2.11$ ,  $p = 6E-71$  in the case of the bulk experiments

Similarly, the shifts in the fluorescence intensity are visible also for platelet in solution, where the expression of PS is evaluated by from the flow cytometry (Figure 5-9).

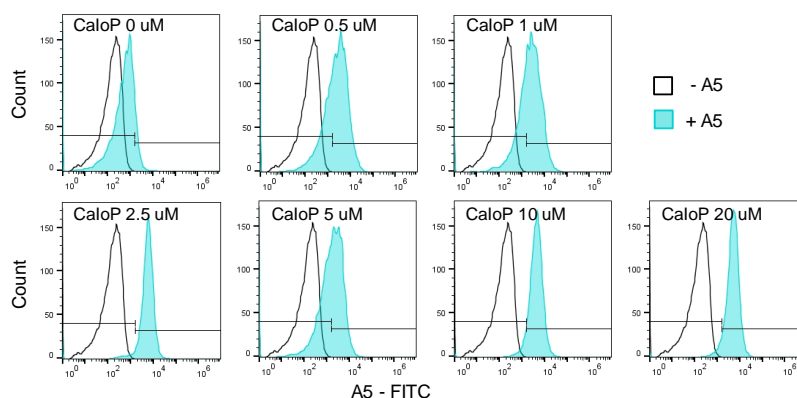


Figure 5-9. Effect of CaloP concentrations on PS exposure on platelets in solution. Fluorescence histograms. Freshly isolated platelets were incubated with various concentrations of CaloP and stained with A5 to detect the PS exposure. The binding of A5 to the PS exposing platelets was evaluated by Flow cytometry and analyzed using the FlowJo software. The shift of the fluorescence intensity is indicative of the exposure level of PS. White peak: background fluorescence recorded in absence of A5. Cyan peak: fluorescence originated from the binding of A5.

Finally, the results of the single platelet experiments are compared with those of the bulk experiments (where CaloP was added to the solution above the adhering platelets) and with those done with platelets in solution, where fluorescence intensities were analyzed by flow cytometry. The corresponding dose response curves, showing the fraction of PS+ platelets as a function of CaloP concentration, are shown in Figure 5-10.

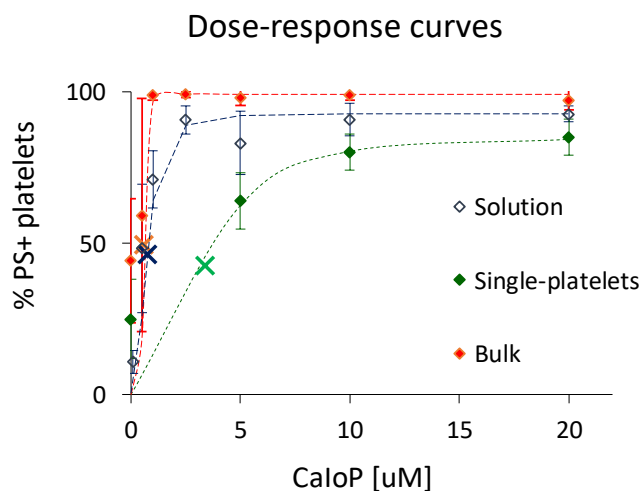


Figure 5-10. Dose-response curves showing the relationship between the fraction of PS+ cells and CaloP concentration for the single platelet experiments (green), “bulk” experiments, where platelets adhering on TiO<sub>2</sub> were treated with CaloP by the addition of the reagent to the bulk solution (red), and for platelets in solution (blue). The latter experiments were analyzed by flow cytometry. Activated platelet fractions were obtained in each case following standard procedures used for analyzing flow cytometry data. EC<sub>50</sub> values for each condition are indicated with crosses.

The dose-response curves can be characterized by two parameters: the CaloP concentration where 50% of the platelets are activated (EC<sub>50</sub>), and the maximal activation level achieved at the plateau. The maximal activation levels from the bulk and the solution experiments are similar:  $99 \pm 2\%$  and  $91 \pm 5\%$ , respectively. The EC<sub>50</sub>s from the bulk and the solution experiments are also similar: 0.6 and 0.7  $\mu\text{M}$ , respectively. On the other hand, in the single platelet experiment, the EC<sub>50</sub> was 3  $\mu\text{M}$  and the maximal activation level that is reached was  $\sim 85\%$ . Fluorescence intensities of platelets labelled with CD62P are similarly different between single platelet and bulk experiments (Figure 5-5).

## 5.8 Discussion

In this Chapter, I describe and validate a method for analyzing activation at the single platelet level. The approach is based on an open-volume microfluidic pipette that is used to deliver agonists and antibodies to the individual platelets. I test its performance on platelets adhering on TiO<sub>2</sub> in the absence of extracellular calcium. Unlike platelets adhering on other substrates, these platelets do not spontaneously secrete  $\alpha$ -granules or express PS upon adhesion.<sup>172</sup> Instead, the secretion and expression events characteristic of platelet activation can be triggered in the adhering platelets by adding CaloP.

### 5.8.1 Multifunctional pipette for single platelet assay

The first conclusion that can be made is that the multifunctional pipette allows to selectively trigger  $\alpha$ -granule secretion and PS expression in individual platelets, and to simultaneously analyze surface activation marker expression by immunofluorescence microscopy. However, the validation study shows differences in platelet PS expression when CaloP is delivered with the pipette, added to the subphase (bulk experiment) or to the platelet in solution. They are reflected in the EC<sub>50</sub> and the maximal PS expression (Figure 5-10). I ascribed these differences to the loss of the reagents due to the non-specific interactions with the PDMS surfaces of the pipette. In particular, I estimate that the effective CaloP concentration in the HCV is  $\sim 4 - 6$  times lower than the nominal (based on the amount of CaloP added to the solution).

## 5.8.2 Expression of CD62P and PS

Some insight can be gained from the analysis of CD62P and PS expression on individual platelets stimulated with the pipette. I found that platelet response in terms of these two markers is quite different. Firstly, the CD62P fluorescence intensities are log-normal (appear symmetrical only in logarithmic coordinates), the fluorescence intensity distributions for PS appear symmetrical both in the linear and logarithmic coordinates and are therefore most likely normal.<sup>255,256</sup> It is possible that this reflects differences in the mechanisms underlying PS expression (redistribution) and the expression of CD62P (granule transport) on the activated platelets: log-normal distributions commonly arise in biology because of random factor correlations contributing to the outcome. In this context, it would appear that CD62P expression is a more complex process (mechanistically) than PS expression. Secondly, CD62P expression requires a much lower CaloP concentration than PS expression, and it is therefore insensitive to the CaloP losses during injection. E.g., the delivery of 5  $\mu\text{M}$  of CaloP induces maximal expression of CD62P, 10  $\mu\text{M}$  CaloP is needed for maximal PS expression. In contrast, other studies report maximal calcium uptake and exposure of PS in washed platelets occurring at a CaloP concentration between 1 and 3  $\mu\text{M}$ .<sup>245,252</sup> Furthermore, the maximal level of PS expression achieved with the pipette is still below that observed in the bulk (Figure 5-10) The different sensitivity of CD62P and PS expression to CaloP stimulation is due to the different intracellular calcium thresholds associated with different platelet responses widely recognized in the literature.<sup>257-259</sup> In particular, Rink et al report different Ca thresholds for platelet shape change (300 nM), aggregation (between 700-900 nM) and secretion events (micromolar range).<sup>260</sup> These differences are also related to the type of agonists, underlying differences in the activation pathways: for example stimulation with thrombin induce an intracellular Ca rise to 200-300 nM sufficient for platelet shape change and aggregation.<sup>259</sup> Similarly, the surface acts as an agonist and its effect might be synergic or antagonist with CaloP.

## 5.9 Conclusion and Outlook

To validate the multifunctional pipette approach to studying single platelets, we relied on a very particular model system: the selectively activated platelets adhering on titanium. In order for this approach to be of interest to platelet biologists, two further steps need to be made. The first is a surface immobilization protocol that does not activate platelets. We have recently developed such a protocol that relies on the passivating properties of the solid-supported lipid bilayers.<sup>261</sup> The second step is the analysis of single platelet secretions collected with the pipette. By combining the immobilization, pipette, and analysis technology, we expect to bring forth a unique method for studying platelet secretions at the single platelet level.

## 6. Discussion

The paradigm of blood-biomaterial interaction holds that protein adsorption is the first event occurring at the biomaterial interface and determines the later interactions with platelets and leukocytes and the activation of the coagulation, cellular inflammation, and complement.<sup>45,262</sup> Protein adsorption is a complex and dynamic process. The composition of the protein layers varies depending on the chemical and physical properties of the surface, but it also subject to changes over time according to the Vroman effect,<sup>224</sup> and protease degradation. Furthermore, not only the composition, but also the conformation of the surface-adsorbed proteins is important in determining the interaction with the blood elements, and it also changes with time.<sup>109,153,203,263</sup>

In this Thesis, the two *in vitro* tests for material hemocompatibility assess this paradigm at two different levels of complexity. The whole-blood quasi-static test gives insight in the role of platelets in the interaction between coagulation and the inflammation systems. The microfluidic assay, more simple and working in PrP, focuses instead on interactions between platelets and the proteins adsorbed at the surface. In both tests, the strategy takes a radical departure from the one used in the past, since neither of the two tests mimic physiological conditions. Taken together, the results that are obtained fit with the accepted blood-biomaterial interaction paradigm that relates surface physico-chemical properties to the properties of the adsorbed protein layers which control platelet, and subsequent cellular responses. Indeed, it is observed in the microfluidic test that different materials act as agonist of different strength, and in the whole blood assays that different materials activate different coagulation/inflammation pathways to different extent.

The concept of materials as agonists, that is supported both by the literature and my data, leads to the essentially new idea that selective platelet activation at biomaterial surfaces can be used to direct wound healing reactions and therefore implant integration. As a first step in this direction, I developed a single-platelet assay for understanding and controlling platelet activation at single platelet level. The assay focuses on the secretion reactions that are thought to be important in the selective platelet activation.

Finally, the behavior of titanium is worthy of a separate discussion. In all the three Chapters, titanium, was found to stand apart from the other materials, in different ways. When it is tested for the activation in the whole blood assay in Chapter 3, it appears superior to CoCr and steel; when it is tested for platelet-protein interactions in Chapter 4, it differs from hydrophobic materials but also from glass, although both TiO<sub>2</sub> and glass are hydrophilic when treated with UV-Ozone, as we did in Chapter 4. Chapter 5 is based on selective platelet activation at the TiO<sub>2</sub> surface, a phenomenon that is not observed on glass.

Titanium also has a long and venerable history of being used as a biomaterial in heart valves, artificial joints, dental implants, extracorporeal devices, and VADs; Ti alloys are also used in stents.<sup>264-268</sup> Its success has always been associated with the particular properties of its oxide, but the reasons for it have never been elucidated, despite many decades of research.<sup>269,270</sup>

On the other hand, reports in literature about titanium performance are discordant, particularly in respect to its thrombogenicity,<sup>271-274</sup> and so my results invite a closer look at the surface properties of TiO<sub>2</sub> with respect to its interactions with biological systems.

## 7. Conclusions

The work presented in this Thesis addresses the problem of material hemocompatibility. All the materials used in clinical practice for CVDs treatment cause thrombotic and inflammatory complications, leading to heart attacks and strokes if they are not managed with the antiplatelet and anticoagulation therapy. The research in the field is stagnant: how to test material hemocompatibility in vitro is still an open question. Therefore, I developed two in vitro assays for material testing. In both tests a series of blood activation parameters were evaluated for their sensitivity in distinguishing between materials. Correlations between various parameters were used to elucidate the mechanism underlying blood-biomaterial interactions.

Taken together, the most striking conclusion is that materials activate the blood responses in different ways. In the whole-blood quasi-static test, these differences are reflected in the extent to which different materials activate the thrombotic and the inflammatory responses. In particular, Ti appears to be less thrombogenic but more pro-inflammatory than CoCr and steel. Furthermore, this test identifies the activation of platelet-monocyte aggregates as the most sensitive parameter to distinguish between materials. On the other hand, the analysis of correlation between parameters highlighted the role of platelet-monocytes aggregates in the interactions between the thrombotic and inflammatory responses. The results with the quasi-static test also show that flow is not absolutely required for evaluating blood activation at biomaterial surfaces.

In the PrP-microfluidic test, the differences between materials are reflected in the platelet-surface adhesion strength. This parameter varied between surfaces, most likely reflecting the differences in composition of the adsorbed proteins at different surfaces. In turn, this depends on the physicochemical properties of the surface. Different surfaces appear to act as agonists of different strength. If it were possible to tune platelet activation at biomaterials to induce regenerative, rather than pathological, responses, new approaches to implant integration could be developed. To explore this possibility, I developed and validated a single platelet microfluidic assay capable of analyzing platelet secretion, because platelets direct the wound healing through secretion of active substances upon activation.

# Appendix

## Characterization of the TiO<sub>2</sub>, glass and PTFEP surfaces used in Chapter 3 and Chapter 4

Figure A-1 shows the surface characterization of TiO<sub>2</sub> (A) and glass (B, C) surfaces by XPS. TiO<sub>2</sub> surface prepared by magnetron reactive sputtering as described in Section 2.8.4 in the Materials and Methods. XPS analysis reveals the expected elements: oxygen, titanium, and carbon. Carbon comes from adventitious surface contamination. No extraneous elements were found. The Ti 2p region (inset) is dominated by the oxide doublet appearing at 458.7 (2p 3/2) and 464.5 eV for (2p 1/2). For comparison, the XPS spectrum of the metallic Ti with a native oxide appears in Section 3.3. No metallic titanium is visible. The energy of the 2p 3/2 peak of is consistent with that of the oxide, 458.8 eV, and the difference between the 2p 1/3 and 2p 3/2 peaks, 5.8 eV, is also consistent with what's expected of the oxide (5.54 – 5.8 eV). Further information can be found in Gonbeau et al and Rossetti and al.<sup>184,185</sup>

The XPS of the glass surfaces before and after cleaning are shown in Figure A- 1B and C. The O and Si peaks, typical of glass, appear. After the SDS/UV-Ozone cleaning procedure (Section 2.8.4 Chapter 2), the C1s peak was reduced from 17 atom% of carbon before cleaning to < 4% after cleaning (Figure A- 1C). No nitrogen was observed on the surfaces, also ruling out protein contamination. The same cleaning procedure has been used on the titanium coatings.<sup>275-277</sup>

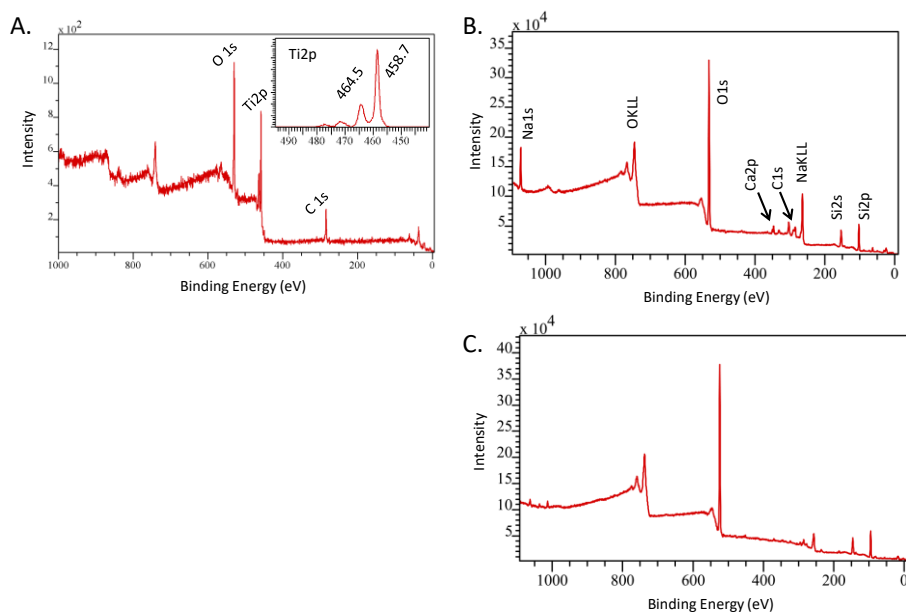


Figure A-1. XPS analysis of  $\text{TiO}_2$  glass surfaces. A. XPS spectrum of  $\text{TiO}_2$  and B of the glass surface before cleaning. C. An XPS spectrum of the glass surface subjected to the SDS-UV/Ozone cleaning procedure.

Figure A-2 shows the surface characterization of PTFEP coating on glass by XPS. The two distinguishable  $\text{C}1s$  peaks of the methylene and the  $\text{CF}_3$  group, typical of perfluorinated polymer, appear.<sup>203</sup> From XPS measurements of bare and coated samples the thickness is estimated to be  $\sim 5$  nm. XPS analysis was performed by Dr. Alexei Nefedov (IFG, KIT).

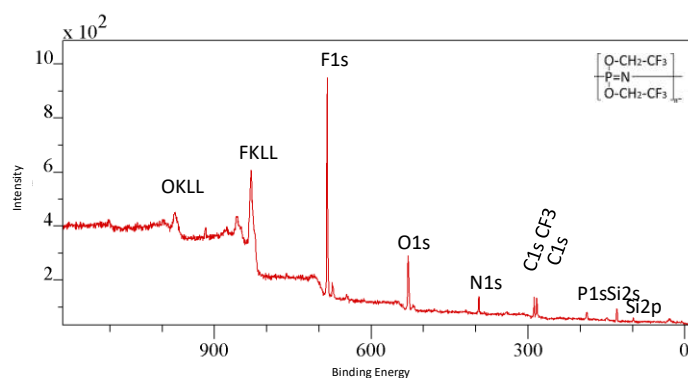


Figure A-2. XPS analysis of PTFEP coating on glass.

# References

- 1 Association, A. H. What is cardiovascular disease? [http://www.heart.org/HEARTORG/Caregiver/Resources/WhatIsCardiovascularDisease/What-is-Cardiovascular-Disease\\_UCM\\_301852\\_Article.jsp#.V6NM-LiLShc](http://www.heart.org/HEARTORG/Caregiver/Resources/WhatIsCardiovascularDisease/What-is-Cardiovascular-Disease_UCM_301852_Article.jsp#.V6NM-LiLShc).
- 2 (WHO), W. H. O. <http://www.who.int/mediacentre/factsheets/fs317/en/>.
- 3 Pirro, M. M., E. Molecular biology of atherosclerosis. *Clinical Cases in Mineral and Bone Metabolism* 5(1), 57-62, (2008).
- 4 National Heart, L., and Blood Institute. What is coronary heart disease? <http://www.nhlbi.nih.gov/health/health-topics/topics/cad>.
- 5 Thom, T. *et al.* Heart disease and stroke statistics—2006 update. *A Report From the American Heart Association Statistics Committee and Stroke Statistics Subcommittee* 113, e85-e151, (2006).
- 6 Lusis, A. J. Atherosclerosis. *Nature* 407, 233-241, (2000).
- 7 (WHO), W. H. O. A global brief on hypertension. [http://ish-world.com/downloads/pdf/global\\_brief\\_hypertension.pdf](http://ish-world.com/downloads/pdf/global_brief_hypertension.pdf).
- 8 Chugh, S. S., Blackshear, J. L., Shen, W.-K., Hammill, S. C. & Gersh, B. J. Epidemiology and natural history of atrial fibrillation: Clinical implications. *Journal of the American College of Cardiology* 37, 371-378, (2001).
- 9 Bui, A. L., Horwich, T. B. & Fonarow, G. C. Epidemiology and risk profile of heart failure. *Nat Rev Cardiol* 8, 30-41, (2011).
- 10 Roger, V. L. Epidemiology of heart failure. *Circulation research* 113, 646-659, (2013).
- 11 Mozaffarian, D. *et al.* Heart disease and stroke statistics—2016 update. *A Report From the American Heart Association*, (2015).
- 12 (WHO), W. H. O. Data and statistics. <http://www.euro.who.int/en/health-topics/noncommunicable-diseases/cardiovascular-diseases/data-and-statistics>.
- 13 Erhardt, L., Moller, R. & García Puig, J. Comprehensive cardiovascular risk management – what does it mean in practice? *Vascular Health and Risk Management* 3, 587-603, (2007).
- 14 Weisfeldt, M. L. & Zieman, S. J. Advances in the prevention and treatment of cardiovascular disease. *Health Affairs* 26, 25-37, (2007).
- 15 Gage, K. L. W., W.R. . Cardiovascular devices, in standard handbook of biomedical engineering & design. *McGraw-Hill:New York* ed M.Kutz, 20, (2003).
- 16 Go, A. S. *et al.* Heart disease and stroke statistics--2014 update: A report from the american heart association. *Circulation* 129, e28-e292, (2014).
- 17 Cook, S., Walker, A., Hugli, O., Togni, M. & Meier, B. Percutaneous coronary interventions in europe: Prevalence, numerical estimates, and projections based on data up to 2004. *Clinical research in cardiology : official journal of the German Cardiac Society* 96, 375-382, (2007).

- 18 Ludman, P. F., O'Neill, D., Whittaker, T. & Donald, A. British cardiovascular intervention society national audit of percutaneous coronary interventional procedures. (2014).
- 19 Grüntzig, A. Transluminal dilatation of coronary-artery stenosis. *The Lancet* 311, 263, (1978).
- 20 Bauters, C. *et al.* Mechanisms and prevention of restenosis: From experimental models to clinical practice. *Cardiovascular Research* 31, 835-846, (1996).
- 21 Chandrasekar, B. & Tanguay, J.-F. Platelets and restenosis. *Journal of the American College of Cardiology* 35, 555-562, (2000).
- 22 Sigwart, U., Puel, J., Mirkovitch, V., Joffre, F. & Kappenberger, L. Intravascular stents to prevent occlusion and restenosis after transluminal angioplasty. *The New England journal of medicine* 316, 701-706, (1987).
- 23 Schomig, A. *et al.* A randomized comparison of antiplatelet and anticoagulant therapy after the placement of coronary-artery stents. *The New England journal of medicine* 334, 1084-1089, (1996).
- 24 Serruys, P. W. *et al.* Angiographic follow-up after placement of a self-expanding coronary-artery stent. *New England Journal of Medicine* 324, 13-17, (1991).
- 25 Iqbal, J., Gunn, J. & Serruys, P. W. Coronary stents: Historical development, current status and future directions. *British Medical Bulletin*, (2013).
- 26 Greenhalgh, J. *et al.* Drug-eluting stents versus bare metal stents for angina or acute coronary syndromes. *Cochrane Database of Systematic Reviews*, (2010).
- 27 Garratt, K. N. Duration of dual anti-platelet therapy post-percutaneous intervention: Is there a correct amount of time? *Progress in Cardiovascular Diseases* 58, 285-298, (2015).
- 28 Windecker, S. *et al.* 2014 esc/eacts guidelines on myocardial revascularization. *EuroIntervention : journal of EuroPCR in collaboration with the Working Group on Interventional Cardiology of the European Society of Cardiology* 10, 1024-1094, (2015).
- 29 National Heart, L., and Blood Institute. What is coronary artery bypass grafting? <https://www.nhlbi.nih.gov/health/health-topics/topics/cabg>.
- 30 Serruys, P. W. *et al.* Percutaneous coronary intervention versus coronary-artery bypass grafting for severe coronary artery disease. *New England Journal of Medicine* 360, 961-972, (2009).
- 31 Smith, S. C. *et al.* Acc/aha/scai 2005 guideline update for percutaneous coronary intervention. *Journal of the American College of Cardiology* 47, e1-e121, (2006).
- 32 Pibarot, P. & Dumesnil, J. G. Prosthetic heart valves: Selection of the optimal prosthesis and long-term management. *Circulation* 119, 1034-1048, (2009).
- 33 Yacoub, M. H. & Takkenberg, J. J. M. Will heart valve tissue engineering change the world? *Nature clinical practice. Cardiovascular medicine* 2, 60-61, (2005).
- 34 Gott, V. L., Alejo, D. E. & Cameron, D. E. Mechanical heart valves: 50 years of evolution. *The Annals of Thoracic Surgery* 76, S2230-S2239.
- 35 Lampropulos, J. F. *et al.* Trends in left ventricular assist device use and outcomes among medicare beneficiaries, 2004–2011. *Open Heart* 1, (2014).

- 36 Susen, S., Rauch, A., Van Belle, E., Vincentelli, A. & Lenting, P. J. Circulatory support devices: Fundamental aspects and clinical management of bleeding and thrombosis. *Journal of thrombosis and haemostasis : JTH* 13, 1757-1767, (2015).
- 37 Miller, L. W. *et al.* Use of a continuous-flow device in patients awaiting heart transplantation. *New England Journal of Medicine* 357, 885-896, (2007).
- 38 Allen, S. J. & Sidebotham, D. Postoperative care and complications after ventricular assist device implantation. *Best Practice & Research Clinical Anaesthesiology* 26, 231-246, (2012).
- 39 Punjabi, P. P. & Taylor, K. M. The science and practice of cardiopulmonary bypass: From cross circulation to ECMO and ICRS. *Global Cardiology Science & Practice* 2013, 249-260, (2013).
- 40 Bing, R. John h. Gibbon, jr. Cardiopulmonary bypass —triumph of perseverance and character. *Clinical Cardiology* 17, 456-457, (1994).
- 41 Edmunds, L. H. Blood-surface interactions during cardiopulmonary bypass. *Journal of Cardiac Surgery* 8, 404-410, (1993).
- 42 B.R., S. & Rinder H.M. in *Platelets* (ed A. D. Michelson) 1075-1096 (Academic Press, 2012).
- 43 Peek, G. J. & Firmin, R. K. The inflammatory and coagulative response to prolonged extracorporeal membrane oxygenation. *ASAIO journal* 45, 250-263, (1999).
- 44 Ratner, B. D. The blood compatibility catastrophe. *Journal of Biomedical Materials Research* 27, 283-287, (1993).
- 45 Gorbet, M. B. & Sefton, M. V. Biomaterial-associated thrombosis: Roles of coagulation factors, complement, platelets and leukocytes. *Biomaterials* 25, 5681-5703, (2004).
- 46 Reviakine, I. *et al.* Stirred, shaken, or stagnant: What goes on at the blood biomaterial interface. *Blood Reviews*, (2016).
- 47 Spaet, T. H. The platelet in hemostasis. *Annals of the New York Academy of Sciences* 115, 31-42, (1964).
- 48 Margetic, S. Inflammation and haemostasis. *Biochemia Medica* 22, 49-62, (2012).
- 49 Markiewski, M. M. & Lambris, J. D. The role of complement in inflammatory diseases from behind the scenes into the spotlight. *The American journal of pathology* 171, 715-727, (2007).
- 50 Gale, A. J. Current understanding of hemostasis. *Toxicologic pathology* 39, 273-280, (2011).
- 51 Mason, R. G. & Saba, H. I. Normal and abnormal hemostasis--an integrated view. A review. *The American journal of pathology* 92, 775-811, (1978).
- 52 Vanhoutte, P. M. & Houston, D. S. in *Central and peripheral mechanisms of cardiovascular regulation* (eds A. Magro, W. Osswald, D. Reis, & P. Vanhoutte) 135-161 (Springer US, 1986).
- 53 Schulze, H. & Shivdasani, R. A. Mechanisms of thrombopoiesis. *Journal of Thrombosis and Haemostasis* 3, 1717-1724, (2005).
- 54 Bessis, M. Living blood cells and their ultrastructure *New York: Springer-Verlag*, 767, (1973).
- 55 Fritsma, G. A. Platelet structure and function. *Clinical laboratory science* 28, 125-131, (2015).
- 56 Michelson, A. D. *Platelets*. Third edn, (Academic Press, 2012).

- 57 Reed, G. L. Platelet secretory mechanisms. *Semin Thromb Hemost* 30, 441-450, (2004).
- 58 Ciferri, S. *et al.* Platelets release their lysosomal content in vivo in humans upon activation. *Thrombosis and Haemostasis* 83, 157-164, (2000).
- 59 Lowenberg, E. C., Meijers, J. C. M. & Levi, M. Platelet-vessel wall interaction in health and disease. *Netherlands Journal of Medicine* 68, 242-251, (2010).
- 60 Stenberg, P. E., McEver, R. P., Shuman, M. A., Jacques, Y. V. & Bainton, D. F. A platelet alpha-granule membrane protein (gmp-140) is expressed on the plasma membrane after activation. *The Journal of cell biology* 101, 880-886, (1985).
- 61 White, J. C. Disorders affecting megakaryocytes and platelets. *Blood and bone marrow pathology* Chapter 32, (2015).
- 62 Rumbaut, R. T., P. . Platelet-vessel wall interactions in hemostasis and thrombosis. . *San Rafael (CA): Morgan & Claypool Life Sciences*, (2010).
- 63 Eyre, L. & Gamlin, F. Haemostasis, blood platelets and coagulation. *ANAESTHESIA AND INTENSIVE CARE MEDICINE* 11, 244-246, (2010).
- 64 Minors, D. Haemostasis, blood platelets and coagulation. *ANAESTHESIA AND INTENSIVE CARE MEDICINE* 8, 214-216, (2007).
- 65 Ruggeri, Z. M. Platelets in atherothrombosis. *Nat Med* 8, 1227-1234, (2002).
- 66 Jackson, S. P., Nesbitt, W. S. & Kulkarni, S. Signaling events underlying thrombus formation. *Journal of Thrombosis and Haemostasis* 1, 1602-1612, (2003).
- 67 Cimmino, G. & Golino, P. Platelet biology and receptor pathways. *Journal of cardiovascular translational research* 6, 299-309, (2013).
- 68 Aalberts, M. *et al.* Identification of distinct populations of prostasomes that differentially express prostate stem cell antigen, annexin a1, and glipr2 in humans. *Biology of reproduction* 86, 82, (2012).
- 69 Reviakine, I. New horizons in platelet research: Understanding and harnessing platelet functional diversity. *Clinical Hemorheology and Microcirculation* 60, 133-152, (2015).
- 70 Nieman, M. T. & Schmaier, A. H. Interaction of thrombin with par1 and par4 at the thrombin cleavage site. *Biochemistry* 46, 8603-8610, (2007).
- 71 Jackson, S. P. & Schoenwaelder, S. M. Antiplatelet therapy: In search of the 'magic bullet'. *Nat Rev Drug Discov* 2, 775-789, (2003).
- 72 Hou, Y. *et al.* Platelets in hemostasis and thrombosis: Novel mechanisms of fibrinogen-independent platelet aggregation and fibronectin-mediated protein wave of hemostasis. *Journal of Biomedical Research* 29, 437-444, (2015).
- 73 Awtry, E. H. & Loscalzo, J. Aspirin. *Circulation* 101, 1206-1218, (2000).
- 74 Topol, E. J., Byzova, T. V. & Plow, E. F. Platelet gpiib-iiiA blockers. *The Lancet* 353, 227-231, (1999).
- 75 Weintraub, W. S., Mandel, L. & Weiss, S. A. Antiplatelet therapy in patients undergoing percutaneous coronary intervention: Economic considerations. *Pharmacoeconomics* 31, 959-970, (2013).

- 76 Bergmeier, W. & Stefanini, L. Novel molecules in calcium signaling in platelets. *Journal of thrombosis and haemostasis : JTH* 7 Suppl 1, 187-190, (2009).
- 77 Varga-Szabo, D., Braun, A. & Nieswandt, B. Calcium signaling in platelets. *J Thromb Haemost* 7, 1057-1066, (2009).
- 78 Nurden, A. T. Platelets, inflammation and tissue regeneration. *Thromb Haemost* 105 Suppl 1, S13-33, (2011).
- 79 Coppinger, J. A. *et al.* Characterization of the proteins released from activated platelets leads to localization of novel platelet proteins in human atherosclerotic lesions. *Blood* 103, 2096-2104, (2004).
- 80 Blair, P. & Flaumenhaft, R. Platelet alpha-granules: Basic biology and clinical correlates. *Blood Reviews* 23, 177-189, (2009).
- 81 Wang, Y. *et al.* Plasma fibronectin supports hemostasis and regulates thrombosis. *The Journal of clinical investigation* 124, 4281-4293, (2014).
- 82 Dahlbäck, B. Blood coagulation. *The Lancet* 355, 1627-1632, (2000).
- 83 Miletich, J., Kane, W., Hofmann, S., Stanford, N. & Majerus, P. Deficiency of factor xa-factor va binding sites on the platelets of a patient with a bleeding disorder. *Blood* 54, 1015-1022, (1979).
- 84 Palta, S., Saroa, R. & Palta, A. Overview of the coagulation system. *Indian Journal of Anaesthesia* 58, 515-523, (2014).
- 85 Bhakdi, S., Hugo, F. & Trandum-Jensen, J. Functions and relevance of the terminal complement sequence. *Blut* 60, 309-318, (1990).
- 86 Rebeck, N. & Finn, A. Polymorphonuclear granulocyte expression of cd11a/cd18, cd11b/cd18 and I-selectin in normal individuals. *FEMS Immunology & Medical Microbiology* 8, 189-195, (1994).
- 87 Wright, H. L., Moots, R. J., Bucknall, R. C. & Edwards, S. W. Neutrophil function in inflammation and inflammatory diseases. *Rheumatology* 49, 1618-1631, (2010).
- 88 Soehnlein, O. *et al.* Neutrophil secretion products pave the way for inflammatory monocytes. *Blood* 112, 1461-1471, (2008).
- 89 Smith, J. A. Neutrophils, host defense, and inflammation: A double-edged sword. *Journal of leukocyte biology* 56, 672-686, (1994).
- 90 Cambien, B. & Wagner, D. D. A new role in hemostasis for the adhesion receptor p-selectin. *Trends in molecular medicine* 10, 179-186, (2004).
- 91 May, A. E., Seizer, P. & Gawaz, M. Platelets: Inflammatory firebugs of vascular walls. *Arteriosclerosis, thrombosis, and vascular biology* 28, s5-s10, (2008).
- 92 Sims, P. J. & Wiedmer, T. The response of human platelets to activated components of the complement system. *Immunology Today* 12, 338-342, (1991).
- 93 Peerschke, E. I., Reid, K. B. & Ghebrehiwet, B. Platelet activation by c1q results in the induction of alpha iib/beta 3 integrins (gpiib-iiiA) and the expression of p-selectin and procoagulant activity. *The Journal of Experimental Medicine* 178, 579-587, (1993).

- 94 Drake, T. A., Ruf, W., Morrissey, J. H. & Edgington, T. S. Functional tissue factor is entirely cell surface expressed on lipopolysaccharide-stimulated human blood monocytes and a constitutively tissue factor-producing neoplastic cell line. *The Journal of cell biology* 109, 389-395, (1989).
- 95 Forsyth, C. B., Solovjov, D. A., Ugarova, T. P. & Plow, E. F. Integrin  $\alpha(m)\beta(2)$ -mediated cell migration to fibrinogen and its recognition peptides. *The Journal of Experimental Medicine* 193, 1123-1134, (2001).
- 96 Verhamme, P. & Hoylaerts, M. F. Hemostasis and inflammation: Two of a kind? *Thrombosis journal* 7, 15, (2009).
- 97 Barragan, P. *et al.* Ticlopidine and subcutaneous heparin as an alternative regimen following coronary stenting. *Catheterization and Cardiovascular Diagnosis* 32, 133-138, (1994).
- 98 Serruys, P. W., Kutryk, M. J. & Ong, A. T. Coronary-artery stents. *The New England journal of medicine* 354, 483-495, (2006).
- 99 Edmunds, L. H. The evolution of cardiopulmonary bypass: Lessons to be learned. *Perfusion* 17, 243-251, (2002).
- 100 Bembea, M. M. *et al.* Variability in anticoagulation management of patients on extracorporeal membrane oxygenation: An international survey. *Pediatric critical care medicine : a journal of the Society of Critical Care Medicine and the World Federation of Pediatric Intensive and Critical Care Societies* 14, e77-e77, (2013).
- 101 Holmes, D. R., Jr. *et al.* Combining antiplatelet and anticoagulant therapies. *Journal of the American College of Cardiology* 54, 95-109, (2009).
- 102 Schomig, A., Sarafoff, N. & Seyfarth, M. Triple antithrombotic management after stent implantation: When and how? *Heart* 95, 1280-1285, (2009).
- 103 Greinacher, A. Platelet activation by heparin. *Blood* 117, 4686-4687, (2011).
- 104 Baier, R. E. & Dutton, R. C. Initial events in interactions of blood with a foreign surface. *Journal of Biomedical Materials Research* 3, 191-206, (1969).
- 105 Plow, E. F. P., M.D.; Ruoslahti, E.; Marguerie, G.; Ginsberg M.H. . Arginyl-glycyl-aspartic acid sequences and fibrinogen binding to platelets. *Blood*, (1987).
- 106 Savage, B., Saldivar, E. & Ruggeri, Z. M. Initiation of platelet adhesion by arrest onto fibrinogen or translocation on von willebrand factor. *Cell* 84, 289-297, (1996).
- 107 Sivaraman, B. & Latour, R. A. The relationship between platelet adhesion on surfaces and the structure versus the amount of adsorbed fibrinogen. *Biomaterials* 31, 832-839, (2012).
- 108 Auton, M., Zhu, C. & Cruz, M. A. The mechanism of vwf-mediated platelet gp1ba binding. *Biophysical Journal* 99, 1192-1201, (2010).
- 109 Sivaraman, B. & Latour, R. A. The adherence of platelets to adsorbed albumin by receptor-mediated recognition of binding sites exposed by adsorption-induced unfolding. *Biomaterials* 31, 1036-1044, (2010).
- 110 Liu, X. *et al.* Blood compatible materials: State of the art. *Journal of Materials Chemistry B* 2, 5718-5738, (2014).

- 111 Horbett, T. A. Principles underlying the role of adsorbed plasma proteins in blood interactions with foreign materials. *Cardiovascular Pathology* 2, 137 - 148, (1993).
- 112 Vroman, L., Adams, A. L., Fischer, G. C. & Munoz, P. C. Interaction of high molecular weight kininogen, factor xii, and fibrinogen in plasma at interfaces. *Blood* 55, 156-159, (1980).
- 113 de Mel, A. C., B.G.; Seifalian, A.M. . Surface modification of biomaterials: A quest for blood compatibility. *International journal of biomaterials* 2012, 8, (2012).
- 114 Mahiout, A., Matata, B. M., Vienken, J. & Courtney, J. M. Ex vivo complement protein adsorption on positively and negatively charged cellulose dialyser membranes. *Journal of Materials Science: Materials in Medicine* 8, 287-296, (1997).
- 115 Ratner, B. D. The catastrophe revisited: Blood compatibility in the 21st century. *Biomaterials* 28, 5144-5147, (2007).
- 116 Amiji, M. P., K. . Prevention of protein adsorption and platelet adhesion on surfaces by peo/ppo/peo triblock copolymers. *Biomaterials* 13, 682-692, (1992).
- 117 Prime, K. L. W., G.M. Adsorption of proteins onto surfaces containing end-attached oligo(ethylene oxide): A model system using self-assembled monolayers *Journal of the American Chemical Society* 115, 10714-10721, (1993).
- 118 Pan, C.-J., Hou, Y.-H., Zhang, B.-B., Dong, Y.-X. & Ding, H.-Y. Blood compatibility and interaction with endothelial cells of titanium modified by sequential immobilization of poly (ethylene glycol) and heparin. *Journal of Materials Chemistry B* 2, 892-902, (2014).
- 119 Chang Chung, Y., Hong Chiu, Y., Wei Wu, Y. & Tai Tao, Y. Self-assembled biomimetic monolayers using phospholipid-containing disulfides. *Biomaterials* 26, 2313-2324, (2005).
- 120 Jordan, S. W. *et al.* Fabrication of a phospholipid membrane-mimetic film on the luminal surface of an eptfe vascular graft. *Biomaterials* 27, 3473-3481, (2006).
- 121 Tegoulia, V. A., Rao, W., Kalambur, A. T., Rabolt, J. F. & Cooper, S. L. Surface properties, fibrinogen adsorption, and cellular interactions of a novel phosphorylcholine-containing self-assembled monolayer on gold. *Langmuir* 17, 4396-4404, (2001).
- 122 Lee, J. H., Lee, H. B. & Andrade, J. D. Blood compatibility of polyethylene oxide surfaces. *Progress in Polymer Science* 20, 1043-1079, (1995).
- 123 Jaffer, I. H., Fredenburgh, J. C., Hirsh, J. & Weitz, J. I. Medical device-induced thrombosis: What causes it and how can we prevent it? *Journal of Thrombosis and Haemostasis* 13, S72-S81, (2015).
- 124 Whelan, D. *et al.* Biocompatibility of phosphorylcholine coated stents in normal porcine coronary arteries. *Heart* 83, 338-345, (2000).
- 125 Hansson, K. M. *et al.* Whole blood coagulation on protein adsorption-resistant peg and peptide functionalised peg-coated titanium surfaces. *Biomaterials* 26, 861-872, (2005).
- 126 Navarese, E. P. *et al.* First-generation versus second-generation drug-eluting stents in current clinical practice: Updated evidence from a comprehensive meta-analysis of randomised clinical trials comprising 31 379 patients. *Open Heart* 1, (2014).

- 127 Wendel, H. P. & Ziemer, G. Coating-techniques to improve the hemocompatibility of artificial devices used for extracorporeal circulation. *European Journal of Cardio-Thoracic Surgery* 16, 342-350, (1999).
- 128 Lev, E. I. *et al.* Comparison of outcomes up to six months of heparin-coated with noncoated stents after percutaneous coronary intervention for acute myocardial infarction. *American Journal of Cardiology* 93, 741-743, (2004).
- 129 Begovac, P. C., Thomson, R. C., Fisher, J. L., Hughson, A. & Gällhagen, A. Improvements in gore-tex® vascular graft performance by carmeda® bioactive surface heparin immobilization. *European Journal of Vascular and Endovascular Surgery* 25, 432-437, (2003).
- 130 Alibeik, S., Zhu, S. & Brash, J. L. Surface modification with peg and hirudin for protein resistance and thrombin neutralization in blood contact. *Colloids and Surfaces B: Biointerfaces* 81, 389-396, (2010).
- 131 Haycox, C. L. & Ratner, B. D. In-vitro platelet interactions in whole human blood exposed to biomaterial surfaces - insights on blood compatibility. *Journal of Biomedical Materials Research* 27, 1181-1193, (1993).
- 132 Jaganathan, S. K., Supriyanto, E., Murugesan, S., Balaji, A. & Asokan, M. K. Biomaterials in cardiovascular research: Applications and clinical implications. *BioMed Research International* 2014, 11, (2014).
- 133 Ratner, B. D. The biocompatibility manifesto: Biocompatibility for the twenty-first century. *J Cardiovasc Transl Res* 4, 523-527, (2011).
- 134 Kusserow, B. K. The use of pathologic techniques in the evaluation of emboli from prosthetic devices. *Bulletin of the New York Academy of Medicine* 48, 468-481, (1972).
- 135 Ratner, B., Hoffman, A., Hanson, S., Harker, L. & Whiffen, J. Blood-compatibility - water-content relationships for radiation-grafted hydrogels. *Journal of Polymer Science: Polymer Symposium* 66, 363 - 375, (1979).
- 136 Gott, V. L. B., R.E. Evaluation of materials by vena cava rings in dogs, vol. I. *National Heart and Lung Institute Annual Report PH 43-68-84-3-1, National Institutes of Health, Bethesda, Maryland* PB, 213-109, (1972).
- 137 Ratner, B. D. Biomaterials science: An introduction to materials in medicine. *Academic Press*, 375, (2004).
- 138 Dawids, S. Test procedures for the blood compatibility of biomaterials. *Springer Science & Business Media*, 684, (2012).
- 139 Bustad, L. K. & McClellan, R. O. Swine in biomedical research. *Science* 152, 1526-1530, (1966).
- 140 Verdouw D, P., Van Den Doel, M. A., De Zeeuw, S. & Duncker, D. J. Animal models in the study of myocardial ischaemia and ischaemic syndromes. *Cardiovascular Research* 39, 121-135, (1998).
- 141 J. Zurbano Gines Escolar Magda Heras Montse Rigol Gloria Gomez Gines Sanz Antonio Ordinas, M. Characterization of adhesive and aggregating functions of pig platelets: Comparative studies with human platelets and differential effects of calcium chelation. *Platelets* 9, 329-337, (1998).

- 142 Grabowski, E. F. D., P.; Lewis, J. C.; Franta, J. T.; Stropp, J. Q. Platelet adhesion to foreign surfaces under controlled conditions of whole blood flow: Human vs rabbit, dog, calf, sheep, pig, macaque, and baboon. *Transactions - American Society for Artificial Internal Organs* 23, 141-151, (1977).
- 143 10993, I. Biological evaluation of medical devices -- part 4: Selection of tests for interactions with blood. (December 2002).
- 144 Jung, F., Braune, S. & Lendlein, A. Haemocompatibility testing of biomaterials using human platelets. *Clinical Hemorheology and Microcirculation* 53, 97-115, (2013).
- 145 van Oeveren, W., Tielliu, I. F. & de Hart, J. Comparison of modified chandler, roller pump, and ball valve circulation models for in vitro testing in high blood flow conditions: Application in thrombogenicity testing of different materials for vascular applications. *International journal of biomaterials* 2012, 673163, (2012).
- 146 van Oeveren, W. Obstacles in haemocompatibility testing. *Scientifica* 2013, 392584, (2013).
- 147 Branchford, B. R., Ng, C. J., Neeves, K. B. & Di Paola, J. Microfluidic technology as an emerging clinical tool to evaluate thrombosis and hemostasis. *Thrombosis Research* 136, 13-19, (2015).
- 148 Westein, E., de Witt, S., Lamers, M., Cosemans, J. & Heemskerk, J. W. M. Monitoring in vitro thrombus formation with novel microfluidic devices. *Platelets* 23, 501-509, (2012).
- 149 de Witt, S. M. *et al.* Identification of platelet function defects by multi-parameter assessment of thrombus formation. *Nature communications* 5, 4257, (2014).
- 150 Fitzgibbon, S., Cowman, J., Ricco, A. J., Kenny, D. & Shaqfeh, E. S. Examining platelet adhesion via stokes flow simulations and microfluidic experiments. *Soft Matter* 11, 355-367, (2015).
- 151 Streller, U., Sperling, C., Hubner, J., Hanke, R. & Werner, C. Design and evaluation of novel blood incubation systems for in vitro hemocompatibility assessment of planar solid surfaces. *Journal of biomedical materials research. Part B, Applied biomaterials* 66, 379-390, (2003).
- 152 Reviakine, I. Implant integration: Problems at the interface. *Biointerphases* 11, 029604, (2016).
- 153 Sivaraman, B. & Latour, R. A. Time-dependent conformational changes in adsorbed albumin and its effect on platelet adhesion. *Langmuir* 28, 2745-2752, (2012).
- 154 Thomas, A. C., Campbell, G. R. & Campbell, J. H. Advances in vascular tissue engineering. *Cardiovascular Pathology* 12, 271-276, (2003).
- 155 Tassiopoulos, A. K. & P.Greisler, H. Angiogenic mechanisms of endothelialization of cardiovascular implants: A review of recent investigative strategies. *Journal of Biomaterials Science, Polymer Edition* 11, 1275-1284, (2000).
- 156 Schopka, S., Schmid, T., Schmid, C. & Lehle, K. Current strategies in cardiovascular biomaterial functionalization. *Materials* 3, 638, (2010).
- 157 Kutryk, M. J. B. & Kuliszewski, M. A. In vivo endothelial progenitor cell seeding for the accelerated endothelialization of endovascular devices. *American Journal of Cardiology* 92, 94L-95L, (2003).
- 158 Aoki, J. *et al.* Endothelial progenitor cell capture by stents coated with antibody against cd34: The healing-fim (healthy endothelial accelerated lining inhibits neointimal growth-first in man) registry. *Journal of the American College of Cardiology* 45, 1574-1579, (2005).

- 159 Rendu, F. & Brohard-Bohn, B. The platelet release reaction: Granules' constituents, secretion and functions. *Platelets* 12, 261-273, (2001).
- 160 Nurden, A. T. N., P.; Sanchez, M.; Andia, I.; Anitua E. Platelets and wound healing *Frontiers in bioscience : a journal and virtual library* 13, 3532-3548, (2008).
- 161 Golebiewska, E. M. & Poole, A. W. Platelet secretion: From haemostasis to wound healing and beyond. *Blood Reviews* 29, 153-162, (2015).
- 162 Piersma, S. R. *et al.* Proteomics of the trap-induced platelet releasate. *J Proteomics* 72, 91-109, (2009).
- 163 Weltermann, A. *et al.* Large amounts of vascular endothelial growth factor at the site of hemostatic plug formation in vivo. *Arteriosclerosis, thrombosis, and vascular biology* 19, 1757-1760, (1999).
- 164 Bambace, N. M., Pace, T. R., Schneider, D. J. & Holmes, C. E. The impact of p2y-mediated activation on release of angiogenic proteins by platelets from healthy individuals. *Blood* 110, 3894-3894, (2007).
- 165 Bambace, N. M., Levis, J. E. & Holmes, C. E. The effect of p2y-mediated platelet activation on the release of vegf and endostatin from platelets. *Platelets* 21, 85-93, (2010).
- 166 Cicha, I., Garlich, C. D., Daniel, W. G. & Goppelt-Struebe, M. Activated human platelets release connective tissue growth factor. *Thrombosis and Haemostasis* 91, 755-760, (2004).
- 167 Eppley, B. L., Pietrzak, W. S. & Blanton, M. Platelet-rich plasma: A review of biology and applications in plastic surgery. *Plastic and Reconstructive Surgery* 118, 147E-159E, (2006).
- 168 Bieback, K. Platelet lysate as replacement for fetal bovine serum in mesenchymal stromal cell cultures. *Transfusion medicine and hemotherapy : offizielles Organ der Deutschen Gesellschaft fur Transfusionsmedizin und Immunhamatologie* 40, 326-335, (2013).
- 169 Kang, I. K., Ito, Y., Sisido, M. & Imanishi, Y. Serotonin and beta-thromboglobulin release reaction from platelet as triggered by interaction with polypeptide derivatives. *J Biomed Mater Res* 22, 595-611, (1988).
- 170 Broberg, M. & Nygren, H. Von willebrand factor, a key protein in the exposure of cd62p on platelets. *Biomaterials* 22, 2403-2409, (2001).
- 171 Gupta, S., Donati, A. & Reviakine, I. Differences in intracellular calcium dynamics cause differences in  $\alpha$ -granule secretion and phosphatidyl serine expression in platelets adhering on glass and tio2. *Submitted*, (2016).
- 172 Gupta, S. & Reviakine, I. Platelet activation profiles on tio2: Effect of ca2+ binding to the surface. *Biointerphases* 7, 28, (2012).
- 173 Heemskerk, J. W. M., Mattheij, N. J. A. & Cosemans, J. M. E. M. Platelet-based coagulation: Different populations, different functions. *Journal of Thrombosis and Haemostasis* 11, 2-16, (2013).
- 174 Heemskerk, J. W., Vuist, W. M., Feijge, M. A., Reutelingsperger, C. P. & Lindhout, T. Collagen but not fibrinogen surfaces induce bleb formation, exposure of phosphatidylserine, and procoagulant activity of adherent platelets: Evidence for regulation by protein tyrosine kinase-dependent ca2+ responses. *Blood* 90, 2615-2625, (1997).

- 175 Munnix, I. C., Cosemans, J. M., Auger, J. M. & Heemskerk, J. W. Platelet response heterogeneity in thrombus formation. *Thrombosis and Haemostasis* 102, 1149-1156, (2009).
- 176 Donati, A., Gupta, S. & Reviakine, I. Subpopulations in purified platelets adhering on glass. *Biointerphases* 11, 029811, (2016).
- 177 Zhu, L., Gregurec, D. & Reviakine, I. Nanoscale departures: Excess lipid leaving the surface during supported lipid bilayer formation. *Langmuir* 29, 15283-15292, (2013).
- 178 Kurrat, R., Textor, M., Ramsden, J. J., Boni, P. & Spencer, N. D. Instrumental improvements in optical waveguide light mode spectroscopy for the study of biomolecule adsorption. *Review of Scientific Instruments* 68, 2172-2176, (1997).
- 179 Vig, J. R. Uv/ozone cleaning of surfaces. *Journal of Vacuum Science & Technology A* 3, 1027-1034, (1985).
- 180 Christophis, C., Grunze, M. & Rosenhahn, A. Quantification of the adhesion strength of fibroblast cells on ethylene glycol terminated self-assembled monolayers by a microfluidic shear force assay. *Physical Chemistry Chemical Physics* 12, 4498-4504, (2010).
- 181 Cho, K. L. *et al.* Shear-induced detachment of polystyrene beads from sam-coated surfaces. *Langmuir* 31, 11105-11112, (2015).
- 182 XPS, T. S. Titanium <http://xpssimplified.com/elements/titanium.php>.
- 183 Moulder, J. F. S., W. F.; Sobol, P. E.; DBomben, K. D. Handbook of x-ray photoelectron spectroscopy. *Physical Electronics Inc.: Chigasaki*, (1995).
- 184 Gonbeau, D. *et al.* Xps study of thin films of titanium oxysulfides. *Surface Science* 254, 81-89, (1991).
- 185 Rossetti, F. F., Reviakine, I. & Textor, M. Characterization of titanium oxide films prepared by the template-stripping method. *Langmuir* 19, 10116-10123, (2003).
- 186 Granja, T. *et al.* Using six-colour flow cytometry to analyse the activation and interaction of platelets and leukocytes--a new assay suitable for bench and bedside conditions. *Thrombosis Research* 136, 786-796, (2015).
- 187 Michelson, A. D., Linden, M. D., Barnard, M. R., Furman, M. I. & Frelinger III, A. L. in *Platelets* (ed A.D. Michelson) (Academic Press, 2007).
- 188 Sinn, S., Scheuermann, T., Deichelbohrer, S., Ziemer, G. & Wendel, H. P. A novel in vitro model for preclinical testing of the hemocompatibility of intravascular stents according to iso 10993-4. *Journal of Materials Science. Materials in Medicine* 22, 1521-1528, (2011).
- 189 Tepe, G. *et al.* Reduced thrombogenicity of nitinol stents—in vitro evaluation of different surface modifications and coatings. *Biomaterials* 27, 643-650, (2006).
- 190 Jenssen, E. K. *et al.* Thrombin generation and platelet activation related to subintimal percutaneous transluminal angioplasty. *Scandinavian Journal of Clinical & Laboratory Investigation* 72, 23-28, (2012).
- 191 Windeløv, N. A. *et al.* Circulating levels of platelet  $\alpha$ -granule cytokines in trauma patients. *Inflammation Research* 64, 235-241, (2015).

- 192 Plicner, D. *et al.* Beta-thromboglobulin as a marker of perioperative myocardial infarction in patients undergoing coronary artery bypass grafting following aspirin discontinuation. *Platelets* 25, 603-607, (2014).
- 193 Michelson, A. D., Barnard, M. R., Krueger, L. A., Valeri, C. R. & Furman, M. I. Circulating monocyte-platelet aggregates are a more sensitive marker of in vivo platelet activation than platelet surface p-selectin: Studies in baboons, human coronary intervention, and human acute myocardial infarction. *Circulation* 104, 1533-1537, (2001).
- 194 Furman, M. I. *et al.* Increased platelet reactivity and circulating monocyte-platelet aggregates in patients with stable coronary artery disease. *Journal of the American College of Cardiology* 31, 352-358, (1998).
- 195 Chang, X. & Gorbet, M. The effect of shear on in vitro platelet and leukocyte material-induced activation. *J Biomater Appl* 28, 407-415, (2013).
- 196 Cerletti, C., Tamburrelli, C., Izzi, B., Gianfagna, F. & de Gaetano, G. Platelet-leukocyte interactions in thrombosis. *Thrombosis Research* 129, 263-266, (2012).
- 197 Cerletti, C., de Gaetano, G. & Lorenzet, R. Platelet – leukocyte interactions: Multiple links between inflammation, blood coagulation and vascular risk. *Mediterranean Journal of Hematology and Infectious Diseases* 2, e2010023, (2010).
- 198 Schoorl, M., Schoorl, M., Nub  e, M. J. & Bartels, P. C. M. Platelet depletion, platelet activation and coagulation during treatment with hemodialysis. *Scandinavian Journal of Clinical & Laboratory Investigation* 71, 240-247, (2011).
- 199 Maugeri, N. *et al.* Human polymorphonuclear leukocytes produce and express functional tissue factor upon stimulation1. *Journal of Thrombosis and Haemostasis* 4, 1323-1330, (2006).
- 200 Barnard, M. R. *et al.* Effects of platelet binding on whole blood flow cytometry assays of monocyte and neutrophil procoagulant activity. *Journal of Thrombosis and Haemostasis* 3, 2563-2570, (2005).
- 201 Rowley, J. W. *et al.* Cardiovascular devices and platelet interactions: Understanding the role of injury, flow, and cellular responses. *Circulation: Cardiovascular Interventions* 5, 296-304, (2012).
- 202 Aarts, P. A. *et al.* Blood platelets are concentrated near the wall and red blood cells, in the center in flowing blood. *Arteriosclerosis* 8, 819-824, (1988).
- 203 Welle, A., Grunze, M. & Tur, D. Plasma protein adsorption and platelet adhesion on poly. *Journal of Colloid and Interface Science* 197, 263-274, (1998).
- 204 Radeleff, B. *et al.* Restenosis of the cypher-select, taxus-express, and polyzene-f nanocoated cobalt-chromium stents in the minipig coronary artery model. *CardioVascular and Interventional Radiology* 31, 971-980, (2008).
- 205 Gutierrez, E. *et al.* Microfluidic devices for studies of shear-dependent platelet adhesion. *Lab on A Chip* 8, 1486-1495, (2008).
- 206 Muthard, R. W., Welsh, J. D., Brass, L. F. & Diamond, S. L. Fibrin, gamma'-fibrinogen, and transclot pressure gradient control hemostatic clot growth during human blood flow over a collagen/tissue factor wound. *Arteriosclerosis, thrombosis, and vascular biology* 35, 645-654, (2015).

- 207 Hosokawa, K. *et al.* Analysing responses to aspirin and clopidogrel by measuring platelet thrombus formation under arterial flow conditions. *Thrombosis and Haemostasis* 109, 102-111, (2013).
- 208 Tronic, E. H. *et al.* Differential surface activation of the  $\alpha 1$  domain of von willebrand factor. *Biointerphases* 11, 029803, (2016).
- 209 Feuerstein, I. A., McClung, W. G. & Horbett, T. A. Platelet adherence and detachment with adsorbed fibrinogen: A flow study with a series of hydroxyethyl methacrylate-ethyl methacrylate copolymers using video microscopy. *Journal of Biomedical Materials Research* 26, 221-237, (1992).
- 210 Jen, C. J., Li, H. M., Wang, J. S., Chen, H. I. & Usami, S. Flow-induced detachment of adherent platelets from fibrinogen-coated surface. *American Journal of Physiology - Heart and Circulatory Physiology* 270, H160-H166, (1996).
- 211 Wu, Y.-P., de Groot, P. G. & Sixma, J. J. Shear stress-induced detachment of blood platelets from various surfaces. *Arteriosclerosis, thrombosis, and vascular biology* 17, 3202-3207, (1997).
- 212 Williams, M. J., Du, X., Loftus, J. C. & Ginsberg, M. H. Platelet adhesion receptors. *Seminars in Cell Biology* 6, 305-314, (1995).
- 213 Ni, H. & Freedman, J. Platelets in hemostasis and thrombosis: Role of integrins and their ligands. *Transfusion and Apheresis Science* 28, 257-264, (2003).
- 214 Chandy, T. & Rao, G. H. R. in *Handbook of platelet physiology and pharmacology* (ed Gundu H. R. Rao) 362-378 (Springer US, 1999).
- 215 Broberg, M., Eriksson, C. & Nygren, H. Gpiib/iii $\alpha$  is the main receptor for initial platelet adhesion to glass and titanium surfaces in contact with whole blood. *Journal of Laboratory and Clinical Medicine* 139, 163-172, (2002).
- 216 Varga-Szabo, D., Pleines, I. & Nieswandt, B. Cell adhesion mechanisms in platelets. *Arteriosclerosis Thrombosis and Vascular Biology* 28, 403-412, (2008).
- 217 Michelson, A. & Shattil, S. J. in *Platelets: A practical approach* (eds S.P. Watson & K.S. Authi) (Oxford University Press, USA, 1996).
- 218 Papaioannou, T. G. & Stefanadis, C. Vascular wall shear stress: Basic principles and methods. *Hellenic journal of cardiology : HJC = Hellenike kardiologike epitheorese* 46, 9-15, (2005).
- 219 Arpa-Sancet, M. P., Christophis, C. & Rosenhahn, A. Microfluidic assay to quantify the adhesion of marine bacteria. *Biointerphases* 7, 26, (2012).
- 220 Alles, M. & Rosenhahn, A. Microfluidic detachment assay to probe the adhesion strength of diatoms. *Biofouling* 31, 469-480, (2015).
- 221 Boudot, C., Recht, S., Eblenkamp, M., Haerst, M. & Wintermantel, E. in *6th european conference of the international federation for medical and biological engineering: Mbec 2014, 7-11 september 2014, dubrovnik, croatia* (eds Igor Lacković & Darko Vasic) 541-544 (Springer International Publishing, 2015).
- 222 Ruggeri, Z. M. Platelet adhesion under flow. *Microcirculation (New York, N.Y. : 1994)* 16, 58-83, (2009).

- 223 Brash, J. L. & Uniyal, S. Dependence of albumin-fibrinogen simple and competitive adsorption on surface-properties of biomaterials. *Journal of Polymer Science Part C-Polymer Symposium*, 377-389, (1979).
- 224 Vroman, L. & Adams, A. L. Identification of rapid changes at plasma-solid interfaces. *Journal of Biomedical Materials Research* 3, 43-67, (1969).
- 225 Ruggeri, Z. M. & Mendolicchio, G. L. Adhesion mechanisms in platelet function. *Circulation research* 100, 1673-1685, (2007).
- 226 Furman, M. I. *et al.* The cleaved peptide of the thrombin receptor is a strong platelet agonist. *Proceedings of the National Academy of Sciences of the United States of America* 95, 3082-3087, (1998).
- 227 Stalker, T. J., Newman, D. K., Ma, P., Wannemacher, K. M. & Brass, L. F. Platelet signaling. *Handbook of experimental pharmacology*, 59-85, (2012).
- 228 Hoffman, A. S., Hanson, S. R., Ratner, B. D., Harker, L. A. & Reynolds, L. O. in *Transactions of the Annual Meeting of the Society for Biomaterials in conjunction with the Interna.* 36.
- 229 Hanson, S. R., Harker, L. A., Ratner, B. D. & Hoffman, A. S. Factors influencing platelet consumption by polyacrylamide hydrogels. *Annals of Biomedical Engineering* 7, 357-367, (1979).
- 230 Cholakis, C. H., Zingg, W. & Sefton, M. V. Effect of heparin-pva hydrogel on platelets in a chronic canine arterio-venous shunt. *Journal of Biomedical Materials Research* 23, 417-441, (1989).
- 231 Freund, E. Über die ursache der blutgerinnung. *Med. Jahrb. Wien* 3, 259, (1985).
- 232 Bordet, J. & Gengou, O. Recherches sur la coagulation du sang. *Ann. de l'Inst. Pasteur* 17, 882, (1903).
- 233 Szott, L. M., Irvin, C., Trollsas, M., Hossainy, S. & Ratner, B. D. Blood compatibility assessment of polymers used in drug eluting stent coatings. *Biointerphases* Submitted, (2016).
- 234 Satzl, S. *et al.* The efficacy of nanoscale poly[bis(trifluoroethoxy) phosphazene] (ptfep) coatings in reducing thrombogenicity and late in-stent stenosis in a porcine coronary artery model. *Investigative radiology* 42, 303-311, (2007).
- 235 Richter, G. M. *et al.* A new polymer concept for coating of vascular stents using ptfep (poly(bis(trifluoroethoxy)phosphazene) to reduce thrombogenicity and late in-stent stenosis. *Investigative radiology* 40, 210-218, (2005).
- 236 Tamburino, C. *et al.* First-in-man 18-month clinical outcomes of the catania (tm) coronary stent system with nanothin polyzene-f in de novo native coronary artery lesions: Assessment of the latest non-thrombogenic angioplasty stent (atlanta) trial. *Journal of the American College of Cardiology* 53, A371-A371, (2009).
- 237 Tamburino, C. *et al.* First-in-man 1-year clinical outcomes of the catania coronary stent system with nanothin polyzene-f in de novo native coronary artery lesions the atlanta (assessment of the latest non-thrombogenic angioplasty stent) trial. *Jacc-Cardiovascular Interventions* 2, 197-204, (2009).
- 238 Tur, D. R. *et al.* Investigation of the thermostability of poly[bis(trifluoroethoxy)phosphazene]. *Acta Polymerica* 36, 627-631, (1985).

- 239 Broberg, M. & Nygren, H. Platelet interactions with surface-adsorbed plasma proteins: Exposure of cd62p induced by von willebrand factor. *Colloids and Surfaces B-Biointerfaces* 11, 67-77, (1998).
- 240 Sakurai, Y. *et al.* Platelet geometry sensing spatially regulates alpha-granule secretion to enable matrix self-deposition. *Blood* 126, 531-538, (2015).
- 241 Leslie, M. Beyond clotting: The powers of platelets. *Science* 328, 562-564, (2010).
- 242 Smyth, S. S. *et al.* Platelet functions beyond hemostasis. *Journal of thrombosis and haemostasis : JTH* 7, 1759-1766, (2009).
- 243 Coller, B. S. Historical perspective and future directions in platelet research. *Journal of thrombosis and haemostasis : JTH* 9 Suppl 1, 374-395, (2011).
- 244 Jonnalagadda, D., Izu, L. T. & Whiteheart, S. W. Platelet secretion is kinetically heterogeneous in an agonist-responsive manner. *Blood* 120, 5209-5216, (2011).
- 245 Dachary-Prigent, J., Pasquet, J. M. & Nurden, A. T. Simultaneous detection of changes in cytoplasmic ca(2+), aminophospholipid exposure and micro-vesiculation in activated platelets. *Platelets* 8, 405-412, (1997).
- 246 Ahemaiti, A. *et al.* A multifunctional pipette for localized drug administration to brain slices. *Journal of Neuroscience Methods* 219, 292-296, (2013).
- 247 Ainla, A., Jeffries, G. D., Brune, R., Orwar, O. & Jesorka, A. A multifunctional pipette. *Lab on A Chip* 12, 1255-1261, (2012).
- 248 Ainla, A., Jansson, E. T., Stepanyants, N., Orwar, O. & Jesorka, A. A microfluidic pipette for single-cell pharmacology. *Analytical Chemistry* 82, 4529-4536, (2010).
- 249 Sarkar, A., Kolitz, S., Lauffenburger, D. A. & Han, J. Microfluidic probe for single-cell analysis in adherent tissue culture. *Nature communications* 5, 3421, (2014).
- 250 Fritz, M., Radmacher, M. & Gaub, H. E. In vitro activation of human platelets triggered and probed by atomic force microscopy. *Exp Cell Res* 205, 187-190, (1993).
- 251 Braune, S., Alagoz, G., Seifert, B., Lendlein, A. & Jung, F. Automated image-based analysis of adherent thrombocytes on polymer surfaces. *Clinical Hemorheology and Microcirculation* 52, 349-355, (2012).
- 252 Dachary-Prigent, J., Freyssinet, J. M., Pasquet, J. M., Carron, J. C. & Nurden, A. T. Annexin v as a probe of aminophospholipid exposure and platelet membrane vesiculation: A flow cytometry study showing a role for free sulfhydryl groups. *Blood* 81, 2554-2565, (1993).
- 253 Gupta, S. & Reviakine, I. The sweeter aspects of platelet activation: A lectin-based assay reveals agonist-specific glycosylation patterns. *Biochimica et Biophysica Acta* 1840, 3423-3433, (2014).
- 254 Gupta, S. *Selective activation of platelets by surfaces and soluble agonists* Ph.D. thesis, University of the Basque Country, , (2014).
- 255 Limpert, E., Stahel, W. A. & Abbt, M. Log-normal distributions across the sciences: Keys and clues. *Bioscience* 51, 341-352, (2001).
- 256 Zhang, L., Schmidt, R. E., Yan, Q. & Snider, W. D. Ngf and nt-3 have differing effects on the growth of dorsal root axons in developing mammalian spinal cord. *The Journal of neuroscience : the official journal of the Society for Neuroscience* 14, 5187-5201, (1994).

- 257 Gerrard, J. M., White, J. G. & Rao, G. H. Effects of the ionophore a23187 on the blood platelets ii. Influence on ultrastructure. *The American journal of pathology* 77, 151-166, (1974).
- 258 Rink, T. J. & Hallam, T. J. What turns platelets on. *Trends in Biochemical Sciences* 9, 215-219, (1984).
- 259 Rink, T. J., Smith, S. W. & Tsien, R. Y. Cytoplasmic free ca<sup>2+</sup> in human platelets: Ca<sup>2+</sup> thresholds and ca-independent activation for shape-change and secretion. *FEBS Letters* 148, 21-26, (1982).
- 260 Rink, T. J. Cytosolic calcium in platelet activation. *Experientia* 44, 97-100, (1988).
- 261 Uhl, E., Donati, A. & Reviakine, I. Platelet immobilization on supported phospholipid bilayers for single platelet studies. *Langmuir : the ACS journal of surfaces and colloids* 32, 8516-8524, (2016).
- 262 Kasemo, B. Biological surface science. *Surface Science* 500, 656-677, (2002).
- 263 Thyparambil, A. A., Wei, Y. & Latour, R. A. Experimental characterization of adsorbed protein orientation, conformation, and bioactivity. *Biointerphases* 10, 019002, (2015).
- 264 Olin, C. in *Titanium in medicine* (eds D. M. Brunette, P. Tengvall, M. Textor, & P. Thomsen) Ch. 26, 890-905 (Springer-Verlag, 2001).
- 265 Windecker, S. *et al.* Stent coating with titanium-nitride-oxide for reduction of neointimal hyperplasia. *Circulation* 104, 928-933, (2001).
- 266 Huang, N. *et al.* Hemocompatibility of titanium oxide films. *Biomaterials* 24, 2177-2187, (2003).
- 267 Yang, Y., Franzen, S. F. & Olin, C. L. In vivo comparison of hemocompatibility of materials used in mechanical heart valves. *The Journal of heart valve disease* 5, 532-537, (1996).
- 268 Sin, D.-C., Kei, H.-L. & Miao, X. Surface coatings for ventricular assist devices. *Expert Review of Medical Devices* 6, 51-60, (2009).
- 269 Parsegian, V. A. Molecular forces governing tight contact between cellular-surfaces and substrates. *Journal of Prosthetic Dentistry* 49, 838-842, (1983).
- 270 Kasemo, B. Biocompatibility of titanium implants - surface science aspects. *Journal of Prosthetic Dentistry* 49, 832-837, (1983).
- 271 Thor, A. *et al.* The role of whole blood in thrombin generation in contact with various titanium surfaces. *Biomaterials* 28, 966-974, (2007).
- 272 Hong, J. *et al.* Titanium is a highly thrombogenic biomaterial: Possible implications for osteogenesis. *Thrombosis and Haemostasis* 82, 58-64, (1999).
- 273 Hong, J., Azens, A., Ekdahl, K. N., Granqvist, C. G. & Nilsson, B. Material-specific thrombin generation following contact between metal surfaces and whole blood. *Biomaterials* 26, 1397-1403, (2005).
- 274 Riescher, S. *et al.* Titaniumcarboxonitride layer increased biocompatibility of medical polyetherurethanes. *Journal of Biomedical Materials Research Part B: Applied Biomaterials* 102, 141-148, (2014).

- 275 Rossetti, F. F. *Interactions of lipidic assemblies with metal oxide surfaces and brush-like polyelectrolytes. Dissertation for the degree of doctor of sciences.* Doctor of Sciences thesis, Swiss Federal Institute of Technology, (2005).
- 276 Rossetti, F. F., Textor, M. & Reviakine, I. Asymmetric distribution of phosphatidyl serine in supported phospholipid bilayers on titanium dioxide. *Langmuir* 22, 3467-3473, (2006).
- 277 Rossetti, F. F., Bally, M., Michel, R., Textor, M. & Reviakine, I. Interactions between titanium dioxide and phosphatidyl serine-containing liposomes: Formation and patterning of supported phospholipid bilayers on the surface of a medically relevant material. *Langmuir* 21, 6443-6450, (2005).